

Universiteit
Leiden
The Netherlands

The contribution of metabolic and adipose tissue inflammation to non-alcoholic fatty liver disease

Mulder, P.C.A.

Citation
Mulder, P. C. A. (2017, February 16). *The contribution of metabolic and adipose tissue inflammation to non-alcoholic fatty liver disease*. Retrieved from https://hdl.handle.net/1887/46137

Version:	Not Applicable (or Unknown)
License:	Licence agreement concerning inclusion of doctoral thesis in the Institutional Repository of the University of Leiden
Downloaded from:	https://hdl.handle.net/1887/46137

Note: To cite this publication please use the final published version (if applicable).

Cover Page



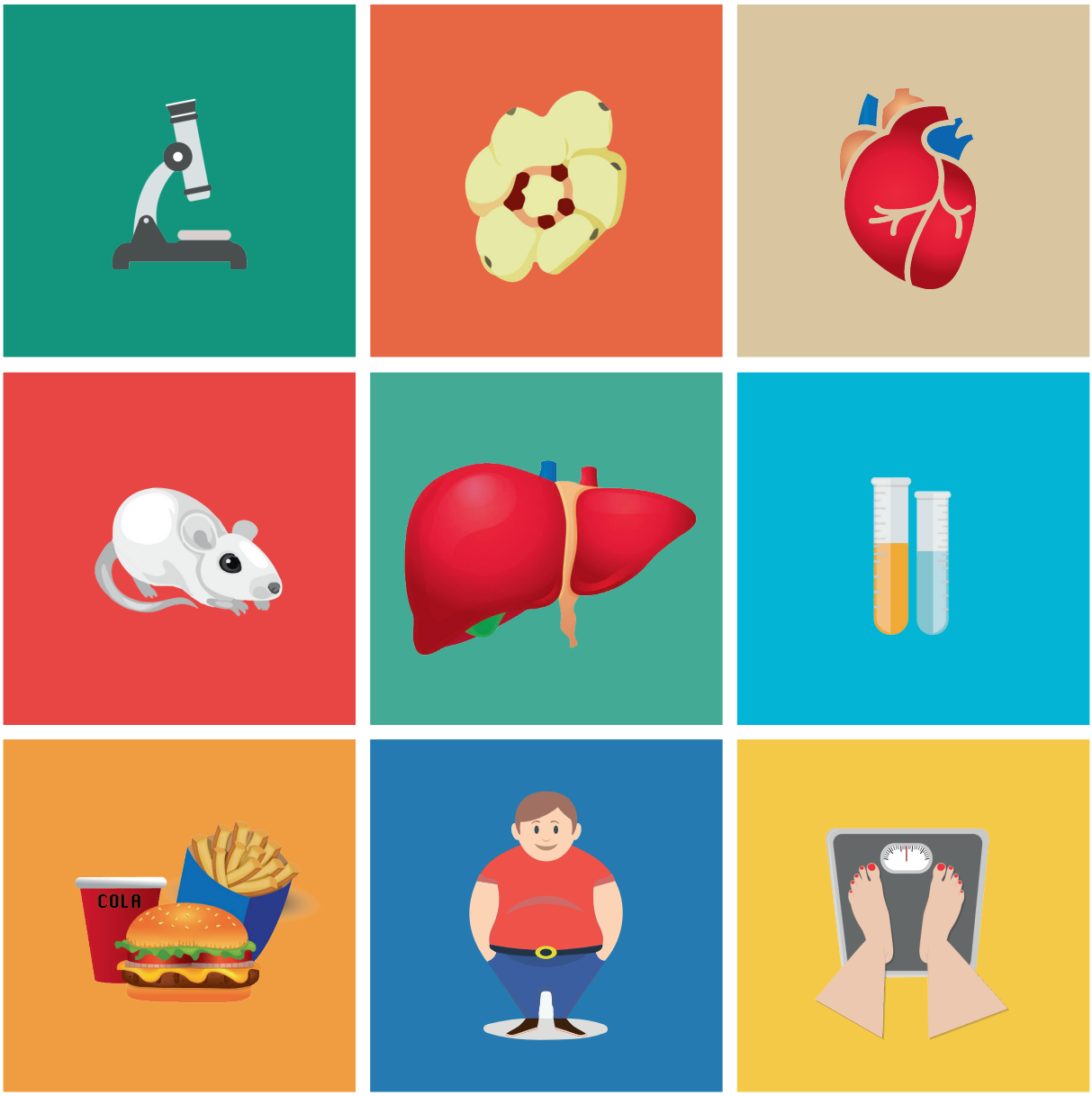
Universiteit Leiden



The handle http://hdl.handle.net/1887/46137 holds various files of this Leiden University dissertation

Author: Mulder, P.C.A.
Title: The contribution of metabolic and adipose tissue inflammation to non-alcoholic fatty liver disease
Issue Date: 2017-02-16

The contribution of metabolic and adipose tissue inflammation to non-alcoholic fatty liver disease



Petra Mulder

The contribution of metabolic and adipose tissue inflammation to non-alcoholic fatty liver disease

© P.C.A. Mulder, 2016
All rights reserved. No part of thesis may be reproduced, stored in a retrieval system or transmitted in any form or by any means without permission from the author or, when appropriate, permission from the publishers.

ISBN: 978-94-6233-486-1
Cover design: Fabian Mulder
Lay-out and printing: Gildeprint, Enschede

The printing of this thesis was kindly supported by:
TNO, Metabolic health Research
Daan Traas fonds

The studies presented in this thesis were performed at the Gaubius Laboratory of TNO, Leiden, The Netherlands. The research was supported by the TNO research programs 'Predictive Health Technologies' and 'Enabling Technology Systems Biology'.

The contribution of metabolic and adipose tissue inflammation to non-alcoholic fatty liver disease

Proefschrift

ter verkrijging van
de graad van doctor aan de Universiteit Leiden,
op gezag van Rector Magnificus prof. mr. C.J.J.M. Stolker,
volgens besluit van het College voor Promoties
te verdedigen op donderdag 16 februari 2017
klokke 16.15 uur

door

Petra Catharina Anne Mulder

geboren te Groningen
in 1987

Promotor

Prof. Dr. J.H. van Bockel

Copromotor

Dr. R. Kleemann

Promotiecommissie

Prof. Dr. Ir. L.M. Havekes

Prof. Dr. Y.M. Smulders (VUmc, Amsterdam)

Dr. J. Verheij (AMC, Amsterdam)

Only the most wise and the most foolish do not change

— Confucius (The analects of Confucius translated by A. Charles Muller, 1990)

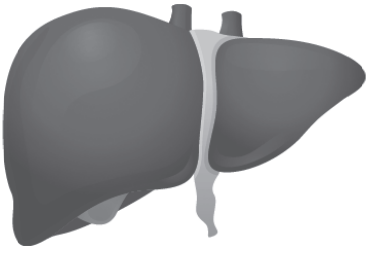
TABLE OF CONTENTS

Chapter 1	General introduction	9
Chapter 2	Surgical removal of inflamed epididymal white adipose tissue attenuates non-alcoholic steatohepatitis in obesity	29
Chapter 3	Reduction of obesity-associated white adipose tissue inflammation by rosiglitazone is associated with reduced non-alcoholic fatty liver disease in LDLr-deficient mice	55
Chapter 4	Intervention with the CCR2 inhibitor propagermanium attenuates diet-induced insulin resistance, adipose tissue inflammation and non-alcoholic steatohepatitis	89
Chapter 5	Intervention with a caspase-1 inhibitor reduces obesity-associated hyperinsulinemia, non-alcoholic steatohepatitis (NASH) and hepatic fibrosis in LDLr-/-.Leiden mice	115
Chapter 6	Replacement of dietary saturated fat by PUFA-rich pumpkin seed oil attenuates non-alcoholic fatty liver disease and atherosclerosis development, with additional health effects of virgin over refined oil	135
Chapter 7	Macrovesicular steatosis is associated with development of lobular inflammation and fibrosis in diet-induced non-alcoholic steatohepatitis (NASH)	165
Chapter 8	Summary and general discussion	183
Chapter 9	Nederlandse samenvatting	207
Appendices	List of publications	215
	Curriculum Vitae	216
	Dankwoord	219

Chapter 1

General introduction







Current lifestyle trends in modern society, characterized by excess energy consumption and reduced physical activity have propelled the incidence of obesity to epidemic proportions [1]. Obesity is associated with increased risk for type 2 diabetes (T2D) and comorbidities, including non-alcoholic fatty liver disease (NAFLD) [2].

NAFLD is a metabolic disorder characterized by fat accumulation in the liver in the absence of chronic alcohol consumption [3]. Clinically, NAFLD encompasses a broad spectrum of liver conditions ranging from fat accumulation (steatosis) to steatosis with inflammation (non-alcoholic steatohepatitis, NASH), which can further progress to fibrosis, cirrhosis and ultimately to hepatocellular carcinoma [4]. Patients with NAFLD are at risk to develop other metabolic complications such as cardiovascular disease (CVD) [5-7] and have a higher overall mortality [7,8].

1. PREVALENCE AND DIAGNOSIS OF NAFLD

Recent estimates suggest that NAFLD is present in 30% of the general population [2,9,10]. NAFLD is tightly linked to obesity as recent estimates suggest that up to 90% of obese patients have NAFLD [11]. Furthermore, the presence of the metabolic syndrome (defined as central obesity accompanied by two or more of the following metabolic risk factors: elevated fasting glucose concentration (reflecting insulin resistance), hypertension, raised triglyceride (TG) levels and lowered high-density lipoprotein cholesterol (HDL) levels), is associated with more progressive disease [12].

NAFLD is often an asymptomatic disease and the majority of patients with NAFLD are identified by increased liver enzymes (alanine aminotransferase, ALT; aspartate aminotransferase, AST) during a routine blood test [13]. Although liver enzymes (i.e. ALT) levels have shown to be a good predictor of hepatic steatosis [14], ALT levels can be found normal in patients with severe liver pathology [15]. While steatosis can be diagnosed by non-invasive imaging, such as ultrasound and magnetic resonance imaging (MRI), none of these techniques can detect inflammation. Consequently, invasive liver biopsy is currently the gold-standard for

diagnosing the advanced stages of NAFLD (NASH and fibrosis) as well as monitoring disease progression [16]. Differentiating NASH from simple steatosis is important, because longitudinal studies have shown that patients with steatosis have similar life expectancy to that of the general population of same age and sex [17], while NASH patients have significantly higher total mortality rates [8]. Moreover, the degree of fibrosis in NASH patients is associated with a higher risk of liver-related morbidity and mortality [7,18].

1.1 Pathophysiology of NAFLD

1.1.1 Histopathology

A distinct hallmark of NAFLD is steatosis, a histological manifestation of fat deposition in the form of triglycerides within hepatocytes [4]. Morphologically, steatosis can manifest in two forms of lipid accumulation, i.e. macrovesicular or microvesicular steatosis. In macrovesicular steatosis, hepatocytes contain a large, single vacuole of fat which fills the cytoplasm and displaces the nucleus to the periphery (see [19] and references therein) (figure 1). By contrast, hepatocytes with microvesicular steatosis contain many small lipid droplets in the cytoplasm [19] (figure 1).

The histological features of NASH include steatosis, hepatocellular injury (usually characterized by hepatocellular ballooning), and lobular inflammation [20] (figure 1). Hepatocellular ballooning refers to swelling of hepatocytes with rarefied cytoplasm and is associated with cytoskeletal injury [21]. The ballooning hepatocytes are mainly located near steatotic hepatocytes and are often, but not always, associated with perisinusoidal fibrosis. Lobular inflammation in NASH is characterized by the presence of inflammatory aggregates, which are typically composed of a mixture of innate and adaptive immune cells, such as neutrophils, lymphocytes and macrophages [22].

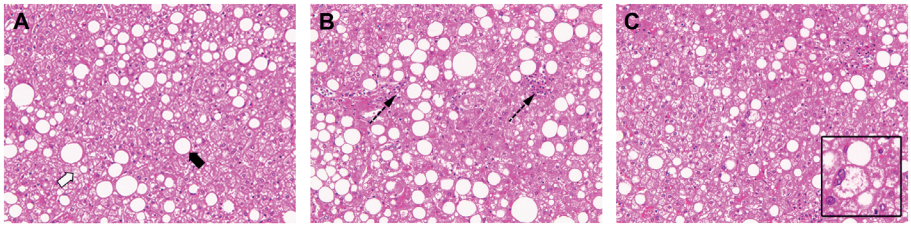


Figure 1. Histological subtypes of human NAFLD. Histological cross-sections of human liver stained with hematoxylin-eosin showing (A) Simple steatosis, predominantly in the form of macrovesicular steatosis (closed arrow) and some microvesicular steatosis (open arrow). (B) Non-alcoholic steatohepatitis (NASH) characterized by steatosis with lobular inflammation (dashed line arrow). (C) NASH characterized by the additional presence of hepatocellular ballooning (insert, magnification x400). (Unless specified otherwise, microphotographs: magnification x200).

1.1.2 Grading and staging of disease

Besides the diagnostic purpose, a liver biopsy is frequently used to assess the severity of disease. In 2005, the NASH Clinical Research Network developed and validated a semiquantitative scoring system for the evaluation of serial biopsies from NAFLD patients in clinical trials [20]. This scoring system, also called NAFLD Activity Score (NAS), unifies important features of NASH into an activity score or a "grade". This grade can range from a score 0 to 8, which consists of the summation of individual scores for steatosis (0-3), lobular inflammation (0-3), and hepatocellular ballooning (0-2). NAS of 1 or 2 indicates no NASH, while a NAS score of 5-8 corresponds to definite NASH. Activity scores 3 and 4 are noted as borderline cases of NASH, as these scores do not fulfill the pathologists' criteria for definite NASH. The scoring system was extended by a fibrosis score or the "stage" of disease, which reflects the unique patterns of fibrosis that can occur in NASH.

Despite the widespread use of NAS in preclinical NAFLD models, this scoring system has never been validated for experimental rodent samples. Therefore, a generic NAFLD grading system for preclinical (mouse) models has been developed based on the human NAS scoring system [23]. Furthermore, with this scoring method for rodents, the individual components of NASH (e.g. number of inflammatory cells) are analyzed on a continuous scale making it possible to investigate more subtle effects of treatments.

1.2 Etiology of disease

Although obesity and insulin resistance has been established as risk factors for NAFLD, the underlying mechanisms that contribute to disease progression from simple steatosis to NASH remain unclear.

The initial stage of NAFLD involves accumulation of fat, predominantly triglycerides, in the liver. The accumulation of fat may be the result of an imbalance between fatty acid transport, synthesis and oxidation or a combination of these factors. Originally, the pathogenesis of NASH was conceptualized as a disease of 'two-hits': the 'first hit', hepatic fat accumulation, sensitized the liver to a 'second hit' which caused tissue injury, inflammation and fibrosis [24]. A number of factors, including pro-inflammatory cytokines, endotoxins, adipokines, mitochondrial dysfunction, oxidative stress and subsequent lipid peroxidation, have been proposed as the second hit [25]. However, inflammatory cytokines such as IL-1β or endotoxin (LPS) that were superimposed on a high-fat diet (HFD) for several weeks failed to induce NASH in experimental models of disease, while metabolic triggers of inflammation (e.g. cholesterol, carbohydrates) caused NASH [26]. However, it is thought that the etiology of NASH is a more complex process and may involve specific metabolic factors, i.e. lipids, that trigger liver injury and disease progression.

The involvement of lipids in the pathogenesis of NASH has led to the concept of 'lipotoxicity', which implies that exposure to, or accumulation of, certain lipids within hepatic cells may directly cause cellular toxicity or act in a pro-inflammatory manner [27]. NASH is associated with two defects that can lead to lipotoxicity: (1) increased delivery of free fatty acids (FFA) to the liver caused by uninhibited lipolysis in insulin-resistant white adipose tissue [28]; and (2) the formation of cholesterol crystals within the lipid droplets of steatotic hepatocytes that can cause lipotoxic injury within these cells [27,29]. The role of white adipose tissue and cholesterol in NASH will be discussed in more detail in the following sections.

1.2.1 The role of white adipose tissue in liver pathology

The principal function of white adipose tissue (WAT) is to store and release fat in response to energy needs. In obesity, WAT mass is expanding in response to excess energy. However, this expansion may be limited, resulting in lipid accumulation in

other organs throughout the body (ectopic fat) [30]. It is hypothesized that ectopic hepatic fat accumulation observed in NAFLD could be due to increased delivery of free fatty acids (FFA) from adipose tissue. In support of this, studies in humans have demonstrated that increased FFA delivery from WAT is a significant source for lipids in the liver [28,31]. Excess FFA, rather than triglyceride accumulation, may result in lipotoxicity in the liver by activating inflammatory and oxidative stress related pathways [32]. Saturated fatty acids, such as palmitic acid, are poorly incorporated into triglycerides and have been shown to cause apoptosis in hepatocytes in vitro [33,34]. By contrast, specific monounsaturated fatty acids (e.g. oleic acid) are thought to have a protective role against palmitic acid-induced apoptosis by promoting incorporation of palmitic acid into triglycerides [33]. When triglyceride accumulation is impaired, free fatty acids may no longer be safely incorporated into triglyceride pools, leading the buildup of lipotoxic metabolites that can cause liver injury and trigger NASH development [32,35].

In insulin-resistant patients, FFA plasma levels are often found to be elevated possibly due to uncontrolled lipolysis in WAT and lead to increased FA flux to the liver [36]. A key mechanism in the pathogenesis of obesity-associated insulin resistance relates to WAT inflammation, which has been well demonstrated in experimental and human studies (reviewed in e.g. [37]). This WAT inflammation is characterized by infiltration of adipose tissue macrophages [38]. These infiltrating macrophages may secrete inflammatory mediators, including the pro-inflammatory cytokine Tumour-Necrosis Factor-alpha (TNFα), which contributes to a local chronic inflammatory state characterized by impaired fat deposition and increased lipolysis in WAT [39].

Although obesity is strongly associated with metabolic complications, the distribution of fat appears more important than the total amount of fat mass per se. Increased intra-abdominal fat, but not subcutaneous fat, has been positively associated with insulin resistance [40] and contributes to increased FFA flux towards the liver in insulin-resistant individuals [31]. Furthermore, intra-abdominal fat mass strongly correlates with liver inflammation and fibrosis, whereas the amount of subcutaneous fat is not associated with histological changes in the liver [40].

Not only the distribution of fat mass in particular WAT depots may be of importance in NASH development, evidence also points to a role of the inflammatory state of WAT [41]. For instance, longitudinal studies in rodents demonstrated that HFD-induced expression of inflammatory genes in WAT precedes the development of NASH in obesity [42,43]. Furthermore, Cancello and colleagues [44] have shown that obese humans with inflamed intra-abdominal WAT have more fibro-inflammatory lesions in the liver than equally obese subjects without WAT inflammation. It is postulated that inflammation in WAT results in increased production of pro-inflammatory cytokines and adipokines (e.g. TNFα, leptin) and decreased production of protective adipokines (adiponectin) [45]. This imbalance in adipokines is thought to contribute to the development of NASH. Although evidence suggests that WAT constitutes an important source of inflammation in NAFLD, experimental proof for a causal role of WAT in NASH is still lacking.

1.2.2 The role of dietary cholesterol in liver pathology

Growing evidence suggest that cholesterol is a critical factor in the development of NASH. Data from epidemiological studies link dietary cholesterol intake to the risk and severity of NAFLD [46,47]. In line with this, expression of inflammatory genes were increased in livers of mice fed a high-cholesterol diet (1% w/w) but not with a lower concentration (0.25% w/w) [48]. Other experimental studies have shown that dietary cholesterol negatively affect the balance between storage and oxidation of fatty acids in the liver [49] and can lead to oxidative stress and hepatic inflammation [50]. Furthermore, increased levels of hepatic free cholesterol are observed in experimental [29,51-53] and human NASH [29,54,55], while lowering of excess hepatic free cholesterol levels improved liver disease severity [27,53,56,57]. Mechanistic studies have shown that free cholesterol accumulation in the liver can promote inflammation and fibrogenesis through the activation of intracellular signaling pathways in hepatic resident macrophages (Kupffer cells) [27] and hepatic stellate cells [58]. However, other studies in mice using dietary cholesterol have shown that hepatic inflammation can develop without steatosis [52] and obesity [59]. Furthermore, cholesterol-induced hepatic inflammation did not contribute to the development of insulin resistance in male LDLr-/-mice [60]

and addition of cholesterol to a high-fat diet (HFD) can protect from HFD-induced insulin resistance in mice (Hanemaaijer, Pieterman unpublished results). These data suggest that dietary cholesterol contributes to NASH development that is independent of insulin resistance.

1.2.3 Inflammatory processes in liver during NASH

Chronic inflammation in the liver is critical in the progression of NAFLD. Activation of the innate immune system – the body's rapid first-line defense against pathogens – is a key component in initiating and for sustaining inflammation in the liver [61]. Innate immune cells recognize pathogen invasion with intracellular or surface-expressed pattern recognition receptors (PRRs) by detecting pathogen-associated molecular patterns (PAMPs). These PRRs are also able to detect endogenous damage and stress signals through damage-associated molecular patterns (DAMPS). Importantly, the DAMP-associated immune response occurs in absence of pathogens and is referred to as 'sterile inflammation', which can occur in all tissues in response to injury and cellular damage. It is thought that metabolic overload (i.e. surplus of energy or macronutrients) triggers this 'sterile' or so-called 'metabolic inflammation' in metabolic diseases. However, underlying mechanisms controlling the inflammatory processes in NASH development remain poorly understood.

Kupffer cells are the primary sensors of PAMPs and DAMPs and considered key players in the pathogenesis of NASH, as depletion of these cells in mice results in resistance to develop hepatic steatosis, inflammation and fibrosis [62,63]. Specifically, the dysregulation between pro-inflammatory macrophages (M1) and anti-inflammatory macrophages (M2) is emerging as a central mechanism driving inflammation [64]. During NASH development, activation of Kupffer cells by inflammatory factors (e.g. FFA) may shift their phenotype towards a pro-inflammatory M1 state. Activation of Kupffer cells may also govern the recruitment of blood–derived monocytes/macrophages during NASH. Both, Kupffer cells and recruited macrophages enhance local inflammation and produce inflammatory mediators (e.g. TNFα, IL-1β) which, in turn, can further stimulate hepatocytes and stellate cells to induce steatosis and fibrosis, respectively [65].

Evidence suggests that recruitment of macrophages into the liver is primarily promoted by monocyte chemotactic protein-1 (MCP-1), a chemokine that is upregulated in livers of NASH patients [66]. In turn, MCP-1 drives the recruitment of C–C chemokine receptor 2 (CCR2) expressing monocytes into the liver. Genetic deletion of MCP-1 or CCR2 has been shown to reduce steatosis and macrophage infiltration in livers of mice [67,68], suggesting that interventions directed at CCR2 can represent an potential target for the treatment of NASH.

Inflammasomes have emerged as an important component of Kupffer cell activation and NAFLD progression. The inflammasome is a protein complex that consists of an intracellular sensor molecule (the NLR), an adaptor sensor protein (ASC) and the effector protein caspase-1 [69]. One of the best characterized inflammasomes is the NLR family pyrin domain-containing 3 (NLRP3) inflammasome. NLRP3 complex becomes activated in response to PAMPs or DAMPs, which results in the maturation of pro-caspase-1 into activated caspase-1. Activated caspase-1 cleaves the precursors of pro-inflammatory cytokines IL-1β and IL-18 into their biologically active counterparts, which are then readily secreted from the cells and initiate an inflammatory response [69]. Experimental studies have shown that knockdown of NLRP3-associated genes (i.e. ASC, NLRP3 or Caspase-1) in HFD-fed mice attenuates obesity-associated inflammation and reduces the development of metabolic complications, including insulin resistance [70,71] and NAFLD [72], suggesting that the NLRP3 inflammasome constitutes a potential target for therapeutic intervention in NASH.

1.3 NAFLD and CVD

Accumulating evidence suggest that patients with NAFLD have a 2-fold higher risk in developing CVD [5-7]. In line with this, NAFLD is associated with atherosclerosis development [73], the underlying pathology of CVD. However, the biological mechanisms linking NAFLD and CVD are still poorly understood.

Patients with NAFLD frequently have a disturbed lipid profile characterized by high triglyceride levels, increased (very) low-density lipoprotein ((V)LDL) cholesterol levels and decreased levels HDL cholesterol [5]. This unfavorable lipid profile drives atherosclerosis development and can, for instance, be the result of increased

hepatic production of triglyceride-rich VLDL to reduce metabolic overload in the liver [74].

Atherosclerosis is increasingly being considered an inflammatory disease in which the liver is thought to be a central mediator in the regulation of inflammation. Support for an atherogenic role of liver inflammation in humans comes from the observation that CVD risk is greater in NASH patients compared to subjects with simple steatosis [75]. Several studies suggest that increased production of pro-inflammatory factors by the liver play an important role in the pathogenesis of atherosclerosis (reviewed in [76,77]). Among them are markers of systemic inflammation, such as cytokines (e.g. IL-6 and TNFα) and acute-phase proteins (e.g. Serum Amyloid A (SAA), fibrinogen).

1.4 Treatments of NAFLD

1.4.1 Lifestyle intervention

Despite its prevalence, treatment options for NAFLD are limited. The recommended mainstay treatment for the majority of NAFLD patients is lifestyle modification (diet and/or increased physical activity) to induce weight loss. Recent studies have shown that reduced energy intake and increased physical activity induces weight loss and improves insulin resistance, liver enzymes, and hepatic fat content [78,79]. Lifestyle modification can also result in improved NAS score in NASH patients [80-82]. More specifically, these studies showed a significant reduction in steatosis grade, but most of them concluded that 7% to 10% weight loss is required for the improvement of hepatic inflammation, hepatocellular ballooning [81,82] and fibrosis [83].

Exercise alone can also improve hepatic fat content and insulin resistance in obese patients [84]. In addition, performing exercise has shown to reduce the likelihood of having NASH by a third [85], but whether exercise affects liver histopathology in NAFLD patients has not been reported so far.

It is important to note that weight loss is seldom maintained in many patients, because (low-caloric) diets and/or physical exercise are often discontinued [86]. In patients who failed to implement lifestyle changes, pharmacological treatments directed at improving NASH might be necessary.

1.4.2 Insulin sensitizers

Current pharmacological treatments of NAFLD aim at modifying risk factors. Insulin resistance is closely associated with NASH, therefore most therapeutic trials have focused on the effect of insulin sensitizers. In particular, the oral antidiabetic drugs thiazolidinediones (TZDs) have been intensively studied in patients with NASH [87,88].

An open label trial of rosiglitazone in 26 biopsy-proven NASH patients [89] and two placebo-controlled trials with pioglitazone [89,90] demonstrated improvements in liver enzymes as well as NAS score during 48 weeks of treatment. A recent meta-analysis of 4 randomized, placebo-controlled clinical trials also confirmed that both, rosiglitazone and pioglitazone significantly improve steatosis, ballooning, lobular inflammation while the effects on fibrosis were less clear [91]. However, the underlying mechanisms mediating the beneficial effects of TZDs in NASH development remain unclear.

TZDs improve insulin sensitivity by acting as selective agonists of the nuclear peroxisome proliferator-activated receptor (PPAR)-γ [92]. PPARγ is predominantly expressed in adipose tissue where it controls inflammatory and metabolic processes [37], suggesting that TZDs exert their hepatoprotective effects via WAT.

The side effects of TZDs however are of great concern, in particular weight gain, which tend to persist after discontinuation of the treatment [86]. Furthermore, the long-term safety of glitazones has been debated concerning the increased risk for cardiovascular events [93]. Hence, rosiglitazone was withdrawn from the market in September 2010. In November 2013, the U.S. Food and Drug Administration (FDA) has lifted its earlier restrictions for the use of rosiglitazone, as recent data did not show increased risk of heart attack compared to the standard type 2 diabetes medicines, such as metformin [94].

1.4.3 Nutritional interventions

Epidemiological studies show that diet is an important determinant for the risk of both NAFLD and associated comorbidities [95-97]. In particular the intake of saturated fatty acids (SFA) is associated with a greater risk of NAFLD [98]. Other studies in patients further support this association, reporting that NAFLD patients

have a higher intake of SFA, fructose and cholesterol with lowered consumption of polyunsaturated fatty acids, fibers, and antioxidants [46,98]. Although it is thought that caloric restriction is most important for improvement of NAFLD [19,99], evidence suggest that modulating the composition of the diet can also be of importance [100]. Data from a recent randomized controlled trial showed that a Mediterranean diet, which is rich in monounsaturated (MUFA) and polyunsaturated fatty acids (PUFA), can reduce liver fat content and improve hepatic insulin resistance, independent of the observed weight loss effect [101]. Supplementation of MUFA and/or PUFA is currently investigated as a potential treatment against NAFLD [100,102,103]. Increased MUFA intake, particularly as a replacement for SFA, is associated with decreased insulin resistance and hepatic steatosis [101]. Others have shown that omega-3 PUFA administration to patients with NAFLD can have beneficial effects on liver enzymes and hepatic steatosis [104,105] and may also improve hepatic inflammation and fibrosis [105]. Despite these encouraging data about the efficacy of PUFAs as a treatment of NAFLD in humans, they have been limited by small sample sizes, lack of randomization or placebo arms. Hence, further studies are needed to assess the feasibility and benefits of such alimentary interventions. Nevertheless, these data suggest that a switch in the type of fat consumed or supplementation of specific fatty acids could be of interest as a treatment to reduce metabolic complications.

1.5 Outline of this thesis

NAFLD is a complex disease, in which the origin and molecular mechanisms controlling the progression of simple steatosis to NASH remain poorly understood. The aim of this thesis is to provide more insight in the mechanisms underlying NAFLD progression, focusing on the role of WAT and specific aspects that can trigger metabolic inflammation.

The first part of this thesis focuses on the link between WAT and liver, in which we studied the potential role of WAT in NASH development (**Chapter 2**). As obesity-induced inflammation in WAT is thought to be critical in NASH development, we first examined the sequence of inflammatory events in different WAT depots and liver in a time-course experiment in context of diet-induced obesity. In a subsequent

experiment, we examined whether WAT is causally involved in NASH development by surgical removal of a specific inflamed WAT depot. As WAT may constitute a new target for the treatment of NAFLD, we next examined whether intervention in WAT inflammation with rosiglitazone (a PPARγ activator) would attenuate NAFLD development (**Chapter 3**).

Chapter 4 and **chapter 5** focused on interventions directed at specific mediators in metabolic inflammation to study whether these interventions can attenuate the development of NAFLD. More specifically, we studied the therapeutic effect of a CCR2 inhibitor (**chapter 4**) and inflammasome inhibition, using a caspase-1 inhibitor, (**chapter 5**) on NAFLD development in context of manifest insulin resistance and WAT inflammation.

In **chapter 6**, we examined the potential of a distinct nutritional strategy to prevent the development of NAFLD, by changing the macronutrient composition of the diet to reduce metabolic overload. We investigated whether replacement of dietary saturated fat with pumpkin seed oil (rich in unsaturated fat) would attenuate NAFLD and atherosclerosis development. In addition, we examined whether phytochemicals present in unrefined (virgin) pumpkin seed oil exerts additional health effects over the refined oil.

Metabolic overload results in the increased fat deposition within the liver, however it is unclear whether a distinct type of fat storage i.e. macrovesicular or microvesicular steatosis, contributes to NAFLD progression. Therefore, in **chapter 7** we studied whether a potential relationship exists between the type of steatosis and the onset of hepatic inflammation in different experimental models of NASH that were also used in the previous chapters. Finally, the results obtained in the studies described herein and their implications are discussed in **chapter 8**.

REFERENCES

1. Hurt RT, Kulisek C, Buchanan LA, McClave SA. The obesity epidemic: challenges, health initiatives, and implications for gastroenterologists. Gastroenterology & hepatology 2010;6:780-792.
2. Marchesini G, Bugianesi E, Forlani G, Cerrelli F, Lenzi M, Manini R, et al. Nonalcoholic fatty liver, steatohepatitis, and the metabolic syndrome. Hepatology 2003;37:917-923.
3. Chalasani N, Younossi Z, Lavine JE, Diehl AM, Brunt EM, Cusi K, et al. The diagnosis and management of non-alcoholic fatty liver disease: Practice guideline by the American Association for the Study of Liver Diseases, American College of Gastroenterology, and the American Gastroenterological Association. The American journal of gastroenterology 2012;107:811-826.
4. Tiniakos DG, Vos MB, Brunt EM. Nonalcoholic fatty liver disease: pathology and pathogenesis. Annual review of pathology 2010;5:145-171.
5. Bhatia LS, Curzen NP, Calder PC, Byrne CD. Non-alcoholic fatty liver disease: a new and important cardiovascular risk factor? European heart journal 2012;33:1190-1200.
6. Armstrong MJ, Adams LA, Canbay A, Syn WK. Extrahepatic complications of nonalcoholic fatty liver disease. Hepatology 2014;59:1174-1197.
7. Adams LA, Lymp JF, St Sauver J, Sanderson SO, Lindor KD, Feldstein A, et al. The natural history of nonalcoholic fatty liver disease: a population-based cohort study. Gastroenterology 2005;129:113-121.
8. Angulo P. Long-term mortality in nonalcoholic fatty liver disease: is liver histology of any prognostic significance? Hepatology 2010;51:373-375.
9. Williams CD, Stengel J, Asike MI, Torres DM, Shaw J, Contreras M, et al. Prevalence of nonalcoholic fatty liver disease and nonalcoholic steatohepatitis among a largely middle-aged population utilizing ultrasound and liver biopsy: a prospective study. Gastroenterology 2011;140:124-131.
10. Loomba R, Sanyal AJ. The global NAFLD epidemic. Nature reviews Gastroenterology & hepatology 2013;10:686-690.
11. Vernon G, Baranova A, Younossi ZM. Systematic review: the epidemiology and natural history of non-alcoholic fatty liver disease and non-alcoholic steatohepatitis in adults. Alimentary pharmacology & therapeutics 2011;34:274-285.
12. Rinella ME. Nonalcoholic fatty liver disease: a systematic review. Jama 2015;313:2263-2273.
13. Armstrong MJ, Houlihan DD, Bentham L, Shaw JC, Cramb R, Olliff S, et al. Presence and severity of non-alcoholic fatty liver disease in a large prospective primary care cohort. Journal of hepatology 2012;56:234-240.
14. Kotronen A, Westerbacka J, Bergholm R, Pietilainen KH, Yki-Jarvinen H. Liver fat in the metabolic syndrome. The Journal of clinical endocrinology and metabolism 2007;92:3490-3497.
15. Mofrad P, Contos MJ, Haque M, Sargeant C, Fisher RA, Luketic VA, et al. Clinical and histologic spectrum of nonalcoholic fatty liver disease associated with normal ALT values. Hepatology 2003;37:1286-1292.
16. Wieckowska A, McCullough AJ, Feldstein AE. Noninvasive diagnosis and monitoring of nonalcoholic steatohepatitis: present and future. Hepatology 2007;46:582-589.
17. Dam-Larsen S, Franzmann M, Andersen IB, Christoffersen P, Jensen LB, Sorensen TI, et al. Long term prognosis of fatty liver: risk of chronic liver disease and death. Gut 2004;53:750-755.

18. Ekstedt M, Hagstrom H, Nasr P, Fredrikson M, Stal P, Kechagias S, et al. Fibrosis stage is the strongest predictor for disease-specific mortality in NAFLD after up to 33 years of follow-up. Hepatology 2015;61:1547-1554.
19. Green CJ, Hodson L. The influence of dietary fat on liver fat accumulation. Nutrients 2014;6:5018-5033.
20. Kleiner DE, Brunt EM, Van Natta M, Behling C, Contos MJ, Cummings OW, et al. Design and validation of a histological scoring system for nonalcoholic fatty liver disease. Hepatology 2005;41:1313-1321.
21. Caldwell S, Ikura Y, Dias D, Isomoto K, Yabu A, Moskaluk C, et al. Hepatocellular ballooning in NASH. Journal of hepatology 2010;53:719-723.
22. Farrell GC, van Rooyen D, Gan L, Chitturi S. NASH is an Inflammatory Disorder: Pathogenic, Prognostic and Therapeutic Implications. Gut and liver 2012;6:149-171.
23. Liang W, Menke AL, Driessen A, Koek GH, Lindeman JH, Stoop R, et al. Establishment of a general NAFLD scoring system for rodent models and comparison to human liver pathology. PloS one 2014;9:e115922.
24. Day CP, James OF. Steatohepatitis: a tale of two "hits"? Gastroenterology 1998;114:842-845.
25. Tilg H, Moschen AR. Evolution of inflammation in nonalcoholic fatty liver disease: the multiple parallel hits hypothesis. Hepatology 2010;52:1836-1846.
26. Liang W, Lindeman JH, Menke AL, Koonen DP, Morrison M, Havekes LM, et al. Metabolically induced liver inflammation leads to NASH and differs from LPS- or IL-1beta-induced chronic inflammation. Laboratory investigation; a journal of technical methods and pathology 2014;94:491-502.
27. Ioannou GN, Van Rooyen DM, Savard C, Haigh WG, Yeh MM, Teoh NC, et al. Cholesterol-lowering drugs cause dissolution of cholesterol crystals and disperse Kupffer cell crown-like structures during resolution of NASH. Journal of lipid research 2015;56:277-285.
28. Donnelly KL, Smith CI, Schwarzenberg SJ, Jessurun J, Boldt MD, Parks EJ. Sources of fatty acids stored in liver and secreted via lipoproteins in patients with nonalcoholic fatty liver disease. The Journal of clinical investigation 2005;115:1343-1351.
29. Ioannou GN, Haigh WG, Thorning D, Savard C. Hepatic cholesterol crystals and crown-like structures distinguish NASH from simple steatosis. Journal of lipid research 2013;54:1326-1334.
30. Virtue S, Vidal-Puig A. It's not how fat you are, it's what you do with it that counts. PLoS Biol 2008;6:e237.
31. Nielsen S, Guo Z, Johnson CM, Hensrud DD, Jensen MD. Splanchnic lipolysis in human obesity. The Journal of clinical investigation 2004;113:1582-1588.
32. Neuschwander-Tetri BA. Hepatic lipotoxicity and the pathogenesis of nonalcoholic steatohepatitis: the central role of nontriglyceride fatty acid metabolites. Hepatology 2010;52:774-788.
33. Listenberger LL, Han X, Lewis SE, Cases S, Farese RV, Jr., Ory DS, et al. Triglyceride accumulation protects against fatty acid-induced lipotoxicity. Proceedings of the National Academy of Sciences of the United States of America 2003;100:3077-3082.
34. Wei Y, Wang D, Topczewski F, Pagliassotti MJ. Saturated fatty acids induce endoplasmic reticulum stress and apoptosis independently of ceramide in liver cells. American journal of physiology Endocrinology and metabolism 2006;291:E275-281.
35. Sahini N, Borlak J. Recent insights into the molecular pathophysiology of lipid droplet formation in hepatocytes. Progress in lipid research 2014;54:86-112.
36. Lomonaco R, Ortiz-Lopez C, Orsak B, Webb A, Hardies J, Darland C, et al. Effect of adipose tissue insulin resistance on metabolic parameters and liver histology in obese patients with nonalcoholic fatty liver disease. Hepatology 2012;55:1389-1397.

37. Shoelson SE, Lee J, Goldfine AB. Inflammation and insulin resistance. The Journal of clinical investigation 2006;116:1793-1801.
38. Weisberg SP, McCann D, Desai M, Rosenbaum M, Leibel RL, Ferrante AW, Jr. Obesity is associated with macrophage accumulation in adipose tissue. The Journal of clinical investigation 2003;112:1796-1808.
39. Olefsky JM, Glass CK. Macrophages, inflammation, and insulin resistance. Annual review of physiology 2010;72:219-246.
40. van der Poorten D, Milner KL, Hui J, Hodge A, Trenell MI, Kench JG, et al. Visceral fat: a key mediator of steatohepatitis in metabolic liver disease. Hepatology 2008;48:449-457.
41. Mirza MS. Obesity, Visceral Fat, and NAFLD: Querying the Role of Adipokines in the Progression of Nonalcoholic Fatty Liver Disease. ISRN gastroenterology 2011;2011:592404.
42. Duval C, Thissen U, Keshtkar S, Accart B, Stienstra R, Boekschoten MV, et al. Adipose tissue dysfunction signals progression of hepatic steatosis towards nonalcoholic steatohepatitis in C57BL/6 mice. Diabetes 2010;59:3181-3191.
43. Liang W, Tonini G, Mulder P, Kelder T, van Erk M, van den Hoek AM, et al. Coordinated and interactive expression of genes of lipid metabolism and inflammation in adipose tissue and liver during metabolic overload. PloS one 2013;8:e75290.
44. Cancello R, Tordjman J, Poitou C, Guilhem G, Bouillot JL, Hugol D, et al. Increased infiltration of macrophages in omental adipose tissue is associated with marked hepatic lesions in morbid human obesity. Diabetes 2006;55:1554-1561.
45. Tilg H, Moschen AR. Adipocytokines: mediators linking adipose tissue, inflammation and immunity. Nature reviews Immunology 2006;6:772-783.
46. Musso G, Gambino R, De Michieli F, Cassader M, Rizzetto M, Durazzo M, et al. Dietary habits and their relations to insulin resistance and postprandial lipemia in nonalcoholic steatohepatitis. Hepatology 2003;37:909-916.
47. Yasutake K, Nakamuta M, Shima Y, Ohyama A, Masuda K, Haruta N, et al. Nutritional investigation of non-obese patients with non-alcoholic fatty liver disease: the significance of dietary cholesterol. Scandinavian journal of gastroenterology 2009;44:471-477.
48. Kleemann R, Verschuren L, van Erk MJ, Nikolsky Y, Cnubben NH, Verheij ER, et al. Atherosclerosis and liver inflammation induced by increased dietary cholesterol intake: a combined transcriptomics and metabolomics analysis. Genome biology 2007;8:R200.
49. Kalaany NY, Gauthier KC, Zavacki AM, Mammen PP, Kitazume T, Peterson JA, et al. LXRs regulate the balance between fat storage and oxidation. Cell metabolism 2005;1:231-244.
50. Subramanian S, Goodspeed L, Wang S, Kim J, Zeng L, Ioannou GN, et al. Dietary cholesterol exacerbates hepatic steatosis and inflammation in obese LDL receptor-deficient mice. Journal of lipid research 2011;52:1626-1635.
51. Van Rooyen DM, Larter CZ, Haigh WG, Yeh MM, Ioannou G, Kuver R, et al. Hepatic free cholesterol accumulates in obese, diabetic mice and causes nonalcoholic steatohepatitis. Gastroenterology 2011;141:1393-1403, 1403 e1391-1395.
52. Wouters K, van Gorp PJ, Bieghs V, Gijbels MJ, Duimel H, Lutjohann D, et al. Dietary cholesterol, rather than liver steatosis, leads to hepatic inflammation in hyperlipidemic mouse models of nonalcoholic steatohepatitis. Hepatology 2008;48:474-486.
53. Morrison MC, Liang W, Mulder P, Verschuren L, Pieterman E, Toet K, et al. Mirtoselect, an anthocyanin-rich bilberry extract, attenuates non-alcoholic steatohepatitis and associated fibrosis in ApoE(*)3Leiden mice. Journal of hepatology 2015;62:1180-1186.

54. Puri P, Baillie RA, Wiest MM, Mirshahi F, Choudhury J, Cheung O, et al. A lipidomic analysis of nonalcoholic fatty liver disease. Hepatology 2007;46:1081-1090.
55. Caballero F, Fernandez A, De Lacy AM, Fernandez-Checa JC, Caballeria J, Garcia-Ruiz C. Enhanced free cholesterol, SREBP-2 and StAR expression in human NASH. Journal of hepatology 2009;50:789-796.
56. Zheng S, Hoos L, Cook J, Tetzloff G, Davis H, Jr., van Heek M, et al. Ezetimibe improves high fat and cholesterol diet-induced non-alcoholic fatty liver disease in mice. Eur J Pharmacol 2008;584:118-124.
57. Wielinga PY, Yakala GK, Heeringa P, Kleemann R, Kooistra T. Beneficial effects of alternate dietary regimen on liver inflammation, atherosclerosis and renal activation. PloS one 2011;6:e18432.
58. Teratani T, Tomita K, Suzuki T, Oshikawa T, Yokoyama H, Shimamura K, et al. A high-cholesterol diet exacerbates liver fibrosis in mice via accumulation of free cholesterol in hepatic stellate cells. Gastroenterology 2012;142:152-164 e110.
59. Sumiyoshi M, Sakanaka M, Kimura Y. Chronic intake of a high-cholesterol diet resulted in hepatic steatosis, focal nodular hyperplasia and fibrosis in non-obese mice. The British journal of nutrition 2010;103:378-385.
60. Funke A, Schreurs M, Aparicio-Vergara M, Sheedfar F, Gruben N, Kloosterhuis NJ, et al. Cholesterol-induced hepatic inflammation does not contribute to the development of insulin resistance in male LDL receptor knockout mice. Atherosclerosis 2014;232:390-396.
61. Kubes P, Mehal WZ. Sterile inflammation in the liver. Gastroenterology 2012;143:1158-1172.
62. Huang W, Metlakunta A, Dedousis N, Zhang P, Sipula I, Dube JJ, et al. Depletion of liver Kupffer cells prevents the development of diet-induced hepatic steatosis and insulin resistance. Diabetes 2010;59:347-357.
63. Neyrinck AM, Cani PD, Dewulf EM, De Backer F, Bindels LB, Delzenne NM. Critical role of Kupffer cells in the management of diet-induced diabetes and obesity. Biochem Biophys Res Commun 2009;385:351-356.
64. Marra F, Lotersztajn S. Pathophysiology of NASH: perspectives for a targeted treatment. Current pharmaceutical design 2013;19:5250-5269.
65. Ramadori G, Armbrust T. Cytokines in the liver. European journal of gastroenterology & hepatology 2001;13:777-784.
66. Haukeland JW, Damas JK, Konopski Z, Loberg EM, Haaland T, Goverud I, et al. Systemic inflammation in nonalcoholic fatty liver disease is characterized by elevated levels of CCL2. Journal of hepatology 2006;44:1167-1174.
67. Kanda H, Tateya S, Tamori Y, Kotani K, Hiasa K, Kitazawa R, et al. MCP-1 contributes to macrophage infiltration into adipose tissue, insulin resistance, and hepatic steatosis in obesity. The Journal of clinical investigation 2006;116:1494-1505.
68. Miura K, Yang L, van Rooijen N, Ohnishi H, Seki E. Hepatic recruitment of macrophages promotes nonalcoholic steatohepatitis through CCR2. American journal of physiology Gastrointestinal and liver physiology 2012;302:G1310-1321.
69. Guo H, Callaway JB, Ting JP. Inflammasomes: mechanism of action, role in disease, and therapeutics. Nat Med 2015;21:677-687.
70. Vandanmagsar B, Youm YH, Ravussin A, Galgani JE, Stadler K, Mynatt RL, et al. The NLRP3 inflammasome instigates obesity-induced inflammation and insulin resistance. Nat Med 2011;17:179-188.
71. Stienstra R, van Diepen JA, Tack CJ, Zaki MH, van de Veerdonk FL, Perera D, et al. Inflammasome is a central player in the induction of obesity and insulin resistance. Proceedings of the National Academy of Sciences of the United States of America 2011;108:15324-15329.

72. Henao-Mejia J, Elinav E, Jin C, Hao L, Mehal WZ, Strowig T, et al. Inflammasome-mediated dysbiosis regulates progression of NAFLD and obesity. Nature 2012;482:179-185.
73. Brea A, Mosquera D, Martin E, Arizti A, Cordero JL, Ros E. Nonalcoholic fatty liver disease is associated with carotid atherosclerosis: a case-control study. Arterioscler Thromb Vasc Biol 2005;25:1045-1050.
74. Fabbrini E, Sullivan S, Klein S. Obesity and nonalcoholic fatty liver disease: biochemical, metabolic, and clinical implications. Hepatology 2010;51:679-689.
75. Targher G, Bertolini L, Padovani R, Rodella S, Zoppini G, Zenari L, et al. Relations between carotid artery wall thickness and liver histology in subjects with nonalcoholic fatty liver disease. Diabetes care 2006;29:1325-1330.
76. Blake GJ, Ridker PM. Novel clinical markers of vascular wall inflammation. Circ Res 2001;89:763-771.
77. Targher G, Marra F, Marchesini G. Increased risk of cardiovascular disease in non-alcoholic fatty liver disease: causal effect or epiphenomenon? Diabetologia 2008;51:1947-1953.
78. Petersen KF, Dufour S, Befroy D, Lehrke M, Hendler RE, Shulman GI. Reversal of nonalcoholic hepatic steatosis, hepatic insulin resistance, and hyperglycemia by moderate weight reduction in patients with type 2 diabetes. Diabetes 2005;54:603-608.
79. Lazo M, Solga SF, Horska A, Bonekamp S, Diehl AM, Brancati FL, et al. Effect of a 12-month intensive lifestyle intervention on hepatic steatosis in adults with type 2 diabetes. Diabetes care 2010;33:2156-2163.
80. Eckard C, Cole R, Lockwood J, Torres DM, Williams CD, Shaw JC, et al. Prospective histopathologic evaluation of lifestyle modification in nonalcoholic fatty liver disease: a randomized trial. Therap Adv Gastroenterol 2013;6:249-259.
81. Huang MA, Greenson JK, Chao C, Anderson L, Peterman D, Jacobson J, et al. One-year intense nutritional counseling results in histological improvement in patients with non-alcoholic steatohepatitis: a pilot study. The American journal of gastroenterology 2005;100:1072-1081.
82. Vilar-Gomez E, Martinez-Perez Y, Calzadilla-Bertot L, Torres-Gonzalez A, Gra-Oramas B, Gonzalez-Fabian L, et al. Weight Loss Through Lifestyle Modification Significantly Reduces Features of Nonalcoholic Steatohepatitis. Gastroenterology 2015;149:367-378 e365; quiz e314-365.
83. Bacchi E, Negri C, Targher G, Faccioli N, Lanza M, Zoppini G, et al. Both resistance training and aerobic training reduce hepatic fat content in type 2 diabetic subjects with nonalcoholic fatty liver disease (the RAED2 Randomized Trial). Hepatology 2013;58:1287-1295.
84. Kistler KD, Brunt EM, Clark JM, Diehl AM, Sallis JF, Schwimmer JB, et al. Physical activity recommendations, exercise intensity, and histological severity of nonalcoholic fatty liver disease. The American journal of gastroenterology 2011;106:460-468; quiz 469.
85. Ratziu V, Goodman Z, Sanyal A. Current efforts and trends in the treatment of NASH. Journal of hepatology 2015;62:S65-75.
86. Ratziu V. Pharmacological agents for NASH. Nature reviews Gastroenterology & hepatology 2013;10:676-685.
87. Cusi K. Role of obesity and lipotoxicity in the development of nonalcoholic steatohepatitis: pathophysiology and clinical implications. Gastroenterology 2012;142:711-725 e716.
88. Neuschwander-Tetri BA, Brunt EM, Wehmeier KR, Oliver D, Bacon BR. Improved nonalcoholic steatohepatitis after 48 weeks of treatment with the PPAR-gamma ligand rosiglitazone. Hepatology 2003;38:1008-1017.

89. Belfort R, Harrison SA, Brown K, Darland C, Finch J, Hardies J, et al. A placebo-controlled trial of pioglitazone in subjects with nonalcoholic steatohepatitis. The New England journal of medicine 2006;355:2297-2307.
90. Promrat K, Lutchman G, Uwaifo GI, Freedman RJ, Soza A, Heller T, et al. A pilot study of pioglitazone treatment for nonalcoholic steatohepatitis. Hepatology 2004;39:188-196.
91. Boettcher E, Csako G, Pucino F, Wesley R, Loomba R. Meta-analysis: pioglitazone improves liver histology and fibrosis in patients with non-alcoholic steatohepatitis. Alimentary pharmacology & therapeutics 2012;35:66-75.
92. Yki-Jarvinen H. Thiazolidinediones. The New England journal of medicine 2004;351:1106-1118.
93. Nissen SE, Wolski K. Rosiglitazone revisited: an updated meta-analysis of risk for myocardial infarction and cardiovascular mortality. Archives of internal medicine 2010;170:1191-1201.
94. Tucker ME. FDA panel advises easing restrictions on rosiglitazone. Bmj 2013;346:f3769.
95. Jia Q, Xia Y, Zhang Q, Wu H, Du H, Liu L, et al. Dietary patterns are associated with prevalence of fatty liver disease in adults. European journal of clinical nutrition 2015;69:914-921.
96. Nettleton JA, Polak JF, Tracy R, Burke GL, Jacobs DR, Jr. Dietary patterns and incident cardiovascular disease in the Multi-Ethnic Study of Atherosclerosis. Am J Clin Nutr 2009;90:647-654.
97. Nettleton JA, Steffen LM, Ni H, Liu K, Jacobs DR, Jr. Dietary patterns and risk of incident type 2 diabetes in the Multi-Ethnic Study of Atherosclerosis (MESA). Diabetes care 2008;31:1777-1782.
98. Zelber-Sagi S, Nitzan-Kaluski D, Goldsmith R, Webb M, Blendis L, Halpern Z, et al. Long term nutritional intake and the risk for non-alcoholic fatty liver disease (NAFLD): a population based study. Journal of hepatology 2007;47:711-717.
99. Sacks FM, Bray GA, Carey VJ, Smith SR, Ryan DH, Anton SD, et al. Comparison of weight-loss diets with different compositions of fat, protein, and carbohydrates. The New England journal of medicine 2009;360:859-873.
100. McCarthy EM, Rinella ME. The role of diet and nutrient composition in nonalcoholic Fatty liver disease. Journal of the Academy of Nutrition and Dietetics 2012;112:401-409.
101. Ryan MC, Itsiopoulos C, Thodis T, Ward G, Trost N, Hofferberth S, et al. The Mediterranean diet improves hepatic steatosis and insulin sensitivity in individuals with non-alcoholic fatty liver disease. Journal of hepatology 2013;59:138-143.
102. Mouzaki M, Allard JP. The role of nutrients in the development, progression, and treatment of nonalcoholic fatty liver disease. Journal of clinical gastroenterology 2012;46:457-467.
103. Finelli C, Tarantino G. Is there any consensus as to what diet or lifestyle approach is the right one for NAFLD patients? Journal of gastrointestinal and liver diseases : JGLD 2012;21:293-302.
104. Capanni M, Calella F, Biagini MR, Genise S, Raimondi L, Bedogni G, et al. Prolonged n-3 polyunsaturated fatty acid supplementation ameliorates hepatic steatosis in patients with non-alcoholic fatty liver disease: a pilot study. Alimentary pharmacology & therapeutics 2006;23:1143-1151.
105. Tanaka N, Sano K, Horiuchi A, Tanaka E, Kiyosawa K, Aoyama T. Highly purified eicosapentaenoic acid treatment improves nonalcoholic steatohepatitis. Journal of clinical gastroenterology 2008;42:413-418.

Chapter 2

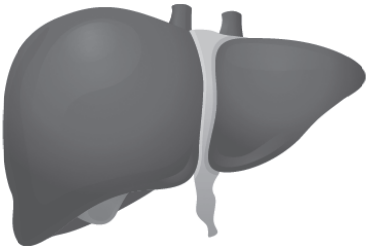
Surgical removal of inflamed epididymal white adipose tissue attenuates the development of non-alcoholic steatohepatitis in obesity

Petra Mulder[1,2], Martine C. Morrison[1], Peter Y. Wielinga[1], Wim van Duyvenvoorde[1], Teake Kooistra[1], Robert Kleemann[1,2]

[1] Department of Metabolic Health Research, Netherlands Organization for Applied Scientific Research (TNO), Zernikedreef 9, 2333 CK Leiden, The Netherlands
[2] Leiden University Medical Center, Department of Cardiovascular Surgery, Leiden, 2333 ZA, The Netherlands

International Journal of Obesity. 2015 Oct 26. doi:10.1038/ijo.2015.226







ABSTRACT

Background: Non-alcoholic fatty liver disease (NAFLD) is strongly associated with abdominal obesity. Growing evidence suggests that inflammation in specific depots of white adipose tissue (WAT) plays a key role in NAFLD progression, but experimental evidence for causal role of WAT is lacking.

Methods: A time-course study in C57BL/6J mice was performed to establish which WAT depot is most susceptible to develop inflammation during high-fat diet (HFD)-induced obesity. Crown-like structures (CLS) were quantified in epididymal (eWAT), mesenteric (mWAT) and inguinal/subcutaneous (iWAT) WAT. The contribution of inflamed WAT to NAFLD progression was investigated by surgical removal of a selected WAT depot and compared to sham surgery. Plasma markers were analyzed by ELISA (cytokines/adipokines) and lipidomics (lipids).

Results: In eWAT, CLS were formed already after 12 weeks of HFD which coincided with maximal adipocyte size and fat depot mass, and preceded establishment of non-alcoholic steatohepatitis (NASH). By contrast, the number of CLS were low in mWAT and iWAT. Removal of inflamed eWAT after 12 weeks (eWATx group), followed by another 12 weeks of HFD feeding, resulted in significantly reduced NASH in eWATx. Inflammatory cell aggregates (-40%; $p<0.05$) and inflammatory genes (e.g. TNFα, -37%; $p<0.05$) were attenuated in livers of eWATx mice, while steatosis was not affected. Concomitantly, plasma concentrations of circulating pro-inflammatory mediators, viz. leptin and specific saturated and monounsaturated fatty acids, were also reduced in the eWATx group.

Conclusion: Intervention in NAFLD progression by removal of inflamed eWAT attenuates the development of NASH and reduces plasma levels of specific inflammatory mediators. These data support the hypothesis that eWAT is causally involved in the pathogenesis of NASH.

INTRODUCTION

Non-alcoholic fatty liver disease (NAFLD) is a significant health problem and the most common form of chronic liver disease world-wide [1,2]. The prevalence of NAFLD parallels the steady increases in the rates of obesity, and consumption of saturated fat is positively associated with the risk of NAFLD [3]. Clinicopathologically, NAFLD comprises a wide spectrum of liver damage ranging from bland steatosis (NAFL) to non-alcoholic steatohepatitis (NASH), fibrosis and ultimately cirrhosis [4]. Bland steatosis is benign whereas NASH is characterized by hepatocyte injury, TNFα-mediated inflammation [4], and a high risk of liver-related morbidity and mortality [1].

The pathogenesis of NAFLD is not fully understood, and the factors that contribute to disease progression from bland steatosis to NASH remain enigmatic. Epidemiological and human observational studies do provide indications that progressive NAFLD is strongly associated with white adipose tissue (WAT) inflammation, insulin resistance, and elevated circulating levels of inflammatory mediators including certain adipokines and lipids [5-10]. Furthermore, longitudinal rodent studies demonstrated that high fat diet (HFD)-induced expression of inflammatory genes in WAT precedes the development of NASH in disease models with obesity, suggesting a potential role of inflamed WAT in NAFLD progression [11]. Also, the severity of the NAFLD pathology appears to be closely linked to WAT dysfunction, i.e. hypertrophy of adipocytes combined with macrophage infiltration, formation of crown-like structures (CLS) and enhanced expression of inflammatory genes [12]. Hence, it has been postulated that obesity-induced inflammation in WAT is critical for the development of NAFLD [13,14], but experimental evidence for an involvement of WAT is still lacking.

WAT is a complex endocrine organ that is composed of different depots among which the intra-abdominal (e.g. epididymal and mesenteric) and subcutaneous (e.g. inguinal) WAT depots [15,16]. These depots are thought to play different roles in energy storage and inflammation [13,15,16] and may thus have different contributions to the pathogenesis of NAFLD. The temporal development of inflammation (i.e. CLS formation) in WAT depots has not been systematically

investigated and it is not known whether a particular depot is more prone to become inflamed during HFD-induced obesity and associated NAFLD.

The present time-course study analyses HFD-evoked changes in epididymal (eWAT), mesenteric (mWAT) and inguinal WAT (iWAT) with specific emphasis on adipocyte hypertrophy and WAT inflammation (CLS formation). To that end, a cohort of male C57BL/6J mice was treated with HFD for a period of 24 weeks. Groups of mice were sacrificed at regular intervals, and compared to chow controls. Longitudinal histological analyses revealed that a particular depot (eWAT) is highly susceptible to develop inflammation with pronounced CLS formation after already 12 weeks. In a separate experiment, the inflamed eWAT depot of obese HFD-fed mice was surgically removed (after 12 weeks on a HFD) to examine a potential role of eWAT in the subsequent development of NASH. Our results provide evidence that inflamed eWAT plays an important role in the pathogenesis of NASH. Analysis of adipokines and circulating lipids by lipidomics supports the view that circulating inflammatory factors derived from eWAT mediate NASH development.

MATERIAL AND METHODS

Animals and housing

Animal experiments were approved by an independent Animal Care and Use Committee and were in compliance with European Community specifications for the use of laboratory animals.

Time-course cohort study

Male 9-week old wild-type C57BL/6J mice (n=84) were obtained from Charles River Laboratories (L'Arbresle Cedex, France). After an acclimatization period of 3 weeks on chow diet (R/M-H, Ssniff Spezialdieten GmbH, Soest, Germany; containing: 33 kcal% protein, 58 kcal% carbohydrate and 9 kcal% fat), mice were matched into 7 groups of n=12 mice each based on body weight. One group was sacrificed after matching to define the starting condition of the experiment (t=0). Three groups were treated with high-fat diet (HFD; D12451, Research Diets Inc., New Brunswick, USA; with 20 kcal%

protein, 35 kcal% carbohydrate and 45 kcal% lard fat) and three control groups remained on chow. Mice had ad libitum access to food and water and groups were sacrificed after 6, 12 and 24 weeks on diet respectively. Plasma samples were collected after 5h fasting at 4-week intervals. Animals were sacrificed by CO_2 asphyxiation, a serum sample was collected by heart puncture; and liver, epididymal (eWAT), mesenteric (mWAT) and inguinal (iWAT) WAT were isolated. A part of the tissues was fixed in formalin and paraffin-embedded for histological analysis, another part was snap-frozen in liquid nitrogen and stored at -80°C for real-time polymerase chain reaction (RT-PCR).

Surgical removal of epididymal adipose tissue depot (eWAT)

In a separate HFD-feeding experiment the contribution of eWAT to NASH development was analyzed. Male 9-week old wild-type C57BL/6J mice (Charles River Laboratories, L'Arbresle Cedex, France) were acclimatized for three weeks and matched in two groups (n=15/group), after 12 weeks of HFD feeding based on body weight and fasting plasma insulin concentrations. All mice were injected subcutaneously with carprofen analgesic (5 mg/kg) 30 minutes prior to surgery and anesthetized with isoflurane during surgery. In the eWATx group, both eWAT fat pads were surgically removed through a mid-ventral abdominal incision as described [17]. Testes were visualized and the attached epididymal fat pads were carefully removed and weighed, without damaging the testicular blood supply. In the sham group, a mid-ventral incision was made and the epididymal fat pads were visualized, i.e. fat pads were pulled out, but were left intact and placed back inside the peritoneal cavity. One animal from the eWATx group died during surgery and was therefore excluded from the study. Daily food intake and body weight regain were evaluated to determine recovery from surgery. After surgery, mice continued HFD feeding for another 12 weeks and were then sacrificed for histological evaluation of livers.

Histological, biochemical, lipidomic and gene expression analyses

A detailed description of biochemical, lipidomic and gene expression analyses is provided as Supplement 1. For histological analysis of livers, 5-µm-thick cross-sections were stained with Hematoxylin-Eosin (HE). NAFLD was scored blindly using a general scoring system for rodent models which is based on the human NAS grading

criteria [18]. Briefly, microvesicular steatosis and macrovesicular steatosis were separately scored and expressed as a percentage of the cross-sectional area. Hepatic inflammation was analyzed by counting the number of inflammatory foci per field at a 100x magnification (view size 3.1 mm^2) in five different fields per specimen. For WAT, paraffin-embedded cross sections (5 µm thick) were stained with Hematoxylin-Phloxine-Saffron (HPS) for quantification of adipocyte size and CLS using an Olympus BX51 microscope and Cellˆ D software (Olympus, Zoeterwoude, The Netherlands). The number of CLS was counted in 5 fields (100x magnification) per mouse and depot and data were expressed as number of CLS per 1000 adipocytes.

Statistical analysis

All data are presented as mean±SEM. Significance of differences of continuous variables between HFD fed and chow fed animals was tested using student's t-test. Changes over time between the different HFD groups (t=0, 6, 12 and 24 weeks) were statistically analyzed by One-way ANOVA and Tukey post-hoc test (normally distributed variables). Non-normally distributed variables were tested by non-parametric Kruskal-Wallis test followed by Mann-Whitney U tests. Statistical significance of differences between SHAM and eWATx was tested using unpaired one-sided t-tests. Paired two-sided t-tests were used to calculate the significance of induction of inflammatory mediators in plasma (fatty acids and adipokines) between week 12 and week 24 (i.e. before and after surgery) within each group. Results were considered statistically significant at $p<0.05$. Analyses were performed using Graphpad Prism software (version 6, Graphpad Software Inc. La Jolla, USA).

RESULTS

Time-resolved analysis of HFD-induced obesity, hyperinsulinemia and hyperglycemia in a cohort of mice

Mice had an average body weight of 26.2±1.0 g at the start of the experiment (t=0). Body weight was significantly higher in mice on a HFD compared to control mice already after 4 weeks of diet feeding and HFD-fed mice reached a final body weight

of 51.6±0.8g versus 33.3±0.7g in chow-fed control mice at 24 weeks of diet feeding (Figure 1A). HFD feeding significantly increased fasting plasma insulin (8.2±0.2 ng/mL) compared to chow (1.6±0.2 ng/mL) (Figure 1B). The HFD effect on insulin was accompanied by a significant increase in fasting plasma glucose (15.1±0.5 mM), compared to on chow (10.9±0.4 mM) (Figure 1C). Plasma triglycerides concentrations were comparable between HFD and chow treated groups and decreased slightly over time (not shown). Altogether, these data show that HFD-treated mice developed obesity, hyperinsulinemia and hyperglycemia, all of which are associated with NAFLD.

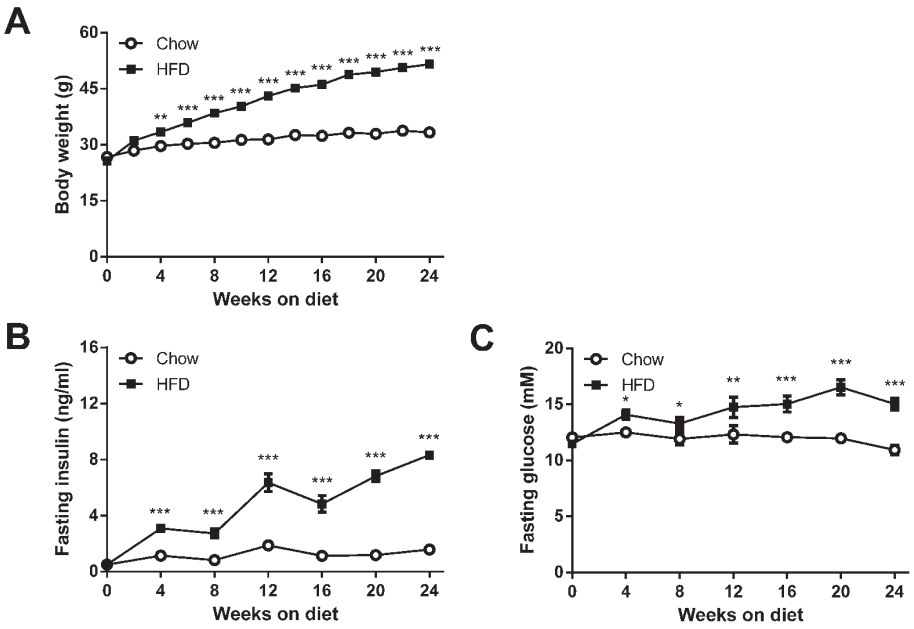


Figure 1. Time-course analysis of the effect of HFD on body weight and metabolic parameters. (A) HFD feeding increased body weight compared to chow control diet. HFD feeding gradually increased fasting plasma concentrations of (B) insulin and (C) glucose compared to chow. Data are mean±SEM (n=12/group per time point), *p<0.05,**p<0.01,***p<0.001 versus chow control.

HFD feeding induces liver steatosis by week 12 which progresses to NASH

Livers collected at t=0, 6, 12 and 24 weeks of diet feeding were analyzed for steatosis and presence of inflammatory cell aggregates to evaluate development of NASH

(representative images shown in Figure 2A). HFD feeding resulted in modest steatosis by week 12 which intensified significantly towards the end of the study, while chow-fed mice showed no steatosis and normal liver histology at all the time points (not shown). Quantification of distinct forms of steatosis, i.e. micro- and macrovesicular steatosis, demonstrated a gradual increase in HFD-induced microvesicular steatosis over time (Figure 2B). By contrast, macrovesicular steatosis (a hallmark of overt human NASH [4]) had hardly developed by week 12, but was significantly increased in week 24 (Figure 2C). HFD-induced liver steatosis can be attributed to significant increases in liver triglycerides as measured biochemically in corresponding liver homogenates (Figure 2D). Lobular inflammation was specifically induced by HFD (Figure 2E), not by chow, and showed a similar time pattern as macrovesicular steatosis. More specifically, the number of inflammatory cell aggregates (an indicator of lobular inflammation [18]) remained low until week 12 and increased significantly by week 24. HFD-induced lobular inflammation was accompanied by significantly increased TNFα and MCP-1/CCL2 gene expression in livers at t=24 weeks (Figure 2F-G).

Taken together, these data demonstrate that 12 weeks of HFD feeding resulted in bland steatosis which progressed to NASH by week 24 as demonstrated by the establishment of pronounced macrovesicular steatosis and lobular inflammation.

Epididymal WAT depot is prone to develop HFD-induced inflammation

We next examined whether the epididymal (eWAT), mesenteric (mWAT) and inguinal (iWAT) depots would differ in their susceptibility to develop inflammation during HFD-feeding and we defined the time point at which CLS formation started in the various depots. HFD-feeding led to an increase in mass of eWAT, mWAT and iWAT depots over time (Figure 3A), while the mass of the depots remained unchanged on chow (not shown). eWAT mass increased strongly at week 6 and reached a maximum already in week 12 (2.4±0.1g). By contrast, the mass of mWAT and iWAT increased continuously over time until the end of the experiment (Figure 3A). In all WAT depots, adipocytes increased in size during HFD feeding indicating that adipocyte expansion is a generic response of all WAT depots. However, the adipocytes of eWAT rapidly reached a maximal size in week 6 (Figure 3B).

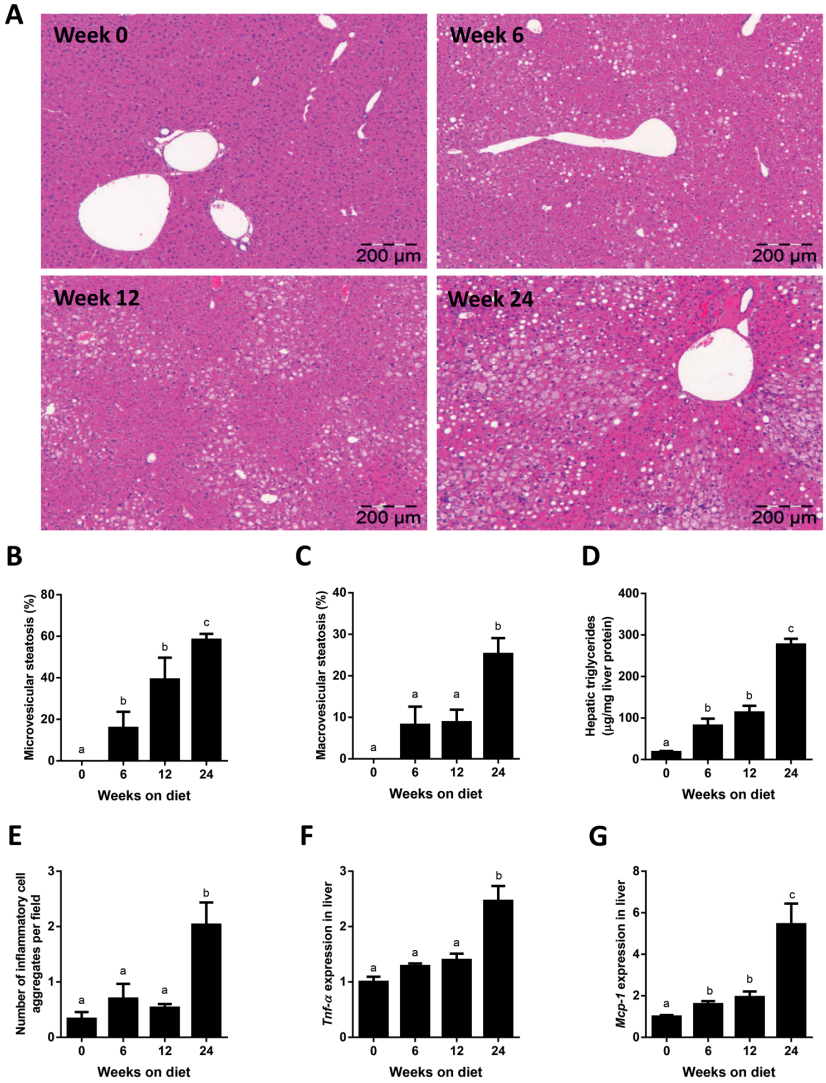


Figure 2. Time-resolved development of NAFLD induced by HFD feeding. (A) Representative photomicrographs of HE-stained liver cross-sections of mice treated with HFD for 0,6,12 or 24 weeks (magnification x100). Histological analysis of (B) microvesicular and (C) macrovesicular steatosis as percentage of the cross-sectional area (n=6-12/group per time point). (D) Biochemical quantification of hepatic triglyceride content (n=11-12/group). (E) Development of lobular inflammation in liver over time defined as the number of inflammatory cell aggregates (n=6-12/group per time point). (F) Gene expression of TNFα and (G) MCP-1 in liver over time. Data (n=8/group) are expressed as fold-change in gene expression relative to t=0. Data are mean±SEM. ^{a,b,c} Mean values with unlike letters differ significantly from each other (p<0.05).

Adipocytes in the other depots were still smaller at this time point and their size increased more slowly and gradually until the end of the study. Notably, in week 6 first CLS were observed in eWAT specifically and their numbers increased greatly in week 12 when the maximal capacity of eWAT seemed to be reached (viz. maximal mass and maximal adipocytes size) (Figure 3C). CLS formation in eWAT was more rapid and pronounced than in mWAT and iWAT (Figure 3C-D) showing that eWAT is most prone to develop HFD-induced inflammation. In mWAT, CLS numbers increased later than in eWAT (by week 24) and when maximal average adipocyte size was reached, essentially as observed in eWAT. These observations show that the expandability of a depot (and its adipocytes) is limited and that this depot-specific restriction seems critical for the development of inflammation. In all, our time-resolved histological analyses show that HFD-induced WAT inflammation starts in a specific depot (eWAT) and increases strongly when eWAT has expanded maximally (at t=12 weeks). Importantly, eWAT inflammation coincides with bland steatosis and hence precedes the development of NASH.

Surgical removal of inflamed eWAT attenuates NASH development

To examine whether eWAT is causally involved in the progression of liver steatosis to NASH, we performed a separate HFD feeding experiment in which eWAT was surgically removed in one group (eWATx) and compared to a SHAM surgery control group (SHAM). The surgery was performed after week 12 of HFD feeding, i.e. the time point at which livers in the above time-course experiment were steatotic and eWAT was inflamed.

Body weight at the time of surgery was comparable between SHAM and eWATx groups (SHAM: 42.3±1.2g, and eWATx: 42.3±0.9g; Figure 4A). On average 1.9±0.1g of eWAT was removed and this reduction in fat mass was reflected in the body weight of eWATx mice the day after surgery (SHAM: 41.6±1.7g; and eWATx: 39.5±1.2g, not shown). CLS were abundantly present in this tissue, confirming pronounced inflammation at the time of surgery (Figure 4B). Food intake was comparable between the eWATx and SHAM group throughout the study. The total body weight at the end of the experiment was 47.1±1.3 g in SHAM and 46.7±0.9 g in eWATx, and whole body fat mass determined by EchoMRI was slightly lower in

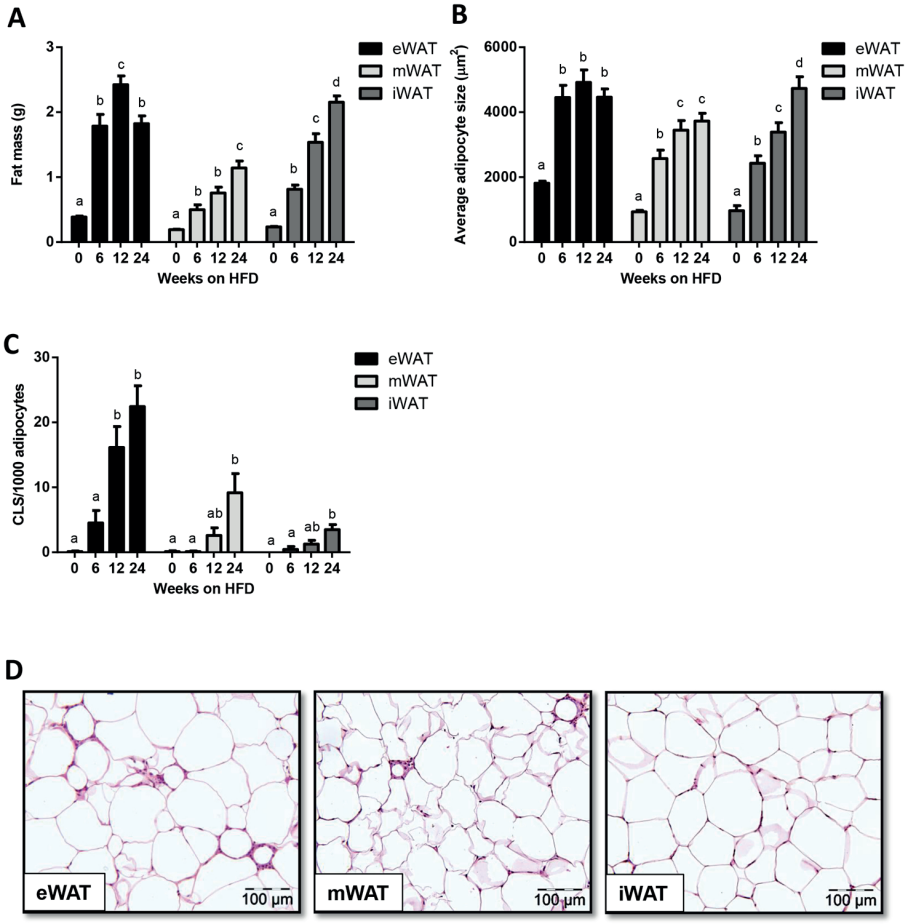


Figure 3. Effect of HFD feeding on the quantity and inflammatory state of the epididymal (eWAT), mesenteric (mWAT) and inguinal (iWAT) white adipose tissue (WAT) depots. (A) WAT mass of eWAT, mWAT and iWAT depot during HFD-feeding time-course experiment (n=12/group per time point). (B) Development of adipocyte cell size of the different WAT depots quantified by morphometric analysis of HPS-stained sections. (C) Quantitative analysis of the number of crown-like structures (CLS) in the different WAT depots over time (n=8-12/group per time point). (D) Representative images of HPS-stained cross-sections of eWAT, mWAT and iWAT after 24 weeks of HFD (magnification x200). Data are mean±SEM. ^{a,b,c,d} Mean values with unlike letters differ significantly from each other (p<0.05).

eWATx mice (not significant, Figure 4C), while lean mass was comparable between the groups (SHAM: 29.1±0.6g vs. eWATx: 29.7 ±0.4g, ns). Fasting plasma glucose concentrations increased during the experiment, essentially as observed in the time-course study, and hyperglycemia was comparable in both groups (SHAM: 14.6±0.7 mM vs. eWATx: 15.2±0.6 mM; ns). Isolation of individual fat depots after sacrifice in week 24 showed that eWAT mass was significantly reduced in eWATx (Figure 4D). The mass of mWAT, iWAT (Figure 4D) and retroperitoneal WAT (not shown) was comparable in both groups indicating that these depots did not compensate for the removed eWAT.

Histological analysis of livers revealed that eWATx mice exhibited a similar degree of micro- and macrovesicular steatosis compared with SHAM mice (Figure 5A-C). Biochemical analysis of liver triglycerides in liver homogenates showed no significant difference between the groups (SHAM: 160.8±18.9 µg/mg liver protein vs. eWATx: 170.5±16.2 µg/mg liver protein; ns). Minor liver lipids (cholesteryl esters and free cholesterol) were also comparable between the groups (data not shown). Remarkably, eWATx livers displayed a significantly reduced number of inflammatory cell aggregates indicating attenuated NASH development upon eWAT removal (Figure 5D). Reduced liver inflammation was substantiated by a significantly decreased gene expression of TNFα (Figure 5E) and MCP-1 (trend p=0.08; Figure 5F) in eWATx livers.

Collectively, these results show that surgical removal of inflamed eWAT significantly attenuates the development of NASH in absence of an effect on hyperglycemia and demonstrates a causal role of eWAT in the pathogenesis of NAFLD. We next analyzed circulating factors that could mediate this effect on liver.

Surgical removal of eWAT affects circulating levels of pro-inflammatory mediators

The effects of eWAT removal on adipokines and lipids associated with NAFLD development were assessed. In eWATx, the IL-6 serum concentrations were slightly lower (5.5±2.6 pg/ml) than in SHAM (7.0±2.5 pg/ml, not shown) but the difference was not statistical significant. The eWATx and SHAM groups also had comparable plasma concentrations of MCP-1 (86.6±11.7 pg/ml vs. 80.8±13.3 pg/ml; ns) and adiponectin (13.6±1.1 µg/ml vs. 14.3±1.2 µg/ml; ns). By contrast, plasma leptin concentrations

increased significantly in SHAM mice and this increase was not observed in eWATx mice (Figure 6A). Plasma leptin levels also correlated positively (r^2=0.7; p=0.01) with hepatic Mcp-1 expression suggesting a link to hepatic inflammation.

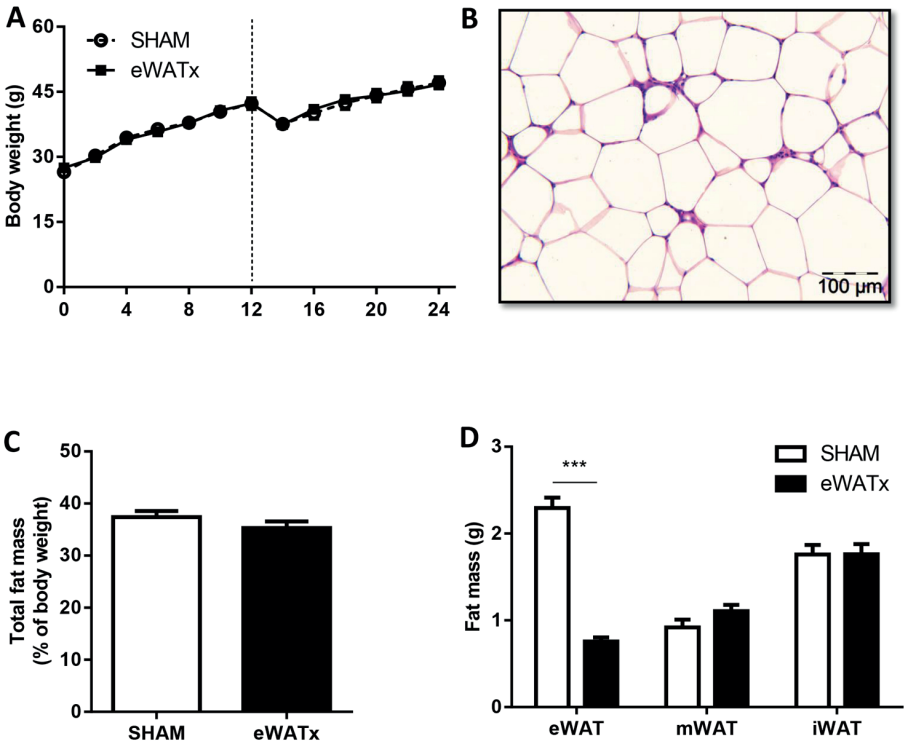


Figure 4. Effect of surgical removal of eWAT on body weight and other WAT depots. Mice were fed HFD and, on average, 1.9 gram of eWAT was carefully removed after 12 weeks of HFD. (A) Body weight development of the eWATx and SHAM group. The dashed line indicates the time point of surgery. (B) Representative image of a HPS-stained eWAT cross-section showing presence of inflammatory cells and CLS at time of removal (magnification x200). (C) Analysis of total fat mass measured by EchoMRI in week 24 of HFD. (D) Mass of eWAT, mWAT and iWAT isolated at the end of the study (24 weeks of HFD) in eWATx and SHAM group. The eWAT mass of eWATx mice was significantly lower than in SHAM. Data also show that mWAT and iWAT did not compensate for the removed eWAT. Data are mean±SEM (n=14-15/group),***p<0.001 versus SHAM.

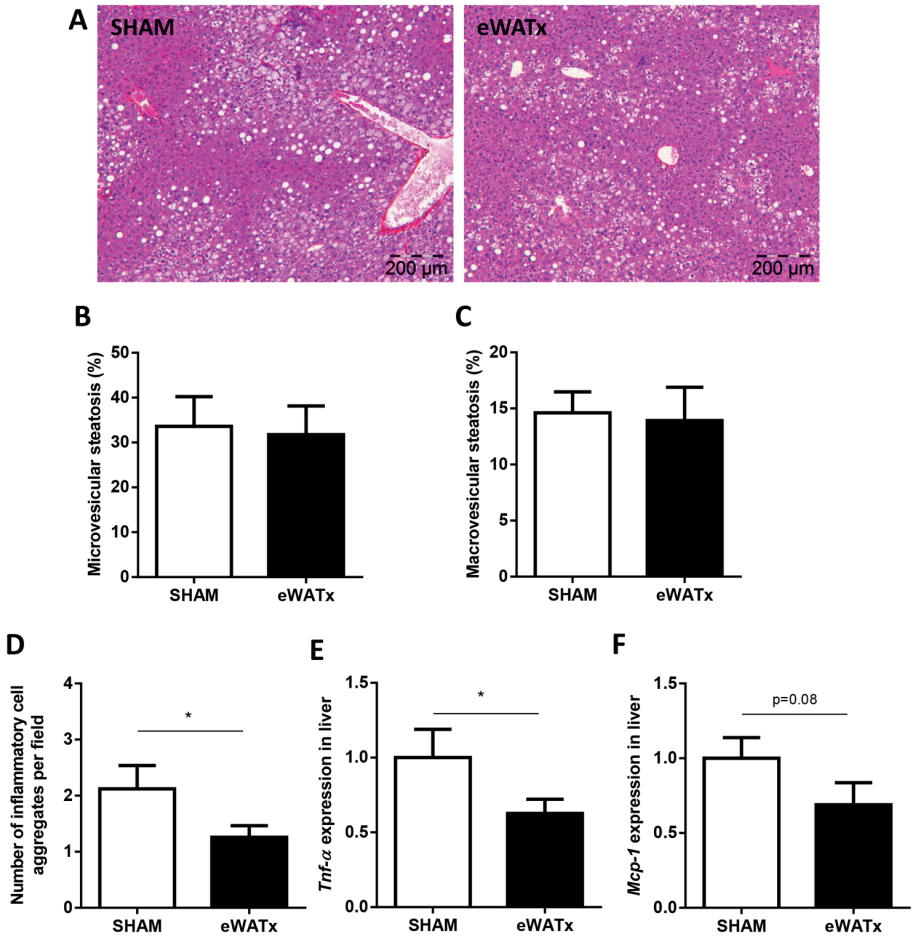


Figure 5. Effect of surgical removal of eWAT on NAFLD development. (A) Representative images of HE-stained liver sections (magnification x100). (B) Quantification of microvesicular steatosis and (C) macrovesicular steatosis as percentage of the cross-sectional liver area (n=14-15/group). (D) Number of inflammatory cell aggregates in livers of eWATx and SHAM mice. Liver gene expression of (E) TNFα and (F) MCP-1 in eWATx and SHAM. Real-time PCR data are expressed as fold-change in gene expression relative to SHAM (n=8/group). Data are mean±SEM,*p<0.05.

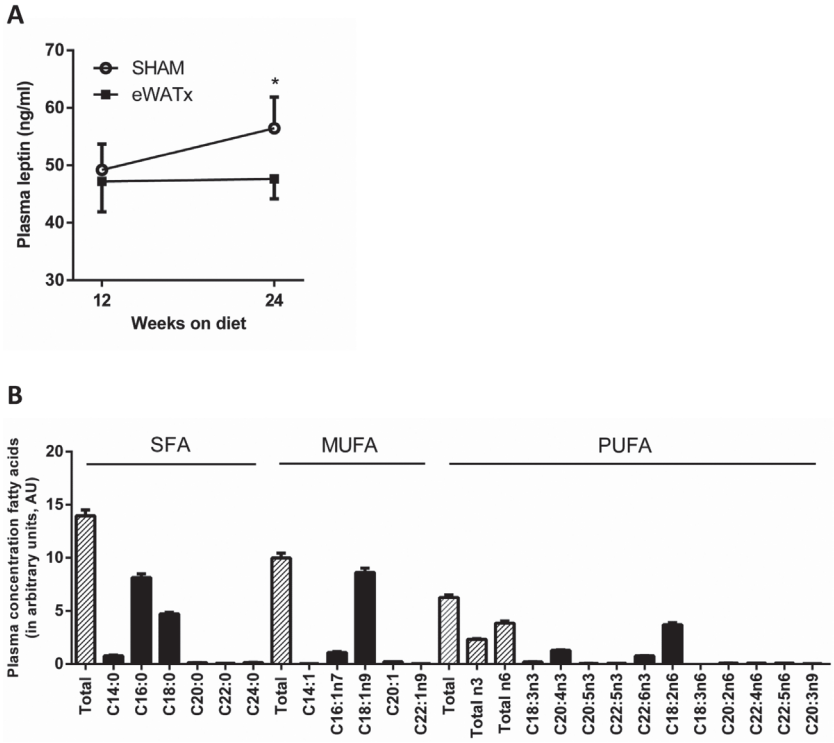


Figure 6. Effect of surgical removal of eWAT on circulating inflammatory mediators and lipids. (A) Plasma concentrations of leptin prior to surgery at 12 weeks of HFD, and at the end of the experiment (24 weeks) in eWATx and SHAM group. Data are mean±SEM,*p<0.05 according to paired Student's t-test. (B) Profiling of plasma lipids after 12 weeks of HFD by lipidomic analysis. Fasting plasma was collected before surgery. The levels of saturated free fatty acids (SFA), monounsaturated fatty acids (MUFA) and polyunsaturated fatty acids (PUFA) are shown and the most abundant lipid species of each category are indicated. Data are mean±SEM and expressed as arbitrary units (AU) relative to internal standard.

We next profiled the circulating (pro-inflammatory) lipids using lipidomics to define the most abundant lipid species in plasma (Figure 6B), and subsequently analyzed whether eWATx removal affected these lipids (Table 1). Saturated fatty acids (SFA) were the most abundant lipid species after 12 weeks of HFD feeding (prior to surgery), followed by monounsaturated fatty acids (MUFA), and n-6 and n-3 polyunsaturated fatty acids (PUFA) (Figure 6B). Within the SFA, C16:0 (palmitic acid), C18:0 (stearic acid) and C14:0 (myristic acid) were most abundant. Within the

class of MUFA C18:1n9 (oleic acid) and C16:1n7 (palmitoleic acid) were circulating at high levels, and within the PUFA, C20:4n3 (eicosatetraenoic acid) and C18:2n6 (linoleic acid) were most abundant.

Table 1 shows that the level of total SFA, and palmitic acid in particular (+1.4; $p<0.05$), increase in SHAM while such an increase was not observed in eWATx. Myristic acid and several of the less abundant SFA (C20:0, C22:0, C24:0) decreased significantly after eWAT removal. Furthermore, total MUFA increased strongly over time in SHAM (+3.7; $p<0.05$), mainly due to significant rises in palmitoleic, oleic and eicosenoic acids. By contrast, there was no significant change over time in any of the MUFA in the eWATx group. Total PUFA levels increased in both, SHAM (+2.0) and eWATx (+1.5). The observed changes in SFA and MUFA support the notion that removal of eWAT prevents the development of a pro-inflammatory state.

DISCUSSION

NAFLD is strongly associated with obesity but the pathogenesis of the disease, and in particular the role of WAT, is poorly understood. It has been proposed that inflammation in WAT may play a critical role in obesity-induced NAFLD development [4,13,19,20], but evidence for causality is lacking. This study shows that HFD-induced inflammation in eWAT develops more rapidly than in mWAT or iWAT, and that this inflammation precedes overt NASH. Notably, pronounced CLS formation was observed in eWAT once the adipocytes of this tissue did not further increase in size and the depot had reached a maximal mass (week 12 of HFD feeding). A subsequent experiment showed that removal of the inflamed eWAT depot at week 12 attenuates liver inflammation and reduces the development of NASH. Removal of eWAT affected the circulating levels of specific pro-inflammatory mediators among which leptin and specific lipids (e.g. palmitic acid), providing a rationale for the observed hepatoprotective effect.

The time-course analysis of HFD-induced NAFLD shows that a particular intra-abdominal depot in mice, eWAT, is prone to develop tissue inflammation characterized by presence of macrophages and CLS. Consistent with this finding,

Table 1. Change in plasma fatty acid levels in SHAM and eWATx

Fatty acids	SHAM Δ change	eWATx Δ change
Saturated fatty acid (SFA)	**1.3 ± 0.8**	**-0.3 ± 1.0**
Myristic acid (C14:0)	0.02 ± 0.1	-0.3 ± 0.2
Palmitic acid (C16:0)	1.4 ± 0.5*	-0.1 ± 0.6
Stearic acid (C18:0)	-0.03 ± 0.3	0.4 ± 0.2
Arachidic acid (C20:0)	-0.01 ± 0.0	-0.05 ± 0.0*
Behenic acid (C22:0)	-0.01 ± 0.0	-0.04 ± 0.0*
Lignoceric acid (C24:0)	-0.02 ± 0.0	-0.1 ± 0.1*
Monounsaturated acid fatty acid (MUFA)	**3.7 ± 0.9*#**	**0.8 ± 0.8**
Myristoleic acid (C14:1)	0.0 ± 0.0	0.0 ± 0.0
Palmitoleic acid (C16:1n7)	0.5 ± 0.2*	0.2 ± 0.1
Oleic acid (C18:1n9)	3.1 ± 0.8*#	0.6 ± 0.7
Eicosenoic acid (C20:1)	0.1 ± 0.0*	0.03 ± 0.0
Erucic acid (C22:1n9)	0.004 ± 0.0	-0.003 ± 0.0
Polyunsaturated fatty acid (PUFA)	**2.0 ± 0.6***	**1.5 ± 0.4***
Total n6-fatty acids	1.7 ± 0.5*	1.0 ± 0.3*
Total n3-fatty acids	0.3 ± 0.1*	0.5 ± 0.1*
Linoleic acid (C18:2n6)	1.7 ± 0.5*	1.0 ± 0.3*
γ-linolenic acid (C18:3n6)	0.0 ± 0.0	0.0 ± 0.0
Eicosadienoic acid (C20:2n6)	0.03 ± 0.0*	0.02 ± 0.0*
Adrenic acid (C22:4n6)	0.02 ± 0.0*	0.03 ± 0.0*
Docosapentaenoic acid (C22:5n6)	0.02 ± 0.0*	0.01 ± 0.0
α-linolenic acid (C18:3n3)	0.1 ± 0.0	0.2 ± 0.0
Eicosatetraenoic acid (C20:4n3)	0.1 ± 0.1	0.3 ± 0.1*
Eicosapentaenoic acid (C20:5n3)	0.01 ± 0.0	0.01 ± 0.0*
Docosapentaenoic acid (C22:5n3)	0.01 ± 0.0*	0.02 ± 0.0*
Docosahexaenoic acid (C22:6n3)	0.1 ± 0.0*	0.1 ± 0.0*
Mead acid (C20:3n9)	0.01 ± 0.0*	0.01 ± 0.0*

Delta (Δ) change in plasma lipids between week 12 and 24, i.e. before and after surgery. Data are in arbitrary units (mean±SEM). *$p \leq 0.05$ indicates significant changes over time within a group. #$p < 0.05$ indicates significant difference between SHAM (n=11) and eWATx (n=12).

other groups have reported that eWAT of obese HFD-treated mice exhibits a higher number of CLS than mesenteric and subcutaneous (inguinal) WAT depots [21,22]. Differences in macrophage content appear to exist already in lean C57BL6 mice: Altinas et al. [21] showed that the subcutaneous depot differs from the intra-abdominal depots with respect to immune cell composition and density. For instance, the density of solitary adipose tissue macrophages (ATM) in subcutaneous WAT is much lower than in intra-abdominal depots such as eWAT [21]. Hence,

the relatively high number of solitary ATM in eWAT may predispose this depot to develop CLS more rapidly in response to HFD than other depots analyzed in this study. In obese subjects, CLS are also more prevalent in abdominal (omental) WAT than in subcutaneous WAT [6,23] suggesting that, in humans, intra-abdominal depots are also more prone to become inflamed than subcutaneous depots, and that our observations are not restricted to mice.

We found that the number of CLS in eWAT increased strongly once this depot had reached a maximal mass and concomitantly no further increase in adipocyte size was observed. In line with this, other groups reported that the weight of eWAT does typically not exceed about 2.5 grams [12,22,24,25]. This limitation in eWAT mass has been observed with different diets and in different strains of mice pointing to a generic threshold of eWAT independent of the experimental conditions employed. Consistent with this, Virtue and Vidal-Puig [26] proposed that organisms possess a maximum capacity for adipose expansion, and failure in the capacity for adipose tissue expansion, rather than obesity per se may underlie the development of inflammation. Indeed, also in the case of mWAT, CLS numbers increased at week 24, i.e. after the average adipocyte size had reached a maximum. Little is known about the mediators that control WAT expansion during diet-induced obesity. It is possible that localized cytokine production limits further WAT expansion: Salles et al. [27] showed that TNFα knockout mice have two-fold more eWAT mass than wild-type mice during HFD feeding. In support of this notion, increased TNFα gene expression in eWAT was observed after attainment of maximal adipocyte size in an experiment conducted under conditions comparable to those applied herein [22]. Together, our time-resolved analysis of the inflammatory component in diet-induced obesity shows that WAT inflammation develops sequentially across depots.

C57BL/6 mice constitute a frequently used model to study diet-induced obesity and associated comorbidities. For the interpretation of these studies, it is important to recognize that development of inflammation upon HFD-feeding is a very complex and dynamic process involving multiple tissues, including WAT and liver [11,15]. As demonstrated herein, the different WAT depots become inflamed at specific time points during HFD feeding, rather than simultaneously. Because animal studies often analyze a single WAT depot (frequently the eWAT) at one

particular time point during HFD feeding, conclusions about the condition 'adipose tissue in general' or the inflammatory state in other depots should be made with caution. Our results support a more comprehensive analysis of WAT (with precise specification of the intra-abdominal depots analyzed), and advocates the study of the cross-talk between organs in NAFLD. For instance, between 12 and 24 weeks of HFD, i.e. the period in which eWAT was inflamed and did not further expand, we observed a pronounced increase of triglyceride concentrations in the liver. This supports the concept that, once the expansion limit of a particular WAT depot has been reached, adipose tissue ceases to store energy efficiently and lipids begin to accumulate as ectopic fat in other tissues [26].

In patients, the accumulation of intra-abdominal WAT is strongly associated with progressive NASH [5]. Hepatic inflammation and fibrosis augmented incrementally with increases in intra-abdominal fat mass. Importantly, intra-abdominal fat of patients was directly associated with liver inflammation and fibrosis independent of insulin resistance and hepatic steatosis [5,7]. Consistent with this, removal of eWAT in the present study attenuated NASH development without an effect on hyperinsulinemia, hyperglycemia and liver steatosis. A possible explanation for the strong association between abdominal WAT mass and NASH severity in the liver may lie in the anatomical distance between both tissues. Inflammatory mediators from the intra-abdominal depots can reach the liver relatively easily (venous drainage via the portal vein) [28]. By contrast, associations between systemically drained adipose tissue depots (e.g. the deep layer of subcutaneous WAT in the abdominal area) and NASH are rare [29] suggesting that these depots only play a minor role in the pathogenesis of NASH.

While the above studies mainly focused on the quantity of adipose tissue, increasing evidence also points to a role of its inflammatory state. Livers of obese subjects with inflamed intra-abdominal (omental) WAT contain more fibro-inflammatory lesions than livers of equally obese subjects without WAT inflammation [6,7]. This observation suggests that inflammation in a specific WAT depot contributes to the inflammatory component in human NASH. The present study supports this view, because surgical removal of inflamed eWAT reduces liver inflammation (about 40% less inflammatory aggregates). Of note, intra-abdominal

eWAT in mice has no human equivalent and our findings should not be generalized with respect to the role of other WAT depots. Because of the close relationship between visceral obesity and NASH development in patients [5], it is possible that inflamed visceral WAT depots, such as mesenteric WAT, may contribute to NASH in a similar way as eWAT. For instance, mesenteric WAT develops similar features of inflammation as observed in eWAT, including formation of CLS during WAT expansion and expression of pro-inflammatory mediators (e.g. cytokines, adipokines, fatty acids), in both, mice [30,31] and humans [32,33]. Furthermore, pro-inflammatory mediators that are released by mesenteric WAT can reach the liver not only via systemic drainage (like eWAT) but also via the portal vein, which constitutes a more direct connection to the liver [28]. However, additional studies are needed to investigate the contribution of inflamed mesenteric WAT to NASH development.

Specific circulating factors have been proposed as inducers of liver inflammation in NASH [19,20]. Among these mediators are cytokines/adipokines (including IL-6, TNFα, leptin, adiponectin) and specific lipids with reported activities on liver cells [4,13,14,20]. Of the adipokines measured in the present study, only plasma leptin differed between the eWATx and the SHAM group. Several studies have shown that leptin exerts pro-inflammatory and pro-fibrogenic effects on liver cells [34,35]. For instance, leptin stimulates hepatic stellate cells to express the pro-inflammatory cytokine MCP-1 [35], a chemotactic factor and critical mediator of lobular inflammation [36]. In line with this, we observed that plasma leptin concentrations correlated with MCP-1 gene expression in the liver. Besides cytokines/adipokines, certain lipid mediators (e.g. SFA with TLR4 binding properties) have also been implicated in the pathogenesis of NASH. For example, *in vitro* studies have shown that SFA, and in particular palmitic acid, can trigger inflammation via the NFκB pathway and thereby induce TNFα production [37]. In SHAM mice, palmitic acid levels increased significantly between 12 and 24 weeks of HFD feeding, i.e. during the progression from NAFL to NASH. This increase was not observed in eWATx mice and in line with this, hepatic TNFα expression was lower than in SHAM. A total plasma lipid analysis in humans showed that obese subjects with NAFL and NASH have significantly elevated MUFA levels when compared with lean controls [38].

Among these MUFA were palmitoleic acid and oleic acid, which also increased after surgery in SHAM while they did not change significantly in eWATx. The observed increases in MUFA (both in humans and mice) may be an adaptive response to protect the liver from the lipotoxic effects of SFA (i.e. palmitic acid). As MUFAs themselves can suppress liver inflammation in mice [39], it is thus likely that increased levels of palmitic acid in SHAM mice are critical for the development of liver inflammation.

Collectively, this study demonstrates that obesity-induced inflammation develops progressively across various WAT depots, starting in eWAT. Surgical removal of inflamed eWAT shows that this depot participates in the development of NASH. Hence, interventions that target WAT may have significant therapeutic benefit for the treatment of NASH in the context of obesity.

ACKNOWLEDGEMENTS

The authors thank Joline Attema, Erik Offerman, Karin Toet and Simone van der Drift-Droog for their excellent technical assistance. This work was funded by TNO research programs ‘Predictive Health Technologies’ and ‘Enabling Technology Systems Biology’.

REFERENCES

1. Loomba R, Sanyal AJ. The global NAFLD epidemic. Nature reviews Gastroenterology & hepatology 2013;10:686-690.
2. de Alwis NM, Day CP. Non-alcoholic fatty liver disease: the mist gradually clears. Journal of hepatology 2008;48 Suppl 1:S104-112.
3. Musso G, Gambino R, De Michieli F, Cassader M, Rizzetto M, Durazzo M, et al. Dietary habits and their relations to insulin resistance and postprandial lipemia in nonalcoholic steatohepatitis. Hepatology 2003;37:909-916.
4. Tiniakos DG, Vos MB, Brunt EM. Nonalcoholic fatty liver disease: pathology and pathogenesis. Annual review of pathology 2010;5:145-171.
5. van der Poorten D, Milner KL, Hui J, Hodge A, Trenell MI, Kench JG, et al. Visceral fat: a key mediator of steatohepatitis in metabolic liver disease. Hepatology 2008;48:449-457.
6. Cancello R, Tordjman J, Poitou C, Guilhem G, Bouillot JL, Hugol D, et al. Increased infiltration of macrophages in omental adipose tissue is associated with marked hepatic lesions in morbid human obesity. Diabetes 2006;55:1554-1561.
7. Tordjman J, Poitou C, Hugol D, Bouillot JL, Basdevant A, Bedossa P, et al. Association between omental adipose tissue macrophages and liver histopathology in morbid obesity: influence of glycemic status. Journal of hepatology 2009;51:354-362.
8. Krawczyk K, Szczesniak P, Kumor A, Jasinska A, Omulecka A, Pietruczuk M, et al. Adipohormones as prognostric markers in patients with nonalcoholic steatohepatitis (NASH). Journal of physiology and pharmacology : an official journal of the Polish Physiological Society 2009;60 Suppl 3:71-75.
9. Lemoine M, Ratziu V, Kim M, Maachi M, Wendum D, Paye F, et al. Serum adipokine levels predictive of liver injury in non-alcoholic fatty liver disease. Liver international : official journal of the International Association for the Study of the Liver 2009;29:1431-1438.
10. Nehra V, Angulo P, Buchman AL, Lindor KD. Nutritional and metabolic considerations in the etiology of nonalcoholic steatohepatitis. Dig Dis Sci 2001;46:2347-2352.
11. Liang W, Tonini G, Mulder P, Kelder T, van Erk M, van den Hoek AM, et al. Coordinated and interactive expression of genes of lipid metabolism and inflammation in adipose tissue and liver during metabolic overload. PloS one 2013;8:e75290.
12. Duval C, Thissen U, Keshtkar S, Accart B, Stienstra R, Boekschoten MV, et al. Adipose tissue dysfunction signals progression of hepatic steatosis towards nonalcoholic steatohepatitis in C57BL/6 mice. Diabetes 2010;59:3181-3191.
13. Tordjman J, Guerre-Millo M, Clement K. Adipose tissue inflammation and liver pathology in human obesity. Diabetes & metabolism 2008;34:658-663.
14. Suganami T, Tanaka M, Ogawa Y. Adipose tissue inflammation and ectopic lipid accumulation. Endocr J 2012;59:849-857.
15. Caesar R, Manieri M, Kelder T, Boekschoten M, Evelo C, Muller M, et al. A combined transcriptomics and lipidomics analysis of subcutaneous, epididymal and mesenteric adipose tissue reveals marked functional differences. PloS one 2010;5:e11525.
16. Cinti S. The adipose organ: morphological perspectives of adipose tissues. The Proceedings of the Nutrition Society 2001;60:319-328.
17. Harris RB, Hausman DB, Bartness TJ. Compensation for partial lipectomy in mice with genetic alterations of leptin and its receptor subtypes. Am J Physiol Regul Integr Comp Physiol 2002;283:R1094-1103.
18. Liang W, Menke AL, Driessen A, Koek GH, Lindeman JH, Stoop R, et al. Establishment of a general NAFLD scoring system for rodent models and comparison to human liver pathology. PloS one 2014;9:e115922.

19. Tilg H, Moschen AR. Evolution of inflammation in nonalcoholic fatty liver disease: the multiple parallel hits hypothesis. Hepatology 2010;52:1836-1846.
20. Mirza MS. Obesity, Visceral Fat, and NAFLD: Querying the Role of Adipokines in the Progression of Nonalcoholic Fatty Liver Disease. ISRN gastroenterology 2011;2011:592404.
21. Altintas MM, Azad A, Nayer B, Contreras G, Zaias J, Faul C, et al. Mast cells, macrophages, and crown-like structures distinguish subcutaneous from visceral fat in mice. Journal of lipid research 2011;52:480-488.
22. Strissel KJ, Stancheva Z, Miyoshi H, Perfield JW, 2nd, DeFuria J, Jick Z, et al. Adipocyte death, adipose tissue remodeling, and obesity complications. Diabetes 2007;56:2910-2918.
23. Harman-Boehm I, Bluher M, Redel H, Sion-Vardy N, Ovadia S, Avinoach E, et al. Macrophage infiltration into omental versus subcutaneous fat across different populations: effect of regional adiposity and the comorbidities of obesity. The Journal of clinical endocrinology and metabolism 2007;92:2240-2247.
24. Lagathu C, Christodoulides C, Tan CY, Virtue S, Laudes M, Campbell M, et al. Secreted frizzled-related protein 1 regulates adipose tissue expansion and is dysregulated in severe obesity. International journal of obesity 2010;34:1695-1705.
25. Larter CZ, Yeh MM, Van Rooyen DM, Teoh NC, Brooling J, Hou JY, et al. Roles of adipose restriction and metabolic factors in progression of steatosis to steatohepatitis in obese, diabetic mice. Journal of gastroenterology and hepatology 2009;24:1658-1668.
26. Virtue S, Vidal-Puig A. Adipose tissue expandability, lipotoxicity and the Metabolic Syndrome--an allostatic perspective. Biochim Biophys Acta 2010;1801:338-349.
27. Salles J, Tardif N, Landrier JF, Mothe-Satney I, Guillet C, Boue-Vaysse C, et al. TNFalpha gene knockout differentially affects lipid deposition in liver and skeletal muscle of high-fat-diet mice. The Journal of nutritional biochemistry 2012;23:1685-1693.
28. Item F, Konrad D. Visceral fat and metabolic inflammation: the portal theory revisited. Obesity reviews : an official journal of the International Association for the Study of Obesity 2012;13 Suppl 2:30-39.
29. Tordjman J, Divoux A, Prifti E, Poitou C, Pelloux V, Hugol D, et al. Structural and inflammatory heterogeneity in subcutaneous adipose tissue: relation with liver histopathology in morbid obesity. Journal of hepatology 2012;56:1152-1158.
30. Kwon EY, Shin SK, Cho YY, Jung UJ, Kim E, Park T, et al. Time-course microarrays reveal early activation of the immune transcriptome and adipokine dysregulation leads to fibrosis in visceral adipose depots during diet-induced obesity. BMC Genomics 2012;13:450.
31. Murano I, Barbatelli G, Parisani V, Latini C, Muzzonigro G, Castellucci M, et al. Dead adipocytes, detected as crown-like structures, are prevalent in visceral fat depots of genetically obese mice. Journal of lipid research 2008;49:1562-1568.
32. Fain JN, Madan AK, Hiler ML, Cheema P, Bahouth SW. Comparison of the release of adipokines by adipose tissue, adipose tissue matrix, and adipocytes from visceral and subcutaneous abdominal adipose tissues of obese humans. Endocrinology 2004;145:2273-2282.
33. Bigornia SJ, Farb MG, Mott MM, Hess DT, Carmine B, Fiscale A, et al. Relation of depot-specific adipose inflammation to insulin resistance in human obesity. Nutrition & diabetes 2012;2:e30.
34. Ikejima K, Honda H, Yoshikawa M, Hirose M, Kitamura T, Takei Y, et al. Leptin augments inflammatory and profibrogenic responses in the murine liver induced by hepatotoxic chemicals. Hepatology 2001;34:288-297.

35. Aleffi S, Petrai I, Bertolani C, Parola M, Colombatto S, Novo E, et al. Upregulation of proinflammatory and proangiogenic cytokines by leptin in human hepatic stellate cells. Hepatology 2005;42:1339-1348.
36. Marra F, Tacke F. Roles for chemokines in liver disease. Gastroenterology 2014;147:577-594 e571.
37. Shi H, Kokoeva MV, Inouye K, Tzameli I, Yin H, Flier JS. TLR4 links innate immunity and fatty acid-induced insulin resistance. The Journal of clinical investigation 2006;116:3015-3025.
38. Puri P, Wiest MM, Cheung O, Mirshahi F, Sargeant C, Min HK, et al. The plasma lipidomic signature of nonalcoholic steatohepatitis. Hepatology 2009;50:1827-1838.
39. Guo X, Li H, Xu H, Halim V, Zhang W, Wang H, et al. Palmitoleate induces hepatic steatosis but suppresses liver inflammatory response in mice. PloS one 2012;7:e39286.

SUPPLEMENTAL DATA

Supplement 1. Detailed material and methods

Biochemical analyses of circulating factors

Plasma was obtained via tail vein bleeding after a 5-hour fast at multiple time points throughout the study. Plasma glucose was quantified by hexokinase method (Instruchemie, Delfzijl, The Netherlands) and plasma insulin was determined by ELISA (Ultrasensitive mouse insulin ELISA, Mercodia, Uppsala, Sweden). Leptin and adiponectin plasma levels and Mcp-1 serum levels were determined by ELISA (all R&D Systems Ltd, Abington, UK). Serum concentrations of IL-6 and TNFα were quantified by quantikine ELISA assay (R&D Systems Ltd, Abington, UK). TNFα levels were below the detection limit, therefore excluded from the analysis. Lipidomic analysis was performed in plasma samples collected after 5 hours of fasting and according an well-established method for polar lipids, and without hydrolysis of lipids as reported earlier [1]. Reported lipids were identified and quantified using respective specific standards, except for C14:1 (reported as myristoleic acid) and C20:1 (reported as eicosenoic acid). Lipids are expressed as arbitrary units (AU) relative to internal standard.

Analysis of intrahepatic triglycerides

For determination of liver triglycerides, lipids were extracted from liver homogenates using the Bligh and Dyer method [2]. High performance thin-layer chromatography (HPTLC) was then used to separate the extracted lipids with a silica-gel-60 pre-coated plate. Density areas were measured with a Hewlett Packard Scanjet 4500c and lipid concentrations were calculated by Tina software (version-2.09).

Body composition

Total body fat and lean mass in SHAM and eWATx mice was determined using a NMR Echo MRI whole body composition analyzer (EchoMRI LLC, Houston, TX, USA) at week 24 of HFD feeding. Total body fat mass was expressed as percentage of total body weight.

Real Time Poly chain reaction (RT-PCR) gene expression analysis

Total RNA was extracted with RNA Bee Total RNA Isolation Kit (Bio-Connect, Huissen, the Netherlands). RNA concentration was determined using Nanodrop 1000 (Isogen Life Science, De Meern, the Netherlands) and RNA quality was measured using 2100 Bioanalyzer (Agilent Technologies, Amstelveen, the Netherlands). One microgram of total RNA was used to generate cDNA for RT-PCR (High-capacity RNA-to-cDNA kit; 4387406, Life Technologies, Bleiswijk, the Netherlands). RT-PCR was performed in duplicate on a Fast-7500 using TaqMan gene expression assays (Life Technologies) and specific probe for TNFα (*Tnf,* Mm00443258_m1) and MCP-1(*Ccl2,* Mm00441242_m1). Glyceraldehyde 3-phosphate dehydrogenase (*Gapdh*; 4308313) and hypoxanthine-guanine phosphoribosyltransferase (*Hprt*; Mm00446968_m1) were used as housekeeping genes. Changes in gene expression were calculated using the comparative Ct (ΔΔCt) method and expressed as fold-change relative to mean expression of control.

References Supplement 1

1. Wopereis S, Radonjic M, Rubingh C, Erk M, Smilde A, Duyvenvoorde W, et al. Identification of prognostic and diagnostic biomarkers of glucose intolerance in ApoE3Leiden mice. Physiol Genomics 2012;44:293-304.
2. Bligh EG, Dyer WJ. A rapid method of total lipid extraction and purification. Canadian journal of biochemistry and physiology 1959;37:911-917.

Chapter 3

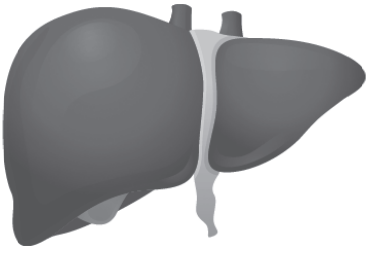
Reduction of obesity-associated white adipose tissue inflammation by rosiglitazone is associated with reduced non-alcoholic fatty liver disease in LDLr-deficient mice

Petra Mulder[1,2], Martine C. Morrison[1], Lars Verschuren[3], Wen Liang[1], J. Hajo van Bockel[2], Teake Kooistra[1], Peter Y. Wielinga[1], Robert Kleemann[1,2]

[1] Department of Metabolic Health Research, Netherlands Organization for Applied Scientific Research (TNO), Zernikedreef 9, 2333 CK Leiden, The Netherlands
[2] Department of Vascular Surgery, Leiden University Medical Center, PO Box 9600, 2300 RC Leiden, The Netherlands
[3] Department of Microbiology and Systems Biology, Netherlands Organization for Applied Scientific Research (TNO), 3704 HE, Zeist, The Netherlands

Scientific Reports. 2016 Aug 22;6:31542. doi: 10.1038/srep31542







ABSTRACT

Obesity is associated with chronic low-grade inflammation that drives the development of metabolic diseases, including non-alcoholic fatty liver disease (NAFLD). We recently showed that white adipose tissue (WAT) constitutes an important source of inflammatory factors. Hence, interventions that attenuate WAT inflammation may reduce NAFLD development. Male LDLr-/- mice were fed a high-fat diet (HFD) for 9 weeks followed by 7 weeks of HFD with or without rosiglitazone. Effects on WAT inflammation and NAFLD development were analyzed using biochemical and (immuno)histochemical techniques, combined with gene expression analyses. Nine weeks of HFD feeding induced obesity and WAT inflammation, which progressed gradually until the end of the study. Rosiglitazone fully blocked progression of WAT inflammation and activated PPARγ significantly in WAT. Rosiglitazone intervention did not activate PPARγ in liver, but improved liver histology and counteracted the expression of genes associated with severe NAFLD in humans. Rosiglitazone reduced expression of pro-inflammatory factors in WAT (TNFα, leptin) and increased expression of adiponectin, which was reflected in plasma. Furthermore, rosiglitazone lowered circulating levels of pro-inflammatory saturated fatty acids. Together, these observations provide a rationale for the observed indirect hepatoprotective effects and suggest that WAT represents a promising therapeutic target for the treatment of obesity-associated NAFLD.

INTRODUCTION

The prevalence of obesity has increased dramatically over the last 30 years and metabolic disorders associated with obesity have become a major health and economic problem worldwide [1]. Obesity is associated with a state of low-grade chronic inflammation, frequently referred to as systemic inflammation or metabolic inflammation [2], which is thought to drive the development of several metabolic diseases including non-alcoholic fatty liver disease (NAFLD) [3,4]. We recently showed that adipose tissue is a critical source of inflammation in obesity and causally involved in NAFLD progression [5]. However, it is unclear whether suppression of adipose tissue inflammation would attenuate NAFLD progression.

White adipose tissue (WAT) is the primary site of energy storage. This storage function involves expansion of WAT through adipocyte hyperplasia (increase in cell number) and adipocyte hypertrophy (increase in cell size) [6]. Adipocyte hypertrophy is closely associated with WAT inflammation: in an in vitro experiment with isolated primary human adipocytes [7], only very hypertrophic cells were found to secrete MCP-1, a key mediator of immune cell recruitment into WAT. Consistent with this observation, adipocyte hypertrophy is associated with infiltration of macrophages and formation of crown-like structures (CLS) [8], a histological hallmark of inflamed WAT. Notably, a strong increase in CLS is observed at the time point at which a WAT depot has reached its maximal mass as shown very recently in a model of diet-induced obesity [5].

It is thought that the inflamed WAT is less insulin sensitive, which enhances lipolysis of stored fat, thereby contributing to ectopic fat deposition and the development of liver steatosis [9]. In line with this, Kolak and colleagues [10] have shown that obese patients with inflamed WAT have more liver fat than equally obese subjects without WAT inflammation. In addition to the increased fat flux, inflamed WAT may produce inflammatory factors that can contribute to systemic inflammation and promote the progression from liver steatosis to non-alcoholic steatohepatitis (NASH) [2,11,12]. However, experimental support for a causal role of WAT in the development of NASH has long been lacking. Recently we have shown that surgical removal of inflamed abdominal (epididymal) WAT in mice reduced

lobular inflammation and attenuated NASH development [5], suggesting that WAT constitutes an possible target for the treatment of NASH.

WAT inflammation may be reduced via the nuclear hormone receptor peroxisome proliferator-activated receptor-γ (PPARγ) which is predominantly expressed in adipose tissue, controlling inflammatory and metabolic processes [13]. Previous studies in humans [14] and animals [15-17], provide indication that pharmacological activators of PPARγ such as rosiglitazone may reduce the inflammatory state of WAT in obesity. We herein investigated whether rosiglitazone intervention can reduce manifest WAT inflammation and would attenuate subsequent NAFLD development. To do so, we first determined the time point at which WAT inflammation develops during high-fat diet treatment in LDLr-/- mice. Subsequently, we studied the therapeutic effect of rosiglitazone on WAT inflammation and associated NAFLD development.

METHODS

Animal experiments

All animal experiments were approved by the institutional Animal Care and Use Committee of the Netherlands Organization of Applied Scientific Research (Zeist, The Netherlands; approval number DEC2935) and were conducted in accordance with the Dutch Law on Animal Experiments, following international guidelines on animal experimentation. Mice (aged 12-14 weeks at the start of the experiment) had ad libitum access to food and water.

Time-course study: Male LDLr-/- mice were fed a high-fat diet (HFD: 45 kcal% lard fat, D12451, Research Diets, New Brunswick, NJ, USA) and were sacrificed after 0, 9 and 16 weeks to collect epididymal WAT (eWAT), mesenteric WAT (mWAT) and inguinal WAT (iWAT). Tissues were prepared essentially as reported [5].

Intervention study: Tissues and plasma were obtained from a large cohort study in which rosiglitazone and other interventions (e.g. fenofibrate) were analyzed [18]. Briefly, one group (n=9) was sacrificed after 9 weeks of HFD to define the condition prior to intervention (reference, REF). The remaining mice continued on

HFD (HFD, n=13) or HFD supplemented with 0.01% w/w rosiglitazone (HFD+Rosi, n=9, Avandia, GSK, Zeist, The Netherlands). A separate control group was kept on chow as a baseline control for microarray and RT-PCR gene expression analysis. In week 16, all animals were sacrificed and WAT depots and liver were collected. Mice (n=2) that did not become obese after 9 weeks of high-fat feeding (i.e. body weight gain 50% less than group mean), were excluded from the analyses.

Histological, biochemical, metabolomics and gene expression analyses

Briefly, WAT characteristics and NAFLD development were quantified histologically as described [5,19]. Immunohistochemistry was performed on frozen, acetone-fixed WAT sections using primary antibodies specific for CCR2 (PA5-23044, Thermo Fisher Scientific, Rockford, IL, USA) and CD11c (BD553800, BD Biosciences, San Diego, CA, USA). After incubation, biotinylated antibodies were detected by incubation with streptavidin-HRP using Nova Red as a substrate (both, Vector Laboratories, Burlingame, CA, USA). All sections were counterstained with hematoxylin. Immunopositive cells were quantified in four different cross-sections per mouse using ImageJ. Intrahepatic triglyceride concentrations were analyzed by high performance thin-layer chromatography (HPTLC) [18]. Plasma parameters were determined with commercially available assays as previously specified [18]. Plasma fatty acids were determined by gas chromatography/mass spectrometry (GC/MS) [18]. The plasma concentration of total free non-esterified fatty acids (NEFAs) was determined with NEFA-HR kit (Instruchemie, Delfzijl, The Netherlands). Illumina microarray gene expression and subsequent pathway analysis of eWAT and liver was performed following established protocols. To analyze potential off-target effects of rosiglitazone in the liver, an upstream transcriptional activator analysis was performed [20]. Microarray data were validated and confirmed by RT-PCR and changes in expression were calculated using the comparative Ct (ΔΔCt) method, expressed as fold-change relative to chow.

Statistical analysis

All data are presented as mean ± SEM. Data were analyzed using one-way ANOVA and least significant difference (LSD) post-hoc test. Non-normally distributed

data were analyzed by Kruskal-Wallis followed by Mann-Whitney U post-hoc test. Correlations were determined by Spearman's rank correlation. Statistically significant differences in plasma fatty acids over time within HFD and HFD+Rosi were analyzed using Student's paired *t*-test. Statistical tests were performed using Graphpad Prism software (version 6, Graphpad Software Inc., La Jolla, USA). $P<0.05$ was considered statistically significant.

RESULTS

WAT inflammation starts in eWAT during high-fat diet-induced obesity

After 16 weeks, CLS formation was most pronounced in eWAT (Figure 1A), while CLS were hardly observed in mWAT and iWAT. Quantitative analysis showed a marked increase in CLS number in eWAT ($p<0.05$; Figure 1B). CLS number correlated with eWAT mass (r=0.80, $p<0.001$, not shown) and with average adipocyte size, a measure of adipocyte hypertrophy (r=0.61, $p<0.01$; Figure 1C). The average adipocyte size in eWAT was greater than in mWAT and iWAT (not shown). Hence, eWAT is most susceptible to develop CLS, with substantial inflammation established after 9 weeks of high-fat feeding.

Rosiglitazone attenuates WAT inflammation independent of obesity and targets WAT

Mice were treated with high-fat diet for 9 weeks to induce obesity (Table 1). At this time point, intervention with rosiglitazone was started. The caloric intake was comparable between the HFD control group and the HFD+Rosi group (14.6±0.7 and 13.4±0.6 kcal/day, respectively). Continuous high-fat feeding increased fasting plasma glucose, while rosiglitazone had a significant lowering effect (Table 1). Rosiglitazone also significantly lowered fasting plasma insulin and HOMA-IR relative to HFD mice (Table 1). Weight gain and total fat mass were comparable between HFD and HFD+Rosi (Table 1), indicating that the observed metabolic effects were independent of obesity.

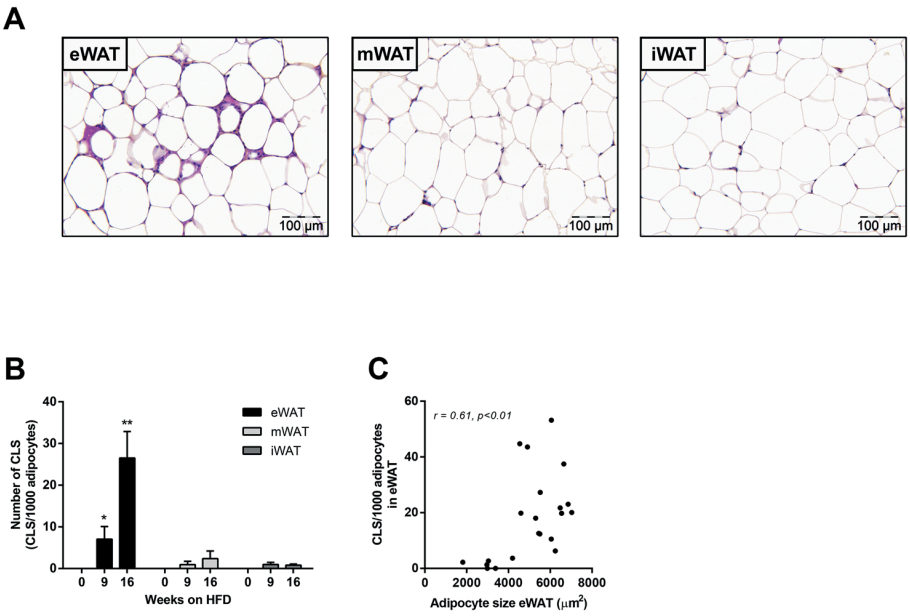


Figure 1. Effect of HFD feeding on development of WAT inflammation. (A) Representative photomicrographs of three WAT depots after 16 weeks of high-fat feeding. (B) Quantitative analysis of CLS formation over time in the major adipose tissue depots, eWAT, mWAT and iWAT. (C) Positive correlation between CLS number and adipocyte size in eWAT. Data are mean±SEM (n=8/group), *p<0.05 compared with t=0; **p<0.05 compared with t=0 and 9 weeks of high-fat feeding.

Table 1 Metabolic parameters of experimental groups

Parameter	Chow	REF	HFD	HFD+Rosi
Body weight gain (g)	3.21 ± 0.48	9.14 ± 1.81*a*	17.49 ± 0.*91b*	17.07 ± 1.*24b*
Total adiposity (g)	1.00 ± 0.11	2.61 ± 0.55*a*	4.41 ± 0.27*b*	4.07 ± 0.28*b*
Glucose (mM)	11.12 ± 0.33	12.52 ± 0.72*a*	15.00 ± 0.48*b*	10.61 ± 0.22*c*
Insulin (ng/ml)	0.65 ± 0.19	2.88 ± 0.80*a*	4.65 ± 0.94*b*	1.40 ± 0.21*c*

Abbreviations: *Chow,* mice fed a chow diet for 16 weeks; *REF,* reference, mice receiving a HFD for 9 weeks to define condition prior to intervention; *HFD,* control mice after 16 weeks of HFD; *HFD+Rosi,* rosiglitazone-treated mice (intervention from 9-16 weeks). *a,* Significantly different from chow; *b,* Significantly different from chow and REF; *c,* Significantly different from HFD (all, p<0.05).

Quantification of CLS in eWAT revealed that CLS numbers were increased in HFD relative to REF, but remained constant in HFD+Rosi (Figure 2A). Hence, rosiglitazone fully blocked further CLS formation but did not resolve existing inflammation (Figure 2B). These effects were paralleled by decreased gene expression of MCP-1 in HFD+Rosi (Figure 2C). Gene expression of macrophage markers revealed that rosiglitazone intervention reduced the pro-inflammatory M1 macrophage markers CD11c and CCR2 (Figure 2D). In addition, rosiglitazone increased the expression of anti-inflammatory M2 macrophage marker Arginase-1, but did not affect CD206 (Figure 2D). Consistent with this, we found less immunoreactivity against CCR2 and CD11c in adipose tissue of mice treated with rosiglitazone as determined by immunohistochemical analysis (Supplement 1). Refined analysis of CLS revealed that CLS contain CCR2+ and CD11c+ cells and some cells expressed both markers in the HFD group as well as the HFD+Rosi group (Supplement 1). Furthermore, rosiglitazone influenced the expression of genes involved in inflammatory and oxidative stress pathways as shown by microarray analysis (Supplement 2). The observed reduction of eWAT inflammation in HFD+Rosi mice was paralleled by a decreased adipocyte size (Figure 2E).

To validate that rosiglitazone affected PPARγ-regulated genes in eWAT under the experimental conditions employed an upstream transcriptional regulator analysis was performed. This analysis demonstrated a highly significantly increased transcriptional activity of PPARγ (Z-score: 4.1, p=5.92e-24). More specifically, rosiglitazone significantly affected the expression of 1049 genes (FDR<0.05), of which 71 are established PPARγ-regulated genes (including fatty acid transporter protein 1, fatty acid binding proteins, perilipin, uncoupling protein-1, acyl-CoA synthetase) (for detailed list, see Supplement 2). By contrast, microarray analysis of corresponding livers under the same statistical cut-off (FDR<0.05) revealed that only 36 genes (among which 4 PPARγ-regulated genes) were differentially expressed by rosiglitazone (Supplement 3), and upstream transcriptional regulator analysis showed no activation of PPARγ. There were also no indications for off-target activation of PPARα or PPARδ from this microarray analysis (Supplement 3). Altogether, these data demonstrated that rosiglitazone significantly activated PPARγ in WAT and attenuated high-fat diet induced WAT inflammation.

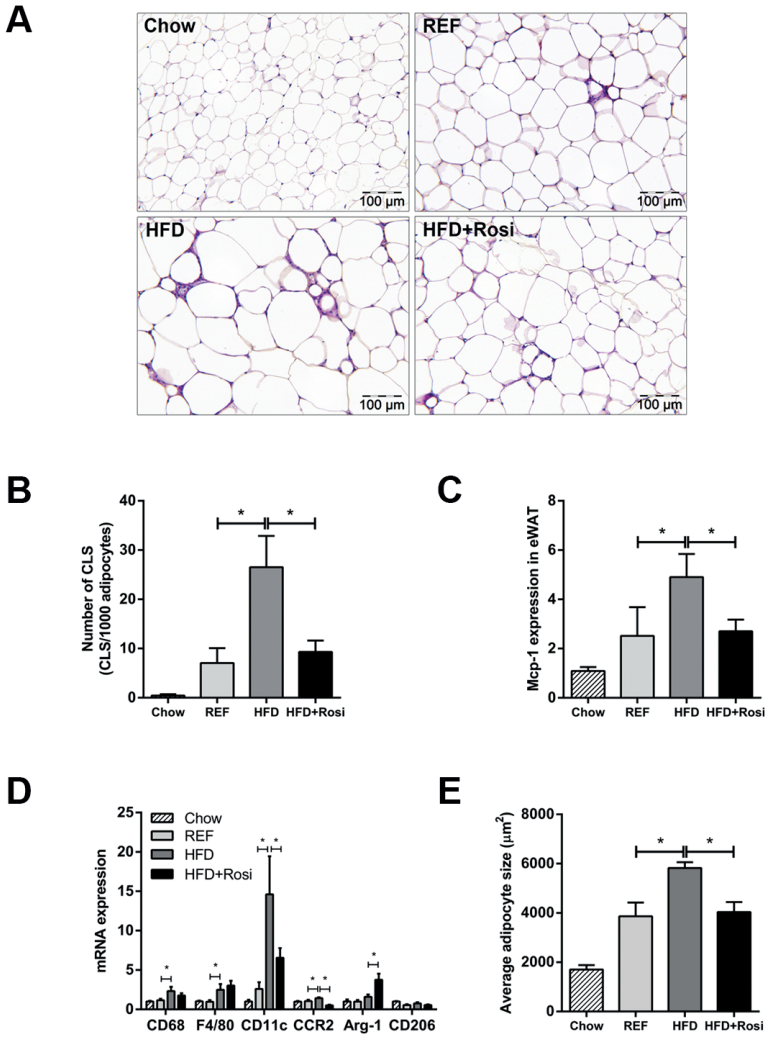


Figure 2. Effects of rosiglitazone intervention on eWAT inflammation. (A) Representative photomicrographs of HPS-stained eWAT cross-sections (magnification x200). (B) High-fat feeding strongly increased CLS formation in eWAT between 9 weeks (REF) and 16 weeks (HFD), while rosiglitazone fully blocked further CLS formation. (C) MCP-1 gene expression was increased in HFD mice, but not in HFD+Rosi. (D) Gene expression of macrophage markers. Rosiglitazone reduced HFD-induced expression of M1 markers (CD11c and CCR2) and increased gene expression of M2 marker Arginase-1 (Arg-1). HFD-induced expression of general macrophage markers, Cd68 and F4/80, was not affected by rosiglitazone. (E) Morphometric analysis of average adipocyte size revealed that rosiglitazone attenuated HFD-induced increase in adipocyte size in eWAT. Data are mean±SEM (n=7-10/group), *p<0.05. Mean expression of RT-PCR data was set 1 for chow-fed mice.

Rosiglitazone prevents progression of NAFLD

Next, we investigated the effects of rosiglitazone intervention on the liver. High-fat feeding resulted in mild/moderate hepatic steatosis after 9 weeks (REF), which was markedly aggravated after 16 weeks (HFD) (Figure 3A). Rosiglitazone blunted the progression of NAFLD and livers resembled those of REF. Biochemical intrahepatic triglyceride analysis showed a significant increase in HFD relative to REF and liver triglyceride concentrations tended to be lower in HFD+Rosi (Figure 3B). Histological analysis revealed a strong increase in microvesicular steatosis in HFD compared with REF and rosiglitazone fully prevented this increase (Figure 3C). Macrovesicular steatosis, a hallmark of NASH in humans [21], was also elevated in HFD and reduced by rosiglitazone (Figure 3D). High-fat treatment activated several pro-inflammatory and pro-fibrotic pathways in liver including those induced by TNFα (Z-score: 2.79; *p*=3.8e-03), IL-6 (Z-score: 2.03; *p*=2.9e-07) and TGFβ1 (Z-score: 1.3; *p*=1.38e-05) as demonstrated by pathway analysis (FDR<0.05). Moreover, high-fat treatment induced several genes which were recently identified in human NASH/fibrosis patients [22] (Table 2). Rosiglitazone treatment attenuated this effect and counteracted the expression of genes including Col14A1, TaxIBP3, EFEMP2, EGFBP7, THBS2, BICC1 and DKK3. Furthermore, RT-PCR analysis of TNFα, which plays an essential role in NASH, showed increased TNFα gene expression in HFD mice and that rosiglitazone treatment quenched this induction (Figure 3E). Similarly, HFD-induced expression of pro-fibrotic genes Col1a1, Col1a2 and TIMP-1 were suppressed by rosiglitazone intervention (Figure 3F). High-fat feeding also resulted in infiltration of neutrophils (MPO-positive inflammatory cells) and formation of inflammatory cell aggregates characteristic for NASH [23] between 9 and 16 weeks which was attenuated by rosiglitazone (Supplement 4). Analysis of Sirius-red stained liver cross-sections of the HFD group revealed onset of perisinusoidal fibrosis, which was not observed in HFD+Rosi (Figure 3G). Altogether, intervention with rosiglitazone attenuated the progression from steatosis to NASH.

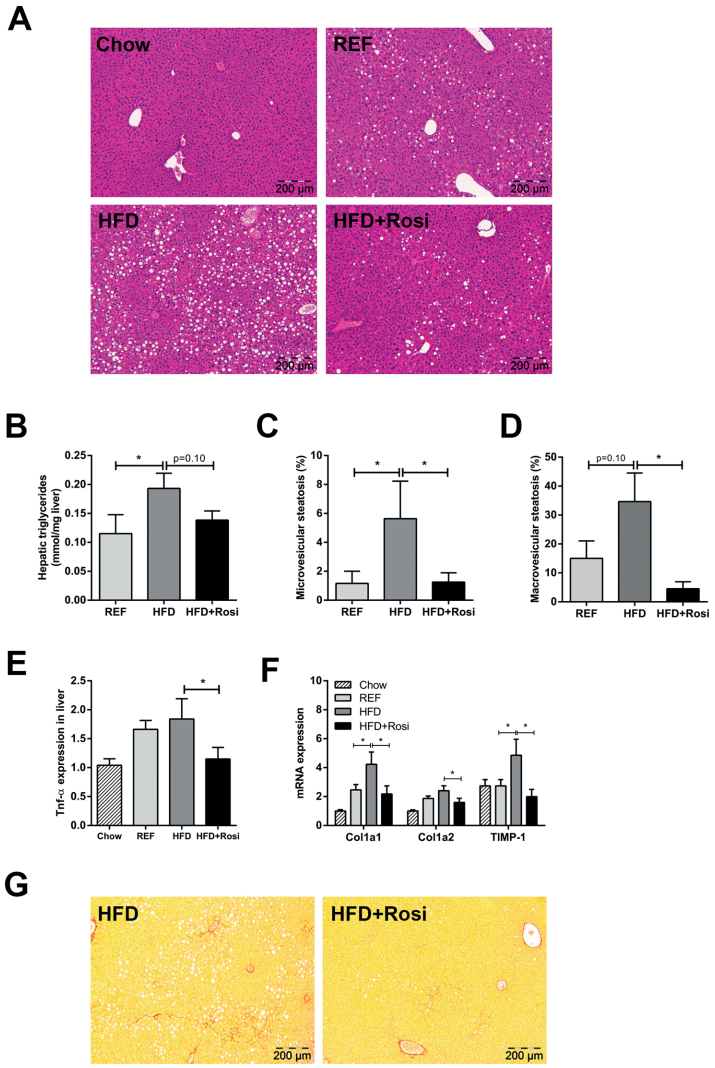


Figure 3. Effects of rosiglitazone intervention on NAFLD development. (A) Representative photomicrographs of HE-stained liver sections of REF, HFD and HFD+Rosi. (B) Biochemical analysis of hepatic triglyceride content. Histological quantification of (C) microvesicular steatosis and (D) macrovesicular steatosis show that steatosis was ameliorated with rosiglitazone compared with HFD (n=7-10/group). (E) TNFα gene expression in liver was diminished in rosiglitazone-treated mice (n=7-8/group). (F) Gene expression of fibrotic genes determined by RT-PCR. Rosiglitazone reduced HFD-induced expression of Col1a1, Col1a2 and TIMP-1. (G) Onset of fibrosis in Sirius Red-stained liver cross-sections in HFD mice, but not in HFD+Rosi. Pictures are shown in magnification x100. Data are mean±SEM, *p<0.05. Mean expression of RT-PCR data was set 1 for chow-fed mice.

Table 2. Microarray analysis of hepatic gene expression profile based on genes identified in human NAFLD

			HFD vs Chow			HFD+Rosi vs HFD		
probeID	**Gene symbol**	**Gene name**	**Fold-Change**		**p-value**	**Fold-Change**		**p-value**
ILMN_2635229	Thbs2	thrombospondin 2	1,740	↑	9,47E-06	0,650	↓	4,62E-04
ILMN_2764588	Igfbp7	insulin-like growth factor binding protein 7	1,465	↑	1,79E-05	0,834	↓	3,52E-02
ILMN_1217309	Tax1bp3	Tax1 (human T-cell leukemia virus type I) binding protein 3	1,360	↑	7,45E-04	0,826	↓	3,28E-02
ILMN_2866901	Efemp2	epidermal growth factor-containing fibulin-like extracellular matrix protein 2	1,556	↑	7,62E-04	0,751	↓	2,70E-02
ILMN_2636424	Itgbl1	integrin, beta-like 1	1,528	↑	1,11E-03	0,905		4,33E-01
ILMN_2746556	Dkk3	dickkopf homolog 3 (Xenopus laevis)	1,402	↑	1,16E-03	0,744	↓	4,27E-03
ILMN_1258629	Col3a1	collagen, type III, alpha 1	1,887	↑	1,61E-03	0,746		1,39E-01
ILMN_2939138	Bicc1	bicaudal C homolog 1 (Drosophila)	1,460	↑	2,69E-03	0,666	↓	1,28E-03
ILMN_2746086	Tax1bp3	Tax1 (human T-cell leukemia virus type I) binding protein 3	1,334	↑	2,94E-03	0,787	↓	1,27E-02
ILMN_2980663	Aqp1	aquaporin 1	0,812	↓	7,68E-03	1,158	↑	5,74E-02
ILMN_2606210	Dpt	dermatopontin	1,459	↑	1,08E-02	0,714	↓	2,26E-02
ILMN_3007428	Sox9	SRY-box containing gene 9	0,694	↓	1,11E-02	1,245		1,23E-01
ILMN_2831656	Epha3	Eph receptor A3	1,334	↑	1,76E-02	0,901		3,84E-01
ILMN_2687872	Col1a1	collagen, type I, alpha 1	1,471	↑	3,99E-02	0,921		6,58E-01
ILMN_2747959	Dcn	decorin	1,151	↑	4,22E-02	0,874	↓	5,21E-02
ILMN_2591027	Col14a1	collagen, type XIV, alpha 1	1,176	↑	4,74E-02	0,820	↓	1,61E-02
ILMN_1223552	Fbn1	fibrillin 1	1,181		6,25E-02	0,885		1,69E-01
ILMN_1233545	Lbh	limb-bud and heart	0,782		6,40E-02	1,089		5,19E-01
ILMN_2669189	Lima1	LIM domain and actin binding 1	1,226		8,23E-02	0,956		6,98E-01
ILMN_1253806	Col1a2	collagen, type I, alpha 2	1,278		8,24E-02	0,837		2,08E-01
ILMN_2852957	Dkk3	dickkopf homolog 3 (Xenopus laevis)	1,184		8,82E-02	0,941		5,38E-01
ILMN_1214954	Cldn10	claudin 10	0,836		1,39E-01	1,143		2,68E-01
ILMN_1228374	Lima1	LIM domain and actin binding 1	1,190		1,48E-01	0,916		4,66E-01
ILMN_2980661	Aqp1	aquaporin 1	0,895		1,89E-01	1,124		1,65E-01
ILMN_1226183	Antxr1	anthrax toxin receptor 1	1,211		1,91E-01	0,815		1,63E-01

Table 2. Microarray analysis of hepatic gene expression profile based on genes identified in human NAFLD (continued)

			HFD vs Chow		HFD+Rosi vs HFD		
probeID	Gene symbol	Gene name	Fold-Change	p-value	Fold-Change		p-value
ILMN_2848305	Pnma1	paraneoplastic antigen MA1	1,144	1,96E-01	0,993		9,43E-01
ILMN_2666018	Mgp	matrix Gla protein	1,162	1,99E-01	0,914		4,39E-01
ILMN_2816180	Lbh	limb-bud and heart	1,137	2,24E-01	0,902		3,29E-01
ILMN_1257077	Jag1	jagged 1	1,160	2,33E-01	0,941		6,22E-01
ILMN_2734683	Fstl1	follistatin-like 1	1,119	2,71E-01	0,949		6,11E-01
ILMN_2596346	Dcn	decorin	1,102	3,26E-01	0,834		6,82E-02
ILMN_2597515	Ehf	ets homologous factor	1,147	3,35E-01	1,055		7,05E-01
ILMN_3001540	Lum	lumican	1,101	4,53E-01	0,817		1,17E-01
ILMN_1227817	Ank3	ankyrin 3, epithelial	1,109	4,57E-01	0,940		6,58E-01
ILMN_2769479	Lama2	laminin, alpha 2	1,116	4,87E-01	0,968		8,38E-01
ILMN_2893417	Sox4	SRY-box containing gene 4	0,929	5,57E-01	0,965		7,75E-01
ILMN_1223963	Ank3	ankyrin 3, epithelial	1,081	5,62E-01	0,835		1,83E-01
ILMN_2836637	Glt8d2	glycosyltransferase 8 domain containing 2	1,078	5,91E-01	1,229		1,45E-01
ILMN_1249021	Bcl2	B-cell leukemia/lymphoma 2	1,058	5,99E-01	0,937		5,50E-01
ILMN_1229643	Antxr1	anthrax toxin receptor 1	1,066	6,02E-01	0,779	↓	4,37E-02
ILMN_2620563	Nexn	nexilin	1,081	6,07E-01	0,771		8,88E-02
ILMN_1238000	Srpx	sushi-repeat-containing protein	1,056	6,75E-01	1,095		4,83E-01
ILMN_2621643	Col4a1	collagen, type IV, alpha 1	1,044	7,12E-01	1,125		3,12E-01
ILMN_2629486	Srpx	sushi-repeat-containing protein	0,958	7,70E-01	0,832		2,12E-01
ILMN_2686036	Tax1bp3	Tax1 (human T-cell leukemia virus type I) binding protein 3	1,030	8,04E-01	1,004		9,72E-01
ILMN_2701712	Plcxd3	phosphatidylinositol-specific phospholipase C, X domain containing 3	0,982	8,80E-01	0,943		6,22E-01
ILMN_2629804	Epha3	Eph receptor A3	0,987	9,04E-01	1,100		3,67E-01

The table lists the genes that were recently reported to be associated with NAFLD severity in humans.[19] HFD feeding of LDLr-/- mice resulted in a significant effect on 16 genes compared to chow (arrows indicate significant up- (↑) or downregulation (↓)). Rosiglitazone counteracted the effect of a HFD as shown by the comparison of HFD+Rosi vs. HFD.

Rationale for the hepatoprotective effects of rosiglitazone

In eWAT, rosiglitazone blocked the HFD-induced gene expression of leptin and TNFα (Figure 4A, B). These effects were paralleled in plasma; HFD+Rosi reduced concentrations of leptin and TNFα (Supplement 5). By contrast, rosiglitazone fully restored the high-fat induced decrease in adiponectin gene expression in eWAT (Figure 4C) which was also reflected in plasma (Supplement 5). In addition, rosiglitazone prevented the high-fat diet-induced increase in total saturated fatty acids in plasma (Figure 4D). In line with this, total NEFA were significantly increased (by 26%, $p<0.05$) in the HFD group, whereas no significant increase was observed in the HFD+Rosi group (11%, n.s.). More specifically, plasma concentrations of palmitic acid (C16:0) and stearic acid (C18:0) were not increased in HFD+Rosi (Figure 4D).

Since WAT inflammation correlated with WAT mass and adipocyte hypertrophy we analyzed effects of rosiglitazone on eWAT, iWAT and mWAT in more detail (Figure 4E). During intervention with rosiglitazone, eWAT mass did not further increase while iWAT mass almost doubled, indicating a shift of fat mass from eWAT towards iWAT. Despite the increase in iWAT mass, this depot did not become inflamed (Figure 4F). Quantification of adipocyte size showed that the expansion in iWAT was mainly attributable to an increase in adipocyte number rather than adipocyte size (Figure 4G). This suggests that increased capability of iWAT to store fat may prevent the development of hypertrophy and associated inflammation in eWAT, and may thereby contribute to beneficial effects of rosiglitazone on NAFLD development.

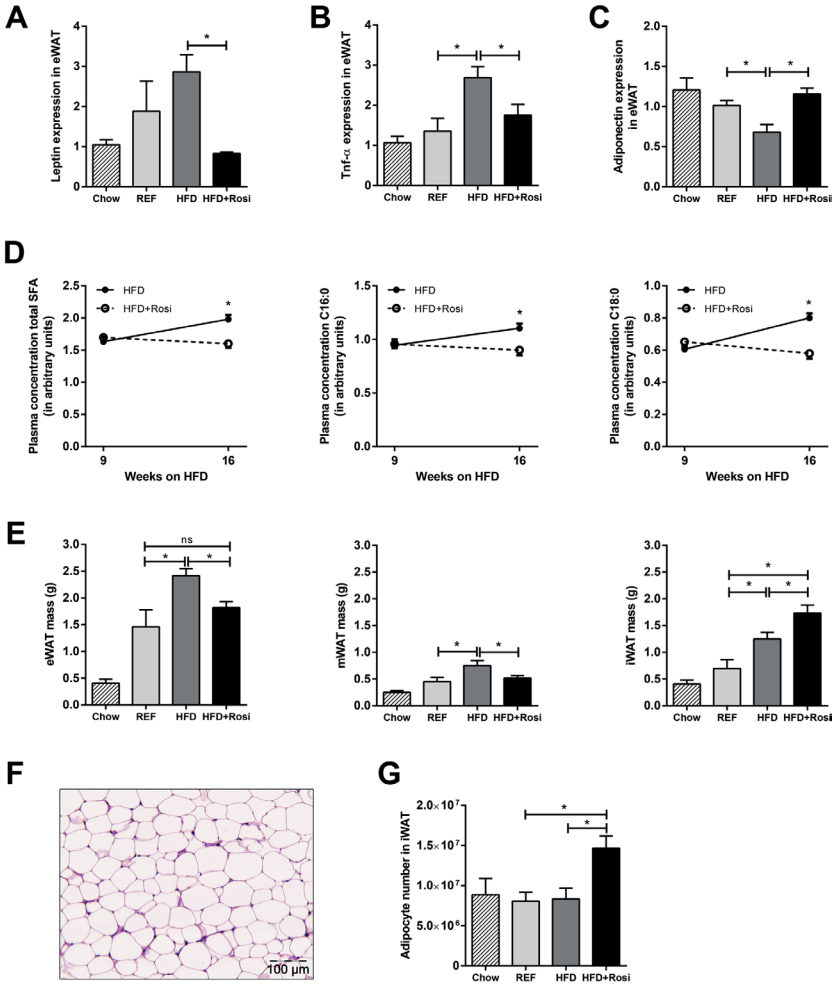


Figure 4. Effects of rosiglitazone on adipokine expression in eWAT, pro-inflammatory fatty acids in plasma and WAT morphology. High-fat feeding increased gene expression in eWAT of pro-inflammatory adipokines (A) leptin, (B) TNFα and decreased expression of (C) anti-inflammatory adipokine adiponectin, while rosiglitazone counteracted these effects. (D) Plasma levels of total saturated fatty acids (SFA) and specific SFAs, palmitic acid (C16:0) and stearic acid (C18:0), were increased between week 9 and 16 of high-fat feeding. This increase was blunted by rosiglitazone (all $p<0.01$; paired t-test; n=9-12/group). (E) The mass of WAT depots was increased in HFD, while rosiglitazone specifically increased iWAT mass. (F) Representative photomicrograph of iWAT in HFD+Rosi, showing absence of CLS. (G) Expansion of iWAT mass in HFD+Rosi was mainly attributable to an increase in adipocyte number. Data are mean±SEM, *$p<0.05$. Mean expression of RT-PCR data was set 1 for chow-fed mice (n=7-8/group). Fatty acid plasma concentration was expressed as arbitrary units relative to internal standard.

DISCUSSION

Recent findings indicate that inflamed (abdominal) WAT plays a causal role in the development of NASH in the context of obesity [5]. WAT may thus constitute a new target for intervention. Compounds that specifically target and quench WAT inflammation have not been developed yet. We therefore used rosiglitazone, an activator of PPARγ with reported anti-inflammatory properties [14-16], as a model compound to intervene in manifest WAT inflammation. Here, we show that rosiglitazone attenuates WAT inflammation and reduces NASH development.

Under the experimental conditions employed herein, rosiglitazone activated PPARγ in WAT, but not in liver, based on a comprehensive analysis of PPARγ-regulated genes. The significant activation of PPARγ in WAT may be important for the observed hepatoprotective effects, because PPARγ activation in liver could cause detrimental effects: Recent knock-out studies have shown that targeted PPARγ deletion in hepatocytes or macrophages protected mice against high-fat induced steatosis [24], while deletion of PPARγ in adipose tissues increased liver steatosis upon high-fat feeding [25]. Furthermore, rosiglitazone treatment remained effective in mice lacking PPARγ specifically in the liver,[26] supporting the view that adipose tissue is an important site of thiazolidinedione action. Consistent with our findings, beneficial effects of rosiglitazone in NAFLD were also observed in aged (12 months old) LDLr-/- mice that develop a more severe disease phenotype than young mice (3 months old) as used herein [27]. However, this study did not examine the effects of rosiglitazone in a therapeutic (intervention) setting and its effects in adipose tissue were not analyzed. In the study by Gupte and colleagues [27], the diet was supplemented with cholesterol which may explain some of the differences observed on liver gene expression and inflammation. Dietary cholesterol has been shown to be a strong inducer of inflammatory gene expression in the liver [28,29]. For instance, treatment with a HFD supplemented with small amounts (0.2% w/w) of cholesterol triggered Kupffer cell activation and inflammatory gene expression after already 2 weeks in LDLr-/- mice, whereas the same diet without cholesterol hardly had an effect on liver inflammation [29]. High-fat diets without cholesterol supplementation induce liver inflammation typically at a slower pace

and, importantly, this liver inflammation is at least partly mediated by the inflamed white adipose tissue (WAT) [5]. However, it is unclear to which extent WAT may contribute to liver inflammation when cholesterol is added to a high-fat diet.

We found that eWAT is more susceptible to develop chronic inflammation than mWAT or iWAT. This observation may be related to the fact that adipocytes in eWAT are more prone to hypertrophy than those in other adipose depots [30]. In the present study, CLS numbers in eWAT correlated with adipocyte size supporting the importance of adipocyte hypertrophy in the development of WAT inflammation [6-8]. Consistent with this, metabolically healthy obese subjects were found to have significantly smaller adipocytes compared with metabolically unhealthy obese patients who had more ectopic liver fat at a comparable body mass index [31]. This suggests that the ability to expand WAT through mechanisms of adipocyte hyperplasia may prevent: a) WAT inflammation and b) ectopic fat accumulation, thereby contributing to a healthy metabolic state.

We observed that rosiglitazone stimulated hyperplasia specifically in subcutaneous WAT thereby preventing adipocyte hypertrophy, which is also observed in patients treated with thiazolidinediones [32,33]. Consequently, this depot did not become inflamed even though its mass was much greater than in control animals, as is seen in humans treated with rosiglitazone.[34] The observed stimulation of hyperplasia specifically in iWAT by rosiglitazone may be explained by depot-specific regulation of perilipin, which is essential for enlargement of lipid droplets. Kim and co-workers showed that perilipin protein expression increased after rosiglitazone treatment in subcutaneous adipose tissue, but did not change in visceral adipose tissue [35].

Clinical trials have shown that treatment with thiazolidinediones can improve liver histology in patients with NASH [36,37]. However, the underlying mechanisms mediating the beneficial effects of thiazolidinediones in NASH development are unclear. Data from the present study support the view that rosiglitazone may attenuate the development of NAFLD via an effect on WAT. Several studies showed that infiltration of macrophages into WAT is strongly associated with NAFLD development [10,38,39]. More specifically, an increase in CD11c+CD206+and CCR2+ macrophages in WAT is associated with enhanced production of pro-inflammatory

adipokines and cytokines in WAT, and NASH severity [39]. Herein we show that rosiglitazone intervention reduced the expression of pro-inflammatory M1 markers, CD11c and CCR2 and increased the expression of anti-inflammatory M2 marker, Arginase-1. An increase in Arginase-1 expression has also been observed in HFD-fed Sv129 mice after treatment with rosiglitazone, but rosiglitazone did not alter the expression of CD11c which may be related to the relatively short intervention period [17]. Long-term rosiglitazone treatment in ob/ob mice resulted in lower CD11c expression level in WAT [40], which is consistent with our findings. Analysis of CLS in the present study shows that long-term rosiglitazone intervention attenuates WAT inflammation by reducing CLS numbers (Figure 2B), rather than altering the activation state of immune cells within a CLS (as determined CD11c and CCR2 immunoreactivity).

Our study indicates that the hepatoprotective effects on NASH by rosiglitazone may at least partly be mediated by adipokines, since plasma leptin and TNFα levels were reduced and plasma adiponectin levels were increased. It is known that leptin can exert pro-inflammatory effects and can activate hepatic stellate cells thereby promoting fibrosis [41]. TNFα plays a crucial role in human and animal NAFLD and neutralization of TNFα activity attenuated the disease.[42] For instance, adiponectin is a potent TNFα-neutralizing cytokine that counteracts inflammation that is relevant for NASH progression [41,42]. It has been demonstrated that also saturated fatty acids can activate inflammatory cascades leading to activation of TNFα.[43] We found that the saturated fatty acids; palmitic acid and stearic acid, were markedly increased by high-fat feeding and reduced with rosiglitazone. Notably, these fatty acids are also increased in patients with diagnosed NASH [44]. Furthermore, surgical excision of inflamed WAT in mice lowered palmitic acid in plasma and reduced progression towards NASH [5]. *In vitro* experiments have shown that conditioned medium from palmitic acid-treated hepatocytes induces the expression of pro-fibrotic genes in hepatic stellate cells [45], providing mechanistic support for a crucial role of inflammatory lipid mediators in NASH. We also observed that rosiglitazone attenuated the HFD-induced hepatic expression of the genes encoding for Col1A1, Col1A2 and TIMP-1. This hepatoprotective effect of rosiglitazone was further substantiated by an effect on genes that are associated

with severity of human NAFLD as shown by Moylan et al [22]. These findings support the view that the experimental conditions established herein (HFD-induced obesity, hyperinsulinemia, WAT inflammation concurrent with histologic NASH) may facilitate preclinical research that aims at translation to the human setting.

In all, intervention with rosiglitazone reduces WAT inflammation, lowers circulating inflammatory mediators and attenuates NAFLD progression. These effects were independent of total adiposity and body weight, indicating that adipose tissue quality (i.e. inflammatory state) rather than absolute mass is critical for NAFLD development. Our results suggest that intervention in WAT may present a new therapeutic option for the treatment of NAFLD.

ACKNOWLEDGEMENTS

The authors would like to thank Erik Offerman, Wim van Duyvenvoorde, Karin Toet, Elvira Fluitsma and Anne Schwerk for their excellent technical assistance. This study was supported by the TNO research programs ‘Enabling Technology Systems Biology’ and ‘Predictive Health Technologies’.

REFERENCES

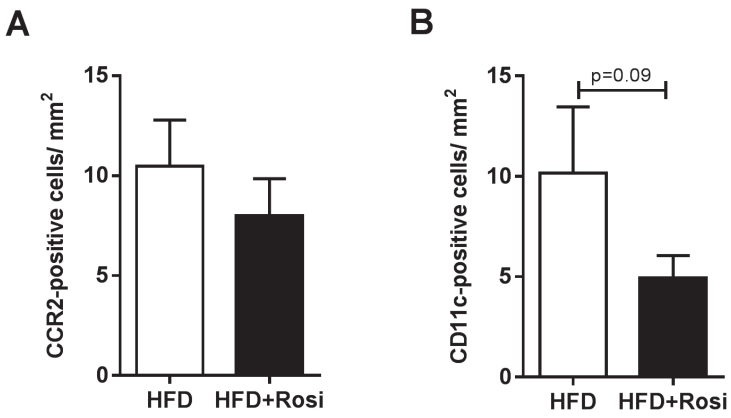
1. Ng M, Fleming T, Robinson M, Thomson B, Graetz N, Margono C, et al. Global, regional, and national prevalence of overweight and obesity in children and adults during 1980-2013: a systematic analysis for the Global Burden of Disease Study 2013. Lancet 2014;384:766-781.
2. Hotamisligil GS. Inflammation and metabolic disorders. Nature 2006;444:860-867.
3. Lumeng CN, Saltiel AR. Inflammatory links between obesity and metabolic disease. The Journal of clinical investigation 2011;121:2111-2117.
4. Tilg H, Moschen AR. Insulin resistance, inflammation, and non-alcoholic fatty liver disease. Trends Endocrinol Metab 2008;19:371-379.
5. Mulder P, Morrison MC, Wielinga PY, van Duyvenvoorde W, Kooistra T, Kleemann R. Surgical removal of inflamed epididymal white adipose tissue attenuates the development of non-alcoholic steatohepatitis in obesity. International journal of obesity 2015.
6. Bays HE, Gonzalez-Campoy JM, Bray GA, Kitabchi AE, Bergman DA, Schorr AB, et al. Pathogenic potential of adipose tissue and metabolic consequences of adipocyte hypertrophy and increased visceral adiposity. Expert review of cardiovascular therapy 2008;6:343-368.
7. Skurk T, Alberti-Huber C, Herder C, Hauner H. Relationship between adipocyte size and adipokine expression and secretion. The Journal of clinical endocrinology and metabolism 2007;92:1023-1033.
8. Cinti S, Mitchell G, Barbatelli G, Murano I, Ceresi E, Faloia E, et al. Adipocyte death defines macrophage localization and function in adipose tissue of obese mice and humans. Journal of lipid research 2005;46:2347-2355.
9. Fabbrini E, Sullivan S, Klein S. Obesity and nonalcoholic fatty liver disease: biochemical, metabolic, and clinical implications. Hepatology 2010;51:679-689.
10. Kolak M, Westerbacka J, Velagapudi VR, Wagsater D, Yetukuri L, Makkonen J, et al. Adipose tissue inflammation and increased ceramide content characterize subjects with high liver fat content independent of obesity. Diabetes 2007;56:1960-1968.
11. Mirza MS. Obesity, Visceral Fat, and NAFLD: Querying the Role of Adipokines in the Progression of Nonalcoholic Fatty Liver Disease. ISRN gastroenterology 2011;2011:592404.
12. Tilg H, Moschen AR. Adipocytokines: mediators linking adipose tissue, inflammation and immunity. Nature reviews Immunology 2006;6:772-783.
13. Olefsky JM, Glass CK. Macrophages, inflammation, and insulin resistance. Annual review of physiology 2010;72:219-246.
14. Kolak M, Yki-Jarvinen H, Kannisto K, Tiikkainen M, Hamsten A, Eriksson P, et al. Effects of chronic rosiglitazone therapy on gene expression in human adipose tissue in vivo in patients with type 2 diabetes. The Journal of clinical endocrinology and metabolism 2007;92:720-724.
15. Xu H, Barnes GT, Yang Q, Tan G, Yang D, Chou CJ, et al. Chronic inflammation in fat plays a crucial role in the development of obesity-related insulin resistance. The Journal of clinical investigation 2003;112:1821-1830.
16. Nguyen MT, Chen A, Lu WJ, Fan W, Li PP, Oh DY, et al. Regulation of chemokine and chemokine receptor expression by PPARgamma in adipocytes and macrophages. PloS one 2012;7:e34976.
17. Stienstra R, Duval C, Keshtkar S, van der Laak J, Kersten S, Muller M. Peroxisome proliferator-activated receptor gamma activation promotes infiltration of alternatively

activated macrophages into adipose tissue. The Journal of biological chemistry 2008;283:22620-22627.
18. Radonjic M, Wielinga PY, Wopereis S, Kelder T, Goelela VS, Verschuren L, et al. Differential effects of drug interventions and dietary lifestyle in developing type 2 diabetes and complications: a systems biology analysis in LDLr-/- mice. PloS one 2013;8:e56122.
19. Liang W, Menke AL, Driessen A, Koek GH, Lindeman JH, Stoop R, et al. Establishment of a general NAFLD scoring system for rodent models and comparison to human liver pathology. PloS one 2014;9:e115922.
20. Liang W, Tonini G, Mulder P, Kelder T, van Erk M, van den Hoek AM, et al. Coordinated and interactive expression of genes of lipid metabolism and inflammation in adipose tissue and liver during metabolic overload. PloS one 2013;8:e75290.
21. Tiniakos DG, Vos MB, Brunt EM. Nonalcoholic fatty liver disease: pathology and pathogenesis. Annual review of pathology 2010;5:145-171.
22. Moylan CA, Pang H, Dellinger A, Suzuki A, Garrett ME, Guy CD, et al. Hepatic gene expression profiles differentiate presymptomatic patients with mild versus severe nonalcoholic fatty liver disease. Hepatology 2014;59:471-482.
23. Liang W, Lindeman JH, Menke AL, Koonen DP, Morrison M, Havekes LM, et al. Metabolically induced liver inflammation leads to NASH and differs from LPS- or IL-1beta-induced chronic inflammation. Laboratory investigation; a journal of technical methods and pathology 2014;94:491-502.
24. Moran-Salvador E, Lopez-Parra M, Garcia-Alonso V, Titos E, Martinez-Clemente M, Gonzalez-Periz A, et al. Role for PPARgamma in obesity-induced hepatic steatosis as determined by hepatocyte- and macrophage-specific conditional knockouts. FASEB journal : official publication of the Federation of American Societies for Experimental Biology 2011;25:2538-2550.
25. He W, Barak Y, Hevener A, Olson P, Liao D, Le J, et al. Adipose-specific peroxisome proliferator-activated receptor gamma knockout causes insulin resistance in fat and liver but not in muscle. Proceedings of the National Academy of Sciences of the United States of America 2003;100:15712-15717.
26. Gavrilova O, Haluzik M, Matsusue K, Cutson JJ, Johnson L, Dietz KR, et al. Liver peroxisome proliferator-activated receptor gamma contributes to hepatic steatosis, triglyceride clearance, and regulation of body fat mass. The Journal of biological chemistry 2003;278:34268-34276.
27. Gupte AA, Liu JZ, Ren Y, Minze LJ, Wiles JR, Collins AR, et al. Rosiglitazone attenuates age- and diet-associated nonalcoholic steatohepatitis in male low-density lipoprotein receptor knockout mice. Hepatology 2010;52:2001-2011.
28. Wouters K, van Gorp PJ, Bieghs V, Gijbels MJ, Duimel H, Lutjohann D, et al. Dietary cholesterol, rather than liver steatosis, leads to hepatic inflammation in hyperlipidemic mouse models of nonalcoholic steatohepatitis. Hepatology 2008;48:474-486.
29. Funke A, Schreurs M, Aparicio-Vergara M, Sheedfar F, Gruben N, Kloosterhuis NJ, et al. Cholesterol-induced hepatic inflammation does not contribute to the development of insulin resistance in male LDL receptor knockout mice. Atherosclerosis 2014;232:390-396.
30. Caesar R, Manieri M, Kelder T, Boekschoten M, Evelo C, Muller M, et al. A combined transcriptomics and lipidomics analysis of subcutaneous, epididymal and mesenteric adipose tissue reveals marked functional differences. PloS one 2010;5:e11525.
31. O'Connell J, Lynch L, Cawood TJ, Kwasnik A, Nolan N, Geoghegan J, et al. The relationship of omental and subcutaneous adipocyte size to metabolic disease in severe obesity. PloS one 2010;5:e9997.

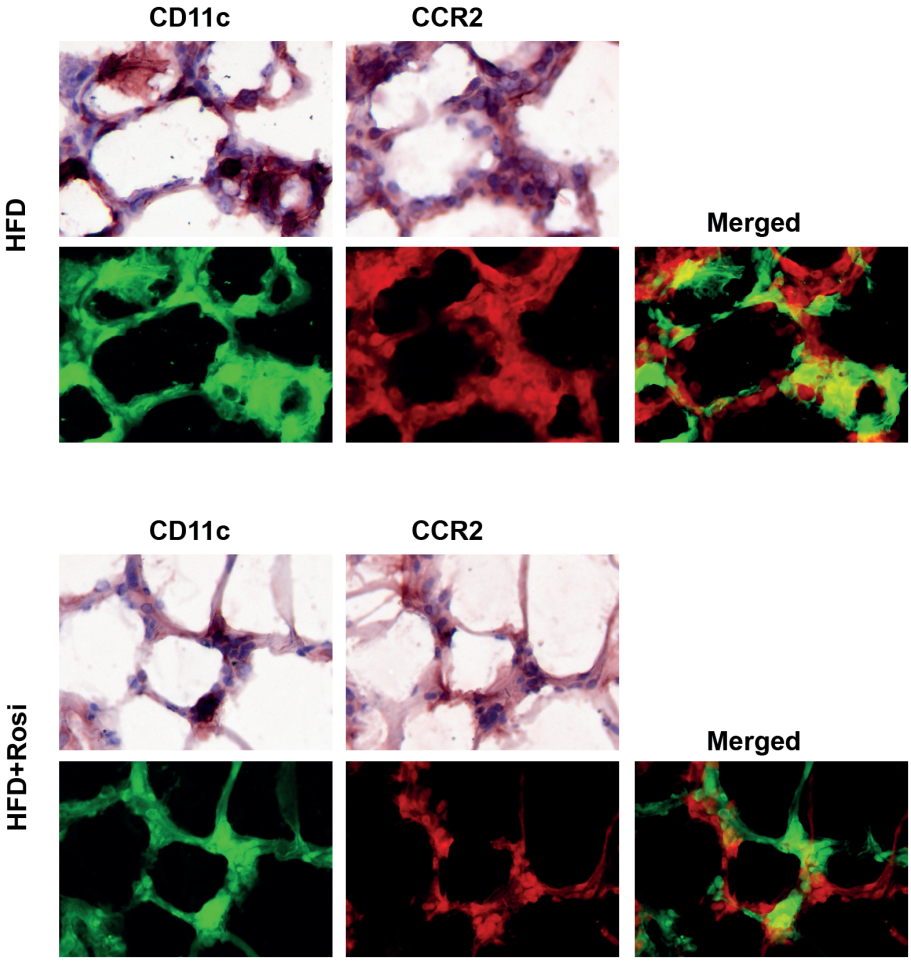
32. Boden G, Cheung P, Mozzoli M, Fried SK. Effect of thiazolidinediones on glucose and fatty acid metabolism in patients with type 2 diabetes. Metabolism: clinical and experimental 2003;52:753-759.
33. McLaughlin TM, Liu T, Yee G, Abbasi F, Lamendola C, Reaven GM, et al. Pioglitazone increases the proportion of small cells in human abdominal subcutaneous adipose tissue. Obesity 2010;18:926-931.
34. Smith U, Hammarstedt A. Antagonistic effects of thiazolidinediones and cytokines in lipotoxicity. Biochim Biophys Acta 2010;1801:377-380.
35. Kim HJ, Jung TW, Kang ES, Kim DJ, Ahn CW, Lee KW, et al. Depot-specific regulation of perilipin by rosiglitazone in a diabetic animal model. Metabolism: clinical and experimental 2007;56:676-685.
36. Neuschwander-Tetri BA, Brunt EM, Wehmeier KR, Oliver D, Bacon BR. Improved nonalcoholic steatohepatitis after 48 weeks of treatment with the PPAR-gamma ligand rosiglitazone. Hepatology 2003;38:1008-1017.
37. Belfort R, Harrison SA, Brown K, Darland C, Finch J, Hardies J, et al. A placebo-controlled trial of pioglitazone in subjects with nonalcoholic steatohepatitis. The New England journal of medicine 2006;355:2297-2307.
38. Cancello R, Tordjman J, Poitou C, Guilhem G, Bouillot JL, Hugol D, et al. Increased infiltration of macrophages in omental adipose tissue is associated with marked hepatic lesions in morbid human obesity. Diabetes 2006;55:1554-1561.
39. du Plessis J, van Pelt J, Korf H, Mathieu C, van der Schueren B, Lannoo M, et al. Association of Adipose Tissue Inflammation With Histologic Severity of Nonalcoholic Fatty Liver Disease. Gastroenterology 2015;149:635-648 e614.
40. Prieur X, Mok CY, Velagapudi VR, Nunez V, Fuentes L, Montaner D, et al. Differential lipid partitioning between adipocytes and tissue macrophages modulates macrophage lipotoxicity and M2/M1 polarization in obese mice. Diabetes 2011;60:797-809.
41. Marra F, Lotersztajn S. Pathophysiology of NASH: perspectives for a targeted treatment. Current pharmaceutical design 2013;19:5250-5269.
42. Tilg H. The role of cytokines in non-alcoholic fatty liver disease. Digestive diseases 2010;28:179-185.
43. Shi H, Kokoeva MV, Inouye K, Tzameli I, Yin H, Flier JS. TLR4 links innate immunity and fatty acid-induced insulin resistance. The Journal of clinical investigation 2006;116:3015-3025.
44. de Almeida IT, Cortez-Pinto H, Fidalgo G, Rodrigues D, Camilo ME. Plasma total and free fatty acids composition in human non-alcoholic steatohepatitis. Clinical nutrition 2002;21:219-223.
45. Wobser H, Dorn C, Weiss TS, Amann T, Bollheimer C, Buttner R, et al. Lipid accumulation in hepatocytes induces fibrogenic activation of hepatic stellate cells. Cell research 2009;19:996-1005.

SUPPLEMENTAL DATA

Supplement 1: Effect of rosiglitazone intervention on inflammatory CCR2-positive and CD11c-positive immune cells in adipose tissue



Supplementary Figure 1. To investigate whether rosiglitazone intervention modulates adipose tissue immune cell activation, we have performed immunohistochemical stainings using primary antibodies against CCR2 and CD11c on adipose tissue cross-sections of mice fed a high-fat diet (HFD) or a HFD supplemented with rosiglitazone (HFD+Rosi). We found less immunoreactivity against CCR2 (**Supplementary figure 1A**) and CD11c (**Supplementary figure 1B**) in mice treated with rosiglitazone, which is consistent with the gene expression data. Values are expressed as mean±SEM and expressed as positively stained cells per mm^2 adipose tissue (n=4/group).

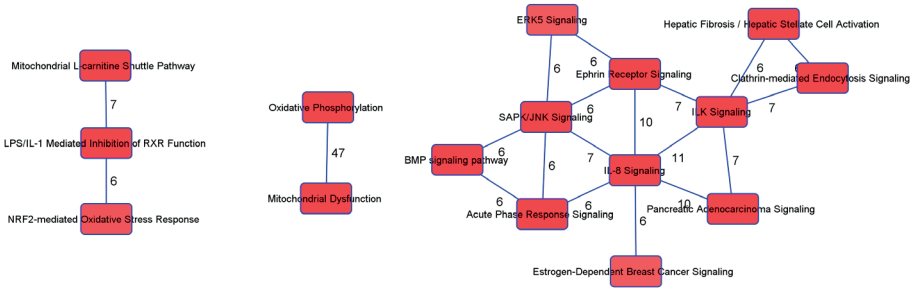


Supplementary Figure 1C shows representative pictures of a crown-like structure (CLS) in adipose tissue of HFD-fed mice and HFD+Rosi mice, which stained positively for CCR2 and CD11c (dark brown staining, upper panels). In order to merge the coloring of the two different immunostainings in a CLS, the bright field images were converted to 8-bit immunofluorescent images (lower panels). The immunoreactivity against CD11c and CCR2 is shown in green and red, respectively. The merged images demonstrate that CLS in the HFD group and the HFD+Rosi group contain CCR2+ and CD11c+ cells and some of these cells express both markers (overlap is indicated by yellow). (Microphotographs: magnification x200).

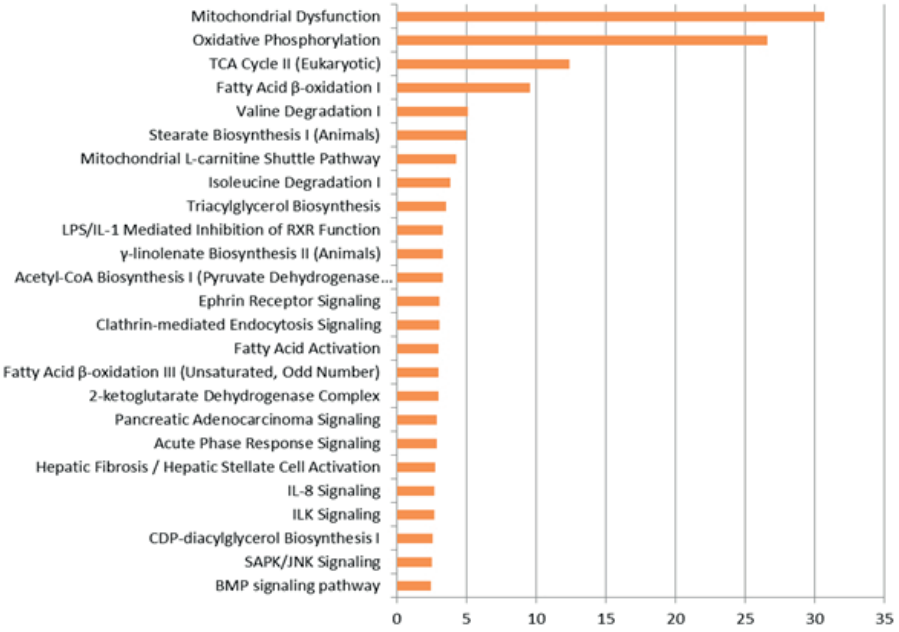
Supplement 2. Microarray analysis of the effects of rosiglitazone intervention in WAT

Gene set enrichment showed that rosiglitazone intervention significantly affected several biological canonical pathways related to inflammatory oxidative stress in WAT. These pathways can be grouped in three main clusters shown below and specified in **Supplementary Figure 2A-1.**

1. Oxidative phosphorylation/ Mitochondrial dysfunction
2. Oxidative stress response/peroxisomal response
3. Acute phase response/ fibrosis



Supplementary Figure 2A-1. Clustering of canonical pathways that are influenced by rosiglitazone intervention. This graph shows three clusters, each of which consisting of canonical pathways. Lines between two pathways indicate that these pathways share genes (the number of overlapping genes is mentioned). The significance of the effect of rosiglitazone on individual pathways is provided in **Supplementary Figure 2A-2.**



Supplementary Figure 2A-2. **Canonical pathways influenced by rosiglitazone.** The bars in the figure indicate significance of the different pathways. Significance is expressed as -log p-values.

As an example for the anti-inflammatory effect of rosiglitazone in WAT, the individual genes of the canonical pathway 'Acute phase response signaling' are listed in **Supplementary Table 2A**. Among the genes that were reduced by rosiglitazone were complement factors, kinases and acute phase reactants such as haptoglobin, serum amyloid A3 and von Willebrand factor.

Supplementary Table 2A.

Symbol	Entrez Gene Name	Exp Log Ratio	Exp p-value
AGT	angiotensinogen (serpin peptidase inhibitor, clade A, member 8)	-2.45	2.50E-08
C2	complement component 2	-1.345	2.69E-07
C4A/C4B	complement component 4B (Chido blood group)	-1.471	7.47E-09
CFB	complement factor B	-1.856	2.67E-08
HP	haptoglobin	-3.09	4.83E-14
HRAS	Harvey rat sarcoma viral oncogene homolog	0.661	3.62E-03
KRAS	Kirsten rat sarcoma viral oncogene homolog	0.677	7.21E-06
LBP	lipopolysaccharide binding protein	-2.18	8.91E-08
MAPK12	mitogen-activated protein kinase 12	-0.527	5.78E-03
MTOR	mechanistic target of rapamycin (serine/threonine kinase)	0.466	1.13E-03
OSMR	oncostatin M receptor	-0.7	4.47E-05
RBP7	retinol binding protein 7, cellular	2.14	8.13E-09
RELA	v-rel avian reticuloendotheliosis viral oncogene homolog A	-0.417	4.28E-03
RIPK1	receptor (TNFRSF)-interacting serine-threonine kinase 1	-0.276	8.71E-03
RRAS	related RAS viral (r-ras) oncogene homolog	-0.649	1.55E-03
Saa3	serum amyloid A 3	-2.635	3.81E-05
SERPINA3	serpin peptidase inhibitor, clade A (alpha-1 antiproteinase, antitrypsin), member 3	-2.923	3.69E-31
SERPING1	serpin peptidase inhibitor, clade G (C1 inhibitor), member 1	-0.659	7.50E-04
SOCS5	suppressor of cytokine signaling 5	0.455	3.79E-03
TAB1	TGF-beta activated kinase 1/MAP3K7 binding protein 1	-0.415	8.28E-03
TF	transferrin	-0.933	1.07E-04
VWF	von Willebrand factor	-1.115	4.49E-04

Supplementary table 2B. Differentially expressed PPARγ regulated genes in epididymal white adipose tissue affected by rosiglitazone intervention in LDLr-/- mice. Transcriptional network analysis demonstrated a significant transcriptional activation of PPARγ (high and positive Z-score of 4.1, *p*=5.92e-24). Rosiglitazone significantly affected the transcription of 71 PPARγ regulated genes in WAT as listed below. False discovery rate of 5% (FDR<0.05) was used.

Supplementary Table 2B

eWAT	**HFD+Rosi compared with HFD**	
Genes in dataset	**Prediction (based on expression direction)**	**Log Ratio**
UCP1	Activated	3.351
TSC22D3	Activated	-0.799
SORBS1	Activated	0.795
SOD1	Activated	0.542
SLC27A1	Activated	1.810
SLC25A20	Activated	1.399
SLC25A1	Activated	0.991
PPARGC1B	Activated	0.935
PMM1	Activated	1.260
PLIN5	Activated	2.068
PDK4	Activated	3.228
MGLL	Activated	1.015
ME1	Activated	1.048
MDH1	Activated	0.863
HP	Activated	-3.090
HADHB	Activated	1.175
GPD1	Activated	2.167
GDF15	Activated	1.279
FABP5	Activated	1.361
FABP3	Activated	2.700
ESRRA	Activated	0.490
EPHX1	Activated	-0.546
EHHADH	Activated	2.244
DLAT	Activated	1.142
CYP4B1	Activated	1.784
CS	Activated	0.911
CRAT	Activated	1.018
CPT2	Activated	1.249
CPT1B	Activated	3.491
CIDEA	Activated	3.514
CAT	Activated	1.016

Supplementary Table 2B (continued)

eWAT	HFD+Rosi compared with HFD	
Genes in dataset	**Prediction (based on expression direction)**	**Log Ratio**
ATP5O	Activated	1.204
AQP7	Activated	1.205
APP	Activated	-0.551
ACTA2	Activated	-1.767
ACSL1	Activated	1.200
ACOX1	Activated	1.222
ACADS	Activated	1.566
ACADM	Activated	1.035
ACAA2	Activated	1.116
Acaa1b	Activated	1.927
VEGFA	Inhibited	-1.435
PRODH	Inhibited	-1.418
PPIC	Inhibited	-0.959
PPARGC1A	Inhibited	0.934
MLYCD	Inhibited	1.078
LAMB3	Inhibited	-1.329
GATA2	Inhibited	-0.889
ELOVL6	Inhibited	-1.391
CFD	Inhibited	-1.274
CCND1	Inhibited	-0.791
APOE	Inhibited	-0.737
ACSL5	Inhibited	-0.576
Abcb1b	Inhibited	-0.826
ACADL	Affected	1.571
ACOT8	Affected	0.575
AGT	Affected	-2.450
CDK2	Affected	-0.597
FBP2	Affected	1.359
HR	Affected	-1.589
HSD3B7	Affected	-0.842
IGFBP3	Affected	-1.141
IGFBP5	Affected	-1.650
IGFBP7	Affected	-0.404
PDHB	Affected	0.850
S100A8	Affected	-2.150
SCNN1G	Affected	1.209
SCP2	Affected	1.216
UGT1A9 (includes others)	Affected	-1.200
VLDLR	Affected	0.723

Supplement 3: Rosiglitazone intervention does not activate PPAR-regulated genes in livers of LDLr-/- mice

Original transcriptomics data: http://www.ebi.ac.uk/arrayexpress/experiments/E-MTAB-1063/

Supplement 3A: Table listing 36 genes that are differentially expressed by rosiglitazone in liver.

probeID	geneSymbol	geneName	Log Ratio	Adjusted p-value
ILMN_2925947	ABAT	4-aminobutyrate aminotransferase	0.505	4.05E-02
ILMN_2629112	ACER2	alkaline ceramidase 2	0.68	5.03E-03
ILMN_2965414	ANKRD22	ankyrin repeat domain 22	0.94	4.83E-06
ILMN_2834123	APOA4	apolipoprotein A-IV	-2.376	4.48E-03
ILMN_2641301	APOA5	apolipoprotein A-V	-0.823	9.36E-03
ILMN_2732601	ARSG	arylsulfatase G	-0.745	9.36E-03
ILMN_2776603	Ccl9	chemokine (C-C motif) ligand 9	0.621	1.75E-02
ILMN_2835423	CFD	complement factor D (adipsin)	4.666	1.33E-06
ILMN_2609813	CHI3L1	chitinase 3-like 1 (cartilage glycoprotein-39)	1.455	1.88E-02
ILMN_1215446	CIDEA	cell death-inducing DFFA-like effector a	3.387	1.99E-03
ILMN_2827217	CLSTN3	calsyntenin 3	1.349	1.03E-02
ILMN_2806996	CREB3L3	cAMP responsive element binding protein 3-like 3	-0.52	3.19E-03
ILMN_2960325	CTSE	cathepsin E	0.926	3.24E-02
ILMN_2664224	EPHX1	epoxide hydrolase 1, microsomal (xenobiotic)	-0.657	4.60E-02
ILMN_2710698	FGF21	fibroblast growth factor 21	-1.51	2.59E-02
ILMN_2605941	GNPAT	glyceronephosphate O-acyltransferase	0.389	1.67E-02
ILMN_3007956	GZF1	GDNF-inducible zinc finger protein 1	0.398	4.72E-02
ILMN_2795520	HLA-A	major histocompatibility complex, class I, A	-0.523	2.71E-02
ILMN_2662160	IMPA2	inositol(myo)-1(or 4)-monophosphatase 2	-0.779	4.48E-03
ILMN_1229605	INHBE	inhibin, beta E	-0.918	3.24E-02
ILMN_2692723	LPL	lipoprotein lipase	1.261	2.51E-04
ILMN_1225764	MFSD2A	major facilitator superfamily domain containing 2A	-1.977	2.58E-02
ILMN_2813830	NT5E	5'-nucleotidase, ecto (CD73)	0.992	3.69E-02
ILMN_2680628	Pbld2	phenazine biosynthesis-like protein domain containing 2	-0.442	3.20E-02
ILMN_2924754	PDZK1	PDZ domain containing 1	-0.315	7.40E-03
ILMN_1249694	PGM3	phosphoglucomutase 3	-0.536	3.20E-02
ILMN_2739760	PRELP	proline/arginine-rich end leucine-rich repeat protein	-0.429	1.88E-02
ILMN_1254902	RDH16	retinol dehydrogenase 16 (all-trans)	1.318	1.33E-06
ILMN_1240471	RETSAT	retinol saturase (all-trans-retinol 13,14-reductase)	-0.719	1.88E-02
ILMN_2825446	SDCBP2	syndecan binding protein (syntenin) 2	1.575	3.19E-03
ILMN_2684145	SDCBP2	syndecan binding protein (syntenin) 2	0.999	7.40E-03

Supplementary Table 3A (continued)

probeID	geneSymbol	geneName	Log Ratio	Adjusted p-value
ILMN_2826264	SERINC2	serine incorporator 2	-0.72	1.88E-02
ILMN_1231573	SERPINB1	serpin peptidase inhibitor, clade B (ovalbumin), member 1	1.994	4.83E-06
ILMN_1256644	SLC6A12	solute carrier family 6 (neurotransmitter transporter), member 12	0.482	2.58E-02
ILMN_2695199	ST3GAL6	ST3 beta-galactoside alpha-2,3-sialyltransferase 6	0.826	5.02E-05
ILMN_2757599	TSPAN31	tetraspanin 31	-0.415	5.62E-04
ILMN_1236758	WFDC2	WAP four-disulfide core domain 2	-2.028	1.18E-03

Supplement 3B: Specific analysis of PPARγ-regulated genes in liver

Only 4 out of the 36 differentially expressed genes in the liver can potentially be regulated by PPARγ. These 4 genes are listed below. However, also other transcriptional regulators control the expression of these genes and a composite analysis of all gene expression changes (see upstream transcriptional regulator analysis below) shows that PPARγ is not activated.

Supplementary Table 3B

Liver	HFD+Rosi compared with HFD control	
Genes in dataset	**Prediction (based on expression direction)**	**Log Ratio**
CFD	Activated	4.666
CIDEA	Activated	3.387
LPL	Activated	1.276
EPHX1	Activated	-0.657

Supplement 3C: Upstream transcriptional regulator analysis for PPARγ, PPARα and PPARδ in liver

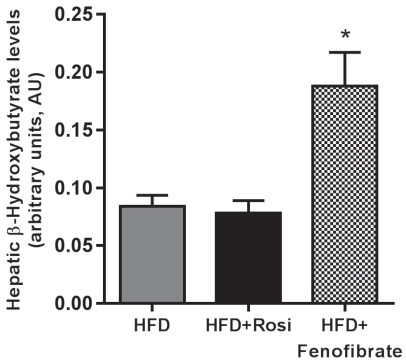
Transcriptional network analysis of differentially expressed genes in liver demonstrated that there is no significant transcriptional activation of upstream regulators PPARγ, PPARα or PPARδ by rosiglitazone. False discovery rate of 5% (FDR<0.05) was used.

As reference for the validity of the method and for PPARα activation, we have used livers from LDLr-/- mice treated with fenofibrate (0.05% w/w), a

pharmacological ligand of PPARα. Diets and duration of intervention were the same as for rosiglitazone. Fenofibrate significantly activates PPARα activity (Z-score: 7.9, *p*=4.5e-55) based on gene expression changes induced by fenofibrate. Consistent with this, a significant activation of several key processes of lipid metabolism in liver was observed with fenofibrate (see **Supplementary Table 3C**). These processes were not affected with rosiglitazone treatment. In line with this, hepatic concentrations of β-hydroxybutyrate (beta-oxidation product) were increased with fenofibrate treatment, but not with rosiglitazone (**Supplementary Figure 3C**), further supporting absence of PPARα activation by rosiglitazone.

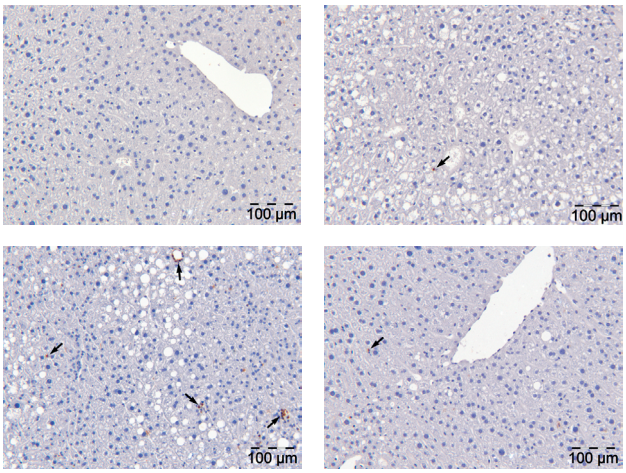
Supplementary Table 3C

Top bio functions in lipid metabolism	Predicted Activation State	Log ratio	p-value
transport of long chain fatty acid	Increased	2,902	1,91E-09
oxidation of fatty acid	Increased	2,782	1,04E-17
uptake of long chain fatty acid	Increased	2,634	1,20E-03
storage of lipid	Increased	2,58	3,39E-06



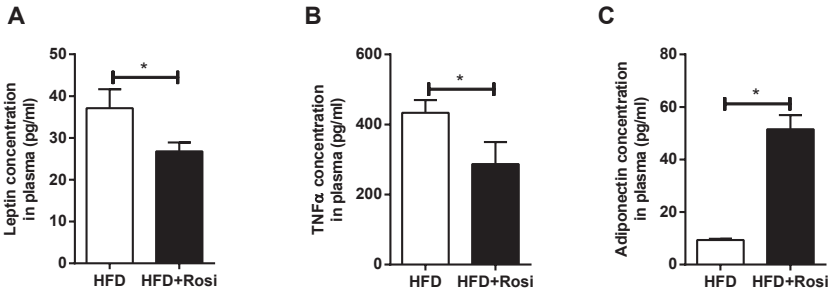
Supplementary figure 3C Using liver tissue homogenates and GC-MS technology, we examined whether rosiglitazone would affect hepatic β-hydroxybutyrate levels (a marker of hepatic fatty acid oxidation) relative to HFD mice. As a positive control for activation of PPARα, livers of fenofibrate-treated LDLr-/- mice were used. The levels of hepatic β-hydroxybutyrate were not increased by rosiglitazone, but were significantly increased by fenofibrate. These data further support absence of PPARα activation by rosiglitazone. Values are expressed as mean ± SEM and expressed as arbitrary units (AU) relative to internal standard. *p<0.05 vs. HFD, HFD+Rosi.

Supplement 4: Effect of rosiglitazone on myeloperoxidase (MPO)-positive cells (neutrophils) in liver



Representative pictures of MPO immunohistochemical stained liver sections of mice after a chow diet (upper left panel), 9 or 16 weeks high-fat diet (REF and HFD, upper right and lower left panel respectively) or rosiglitazone intervention (HFD+Rosi Lower right panel). Infiltration of neutrophils into the liver was observed after 16 weeks of HFD (both single cells and cell aggregates). Only a few MPO-positive cells were observed in HFD+Rosi, which resembled the condition prior to intervention (REF). (magnification x100).

Supplement 5: Effect of rosiglitazone on adipokine plasma concentrations of leptin, TNFα and adiponectin



Plasma concentrations of leptin, TNFα and adiponectin of mice fed either a high-fat diet (HFD) or a HFD supplemented with rosiglitazone (HFD+Rosi). Rosiglitazone intervention reduced levels of pro-inflammatory adipokines leptin and TNFα. By contrast, rosiglitazone increased levels of anti-inflammatory adipokine adiponectin. Values are expressed as mean±SEM and expressed as plasma concentrations in pg/ml. *p<0.05.

Chapter 4

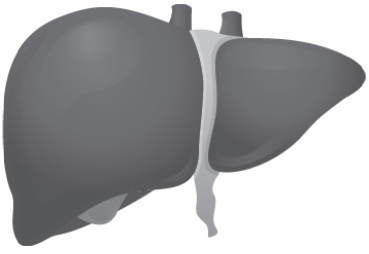
The CCR2 inhibitor propagermanium attenuates diet-induced insulin resistance, adipose tissue inflammation and non-alcoholic steatohepatitis

Petra Mulder[1,2], Anita M. van den Hoek[1], Robert Kleemann[1,2]

[1] Department of Metabolic Health Research, Netherlands Organization for Applied Scientific Research (TNO), Zernikedreef 9, 2333 CK Leiden, The Netherlands
[2] Department of Vascular Surgery, Leiden University Medical Center, PO Box 9600, 2300 RC Leiden, The Netherlands

Accepted - PloS one







ABSTRACT

Background and aim: Obese patients with chronic inflammation in white adipose tissue (WAT) have an increased risk of developing non-alcoholic steatohepatitis (NASH). The C-C chemokine receptor-2 (CCR2) has a crucial role in the recruitment of immune cells to WAT and liver, thereby promoting the inflammatory component of the disease. Herein, we examined whether intervention with propagermanium, an inhibitor of CCR2, would attenuate tissue inflammation and NASH development.

Methods: Male C57BL/6J mice received a high-fat diet (HFD) for 0, 6, 12 and 24 weeks to characterize the development of early disease symptoms of NASH, i.e. insulin resistance and WAT inflammation (by hyperinsulinemic-euglycemic clamp and histology, respectively) and to define the optimal time point for intervention. In a separate study, mice were pretreated with HFD followed by propagermanium treatment (0.05% w/w) after 6 weeks (early intervention) or 12 weeks (late intervention). NASH was analyzed after 24 weeks of diet feeding.

Results: Insulin resistance in WAT developed after 6 weeks of HFD, which was paralleled by modest WAT inflammation. Insulin resistance and inflammation in WAT intensified after 12 weeks of HFD, and preceded NASH development. The subsequent CCR2 intervention experiment showed that early, but not late, propagermanium treatment attenuated insulin resistance. Only the early treatment significantly decreased Mcp-1 and CD11c gene expression in WAT, indicating reduced WAT inflammation. Histopathological analysis of liver demonstrated that propagermanium treatment decreased macrovesicular steatosis and tended to reduce lobular inflammation, with more pronounced effects in the early intervention group. Propagermanium improved the ratio between pro-inflammatory (M1) and anti-inflammatory (M2) macrophages, quantified by CD11c and Arginase-1 gene expression in both intervention groups.

Conclusions: Overall, early propagermanium administration was more effective to improve insulin resistance, WAT inflammation and NASH compared to late intervention. These data suggest that therapeutic interventions for NASH directed at the MCP-1/CCR2 pathway should be initiated early.

INTRODUCTION

Non-alcoholic fatty liver disease (NAFLD) is the most common cause of chronic liver disease worldwide [1]. NAFLD encompasses a spectrum of liver conditions ranging from steatosis (NAFL) to steatosis with hepatic inflammation (non-alcoholic steatohepatitis, NASH) which can lead to liver fibrosis, cirrhosis and liver-related mortality [2]. The rise in prevalence of NAFLD parallels the dramatic increase in obesity [1]. It has been postulated that the chronic, low-grade inflammatory state that characterizes obesity may play a central role in driving the development of NASH [3]. Thus, anti-inflammatory treatments may have therapeutic potential to reduce obesity-associated NASH development.

The expanding white adipose tissue (WAT) in obesity may constitute an important source of inflammation during the development of NASH [4]. Many studies have demonstrated that WAT inflammation in obese subjects is promoted by infiltrating macrophages [5, 6]. Recently, we have shown that surgical excision of inflamed WAT can attenuate NASH, providing first evidence for a causal role of WAT in NASH development [7].

The chemokine monocyte chemoattractant protein (MCP)-1 and its receptor C-C chemokine receptor-2 (CCR2) play a pivotal role in the recruitment of macrophages/monocytes to the sites of inflammation both in WAT [8, 9] as well as in liver [9-11]. For instance, mouse models with genetic deletion of MCP-1 or CCR2 have shown that these factors control the infiltration of macrophages into WAT and are crucial for the development of insulin resistance and hepatic steatosis in high-fat diet (HFD)-induced obese mice [12, 13]. It also has been reported that CCR2-deficient mice have decreased accumulation of inflammatory cells in liver [10, 14]. Furthermore, previous studies have shown that the CCR2 inhibitor propagermanium can prevent insulin resistance and steatosis in db/db mice [15] and wild-type mice [16]. However, *prophylactic* administration was used in the latter experiments and it therefore remains unknown whether therapeutic intervention with propagermanium in the ongoing disease process of NASH, i.e. reflecting the clinical setting, will be effective. To answer this question, we first examined the development of disease symptoms insulin resistance, WAT and liver inflammation

in time, in order to define adequate time points for propagermanium intervention. To do so, male C57BL/6J mice were fed a high-fat diet (HFD) for 0, 6, 12 and 24 weeks and insulin resistance was characterized by hyperinsulinemic-euglycemic clamp, and WAT and liver inflammation by histology. In a subsequent *intervention* study, we investigated whether propagermanium treatment, started at different time points in the disease development (early vs. late), would attenuate NASH development in mice with manifest disease symptoms.

MATERIALS AND METHODS

Animal experiments were approved by an independent Ethical Committee on Animal Care and Experimentation (DEC-Zeist, the Netherlands) and were in compliance with European Community specifications for the use of laboratory animals. Male 9-week old wild type C57BL/6J mice were obtained from Charles River Laboratories (L'Arbresle Cedex, France) and were kept on chow control diet during a 3-week acclimatization period until the start of the experiment (R/M-H, Ssniff Spezialdieten GmbH, Soest, Germany). Mice were housed in a temperature-controlled room with a regular 12-h light/dark cycle, with ad libitum access to food and water.

Time-course hyperinsulinemic–euglycemic clamp experiment

A group of mice (n=12) was used as reference to define the condition prior to HFD feeding (at t=0). Three groups (n=12 each) were treated with a high-fat diet (HFD) for 6, 12 and 24 weeks (D12451, Research Diets Inc., New Brunswick, USA) to determine the development of whole-body and tissue-specific insulin resistance. A hyperinsulinemic-euglycemic clamp analysis was performed in all groups as described previously [17]. Briefly, after an overnight fast, mice were anesthetized with 6.25 mg/kg vetranquil (Sanofi Santé Nutrition Animale, Libourne Cedex, France), 6.25 mg/kg dormicum (Roche, Mijdrecht, The Netherlands) and 0.3125 mg/kg fentanyl (Janssen-Cilag, Tilburg, the Netherlands) and an infusion needle was placed in one of the tail veins. Basal rates of glucose turnover were determined by administering a

primed (0.72 µCi/µl), continuous (1.2 µCi/h) infusion of [^{14}C]-glucose for 60 minutes. Subsequently, the hyperinsulinemic condition was started with a primed (4.1 mU) continuous (6.8 mU/h) infusion of insulin (Actrapid, Novo Nordisk, Alphen a/d Rijn, The Netherlands). A variable infusion of 12.5% D-glucose was used to maintain euglycemia (measured at 10 min intervals via tail bleeding using the 'Freestyle glucose measurement system' from Abbott (Abbott Park, IL, USA). Blood samples (75 µl) were collected during the basal period (after 50 and 60 minutes) and during the clamp (hyperinsulinemic) period (after 70, 80 and 90 minutes) for determination of plasma glucose, insulin and ^{14}C-glucose specific activities. To assess insulin-mediated glucose uptake in white adipose tissue (WAT), 2-deoxy-D-[3H] glucose (2-DG glucose; Amersham, Little Chalfont, UK) was administered as a bolus (1 µCi), 40 minutes before the end of the clamp experiment. After the clamp, mice were sacrificed, plasma was collected by heart puncture and liver and adipose tissue were isolated. One part of the tissues was fixed in formalin and paraffin-embedded for histological analysis, another part was frozen in liquid nitrogen for subsequent analysis.

CCR2 inhibitor intervention experiment

Mice were matched based on body weight and fasting insulin plasma concentration and divided into a chow control diet (n=5) control group and a HFD treatment group (n=45). Mice on HFD were matched again after 6 weeks of HFD feeding and divided into three groups (n=15 each). One group continued on HFD until the end of the study (24 weeks). The early intervention group received HFD supplemented with propagermanium from 6 weeks onwards, for a total of 18 weeks (HFD+Pro_6w, 0.05% w/w; Sigma Aldrich, Zwijndrecht, The Netherlands). The late intervention group received HFD supplemented with propagermanium from 12 weeks onwards for another 12 weeks (HFD+Pro_12w). In week 24, all animals were sacrificed by CO_2 asphyxiation. Serum was collected by heart puncture and major WAT depots and livers were isolated. One part of the tissues was fixed in formalin and paraffin-embedded for histological analysis. Another part was snap-frozen in liquid nitrogen and stored at -80°C for real-time polymerase chain reaction (RT-PCR). Two mice that were resistant to develop diet-induced obesity on HFD (i.e. body weight gain 50% less than group mean) were excluded from the study at sacrifice.

Body composition

Total body fat was determined using a NMR Echo MRI whole body composition analyzer (EchoMRI LLC, Houston, TX, USA) at the end of the study (week 24).

Blood and plasma analyses

Blood samples were taken at regular intervals by tail incision after a 5-hour fast. Blood glucose was measured immediately using the 'Freestyle glucose measurement system' from Abbott (Abbott Park, IL, USA). Plasma insulin levels (Ultrasensitive mouse insulin ELISA, Mercodia, Uppsala, Sweden) and plasma adiponectin levels (R&D Systems Ltd, Abington, UK) were determined by ELISA. Homeostasis model assessment (HOMA) was used to calculate relative insulin resistance (IR). Five hours fasting plasma insulin and fasting blood glucose values were used to calculate IR, as follows: IR = [insulin (ng/ml) × glucose (mM)]/22.5.

Histological and biochemical analysis of adipose tissue and liver

Paraffin-embedded cross-sections (5 µm) of adipose tissue were stained with hematoxylin-phloxine-saffron (HPS). WAT inflammation was quantified blindly by counting the number of crown-like structures (CLS) in 3 non-overlapping fields (at x100 magnification) and expressed as number of CLS per mm^2.

Hematoxylin and eosin-stained (HE) cross-sections (3µm) of the medial liver lobe (lobus medialis hepatis) were scored blindly using an adapted grading method for human NASH [18]. Briefly, two cross-sections per mouse were examined and the level of macrovesicular and microvesicular steatosis was assessed relative to the liver area analyzed and expressed as a percentage. Hepatic inflammation was evaluated by counting the number of inflammatory cell aggregates per field at a x100 magnification (view size of 3.1 mm^2) in five non-overlapping fields per specimen, and expressed as average number of cell aggregates per field. Biochemical analysis of intrahepatic triglyceride content was determined by high-performance thin-layer chromatography (HPTLC) as previously described [7].

Gene expression analyses

Liver RNA was extracted using RNA Bee Total RNA Isolation Kit (Bio-Connect, Huissen, the Netherlands) and Ambion Total RNA isolation was used for RNA extraction of WAT (AM1912, Life Technologies, Bleiswijk, The Netherlands). RNA concentration was assessed spectrophotometrically using Nanodrop 1000 (Isogen Life Science, De Meern, the Netherlands) and RNA quality was determined by Lab-on-Chip analysis using 2100 Bioanalyzer (Agilent Technologies, Amstelveen, the Netherlands). cDNA was synthesized from total RNA using a High Capacity RNA-to-cDNA™ Kit (Life Technologies). Gene expression analyses were performed by RT-PCR on an Applied Biosystems 7500 Fast Real-time PCR system. TaqMan® Gene Expression Assays (Life Technologies) were used to detect the expression of the following genes: CD68 (Mm03047340_m1), CD11c (*Itgax*, Mm00498698_m1), Arginase-1 (*Arg1*, Mm00475988_m1), Mcp-1 (*Ccl2,* Mm00441242_m1), Tnf-α (*Tnf*, Mm00443258_m1). Glyceraldehyde 3-phosphate dehydrogenase (*Gapdh*; 4308313), hypoxanthine-guanine phosphoribosyltransferase (*Hprt*; Mm00446968_m1) and peptidylprolyl isomerase F (*Ppif*; Mm00506384_m1) were used as housekeeping genes. Changes in gene expression were calculated using the comparative Ct (ΔΔCt) method and expressed as fold-change relative to HFD control group.

Statistical analysis

Results are shown as mean±SEM. Significance of difference between groups were statistically analyzed by One-way ANOVA and Tukey post-hoc tests (for normally distributed variables). Non-normally distributed variables were tested by non-parametric Kruskal-Wallis followed by one-sided Mann-Whitney U test using Graphpad Prism software (version 6, Graphpad Software Inc. La Jolla, USA). Correlations were determined by Spearman's rank correlation. Differences were considered significant at $p<0.05$.

RESULTS

Insulin resistance in WAT precedes hepatic insulin resistance in diet-induced NASH

The development of whole body and tissue-specific insulin resistance was determined by hyperinsulinemic-euglycemic clamps prior to (t=0) and after 6, 12, 24 weeks of HFD feeding. The glucose infusion rate (GIR), a measure of whole body insulin sensitivity, was markedly lowered after 6 weeks and decreased further at 24 weeks (Figure 1A). The use of radioactive glucose tracers allowed us to determine development of insulin resistance in WAT and liver. The 2-deoxyglucose (2DG) uptake by WAT was already significantly lowered after 6 weeks of HFD feeding, clearly indicating that this tissue had become insulin resistant (Figure 1B), whereas the liver was still insulin sensitive at that time point (Figure 1C). Hepatic glucose production was suppressed by insulin until week 12 of HFD feeding, but thereafter insulins' inhibitory effect became weaker and hepatic insulin resistance developed after 24 weeks of HFD feeding (Figure 1C). The development of insulin resistance in WAT after 6 weeks of HFD was paralleled by the occurrence of crown-like structures (CLS), a defining characteristic of macrophage-driven WAT inflammation (Figure 1D and Figure 1F). Also, the development of hepatic insulin resistance after 24 weeks of HFD coincided with formation of inflammatory cell aggregates indicating liver inflammation (Figure 1E and Figure 1G). In all, these data demonstrate that insulin resistance in WAT develops rapidly (detectable after 6 and 12 weeks) and precedes liver insulin resistance (24 weeks) and diet-induced NASH.

Intervention with propagermanium improves insulin resistance independent of obesity

In a separate study, propagermanium interventions were started after 6 weeks (HFD+Pro_6w; early intervention) and 12 weeks (HFD+Pro_12w group; late intervention) of HFD feeding.

The body weight of mice on a HFD increased strongly over time relative to chow control mice (HFD: 49.1±1.0g vs. Chow: 33.7±1.5g, $p<0.0001$; Figure 2A). The increase in body weight in the HFD group was reflected by increased total body fat mass (HFD: 18.6±0.8g vs. Chow: 4.3±1.2g; $p<0.001$). Early and late treatment

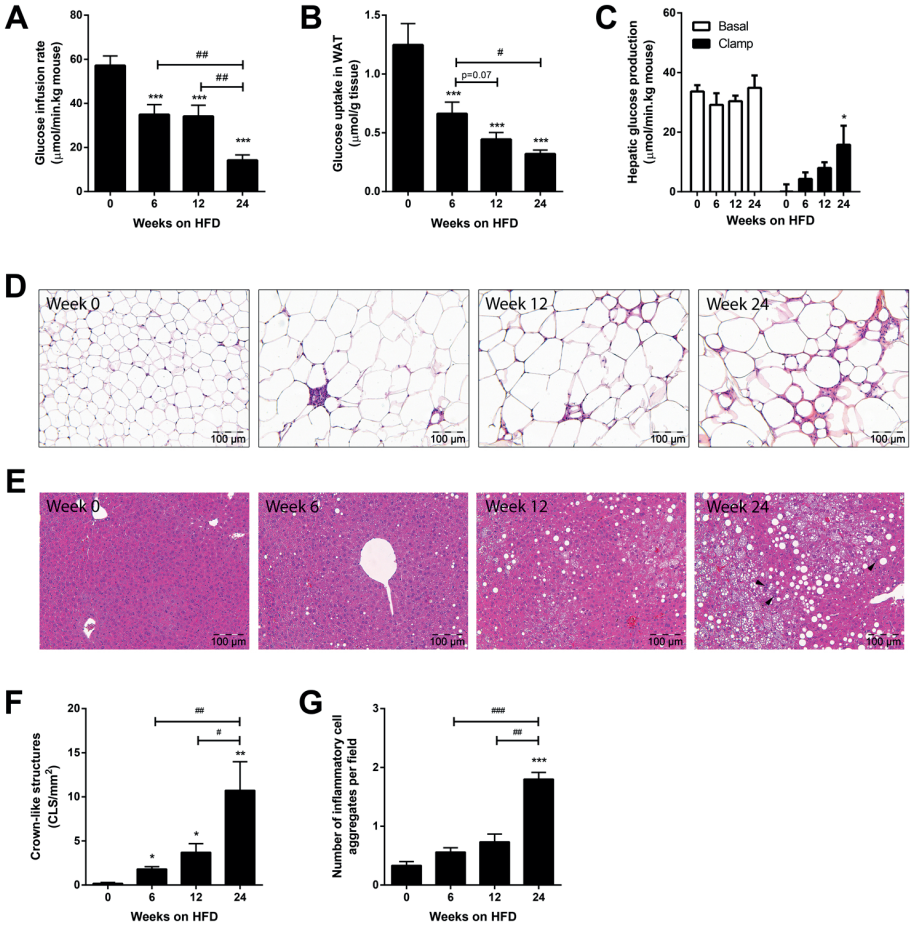


Figure 1. Time course development of insulin resistance, adipose and liver inflammation. Mice were maintained on a high-fat diet (HFD) 0, 6, 12 and 24 weeks prior to clamp experiment to induce insulin resistance. (A) shows HFD-induced decrease in glucose infusion rate (GIR) under hyperinsulinemic conditions, indicating development of whole body insulin resistance. (B) HFD feeding resulted in a gradual decrease of tissue-specific uptake of glucose into white adipose tissue (WAT). (C) HFD feeding increased hepatic glucose production after 24 weeks of HFD, indicating development of hepatic insulin resistance. 'Basal' indicates prior to hyperinsulinemic clamp conditions and 'clamp' indicates hyperinsulinemic clamp conditions. (D) Representative microphotographs of HPS-stained WAT cross-sections, showing WAT inflammation (i.e. crown-like structures) already after 6 weeks of HFD feeding. (E) Representative microphotographs of HE-stained liver cross-sections, showing NASH development after 24 weeks of HFD feeding (arrow heads indicate clusters of inflammatory cells). (F) Quantitative analysis of crown-likes structures (CLS), demonstrating gradual development of WAT inflammation by HFD feeding. (G) Hepatic inflammation (number of inflammatory cell aggregates per 100x field) was induced after 24 weeks of HFD feeding. All data are mean±SEM, n=7-11/group. * p<0.05 ** p<0.01 *** p<0.001 compared with t=0. # p<0.05, ###p<0.01 compared to week 24.

with propagermanium did not affect body weight (HFD+Pro_6w: 48.2±1.3g and HFD+Pro_12w: 47.7±0.7g, ns; Figure 2A) and total fat mass (HFD+Pro_6w: 18.4±0.8g and HFD+Pro_12w: 17.9±0.4g; ns).

HFD feeding increased fasting blood glucose (9.2±0.3 mM vs. 7.6±0.3 mM in chow; $p<0.01$; Figure 2B), and comparable levels were observed in the intervention groups (HFD+Pro_6w: 8.9±0.2 mM and HFD+Pro_12w: 8.9±0.2 mM, ns; Figure 2B). Moreover, HFD feeding strongly increased fasting insulin levels compared to chow (HFD: 18.6 ±3.7 ng/ml vs. Chow: 1.2±0.3 ng/ml; $p<0.001$). This increase was significantly attenuated in the early intervention group, but not in the late intervention group (Figure 2C). Consistent with this, C-peptide was significantly reduced by the early propagermanium intervention, but not by the late intervention (Figure 2D). Moreover, early intervention with propagermanium significantly lowered fasting HOMA-IR which remained at a lower level until the end of the study (Figure 2E). The anti-inflammatory adipokine adiponectin was increased in plasma at week 24 in those mice receiving early propagermanium treatment (Figure 2F).

Taken together, early intervention, but not late intervention, with propagermanium attenuates insulin resistance and increases plasma adiponectin levels. These effects were independent of body mass and adiposity, suggesting an effect on the inflammatory state of WAT.

Intervention with propagermanium attenuates WAT inflammation

MCP-1 and its receptor CCR2 are important for macrophage recruitment [8, 9] as well as polarization of macrophages from an anti-inflammatory M2 toward a pro-inflammatory M1 phenotype in adipose tissue [19]. Both processes contribute to WAT inflammation and have been associated with the development of insulin resistance. As shown in Figure 3A, HFD feeding resulted in increased gene expression of CD68 (a generic macrophage marker) compared to chow ($p<0.05$), indicating that more macrophages are present in WAT of the HFD-fed mice. Propagermanium interventions did not affect CD68 expression in WAT. A more refined analysis of the macrophage phenotype revealed that HFD treatment strongly increased the gene expression of CD11c, a M1 marker. This increase was significantly reduced by early propagermanium treatment ($p<0.05$ vs. HFD) and tended to be lower in the late

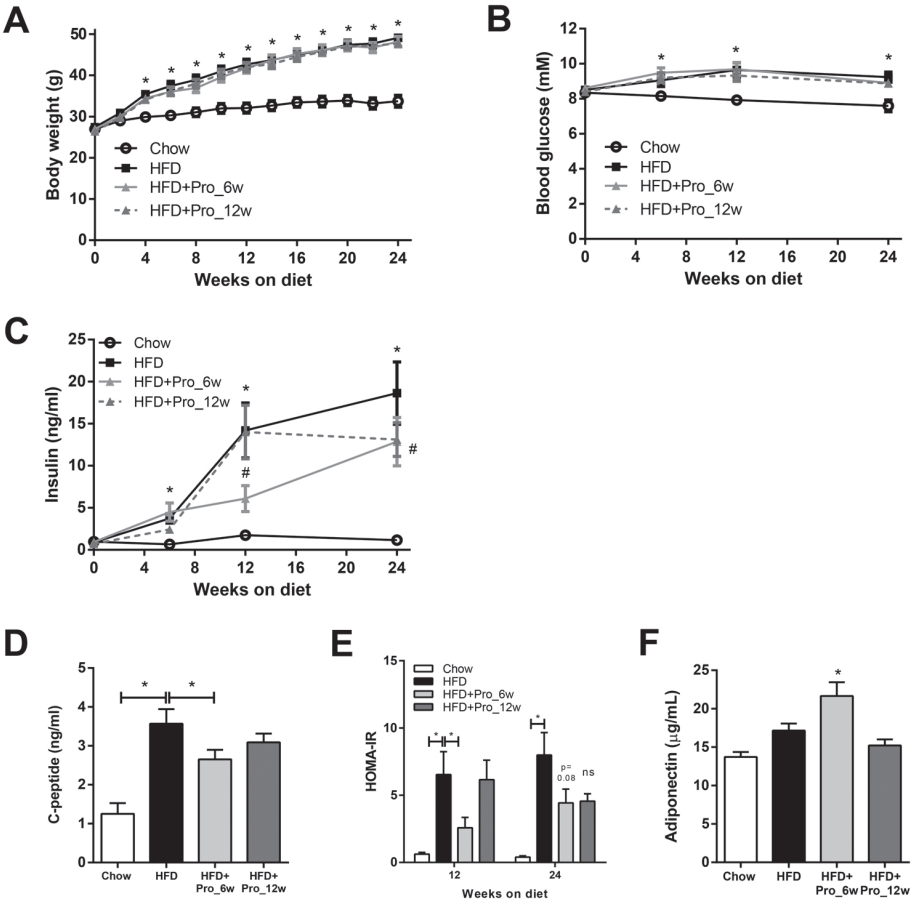


Figure 2. Effects of propagermanium intervention on body weight and metabolic parameters. Mice were fed a high-fat diet (HFD) for 24 weeks or treated with the CCR2 inhibitor propagermanium started after 6 weeks (HFD+Pro_6w, early intervention) or 12 weeks of HFD (HFD+Pro_12w, late intervention). Chow-fed mice were included as a reference. (A) HFD feeding increased body weight compared with chow and was not affected by propagermanium intervention. (B) Fasting blood glucose levels over time. (C) HFD-induced increased fasting plasma insulin levels, which were reduced in HFD+Pro_6w. (D) C-peptide levels were increased at week 24 in HFD-fed mice and attenuated by early propagermanium intervention. (E) HFD-induced increases in HOMA-IR relative to chow were significantly reduced by early, but not late, propagermanium intervention. (F) Plasma adiponectin levels were increased by early propagermanium treatment in week 24. All data are mean±SEM, n=5 (chow), and n=13-15 for HFD and intervention groups. * $p<0.05$ (compared with chow) # $p<0.05$ compared with HFD.

intervention group (p=0.09 vs. HFD, Figure 3B). By contrast, expression of arginase-1 (a M2 marker) did not differ between the groups (Figure 3C). In agreement with the observed decrease in expression of CD11c, Mcp-1 expression was significantly attenuated in the HFD+Pro_6w group (p<0.05 vs. HFD, Figure 3D). The HFD-induced expression of Tnf-α was diminished in both intervention groups, but this effect did not reach statistical significance (p=0.10; HFD vs. HFD+Pro_6w, Figure 3E).

Collectively, these results indicate that early intervention with propagermanium reduces WAT inflammation as shown by decreased expression of pro-inflammatory M1 macrophage markers.

Propagermanium intervention attenuates NASH development

Histological analysis revealed a significant decrease in macrovesicular steatosis vs. HFD control group by early intervention only (with -37%, p<0.05 for HFD+Pro_6wk and -31%, p=0.14 for HFD+Pro_12 wk; Figure 4A), while microvesicular steatosis was not affected (Figure 4B). Biochemical analysis showed that hepatic triglycerides were slightly reduced by early propagermanium treatment, but did not reach statistical significance (HFD: 168.5±19.0 µg/mg liver protein vs. HFD+Pro_6w: 149.7±22.9 µg/mg liver protein, p=0.27; not shown).

Quantification of inflammatory cell aggregates (a hallmark of NASH) revealed that lobular inflammation was reduced by intervention with propagermanium (Figure 4C), with borderline significant effect of early propagermanium treatment (p=0.05 for HFD+Pro_6wk and p=0.18 for HFD+Pro_12wk, respectively). Lobular inflammation in the HFD group was accompanied by increased hepatic Tnf-α gene expression and increased CD68 gene expression (both, p<0.05 vs. chow), which were not affected by propagermanium (not shown). Notably, lobular inflammation positively correlated with the ratio of M1/M2 macrophages (CD11c/Arginase-1 gene expression; r=0.72, p<0.0001, Figure 4D). HFD feeding strongly increased the M1/M2 ratio compared to chow and propagermanium intervention attenuated this HFD effect (Figure 4E). The improvement in M1/M2 ratio by propagermanium is the result of lowered CD11c expression as well as an increase in Arginase-1 expression (Supplemental figure 1). Taken together, propagermanium treatment reduced NASH development with a more pronounced hepatoprotective effect of early intervention.

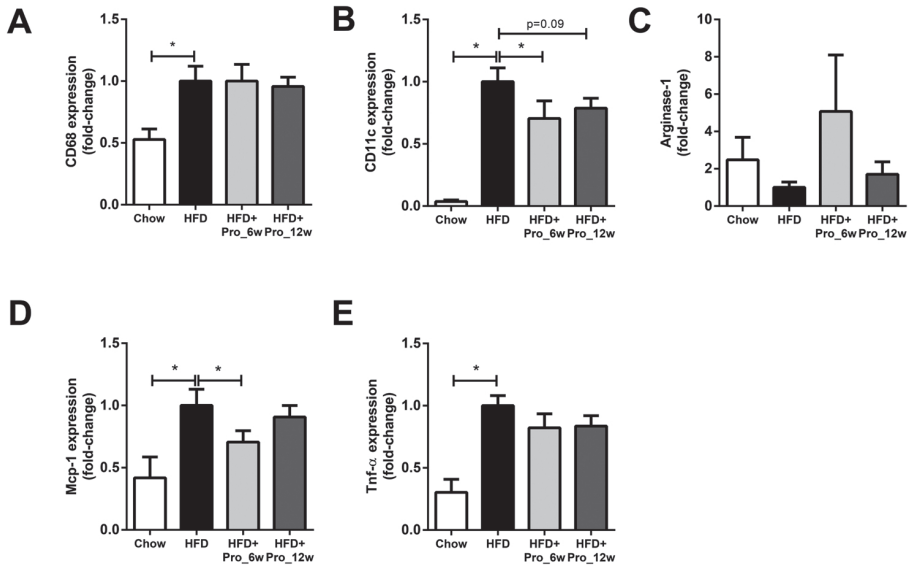


Figure 3. Effects of propagermanium intervention on WAT inflammation markers. (A) HFD feeding increased CD68 expression (general macrophage marker), which was not affected by propagermanium. (B) HFD increased CD11c expression, suggesting increased number of 'pro-inflammatory' (M1) macrophages in WAT. (C) Arginase-1 expression (anti-inflammatory M2 macrophage marker) did not differ between the groups. Early intervention significantly lowered HFD-induced expression of (D) Mcp-1 and showed slightly lowered (E) Tnf-α expression levels in WAT. All data are mean±SEM.* $p<0.05$.

DISCUSSION

Accumulating evidence points to an important role of the MCP-1/CCR2 pathway in the development of obesity-associated inflammation in WAT [6, 8, 9, 12, 13] and subsequent development of NASH [9, 10, 14]. Herein, we examined whether therapeutic intervention with the CCR2 inhibitor propagermanium in ongoing disease would attenuate NASH development. We demonstrate that early risk factors of the disease, i.e. insulin resistance and WAT inflammation, can be reduced by propagermanium and that this effect is independent of obesity. Moreover, intervention with propagermanium reduced macrovesicular steatosis and reduced lobular inflammation, indicating an attenuation of NASH development. The effects

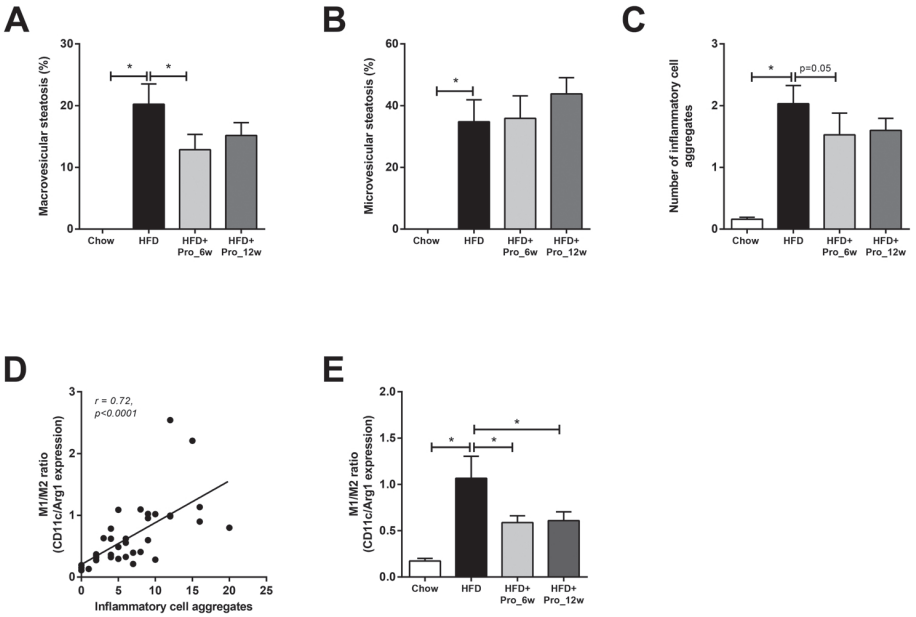


Figure 4. Effects of propagermanium intervention on NASH development. (A) HFD feeding induced pronounced macrovesicular steatosis, which was reduced in HFD+Pro_6w group. (B) Microvesicular steatosis was induced by HFD and was not affected by propagermanium treatment. (C) Quantification of inflammatory cell aggregates number per field in the liver (lobular inflammation), which was increased by HFD and tended to be reduced by early propagermanium treatment. (D) Lobular inflammation strongly correlates with the ratio of M1/M2 markers (CD11c/Arginase-1 gene expression). (E) M1/M2 ratio is decreased by propagermanium treatment, indicating a shift towards M2 phenotype. All data are mean±SEM. * $p<0.05$.

of propagermanium were more pronounced when the intervention was started early (after 6 weeks of HFD feeding).

NASH is strongly associated with insulin resistance [20, 21]. More specifically, it has been shown the degree of adipose tissue insulin resistance is associated with progressive NASH in patients [22], supporting the view that insulin resistance in WAT is an early disease symptom that may contribute to NASH development [23]. In line with this, our data show that WAT insulin resistance precedes NASH development. Interestingly, hepatic insulin resistance develops much later in time (after 24 weeks of HFD). We observed that development of insulin resistance was

paralleled by an increase in inflammatory cells in both, WAT and liver. In addition to changes in number of inflammatory cells, macrophage phenotype may also play a role in the development of insulin resistance.

Macrophages are phenotypically heterogeneous and have been characterized based on their polarization state as 'pro-inflammatory M1' or 'anti-inflammatory M2' macrophages [24]. The ratio of M1/M2 macrophages may be of particular importance in the development of insulin resistance. For instance, mice lacking M2 polarized macrophages show increased WAT inflammation (e.g. CLS) and worsened insulin resistance [25, 26]. In the present study, we observed a significantly increase in M1 marker CD11c expression in WAT upon HFD feeding and propagermanium attenuated this effect and lowered plasma insulin levels. Notably, therapeutic propagermanium administration did not result in decreased expression of total macrophage marker (CD68) or increased M2 macrophage marker expression, indicating that decreasing pro-inflammatory M1 macrophage content is sufficient to improve obesity-associated insulin resistance. In support of this notion, CD11c depletion in obese mice resulted in a rapid normalization of glucose and insulin tolerance and decreased inflammatory markers in WAT, both at the level of gene transcription and protein expression [27].

The dysregulation of the M1/M2 phenotypic balance in the liver is also emerging as a central mechanism in NASH development [24]. Herein, we observed that HFD feeding increased the ratio M1/M2 macrophage expression in the liver, whereas propagermanium intervention counteracted this effect. Moreover, lobular inflammation positively correlated with the ratio of M1/M2 expression in liver, suggesting that a shift towards M1 macrophages may be critical for NAFLD progression. Consistent with this, Maina and colleagues have shown that hepatic expression of M1 markers (i.e. iNOS, IL-12p40) positively correlated with number of inflammatory foci in livers of C57BL/6 mice [28]. These and our data suggest that suppressing M1 macrophage polarization and/or favoring the differentiation of M2 macrophages in the liver can attenuate NASH development.

Recently, in a randomized controlled clinical trial the effect of the CCR2 antagonist, JNJ-41443532, was examined in obese patients with type 2 diabetes [29]. The administration of this CCR2 antagonist resulted in decreased levels of

fasting blood glucose over a 4-week treatment period. HOMA-IR was also lowered in these patients, but did not reach statistical significance. Herein, intervention with propagermanium in obese mice resulted also in reduced plasma insulin and HOMA-IR, but only early treatment showed significant reductions. These data indicate that CCR2 inhibitors may be beneficial to treat insulin resistance, but only when administered early in the disease development, essentially as shown by Tamura and co-workers [15, 16].

Importantly, the effect of CCR2 antagonism on NASH development has not been investigated so far. This study provides experimental evidence that early CCR2 intervention attenuates adipose tissue inflammation in obesity and subsequent NASH development. Late intervention (12 week onwards) showed similar effects, yet not significant. The late intervention was started at a time point were insulin resistance, WAT inflammation and hepatic steatosis were progressing, but without manifest hepatic inflammation. Since the propagermanium treatment already lost effectiveness when started at this time point, it's unlikely that propagermanium would be able to reverse the disease process when given at a later time point, i.e. when NAFLD has progressed to NASH. Nonetheless, we cannot exclude the possibility that a longer treatment period with propagermanium may be required to achieve a beneficial effect on NASH. Furthermore, it should be noted that propagermanium selectively inhibits MCP-1-induced chemotaxis of CCR2-positive monocytes in vitro [30]. Based on published data [31-33], it is thus likely that disease pathways other than MCP-1/CCR2 become upregulated at later stages of disease process (e.g. RANTES/CCR5) and that interventions merely targeting MCP-1/CCR2 become less efficient.

In all, early propagermanium intervention was more effective than late intervention in attenuating insulin resistance, WAT inflammation, and NASH development. The results of this study suggest that therapeutic interventions for NASH directed at the MCP-1/CCR2 pathway should be initiated in an early stage of the disease development in order to be effective.

ACKNOWLEDGEMENTS

The authors thank Wim van Duyvenvoorde, Anita van Straalen-van Nieuwkoop and Annemarie Maas for excellent technical assistance. This study was supported by the TNO research programs ‘Predictive Health Technologies’ and ‘Enabling Technology Systems Biology’.

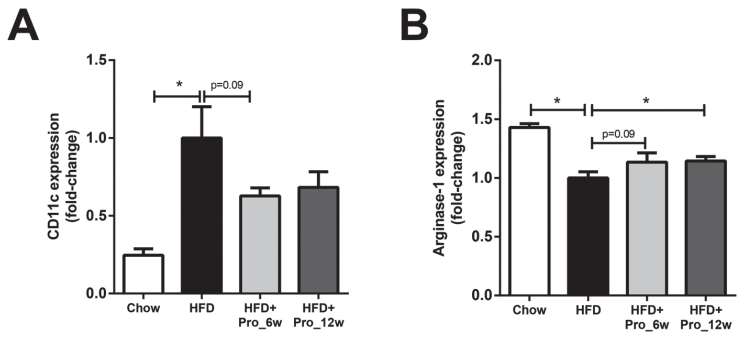
REFERENCES

1. Loomba R, Sanyal AJ. The global NAFLD epidemic. Nat Rev Gastroenterol Hepatol. 2013;10(11):686-90. doi: 10.1038/nrgastro.2013.171.
2. Tiniakos DG, Vos MB, Brunt EM. Nonalcoholic fatty liver disease: pathology and pathogenesis. Annu Rev Pathol. 2010;5:145-71. doi: 10.1146/annurev-pathol-121808-102132.
3. Tilg H, Hotamisligil GS. Nonalcoholic fatty liver disease: Cytokine-adipokine interplay and regulation of insulin resistance. Gastroenterology. 2006;131(3):934-45. doi: 10.1053/j.gastro.2006.05.054.
4. Mirza MS. Obesity, Visceral Fat, and NAFLD: Querying the Role of Adipokines in the Progression of Nonalcoholic Fatty Liver Disease. ISRN Gastroenterol. 2011;2011:592404. doi: 10.5402/2011/592404.
5. Weisberg SP, McCann D, Desai M, Rosenbaum M, Leibel RL, Ferrante AW, Jr. Obesity is associated with macrophage accumulation in adipose tissue. J Clin Invest. 2003;112(12):1796-808. doi: 10.1172/JCI19246.
6. Xu H, Barnes GT, Yang Q, Tan G, Yang D, Chou CJ, et al. Chronic inflammation in fat plays a crucial role in the development of obesity-related insulin resistance. J Clin Invest. 2003;112(12):1821-30. doi: 10.1172/JCI19451.
7. Mulder P, Morrison MC, Wielinga PY, van Duyvenvoorde W, Kooistra T, Kleemann R. Surgical removal of inflamed epididymal white adipose tissue attenuates the development of non-alcoholic steatohepatitis in obesity. Int J Obes (Lond). 2015. doi: 10.1038/ijo.2015.226.
8. Ito A, Suganami T, Yamauchi A, Degawa-Yamauchi M, Tanaka M, Kouyama R, et al. Role of CC chemokine receptor 2 in bone marrow cells in the recruitment of macrophages into obese adipose tissue. J Biol Chem. 2008;283(51):35715-23. doi: 10.1074/jbc.M804220200.
9. Oh DY, Morinaga H, Talukdar S, Bae EJ, Olefsky JM. Increased macrophage migration into adipose tissue in obese mice. Diabetes. 2012;61(2):346-54. doi: 10.2337/db11-0860.
10. Obstfeld AE, Sugaru E, Thearle M, Francisco AM, Gayet C, Ginsberg HN, et al. C-C chemokine receptor 2 (CCR2) regulates the hepatic recruitment of myeloid cells that promote obesity-induced hepatic steatosis. Diabetes. 2010;59(4):916-25. doi: 10.2337/db09-1403.
11. Gadd VL, Skoien R, Powell EE, Fagan KJ, Winterford C, Horsfall L, et al. The portal inflammatory infiltrate and ductular reaction in human nonalcoholic fatty liver disease. Hepatology. 2014;59(4):1393-405. doi: 10.1002/hep.26937.
12. Weisberg SP, Hunter D, Huber R, Lemieux J, Slaymaker S, Vaddi K, et al. CCR2 modulates inflammatory and metabolic effects of high-fat feeding. J Clin Invest. 2006;116(1):115-24. doi: 10.1172/JCI24335.
13. Kanda H, Tateya S, Tamori Y, Kotani K, Hiasa K, Kitazawa R, et al. MCP-1 contributes to macrophage infiltration into adipose tissue, insulin resistance, and hepatic steatosis in obesity. J Clin Invest. 2006;116(6):1494-505. doi: 10.1172/JCI26498.
14. Miura K, Yang L, van Rooijen N, Ohnishi H, Seki E. Hepatic recruitment of macrophages promotes nonalcoholic steatohepatitis through CCR2. Am J Physiol Gastrointest Liver Physiol. 2012;302(11):G1310-21. doi: 10.1152/ajpgi.00365.2011.
15. Tamura Y, Sugimoto M, Murayama T, Ueda Y, Kanamori H, Ono K, et al. Inhibition of CCR2 ameliorates insulin resistance and hepatic steatosis in db/db mice. Arterioscler Thromb Vasc Biol. 2008;28(12):2195-201. doi: 10.1161/ATVBAHA.108.168633.

16. Tamura Y, Sugimoto M, Murayama T, Minami M, Nishikaze Y, Ariyasu H, et al. C-C chemokine receptor 2 inhibitor improves diet-induced development of insulin resistance and hepatic steatosis in mice. J Atheroscler Thromb. 2010;17(3):219-28.
17. Kleemann R, van Erk M, Verschuren L, van den Hoek AM, Koek M, Wielinga PY, et al. Time-resolved and tissue-specific systems analysis of the pathogenesis of insulin resistance. PLoS One. 2010;5(1):e8817. doi: 10.1371/journal.pone.0008817.
18. Liang W, Menke AL, Driessen A, Koek GH, Lindeman JH, Stoop R, et al. Establishment of a general NAFLD scoring system for rodent models and comparison to human liver pathology. PLoS One. 2014;9(12):e115922. doi: 10.1371/journal.pone.0115922.
19. Lumeng CN, Bodzin JL, Saltiel AR. Obesity induces a phenotypic switch in adipose tissue macrophage polarization. J Clin Invest. 2007;117(1):175-84. doi: 10.1172/JCI29881.
20. Bellentani S, Scaglioni F, Marino M, Bedogni G. Epidemiology of non-alcoholic fatty liver disease. Dig Dis. 2010;28(1):155-61. doi: 10.1159/000282080.
21. Marchesini G, Bugianesi E, Forlani G, Cerrelli F, Lenzi M, Manini R, et al. Nonalcoholic fatty liver, steatohepatitis, and the metabolic syndrome. Hepatology. 2003;37(4):917-23. doi: 10.1053/jhep.2003.50161.
22. Lomonaco R, Ortiz-Lopez C, Orsak B, Webb A, Hardies J, Darland C, et al. Effect of adipose tissue insulin resistance on metabolic parameters and liver histology in obese patients with nonalcoholic fatty liver disease. Hepatology. 2012;55(5):1389-97. doi: 10.1002/hep.25539.
23. Bugianesi E, McCullough AJ, Marchesini G. Insulin resistance: a metabolic pathway to chronic liver disease. Hepatology. 2005;42(5):987-1000. doi: 10.1002/hep.20920.
24. Marra F, Lotersztajn S. Pathophysiology of NASH: perspectives for a targeted treatment. Curr Pharm Des. 2013;19(29):5250-69.
25. Odegaard JI, Ricardo-Gonzalez RR, Goforth MH, Morel CR, Subramanian V, Mukundan L, et al. Macrophage-specific PPARgamma controls alternative activation and improves insulin resistance. Nature. 2007;447(7148):1116-20. doi: 10.1038/nature05894.
26. Hevener AL, Olefsky JM, Reichart D, Nguyen MT, Bandyopadyhay G, Leung HY, et al. Macrophage PPAR gamma is required for normal skeletal muscle and hepatic insulin sensitivity and full antidiabetic effects of thiazolidinediones. J Clin Invest. 2007;117(6):1658-69. doi: 10.1172/JCI31561.
27. Patsouris D, Li PP, Thapar D, Chapman J, Olefsky JM, Neels JG. Ablation of CD11c-positive cells normalizes insulin sensitivity in obese insulin resistant animals. Cell Metab. 2008;8(4):301-9. doi: 10.1016/j.cmet.2008.08.015.
28. Maina V, Sutti S, Locatelli I, Vidali M, Mombello C, Bozzola C, et al. Bias in macrophage activation pattern influences non-alcoholic steatohepatitis (NASH) in mice. Clin Sci (Lond). 2012;122(11):545-53. doi: 10.1042/CS20110366.
29. Di Prospero NA, Artis E, Andrade-Gordon P, Johnson DL, Vaccaro N, Xi L, et al. CCR2 antagonism in patients with type 2 diabetes mellitus: a randomized, placebo-controlled study. Diabetes Obes Metab. 2014;16(11):1055-64. doi: 10.1111/dom.12309.
30. Yokochi S, Hashimoto H, Ishiwata Y, Shimokawa H, Haino M, Terashima Y, et al. An anti-inflammatory drug, propagermanium, may target GPI-anchored proteins associated with an MCP-1 receptor, CCR2. J Interferon Cytokine Res. 2001;21(6):389-98. doi: 10.1089/107999001750277862.
31. Kitade H, Sawamoto K, Nagashimada M, Inoue H, Yamamoto Y, Sai Y, et al. CCR5 plays a critical role in obesity-induced adipose tissue inflammation and insulin resistance by regulating both macrophage recruitment and M1/M2 status. Diabetes. 2012;61(7):1680-90. doi: 10.2337/db11-1506.

32. Berres ML, Koenen RR, Rueland A, Zaldivar MM, Heinrichs D, Sahin H, et al. Antagonism of the chemokine Ccl5 ameliorates experimental liver fibrosis in mice. J Clin Invest. 2010;120(11):4129-40. doi: 10.1172/JCI41732.
33. Seki E, De Minicis S, Gwak GY, Kluwe J, Inokuchi S, Bursill CA, et al. CCR1 and CCR5 promote hepatic fibrosis in mice. J Clin Invest. 2009;119(7):1858-70.

SUPPLEMENTAL DATA



Supplemental Figure 1. The effect on propagermanium intervention on hepatic gene expression of M1 and M2 macrophage markers. (A) HFD increased CD11c expression in liver, suggesting increased number of 'pro-inflammatory' (M1) macrophages. Early treatment tended to reduce M1 macrophage expression. (B) HFD reduced expression of Arginase-1 in liver, reflecting lower number of anti-inflammatory (M2) macrophages. Propagermanium treatment increased expression of M2 macrophages. All data are mean±SEM. * p<0.05.

Chapter 5

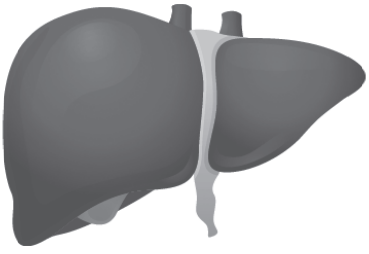
Intervention with a caspase-1 inhibitor reduces obesity-associated hyperinsulinemia, non-alcoholic steatohepatitis (NASH) and hepatic fibrosis in LDLr-/-.Leiden mice

Martine C. Morrison[1,2,3], Petra Mulder[1], Kanita Salic[1], Joanne Verheij[4], Wen Liang[1], Wim van Duyvenvoorde[1], Aswin Menke[5], Teake Kooistra[1], Robert Kleemann[1], Peter Y. Wielinga[1]

[1]Department of Metabolic Health Research, Netherlands Organization for Applied Scientific Research (TNO), Zernikedreef 9, 2333 CK Leiden, The Netherlands
[2]Department of Pathology and Medical Biology, University of Groningen, University Medical Center Groningen, Hanzeplein 1 (EA11), 9713 GZ Groningen, The Netherlands
[3]Top Institute Food and Nutrition, Nieuwe Kanaal 9A, 6709 PA Wageningen, The Netherlands
[4]Department of Pathology, Academic Medical Center, University of Amsterdam, Meibergdreef 9, 1105 AZ Amsterdam, The Netherlands
[5]TNO Triskelion, Utrechtseweg 48, 3704 HE Zeist, The Netherlands

International Journal of Obesity. 2016 Sep; 40(9):1416-23. doi: 10.1038/ijo.2016.74.







ABSTRACT

Background/Objectives: Non-alcoholic steatohepatitis (NASH) is a serious liver condition, closely associated with obesity and insulin resistance. Recent studies have suggested an important role for inflammasome/caspase-1 in the development of NASH, but the potential therapeutic value of caspase-1 inhibition remains unclear. Therefore, we aimed to investigate the effects of caspase-1 inhibition in the ongoing disease process, to mimic the clinical setting.

Subjects/Methods: To investigate effects of caspase-1 inhibition under therapeutic conditions, male LDLr-/-.Leiden mice were fed a high-fat diet (HFD) for 9 weeks to induce a pre-diabetic state before start of treatment. Mice were then continued on HFD for another 12 weeks, without (HFD) or with (HFD-YVAD) treatment with the caspase-1 inhibitor Ac-YVAD-cmk (40 mg/kg/day).

Results: 9 weeks of HFD feeding resulted in an obese phenotype, with obesity-associated hypertriglyceridemia, hypercholesterolemia, hyperglycemia, and hyperinsulinemia. Treatment with Ac-YVAD-cmk did not affect further body weight gain or dyslipidemia, but did attenuate further progression of insulin resistance. Histopathological analysis of livers clearly demonstrated prevention of NASH development in HFD-YVAD mice: livers were less steatotic and neutrophil infiltration was strongly reduced. In addition, caspase-1 inhibition had a profound effect on hepatic fibrosis, as assessed by histological quantification of collagen staining and gene expression analysis of fibrosis-associated genes *Col1a1, Acta2,* and *Tnfa*.

Conclusions: Intervention with a caspase-1 inhibitor attenuated the development of NASH, liver fibrosis and insulin resistance. Our data support the importance of inflammasome/caspase-1 in the development of NASH and demonstrate that therapeutic intervention in the already ongoing disease process is feasible.

INTRODUCTION

Non-alcoholic fatty liver disease (NAFLD) has become the most common cause of chronic liver disease in Western countries, and its prevalence continues to rise in parallel with increasing rates of obesity and type 2 diabetes (T2D), to which it is strongly related [1,2]. NAFLD encompasses a spectrum of liver disease, that ranges from the clinically benign intrahepatic accumulation of lipids (steatosis) to the more progressive non-alcoholic steatohepatitis (NASH), which is characterized by the presence of hepatic inflammation, ballooning and fibrosis [3]. NASH is a serious liver disease that can further progress to cirrhosis and hepatocellular carcinoma [4], and is projected to become the leading indication for liver transplantation in the next several years [5], particularly since there is currently no approved pharmacological therapy for NAFLD/NASH.

A crucial factor in the pathogenesis of NAFLD is considered to be the chronic low-grade inflammatory state that characterizes metabolic overload and obesity [6]. It is assumed that this metabolically induced inflammation results from excess nutrient and energy intake and originates in the adipose tissue [7]. A key component in metabolic inflammation is the NLRP3 inflammasome, a multi-protein danger-sensing complex that is thought to form the crossroads between metabolism and inflammation [8]. This large cytoplasmic complex comprises the receptor protein NLRP3, which can be activated by classical pro-inflammatory signals as well as by metabolic signals such as free fatty acids [9,10]. Activation of NLRP3 facilitates the recruitment and activation of caspase-1, which cleaves the biologically inactive precursors of the cytokines IL-1β and IL-18 into their mature, pro-inflammatory counterparts [11].

Several studies provide indication that inflammasome activation indeed plays an important role in the development of NAFLD. Analyses of human liver biopsies have shown that mRNA expression of NLRP3 inflammasome-related proteins (e.g. NLRP3, caspase-1, pro-IL-1β, pro-IL-18) is increased in livers of NASH patients [9,12] and that their expression correlates with the extent of fibrosis development [12]. In line with this, studies in experimental models of NASH have shown that caspase-1 is activated in NASH livers [9,13,14] and that development of NASH is

clearly reduced in mice in which inflammasome-associated genes are knocked out [12-14] while constitutive hyperactivation of the NLRP3 inflammasome results in severe liver inflammation and fibrosis [15].

However, since most of these studies were performed in genetically engineered mouse strains that are completely deficient in inflammasome-associated genes like NLRP3 or caspase-1, the potential therapeutic value of inflammasome inhibition in the ongoing disease process, i.e. conditions reflective of the clinical setting, remains unclear. Therefore, we aimed to investigate the effect of treatment with an inflammasome inhibitor on the development of obesity-associated NAFLD. To this end we used LDLr-/-.Leiden mice, a translational model for obesity-associated diseases [16]. When fed a HFD, these mice develop diet-induced obesity, metabolic inflammation and insulin resistance that progresses to development of T2D and NASH [17,18]. We treated HFD-fed LDLr-/-.Leiden mice with the caspase-1 inhibitor Ac-YVAD-cmk [19-21], starting treatment once early disease symptoms were present, to allow us to study the effects of inflammasome inhibition in a therapeutic setting.

MATERIAL AND METHODS

Animals

Animal experiments were approved by an independent Committee on the Ethics of Animal Experiments (DEC-Zeist, The Netherlands; Permit Number: 3216). Male LDLr-/-.Leiden mice were kept on chow (Sniff-R/M-V1530, Uden, the Netherlands) until the start of the study (at 12-14 weeks of age). The mice were then matched into three groups (n=15/group) based on body weight (sample size based on previously performed pilot studies). The first group received a low-fat reference diet (LFD, 10 kcal% fat from lard; D12450B Research Diets, New Brunswick, USA). The other two groups were fed a high-fat diet (HFD, 45 kcal% fat from lard; D12451, Research Diets) for nine weeks, after which the intervention was started. Both groups continued on HFD for the remainder of the study, and from t=9w onwards group 3 (HFD-YVAD) received daily i.p. injections with the caspase-1 inhibitor Ac-YVAD-cmk (40 mg/

kg; Bachem, Weil a.Rhein, Germany). Body weight (individual) and food intake (per cage) were measured every 3 weeks. Body fat percentage was determined by EchoMRI (EchoMRI-LLC, Houston, USA). Tail blood samples (for EDTA plasma) were taken at regular intervals after a 5-hour fast. At t=20w, an intraperitoneal glucose tolerance test (ipGTT) was performed (n=8/group, randomly selected). For this, mice were fasted for 5 hours before they were injected with 33 mg glucose (comparable to 1g/kg body weight based on average body weight of 33 g in the LFD control group). Tail blood samples were taken before (t=0), and at 5, 15, 30, 60 and 120 minutes post-injection to determine blood glucose and plasma insulin levels. At t=21 weeks, the mice were sacrificed by CO_2, terminal blood (for serum collection) was obtained via cardiac puncture and isolated organs were weighed.

Blood and plasma analyses

Blood glucose was measured immediately using a hand-held glucose analyser (Freestyle Disectronic, Vianen, the Netherlands). Plasma insulin levels were determined by ELISA (Mercodia, Uppsala, Sweden). Total plasma cholesterol and triglyceride levels were measured with enzymatic assays (Roche Diagnostics, Almere, the Netherlands). Plasma alanine aminotransferase (ALAT) levels were measured using a spectrophotometric activity assay (Reflotron-Plus, Roche).

Histological analysis of adipose tissue and liver

White adipose tissue (WAT) inflammation was assessed in the three major WAT depots (inguinal, mesenteric and epididymal). Tissues were formalin-fixed and paraffin-embedded, and cross-sections (5µm) were stained with hematoxylin-phloxine-saffron. WAT inflammation was quantified blindly by counting the number of crown-like structures (CLS) in 3 non-overlapping fields (at 100x magnification, view size 3.1 mm^2) for each depot, expressed as number of CLS per mm^2.

Formalin-fixed and paraffin-embedded cross-sections (5µm) of the median lobe were stained with hematoxylin and eosin and scored blindly by a board-certified pathologist using an adapted grading method for human NASH [16]. Briefly, two cross-sections/mouse were examined and the level of microvesicular and macrovesicular steatosis was determined relative to the liver area analyzed

(expressed as a percentage). Hepatic inflammation was assessed by counting the number of inflammatory foci per field at a 100× magnification (view size 3.1 mm^2) in five non-overlapping fields per specimen, expressed as the average number of foci per field. Immunohistochemical staining for myeloperoxidase (ab9535; Abcam, Cambridge, UK) was used to identify neutrophils, and the number of myeloperoxidase-positive inflammatory clusters was counted as described above. Fibrosis was assessed histochemically by Picro-Sirius Red staining (Chroma, WALDECK-Gmbh, Münster, Germany). Collagen content was quantified using ImageJ software (version 1.48, NIH, Bethesda, MD, USA) to assess the area of liver tissue that was positively stained (expressed as the percentage of total tissue area). In addition, development of fibrosis was assessed by a pathologist to gain insight into the distribution pattern of the collagen and to quantify the percentage of pericellular fibrosis specifically (expressed as the percentage of pericellular fibrosis relative to the total perisinusoidal area).

Analysis of liver lipids

Liver lipids were analyzed by high performance thin layer chromatography (HPTLC) as described previously [22]. In brief, lipids were extracted from liver homogenates using methanol and chloroform following the Bligh and Dyer method [23], after which they were separated by HPTLC on silica gel plates. Lipid spots were stained with color reagent (5 g of MnCl24H2O, 32 ml of 95–97% H2SO4 added to 960 ml of CH3OH:H2O 1:1 v/v) and triglycerides, cholesteryl esters and free cholesterol were quantified using TINA version 2.09 software (Raytest, Straubenhardt, Germany). Liver lipids were expressed per mg liver protein, which was determined in the same liver homogenates used for the liver lipid analysis, using the Lowry protein assay [24].

Hepatic gene expression analyses

RNA-Bee Total-RNA Isolation Kit (Bio-Connect, Huissen, the Netherlands) was used for RNA extraction. RNA concentration was determined spectrophotometrically using Nanodrop 1000 (Isogen Life Science, De Meern, the Netherlands) and RNA quality was assessed using 2100 Bioanalyzer (Agilent Technologies, Amstelveen,

the Netherlands). cDNA was synthesized from 1 µg of RNA using a High-Capacity RNA-to-cDNA™ Kit (Life Technologies, Bleiswijk, the Netherlands). Transcripts were quantified using TaqMan® Gene Expression Assays (Life Technologies) and the following primer/probe-sets: F4/80 (Mm00802529_m1), Col1a1 (Mm00801666_g1), Tnf (Mm00443258_m1), Acta2 (Mm01546133_m1), and the endogenous control Ppif (Mm01273726_m1). Changes in gene expression were calculated using the comparative Ct (ΔΔCt) method and expressed as fold-change relative to LFD as described previously [25].

Statistical analysis

Data were analyzed with SPSS 22.0 (IBM, Armonk, USA). Differences between groups were analyzed by one-way ANOVA followed by LSD post-hoc analysis. Variables with unequal variances were analyzed by ANOVA (Brown-Forsythe) and Dunnett's T3 post-hoc test. Non-normally distributed variables were analyzed by non-parametric Kruskal-Wallis followed by Mann-Whitney U. To test the hypothesis that treatment with Ac-YVAD-cmk may attenuate development of WAT inflammation, insulin resistance and NASH, a one-sided $p<0.05$ was considered statistically significant. All Results are shown as mean±SEM.

RESULTS

In order to investigate the effects of caspase-1 inhibition under therapeutic conditions, LDLr-/-.Leiden mice were fed a HFD for 9 weeks to induce a pre-diabetic state prior to the start of treatment with the caspase-1 inhibitor Ac-YVAD-cmk. This HFD-feeding resulted in an obese phenotype with obesity-associated hypertriglyceridemia, hypercholesterolemia, hyperglycemia, and hyperinsulinemia (Table 1, all $p<0.05$ compared with t=0). As a reference, a LFD-fed group of LDLr-/-.Leiden mice was included that developed a milder obese pre-diabetic phenotype (Table 1).

Table 1. Pre-treatment characteristics

	t=0	t=9 weeks	
	chow	LFD	HFD
Body weight (g)	26.3 ± 0.3[a]	32.3 ± 0.9[b]	39.0 ± 1.0[c]
Plasma cholesterol (mM)	5.4 ± 0.1[a]	16.1 ± 2.0[b]	16.8 ± 1.1[b]
Plasma triglycerides (mM)	1.0 ± 0.0[a]	2.6 ± 0.4[b]	2.6 ± 0.2[b]
Blood glucose (mM)	6.5 ± 0.1[a]	6.5 ± 0.4[a]	8.5 ± 0.2[b]
Plasma insulin (ng/ml)	1.1 ± 0.1[a]	2.2 ± 0.4[b]	5.2 ± 0.5[c]

All data are mean ± SEM. Means in a row with superscripts without a common letter differ significantly ($p<0.05$).

Caspase-1 inhibition does not affect obesity or dyslipidemia, but does improve adipose tissue inflammation and insulin sensitivity

After these first 9 weeks of HFD-feeding, treatment with Ac-YVAD-cmk was started in half of the HFD-fed animals (HFD-YVAD) while the other 15 mice remained on the HFD alone (HFD). The LFD reference group continued on the LFD until the end of the study. Ac-YVAD-cmk treatment did not affect food intake (average food intake during treatment period: 12.5±0.3 kcal/mouse/day in HFD, 11.9±0.8 kcal/mouse/day in HFD+YVAD, n.s.), HFD-induced body weight gain (Figure 1A), body fat percentage (Figure 1B) or dyslipidemia (Supplemental figure 1). Refined histological analysis of WAT quality revealed that HFD-feeding resulted in WAT inflammation in the epididymal depot, as reflected by a clear presence of CLS in this depot specifically (Figure 1C). Ac-YVAD-cmk treatment reduced (-41%, $p<0.05$) the presence of CLS in epididymal WAT (Figure 1D). This reduction in WAT inflammation was observed in absence of an effect of Ac-YVAD-cmk on WAT mass or the distribution of WAT mass over the epididymal, mesenteric, or inguinal depots (Supplemental figure 2).

The observed improvement in WAT quality was accompanied by improved insulin sensitivity in HFD-YVAD mice. The HFD-induced increases in fasting glucose (Figure 2A) and fasting insulin levels (Figure 2B) were significantly reduced in HFD-YVAD mice (absolute blood glucose and plasma insulin levels are shown in Supplemental figure 3). An ipGTT performed at t=20w (after 11 weeks of treatment) further confirmed these beneficial effects (Figure 2C-D, showing the delta changes in glucose and insulin post-injection). In HFD mice, the glucose injection resulted in a rapid increase in blood glucose, with peak levels reached

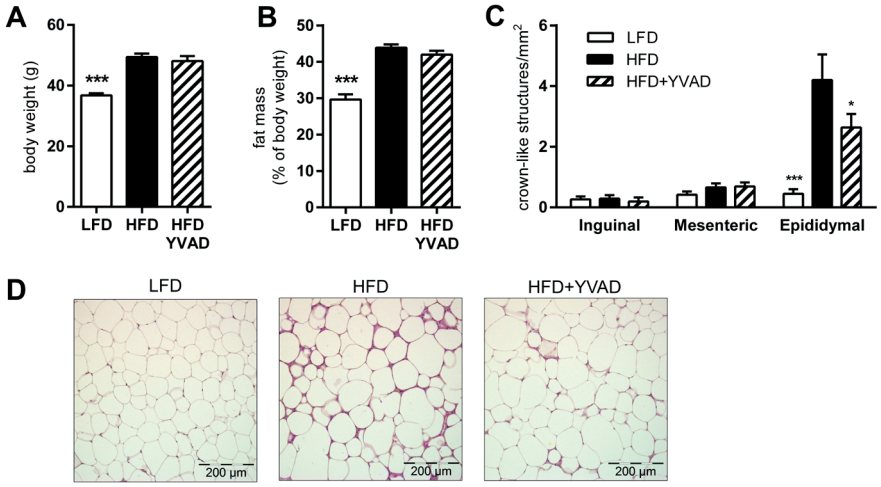


Figure 1. Effects of caspase-1 inhibition on high-fat diet-induced body weight, adiposity, and adipose tissue inflammation. LDLr-/-.Leiden mice were fed a high-fat diet for 21 weeks (HFD; n=15) or HFD + caspase 1 inhibitor Ac-YVAD-cmk (40 mg/kg daily) starting treatment after 9 weeks of HFD (HFD+YVAD; n=15). Low-fat diet (LFD)-fed mice (n=15) were included as a reference. A: HFD-feeding significantly induced body weight relative to LFD, which was not affected by caspase-1 inhibition. B: Body fat percentage was induced by HFD and was not affected in HFD+YVAD mice. C: HFD induced pronounced adipose tissue inflammation specifically in the epididymal depot, which tended to be reduced in HFD+YVAD mice. D: representative photomicrographs of HPS-stained epididymal adipose tissue sections. All data are from the t=21 weeks time point and are mean±SEM. * $p<0.05$, *** $p<0.001$ compared with HFD.

after 15 min (17.8±1.4 mM), after which they gradually decreased to 12.3±0.8 mM at 120 min post-injection. This glucose response was slightly more pronounced than that of LFD mice. In HFD-YVAD, the increase in blood glucose was much slower and the peak was not reached until 60 min post-injection (15.7±1.2 mM), after which it decreased to 9.9±0.8 mM at t=120 min. The area under the curve did not differ significantly between HFD and HFD-YVAD animals (not shown). While LFD mice needed only a slight increase in insulin to clear the glucose, the glucose injection triggered a strong and rapid insulin response in HFD mice, with plasma insulin levels increasing from 14.3±3.3 ng/ml at baseline, to 23.8±6.7 ng/ml at 15 min after the injection. From t=15 min onward, plasma insulin levels then gradually declined back to baseline levels (15.1±5.0 ng/ml). Remarkably, HFD-YVAD mice showed no insulin response to the injected glucose, with insulin levels remaining

comparable to baseline levels for the duration of the GTT. Together, these data indicate improved glucose tolerance and insulin sensitivity in Ac-YVAD-cmk-treated mice.

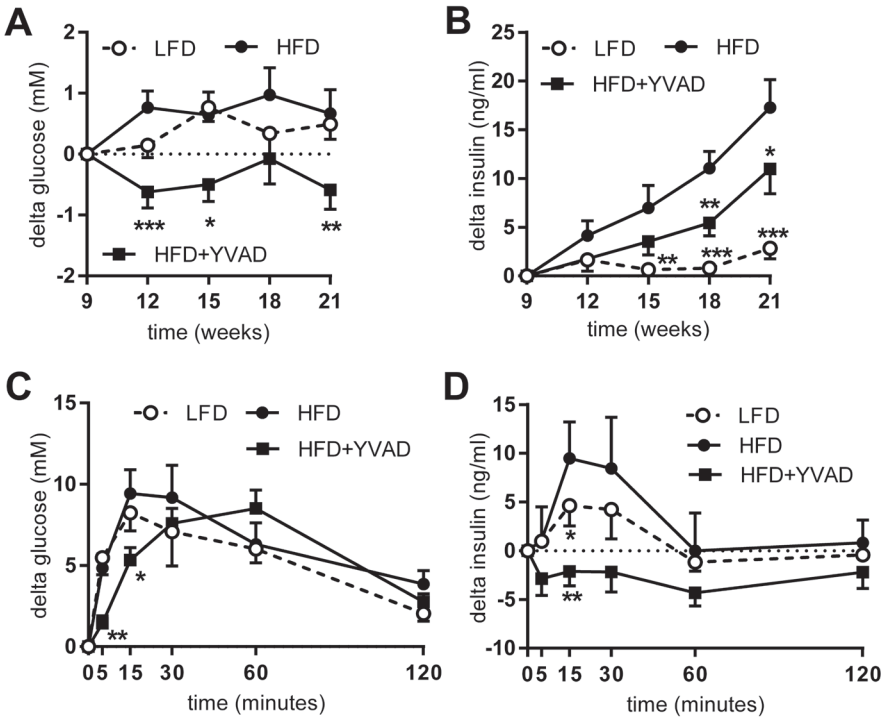


Figure 2. Effects of caspase-1 inhibition on fasting glucose and insulin and glucose tolerance. LDLr-/-.Leiden mice were fed a high-fat diet for 21 weeks (HFD; n=15) or HFD + caspase 1 inhibitor Ac-YVAD-cmk (40 mg/kg daily) starting treatment after 9 weeks of HFD (HFD+YVAD; n=15). Low-fat diet (LFD)-fed mice (n=15) were included as a reference. (A) HFD-induced increases in fasted blood glucose relative to treatment start (t=9 weeks) were reduced in HFD+YVAD. (B) HFD-induced increases in fasted plasma insulin relative to treatment start (t=9 weeks) were reduced in HFD+YVAD. (C) The glucose response to an intraperitoneal glucose tolerance test (ipGTT; performed at t=20 weeks) was modified by caspase-1 inhibition. (D) HFD mice showed a clear insulin response during the ipGTT, while HFD+YVAD mice showed no response in plasma insulin. Data are mean±SEM. * $p<0.05$, ** $p<0.01$, *** $p<0.001$ compared with HFD.

Caspase-1 inhibition improves hepatic steatosis

To investigate whether these improvements in glucose handling are accompanied by an effect on the development of hepatic steatosis, we analyzed liver cross-sections (Figure 3A) using an adapted scoring system for human NASH [16]. We observed pronounced hepatic steatosis in HFD-fed animals, with 48.5±5.6 % of hepatocytes affected by macrovesicular steatosis (Figure 3B) and 40.0±5.4 % affected by microvesicular steatosis (Figure 3C). Though treatment with Ac-YVAD-cmk did not affect development of macrovesicular steatosis (54.5±3.6 %, Figure 3B), microvesicular steatosis was significantly reduced (27.8±5.6 %, $p<0.01$, Figure 3C) in livers of HFD-YVAD mice compared with HFD mice. Liver lipid analysis by HPTLC revealed that Ac-YVAD-cmk treatment tended to reduce the accumulation of triglycerides in the liver (233.2±10.0 µg/mg liver protein in HFD, 205.3±13.8 µg/mg liver protein in HFD-YVAD, $p=0.08$, Figure 3D), while the accumulation of cholesterol (in both free- and esterified form) was not affected by the treatment (Supplemental figure 4).

Caspase-1 inhibition reduces hepatic inflammation

In addition to the observed reduction in hepatic steatosis, Ac-YVAD-cmk had a strong effect on plasma ALAT, a marker of hepatocellular damage (HFD: 390.5±16.4 U/l, HFD-YVAD: 237.0±35.7 U/l, $p<0.05$, Figure 4A). To investigate whether this was reflected by a reduction in NASH development, we next analyzed hepatic inflammation, a defining characteristic of NASH that can be observed histologically as the presence of inflammatory cell foci. Analysis of the number of these inflammatory cell foci showed marked lobular inflammation in HFD mice (3.6±0.6 foci per 100x field, Figure 4B), while Ac-YVAD-cmk treatment strongly reduced (-51%) the number of these inflammatory cell clusters (1.8±0.3 foci per 100x field, $p<0.01$, Figure 4B). As hepatic gene expression analysis for the macrophage marker *Emr1* (F4/80) indicated that this anti-inflammatory effect of Ac-YVAD-cmk was not due to an effect on macrophages (Figure 4C) we next investigated whether Ac-YVAD-cmk may have an effect on neutrophilic cells, the influx of which is considered a hallmark of human

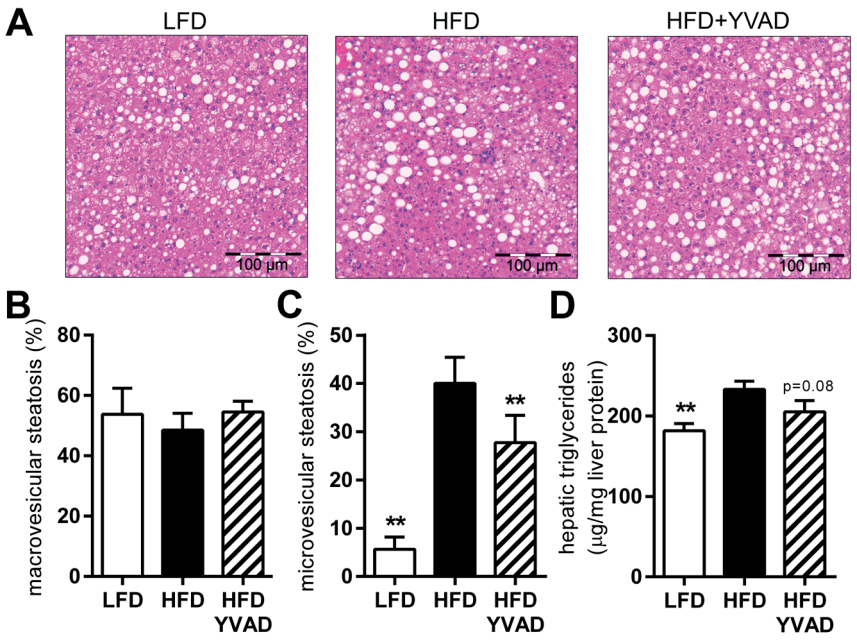


Figure 3. Effects of caspase-1 inhibition on hepatic steatosis. LDLr-/-.Leiden mice were fed a high-fat diet for 21 weeks (HFD; n=15) or HFD + caspase 1 inhibitor Ac-YVAD-cmk (40 mg/kg daily) starting treatment after 9 weeks of HFD (HFD+YVAD; n=15). Low-fat diet (LFD)-fed mice (n=15) were included as a reference. (A) representative photomicrographs of H&E stained liver sections. (B) Macrovesicular steatosis did not differ between groups. (C) HFD feeding induced pronounced microvesicular steatosis, which was reduced in HFD+YVAD. (D) HFD-induced hepatic triglycerides tended to be reduced in HFD+YVAD. All data are from the t=21 weeks time point and are mean±SEM. ** $p<0.01$ compared with HFD.

NASH [22,26,27]. Immunohistochemical staining for the neutrophil marker myeloperoxidase showed distinct presence of neutrophils in HFD animals, which was clearly reduced in HFD-YVAD mice (Figure 4D), as is also evident from the quantification of the number of MPO-positive inflammatory foci per field (Figure 4E). In line with these results, we observed a profound reduction (43%) in the mRNA levels of the pro-inflammatory cytokine *Tnfa* (TNF-α) in HFD-YVAD mice (1.0±0.14 in HFD, 0.6±0.06 in HFD-YVAD, $p<0.05$, Figure 4F).

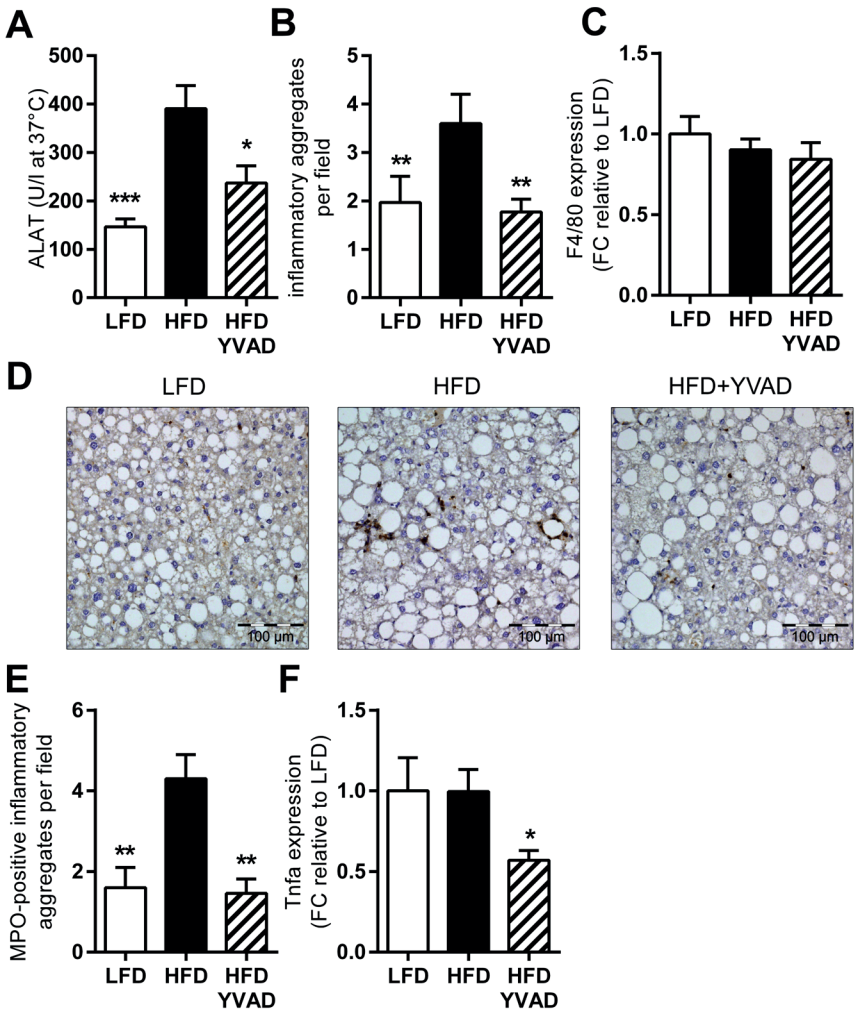


Figure 4. Effects of caspase-1 inhibition on hepatic inflammation. LDLr-/-.Leiden mice were fed a high-fat diet for 21 weeks (HFD; n=15) or HFD + caspase 1 inhibitor Ac-YVAD-cmk (40 mg/kg daily) starting treatment after 9 weeks of HFD (HFD+YVAD; n=15). Low-fat diet (LFD)-fed mice (n=15) were included as a reference. (A) HFD-induced plasma alanine aminotransferase (ALAT) was reduced in HFD+YVAD. (B) Lobular inflammation (number of inflammatory foci per 100x field) was induced by HFD, this induction was prevented by Ac-YVAD-cmk treatment. (C) F4/80 mRNA expression did not differ between groups. (D) Representative photomicrographs of immunohistochemical analysis of MPO-positive neutrophils. (E) Quantification of the number of MPO-positive inflammatory foci (per 100x field) revealed a clear induction in HFD, which was not apparent in YVAD. (F) Hepatic Tnf-α mRNA was reduced in HFD+YVAD. All data are from the t=21 weeks time point and are mean±SEM. * $p<0.05$, ** $p<0.01$, *** $p<0.001$ compared with HFD.

Caspase-1 inhibition reduces hepatic fibrosis

As hepatocellular damage and hepatic inflammation are thought to drive the development of hepatic fibrosis, we next questioned whether Ac-YVAD-cmk treatment may also reduce fibrosis development. Picro-sirius red staining for collagen content revealed presence of periportal and pericellular fibrosis without bridging in HFD, which was attenuated by Ac-YVAD-cmk (Figure 5A). Automated quantification of the area stained positively for collagen showed a strong reduction in the total fibrotic area (-65%) in HFD-YVAD mice compared with HFD (1.14±0.28 in HFD, 0.40±0.04 in HFD-YVAD, $p<0.05$, Figure 5B). The pathologist-assessed percentage of pericellular fibrosis specifically was also lower in HFD-YVAD, although this effect was not statistically significant (1.4±0.57 in LFD, 2.3±0.73 in HFD, 1.3±0.51 in HFD-YVAD, $p=0.14$ for HFD-YVAD compared with HFD). Hepatic gene expression analysis of *Col1a1* confirmed the observed effect on hepatic collagen deposition (1.80±0.36 in HFD, 0.68±0.17 in HFD-YVAD, 62% reduction, $p<0.01$, Figure 5C). Consistently, we observed a marked reduction (49%) in expression of the stellate cell activation marker *Acta2* (αSMA) (1.65±0.23 in HFD, 0.84±0.09 in HFD-YVAD, $p<0.01$, Figure 5D). Collectively, these data indicate that therapeutic intervention with Ac-YVAD-cmk attenuates hepatocellular inflammation and activation of the primary collagen-producing cell type in the liver.

DISCUSSION

A growing body of evidence supports an important role for NLRP3 inflammasome activation in the development of obesity-related diseases such as insulin resistance/T2D and NASH. However, the potential therapeutic value of inhibitors of the inflammasome/caspase-1 to treat NASH remains unclear. Here we show that intervention with the caspase-1 inhibitor Ac-YVAD-cmk reduces development of NASH and associated fibrosis. Importantly, efficacy of Ac-YVAD-cmk was demonstrated in mice with established obesity-associated hypertriglyceridemia, hypercholesterolemia, hyperglycemia, and hyperinsulinemia.

We found that treatment with Ac-YVAD-cmk substantially retarded the progression of NAFLD, with reductions in hepatic steatosis, inflammation and

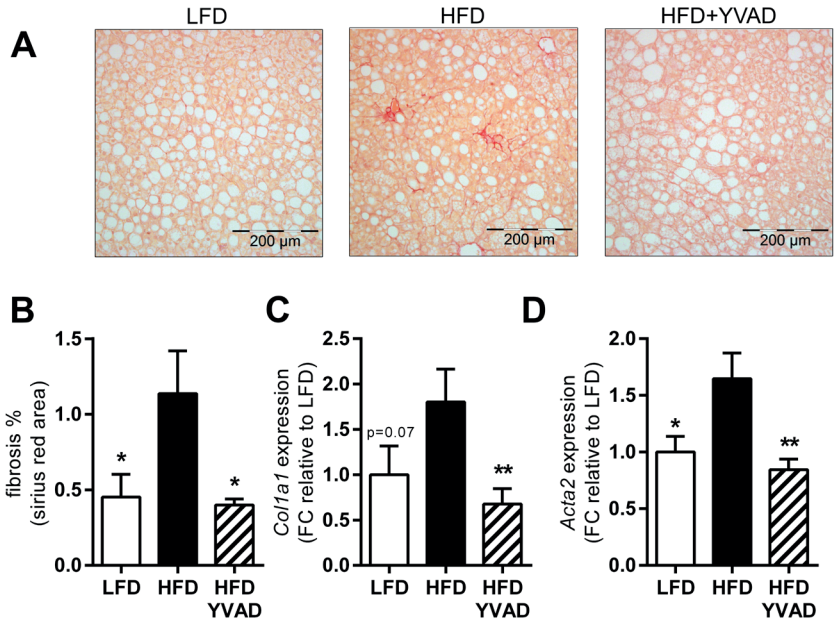


Figure 5. Effects of caspase-1 inhibition on hepatic fibrosis. LDLr-/-.Leiden mice were fed a high-fat diet for 21 weeks (HFD; n=15) or HFD + caspase 1 inhibitor Ac-YVAD-cmk (40 mg/kg daily) starting treatment after 9 weeks of HFD (HFD+YVAD; n=15). Low-fat diet (LFD)-fed mice (n=15) were included as a reference. (A) Representative photomicrographs of Picro-Sirius Red stained liver sections show hepatopericellular fibrosis in HFD animals which is reduced in HFD+YVAD. (B) Quantification of positively-stained area in Picro-Sirius red stained liver sections show a clear induction of fibrosis in HFD which is reduced in HFD+YVAD. (C) Col1a1 mRNA expression is reduced in HFD+YVAD. (D) mRNA expression of hepatic stellate cell activation marker Acta2 (α-SMA) tended to be induced in HFD and was reduced in HFD+YVAD. All data are from the t=21 weeks time point and are mean±SEM. * $p<0.05$, ** $p<0.01$ compared with HFD.

fibrosis. In accordance with our observations, others have reported that genetic deletion of caspase-1 reduces HFD-induced hepatic triglyceride levels and lipogenic gene expression (*Pparg, Srebp1c, Acc, Scd1*) [14] and deletion of NLRP3 attenuates HFD-induced hepatic steatosis with increased expression of fatty acid oxidation regulators [28]. Furthermore, deletion of caspase-1 was shown to reduce intestinal triglyceride absorption after an oral lipid load, with consequent reductions in the uptake and incorporation of these intestinally-derived triglycerides into peripheral tissues [29]. Together, these effects on hepatic lipid metabolism and intestinal lipid

uptake may promote a reduction in hepatic steatosis in absence of active caspase-1, as observed herein.

Although the effects of Ac-YVAD-cmk treatment on hepatic steatosis in the current study were modest, we did observe a strong effect on hepatic inflammation. In line with this, Dixon et al. have shown that deletion of caspase-1 leads to dissociation between hepatic triglyceride levels and inflammatory activity [13]. Results from our analysis of hepatic inflammation indicate that the anti-inflammatory effects of Ac-YVAD-cmk treatment are attributable to an effect on the influx of myeloperoxidase-positive neutrophilic cells, without affecting expression of the monocyte/macrophage marker F4/80. Consistent with this, others report that caspase-1 deficiency does not affect HFD-induced hepatic F4/80 expression and suggest that caspase-1 may be of importance in regulating the sensitivity of Kupffer cells to activation rather than recruitment and/or proliferation of Kupffer cells in the liver [14]. Furthermore, constitutively expressed hyperactive NLRP3 resulted in severe liver inflammation with many inflammatory foci composed predominantly of neutrophils, in absence of an effect on F4/80 expression [15]. Together these results indicate that modulation of caspase-1 expression or activity primarily influences the influx of neutrophils into the liver, which is considered a defining characteristic of human NASH [30]. Since neutrophils have the ability to release a potent cocktail of reactive oxygen species and proteases, they are a potential cause of extensive tissue damage that may contribute to amplification of the inflammatory response and development of hepatic fibrosis [31,32]. More specifically, a recent study has shown that neutrophilic myeloperoxidase promotes progression of NASH to fibrosis, potentiating oxidative stress, causing hepatocyte injury and activating hepatic stellate cells [33].

In line with the observed reductions in hepatic inflammation and, more specifically, neutrophil infiltration, we observed a reduction in the development of hepatic fibrosis in Ac-YVAD-cmk-treated mice. Multiple lines of evidence indicate that caspase-1 activation is required and essential for hepatic fibrogenesis. Watanabe and colleagues demonstrated that NLRP3 inflammasome activation in hepatic stellate cells results in activation of and collagen production by these cells [34]. Furthermore, they showed that chemically-induced (with CCl_4 or

Thioacetamide) hepatic stellate cell activation and liver fibrosis was reduced in mice deficient in NLRP3 or the inflammasome adaptor protein ASC. In line with this, Dixon et al. have shown reduced hepatic stellate cell activation and collagen deposition in *Casp1*-/- mice fed an MCD diet [13] or a HFD [14]. Similarly, hepatic stellate cell activation and collagen deposition was also reduced in NLRP3-/- mice on a choline-deficient amino acid-defined diet [12], while mice that express constitutively hyperactive NLRP3 showed increased collagen deposition relative to wild-type mice [15]. Altogether these studies indicate that NLRP3 inflammasome activation is a generic process that is observed during fibrogenesis across a range of different (both chemically- and dietary-induced) models of hepatic fibrosis. Our observations of reduced hepatic stellate cell activation and collagen deposition further corroborate these observations, and show that therapeutic intervention with a caspase-1 inhibitor in the ongoing disease process can reduce development of hepatic fibrogenesis.

Since obesity-associated insulin resistance is thought to play a causal role in the pathogenesis of NASH [35], we studied the effects of caspase-1 inhibition in the LDLr-/-.Leiden model, which develops NAFLD in the context of insulin resistance. We found that treatment with Ac-YVAD-cmk retarded HFD-induced increases in fasting plasma glucose and insulin levels. This is in line with findings by others, who have shown improved insulin sensitivity in Casp1-/- mice [36,37]. It is thought that this effect of caspase-1 on insulin sensitivity may be mediated for a large part by the role that caspase-1 plays in expanding WAT. Stienstra et al. [36] demonstrated that obesity-induced inflammation originating from expanding WAT is represented by inflammasome and caspase-1 activation, which governs adipocyte differentiation and insulin sensitivity and contributes to insulin resistance. *In vitro* studies in mature human SGBS adipocytes showed that treatment with the caspase-1 inhibitor pralnacasan directly enhanced insulin signaling in these cells, indicating that caspase-1 activation within adipocytes may have direct detrimental effects on insulin sensitivity of these cells. These effects were further substantiated *in vivo* in a proof-of-concept experiment in which ob/ob mice were treated with pralnacasan for two weeks [36], showing that caspase-1 inhibition can improve insulin sensitivity *in vivo*.

Remarkably, we observed no elevation in plasma insulin in Ac-YVAD-cmk-treated mice during the ipGTT. There are several potential explanations for this phenomenon. Firstly, we cannot exclude that insulin levels may have peaked between two of the time points of blood sampling, although this seems unlikely given the plasma half-life of insulin of around 10 minutes in mice [38]. Secondly, it is possible that Ac-YVAD-cmk affected non-insulin-dependent glucose uptake. All cell types have the capacity to take up glucose independently of insulin, ensuring basal as well as hyperglycemia-promoted supply of glucose. As much as 75% of whole-body glucose uptake is considered to be operated through pathways that are non-insulin dependent [39], for instance through effects on cell membrane fluidity, which is known to influence glucose transporter activity [40]. Thirdly, Ac-YVAD-cmk may stimulate proteins and their actions downstream of the insulin receptor (at the post-receptor level or in the lower part of the insulin cascade) and may thus generate a more efficacious effect with the available insulin [39]. The relatively high absolute insulin levels observed in Ac-YVAD-cmk treated mice (~11 ng/mL) are in support of this notion. Another possible rationale may be found in an effect of Ac-YVAD-cmk on the potency of the insulin molecules themselves (either through direct interaction with insulin or indirectly through its effects on caspase-1), in a manner similar to that which has been observed for instance for the chemokine MIF, which affects insulin conformation and thereby increases the potency of insulin molecules [41]. Which of these mechanisms – alone or in concert – is responsible for the observed effects merits further investigation.

In the present study, reduced progression of insulin resistance and NAFLD development coincided with improvement of WAT inflammation in Ac-YVAD-cmk-treated animals. This corresponds with findings by others, who have shown that absence of caspase-1 reduces macrophage infiltration into WAT and protects against HFD-induced WAT inflammation [37]. Inflammation of WAT (i.e. macrophage infiltration and CLS formation) is increasingly considered to be a crucial event in the development of obesity-associated insulin resistance and NAFLD [42]. Besides associative studies demonstrating associations between progressive NAFLD and WAT inflammation in obese subjects [43,44], experimental studies have shown that obesity-associated inflammation in WAT precedes hepatic inflammation in HFD-fed

mice [45,46]. Surgical removal of inflamed WAT provided evidence for a causal role of inflamed WAT in the progression of NASH [47]. The observed reduction of WAT inflammation herein may thus indirectly have contributed to the attenuation of NASH development by Ac-YVAD-cmk.

Overall, we show that intervention with the caspase-1 inhibitor Ac-YVAD-cmk improves insulin resistance and retards the progression of NASH and fibrosis development in male LDLr-/-.Leiden mice. Data from this study further support the importance of inflammasome/caspase-1 in the development of insulin resistance and NASH and demonstrate that therapeutic intervention in the already ongoing disease process is feasible.

ACKNOWLEDGEMENTS

We would like to thank Simone van der Drift-Droog, Erik Offerman and Karin Toet for their excellent technical assistance.

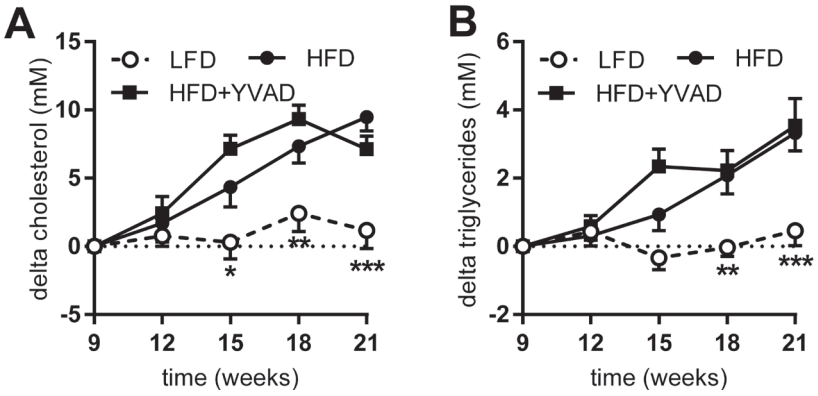
REFERENCES

1. Fabbrini E, Sullivan S, Klein S. Obesity and nonalcoholic fatty liver disease: biochemical, metabolic, and clinical implications. Hepatology 2010;51:679-689.
2. Birkenfeld AL, Shulman GI. Nonalcoholic fatty liver disease, hepatic insulin resistance, and type 2 diabetes. Hepatology 2014;59:713-723.
3. Tiniakos DG, Vos MB, Brunt EM. Nonalcoholic fatty liver disease: Pathology and pathogenesis. Annu Rev Pathol 2010;5:145-171.
4. Angulo P. Nonalcoholic fatty liver disease. N Engl J Med 2002;346:1221-1231.
5. Charlton MR, Burns JM, Pedersen RA, Watt KD, Heimbach JK, Dierkhising RA. Frequency and outcomes of liver transplantation for nonalcoholic steatohepatitis in the United States. Gastroenterology 2011;141:1249-1253.
6. Hotamisligil GS. Inflammation and metabolic disorders. Nature 2006;444:860-867.
7. Exley MA, Hand L, O'Shea D, Lynch L. Interplay between the immune system and adipose tissue in obesity. J Endocrinol 2014;223:R41-48.
8. Horng T, Hotamisligil GS. Linking the inflammasome to obesity-related disease. Nat Med 2011;17:164-165.
9. Csak T, Ganz M, Pespisa J, Kodys K, Dolganiuc A, Szabo G. Fatty acid and endotoxin activate inflammasomes in mouse hepatocytes that release danger signals to stimulate immune cells. Hepatology 2011;54:133-144.
10. Wen H, Gris D, Lei Y, Jha S, Zhang L, Huang MT, et al. Fatty acid-induced NLRP3-ASC inflammasome activation interferes with insulin signaling. Nat Immunol 2011;12:408-415.
11. Gross O, Thomas CJ, Guarda G, Tschopp J. The inflammasome: an integrated view. Immunol Rev 2011;243:136-151.
12. Wree A, McGeough MD, Pena CA, Schlattjan M, Li H, Inzaugarat ME, et al. NLRP3 inflammasome activation is required for fibrosis development in NAFLD. J Mol Med 2014;92:1069-1082.
13. Dixon LJ, Berk M, Thapaliya S, Papouchado BG, Feldstein AE. Caspase-1-mediated regulation of fibrogenesis in diet-induced steatohepatitis. Lab Invest 2012;92:713-723.
14. Dixon LJ, Flask CA, Papouchado BG, Feldstein AE, Nagy LE. Caspase-1 as a central regulator of high fat diet-induced non-alcoholic steatohepatitis. PLoS One 2013;8:e56100.
15. Wree A, Eguchi A, McGeough MD, Pena CA, Johnson CD, Canbay A, et al. NLRP3 inflammasome activation results in hepatocyte pyroptosis, liver inflammation, and fibrosis in mice. Hepatology 2014;59:898-910.
16. Liang W, Menke AL, Driessen A, Koek GH, Lindeman JH, Stoop R, et al. Establishment of a general NAFLD scoring system for rodent models and comparison to human liver pathology. PloS one 2014;9:e115922.
17. Radonjic M, Wielinga PY, Wopereis S, Kelder T, Goelela VS, Verschuren L, et al. Differential effects of drug interventions and dietary lifestyle in developing type 2 diabetes and complications: a systems biology analysis in LDLr-/- mice. PloS one 2013;8:e56122.
18. Mulder P, Liang W, Wielinga PY, Verschuren L, Toet K, Havekes LM, et al. Macrovesicular steatosis is associated with development of lobular inflammation and fibrosis in diet-induced non-alcoholic steatohepatitis (NASH). Inflammation and Cell Signaling 2015;2.
19. Lipinska K, Malone KE, Moerland M, Kluft C. Applying caspase-1 inhibitors for inflammasome assays in human whole blood. J Immunol Methods 2014;411:66-69.

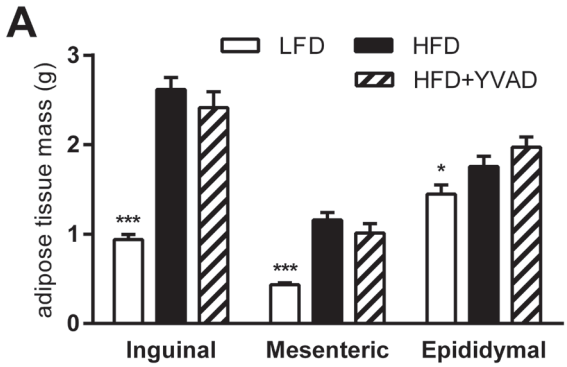
20. Osuka A, Hanschen M, Stoecklein V, Lederer JA. A protective role for inflammasome activation following injury. Shock 2012;37:47-55.
21. Suzuki H, Sozen T, Hasegawa Y, Chen W, Zhang JH. Caspase-1 inhibitor prevents neurogenic pulmonary edema after subarachnoid hemorrhage in mice. Stroke 2009;40:3872-3875.
22. Liang W, Lindeman JH, Menke AL, Koonen DP, Morrison M, Havekes LM, et al. Metabolically induced liver inflammation leads to NASH and differs from LPS- or IL-1beta-induced chronic inflammation. Lab Invest 2014;94:491-502.
23. Bligh EG, Dyer WJ. A rapid method of total lipid extraction and purification. Can J Biochem Physiol 1959;37:911-917.
24. Lowry OH, Rosebrough NJ, Farr AL, Randall RJ. Protein measurement with the Folin phenol reagent. J Biol Chem 1951;193:265-275.
25. Morrison MC, Liang W, Mulder P, Verschuren L, Pieterman E, Toet K, et al. Mirtoselect, an anthocyanin-rich bilberry extract, attenuates non-alcoholic steatohepatitis and associated fibrosis in ApoE *3Leiden mice. J Hepatol 2015;62:1180-1186.
26. Hubscher SG. Histological assessment of non-alcoholic fatty liver disease. Histopathology 2006;49:450-465.
27. Rensen SS, Slaats Y, Nijhuis J, Jans A, Bieghs V, Driessen A, et al. Increased hepatic myeloperoxidase activity in obese subjects with nonalcoholic steatohepatitis. Am J Pathol 2009;175:1473-1482.
28. Vandanmagsar B, Youm YH, Ravussin A, Galgani JE, Stadler K, Mynatt RL, et al. The NLRP3 inflammasome instigates obesity-induced inflammation and insulin resistance. Nat Med 2011;17:179-188.
29. van Diepen JA, Stienstra R, Vroegrijk IO, van den Berg SA, Salvatori D, Hooiveld GJ, et al. Caspase-1 deficiency in mice reduces intestinal triglyceride absorption and hepatic triglyceride secretion. J Lipid Res 2013;54:448-456.
30. Brunt EM, Janney CG, Di Bisceglie AM, Neuschwander-Tetri BA, Bacon BR. Nonalcoholic steatohepatitis: a proposal for grading and staging the histological lesions. Am J Gastroenterol 1999;94:2467-2474.
31. Kubes P, Mehal WZ. Sterile inflammation in the liver. Gastroenterology 2012;143:1158-1172.
32. Xu R, Huang H, Zhang Z, Wang FS. The role of neutrophils in the development of liver diseases. Cellular and Molecular Immunology 2014;11:224-231.
33. Pulli B, Ali M, Iwamoto Y, Zeller MW, Schob S, Linnoila JJ, et al. Myeloperoxidase-hepatocyte-stellate cell cross talk promotes hepatocyte injury and fibrosis in experimental nonalcoholic steatohepatitis. Antioxidants and Redox Signaling 2015.
34. Watanabe A, Sohail MA, Gomes DA, Hashmi A, Nagata J, Sutterwala FS, et al. Inflammasome-mediated regulation of hepatic stellate cells. American Journal of Physiology - Gastrointestinal and Liver Physiology 2009;296:G1248-1257.
35. Pagano G, Pacini G, Musso G, Gambino R, Mecca F, Depetris N, et al. Nonalcoholic steatohepatitis, insulin resistance, and metabolic syndrome: Further evidence for an etiologic association. Hepatology 2002;35:367-372.
36. Stienstra R, Joosten LA, Koenen T, van Tits B, van Diepen JA, van den Berg SA, et al. The inflammasome-mediated caspase-1 activation controls adipocyte differentiation and insulin sensitivity. Cell Metab 2010;12:593-605.
37. Stienstra R, van Diepen JA, Tack CJ, Zaki MH, van de Veerdonk FL, Perera D, et al. Inflammasome is a central player in the induction of obesity and insulin resistance. Proc Natl Acad Sci U S A 2011;108:15324-15329.
38. Cresto J, Lavine R, Buchly M, Penhos J, Bhathena S, Recant L. Half life of injected 125I-insulin in control and ob/ob mice. Acta physiologica latino americana 1976;27:7-15.

39. Wiernsperger NF. Is non-insulin dependent glucose uptake a therapeutic alternative? Part 1: physiology, mechanisms and role of non insulin-dependent glucose uptake in type 2 diabetes. Diabetes Metab 2005;31:415-426.
40. Pilch PF, Thompson PA, Czech MP. Coordinate modulation of D-glucose transport activity and bilayer fluidity in plasma membranes derived from control and insulin-treated adipocytes. Proc Natl Acad Sci U S A 1980;77:915-918.
41. Vujicic M, Senerovic L, Nikolic I, Saksida T, Stosic-Grujicic S, Stojanovic I. The critical role of macrophage migration inhibitory factor in insulin activity. Cytokine 2014;69:39-46.
42. Esser N, Legrand-Poels S, Piette J, Scheen AJ, Paquot N. Inflammation as a link between obesity, metabolic syndrome and type 2 diabetes. Diabetes Res Clin Pract 2014;105:141-150.
43. Cancello R, Tordjman J, Poitou C, Guilhem G, Bouillot JL, Hugol D, et al. Increased infiltration of macrophages in omental adipose tissue is associated with marked hepatic lesions in morbid human obesity. Diabetes 2006;55:1554-1561.
44. Tordjman J, Poitou C, Hugol D, Bouillot J-L, Basdevant A, Bedossa P, et al. Association between omental adipose tissue macrophages and liver histopathology in morbid obesity: Influence of glycemic status. J Hepatol 2009;51:354-362.
45. Liang W, Tonini G, Mulder P, Kelder T, van Erk M, van den Hoek AM, et al. Coordinated and interactive expression of genes of lipid metabolism and inflammation in adipose tissue and liver during metabolic overload. PLoS One 2013;8:e75290.
46. van der Heijden RA, Sheedfar F, Morrison MC, Hommelberg PP, Kor D, Kloosterhuis NJ, et al. High-fat diet induced obesity primes inflammation in adipose tissue prior to liver in C57BL/6j mice. Aging 2015;7:256.
47. Mulder P, Morrison MC, Wielinga PY, van Duyvenvoorde W, Kooistra T, Kleemann R. Surgical removal of inflamed epididymal white adipose tissue attenuates the development of non-alcoholic steatohepatitis in obesity. Int J Obes 2015:e-pub ahead of print 26 October 2015.

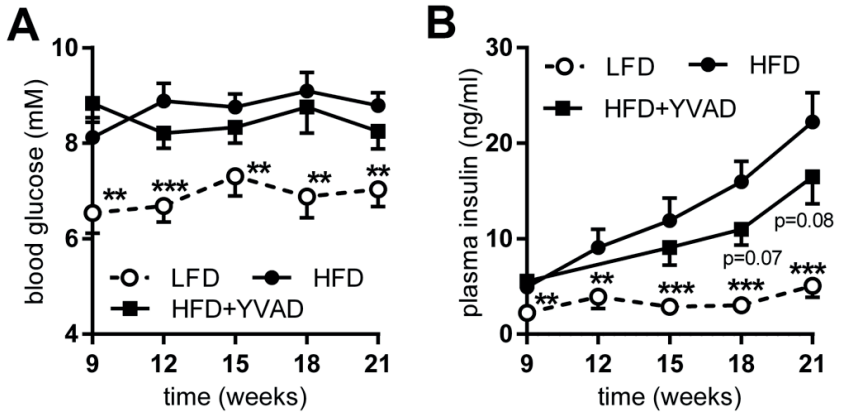
SUPPLEMENTAL DATA



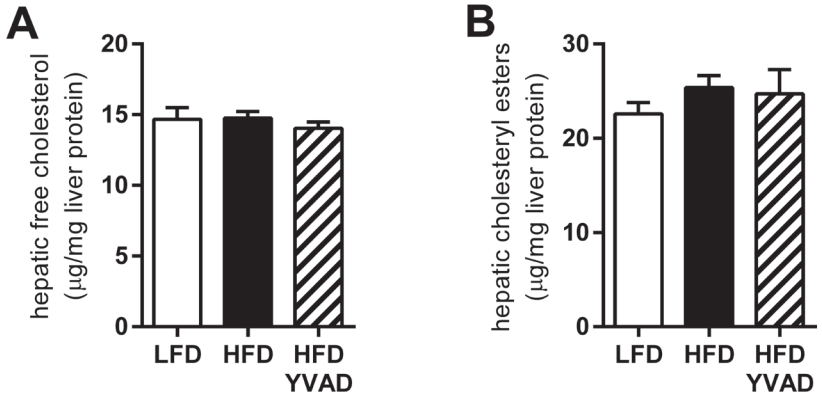
Supplementary Figure 1. Effects of caspase-1 inhibition on plasma lipids. LDLr-/-.Leiden mice were fed a high-fat diet for 21 weeks (HFD; n=15) or a HFD with caspase 1 inhibitor Ac-YVAD-cmk (40 mg/kg daily) starting treatment after 9 weeks of HFD (HFD+YVAD; n=15). Low-fat diet (LFD)-fed mice (n=15) were included as a reference. (A) HFD-induced increases in plasma cholesterol relative to treatment start (t=9 weeks) were not affected by HFD+YVAD. (B) HFD-induced increases in plasma triglycerides relative to treatment start (t=9 weeks) were not affected by HFD+YVAD. All data are mean±SEM. * p<0.05, compared with HFD, ** p<0.01 compared with HFD, *** p<0.001 compared with HFD.



Supplementary Figure 2. Effects of caspase-1 inhibition on adipose tissue mass. LDLr-/-.Leiden mice were fed a high-fat diet for 21 weeks (HFD; n=15) or HFD + caspase 1 inhibitor Ac-YVAD-cmk (40 mg/kg daily) starting treatment after 9 weeks of HFD (HFD+YVAD; n=15). Low-fat diet (LFD)-fed mice (n=15) were included as a reference. Distribution of fat mass over the inguinal, mesenteric and epididymal depots was not affected by HFD+YVAD. All data are mean±SEM. * p<0.05, compared with HFD, *** p<0.001 compared with HFD.



Supplementary Figure 3. Effects of caspase-1 inhibition on blood glucose and plasma insulin. LDLr-/-.Leiden mice were fed a high-fat diet for 21 weeks (HFD; n=15) or HFD + caspase 1 inhibitor Ac-YVAD-cmk (40 mg/kg daily) starting treatment after 9 weeks of HFD (HFD+YVAD; n=15). Low-fat diet (LFD)-fed mice (n=15) were included as a reference. (A) Blood glucose levels were not significantly affected by Ac-YVAD-cmk treatment. (B) Ac-YVAD-cmk treatment tended to reduce plasma insulin levels. All data are mean±SEM. ** p<0.01, *** p<0.001 compared with HFD.



Supplementary Figure 4. Effects of caspase-1 inhibition on hepatic cholesterol. LDLr-/-.Leiden mice were fed a high-fat diet for 21 weeks (HFD; n=15) or HFD + caspase 1 inhibitor Ac-YVAD-cmk (40 mg/kg daily) starting treatment after 9 weeks of HFD (HFD+YVAD; n=15). Low-fat diet (LFD)-fed mice (n=15) were included as a reference. (A) Ac-YVAD-cmk treatment did not affect intrahepatic free cholesterol levels. (B) Hepatic cholesteryl esters were not affected in HFD+YVAD. All data are mean±SEM.

Chapter 6

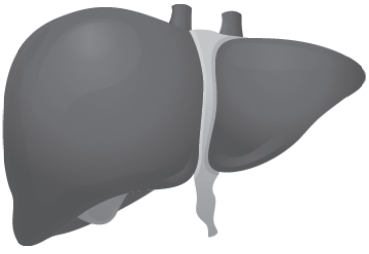
Replacement of Dietary Saturated Fat by PUFA-rich Pumpkin Seed Oil Attenuates Non-Alcoholic Fatty Liver Disease and Atherosclerosis Development, with Additional Health Effects of Virgin over Refined Oil

Martine C. Morrison[1,2], Petra Mulder[1], P. Mark Stavro[3], Manuel Suárez [4,5], Anna Arola-Arnal[4,5], Wim van Duyvenvoorde[1], Teake Kooistra[1], Peter Y. Wielinga[1], Robert Kleemann[1,6]

[1] Department of Metabolic Health Research, Netherlands Organization for Applied Scientific Research (TNO), Leiden, the Netherlands
[2] Department of Pathology and Medical Biology, University of Groningen, University Medical Center Groningen, Groningen, the Netherlands
[3] Bunge Ltd., White Plains, NY, USA
[4] Department of Biochemistry and Biotechnology, Rovira iVirgili University, Tarragona, Spain
[5] Centre Tecnològic de Nutrició i Salut (CTNS), TECNIO, CEICS, Reus, Spain
[6] Department of Human and Animal Physiology, Wageningen University, Wageningen, the Netherlands

PloS one. 2015 Sep 25;10(9):e0139196.







ABSTRACT

Background and aims: As dietary saturated fatty acids are associated with metabolic and cardiovascular disease, a potentially interesting strategy to reduce disease risk is modification of the quality of fat consumed. Vegetable oils represent an attractive target for intervention, as they largely determine the intake of dietary fats. Furthermore, besides potential health effects conferred by the type of fatty acids in a vegetable oil, other minor components (e.g. phytochemicals) may also have health benefits. Here, we investigated the potential long-term health effects of isocaloric substitution of dietary fat (i.e. partial replacement of saturated by unsaturated fats), as well as putative additional effects of phytochemicals present in unrefined (virgin) oil on development of non-alcoholic fatty liver disease (NAFLD) and associated atherosclerosis. For this, we used pumpkin seed oil, because it is high in unsaturated fatty acids and a rich source of phytochemicals.

Methods: ApoE*3Leiden mice were fed a Western-type diet (CON) containing cocoa butter (15% w/w) and cholesterol (1% w/w) for 20 weeks to induce risk factors and disease endpoints. In separate groups, cocoa butter was replaced by refined (REF) or virgin (VIR) pumpkin seed oil (comparable in fatty acid composition, but different in phytochemical content).

Results: Both oils improved dyslipidemia, with decreased (V)LDL-cholesterol and triglyceride levels in comparison with CON, and additional cholesterol-lowering effects of VIR over REF. While REF did not affect plasma inflammatory markers, VIR reduced circulating serum amyloid A and soluble vascular adhesion molecule-1. NAFLD and atherosclerosis development was modestly reduced in REF, and VIR strongly decreased liver steatosis and inflammation as well as atherosclerotic lesion area and severity.

Conclusions: Overall, we show that an isocaloric switch from a diet rich in saturated fat to a diet rich in unsaturated fat can attenuate NAFLD and atherosclerosis development. Phytochemical-rich virgin pumpkin seed oil exerts additional anti-inflammatory effects resulting in more pronounced health effects.

INTRODUCTION

Cardiometabolic diseases such as non-alcoholic fatty liver disease (NAFLD) and cardiovascular disease (CVD) constitute a major health burden in modern societies. Accumulating evidence suggests that NAFLD, besides increasing liver morbidity and mortality, is associated with development of atherosclerosis, the major underlying pathology of CVD [1]. As dyslipidemia and chronic inflammation are recognized to drive the development of NAFLD as well as atherosclerosis [2-4], dietary regimens that influence one or both of these risk factors may be of great preventive and possibly even therapeutic benefit. Support for this concept comes from epidemiological and experimental studies that show that the type of dietary fat consumed plays an important role in the development of both NAFLD and associated CVD (reviewed in [5,6]). Therefore, a potentially interesting strategy to reduce cardiometabolic risk is a modification of the quality of fat in diets. This is further supported by results from a recent systematic review indicating that partial replacement of saturated fat by unsaturated fat may reduce CVD risk [7].

The daily intake of dietary fats is largely determined by vegetable oils, which makes them an attractive target for intervention. The more so, since besides potential health effects conferred by the type of fatty acids in a vegetable oil, other minor components of an oil (e.g. phytochemicals) may also significantly contribute to cardiometabolic health. Typically, vegetable oils are consumed in their fully refined form that consists almost exclusively of triglycerides. Virgin oils on the other hand, the completely unrefined first press form of an oil, are rich in a collection of phytochemicals (e.g. vitamins E and K, phytosterols and polyphenols) that may influence the critical risk factors dyslipidemia as well as inflammation [8,9].

Herein we investigated the potential long-term health effects of substitution of dietary saturated fat by unsaturated fat from refined oil, as well as putative additional effects of the unrefined counterpart rich in phytochemicals (virgin oil). For this, we used pumpkin seed oil, because it is high in unsaturated fatty acids (about 80%) and known to contain large amounts of phytochemicals [10,11]. In short-term studies, pumpkin seed oil has been shown to reduce surrogate markers of liver health [12] and improve dyslipidemia [13-15]. However, potential anti-

inflammatory properties have not been examined and its effects on cardiometabolic disease endpoints are unknown.

The ApoE*3Leiden (E3L) mouse is a well-established diet-inducible model for NAFLD [16] and atherosclerosis [17]. The model develops human-like dyslipidemia, inflammation and disease endpoints in response to a well-defined Western-type diet, containing cocoa butter (±60% saturated fat) as the major fat source [17,18]. This diet also contains cholesterol (1% w/w), which is required for induction of dyslipidemia, inflammation and disease endpoints [16,18,19]. Groups of E3L mice were fed the Western-type control diet (CON) or pumpkin seed oil-substituted diets, REF (refined oil) and VIR (virgin oil) for 20 weeks, all of which contained 1% cholesterol. The refined and virgin pumpkin seed oils were comparable in fatty acid profile but differed in phytochemical content. This allowed us to define the health effects of refined pumpkin seed oil, as well as the additional effects of the phytochemicals present in its unrefined counterpart. Plasma lipids and markers of inflammation were monitored over time and NAFLD and atherosclerosis endpoints were scored according to established human grading systems [20-22]. Results from this study indicate that an isocaloric switch from a diet rich in saturated fat to a diet rich in unsaturated fat has beneficial effects on risk factors, and that phytochemical-rich virgin oil has additional anti-inflammatory properties and more strongly reduces disease endpoints.

MATERIALS AND METHODS

All animal experiments were approved by an independent Ethical Committee on Animal Care and Experimentation (DEC-Zeist, the Netherlands) and were in compliance with European Community specifications regarding the use of laboratory animals. Female ApoE*3Leiden transgenic (E3L) mice were obtained from the breeding facility of TNO Metabolic Health Research, Leiden, the Netherlands, and were characterized for expression of human APOE by ELISA. 12-week old E3L mice were matched into 3 groups based on plasma cholesterol and triglycerides. All animals were group-housed (3-4 mice per cage) in the SPF animal

facility of TNO Metabolic Health Research, in a temperature-controlled room on a 12 hour light/dark cycle and had free access to food and water. Diets were based on a standardized atherogenic Western-type diet (WTD) that contains 15% cocoa butter, 1% corn oil, 40.5% sucrose, 20% acid casein, 10% corn starch and 6.2% cellulose (all w/w; diet-T; AB-Diets, Woerden, the Netherlands), supplemented with 1% (w/w) cholesterol (Sigma-Aldrich, Zwijndrecht, the Netherlands). Control mice (CON, n=18) were fed this standard WTD, while the treatment groups received the WTD with 9% (w/w of total diet) of the cocoa butter replaced by either 9% refined pumpkin seed oil (REF, n=15; Bunge Ltd., White Plains, USA) or 9% virgin pumpkin seed oil (VIR, n=15; Bunge Ltd). As the cholesterol in this diet is required to induce inflammation and dyslipidemia [16,18,19], the cholesterol concentration was the same (1%) in all three groups.

Detailed methods of the analysis of the composition of the cocoa butter and pumpkin seed oils are described in Supplement 1. Briefly, the fatty acid composition was determined by gas chromatography, the total phenolic content was determined spectrophotometrically by the Folin-Ciolcalteau method, and individual phenolic content of the pumpkin seed oils was determined by LC-QTOF-MS.

Food intake was measured per cage (3-4 mice per cage) every 4 weeks, expressed as the average food intake per mouse per day. The energy content of the diets was determined by bomb calorimetry. Blood samples were collected from the tail vein after a 4h fasting period for EDTA plasma isolation at week 0, 3, 6, 12 and 20 of the study. Total plasma cholesterol and triglyceride levels were measured in these fasted plasma samples by commercially available enzymatic assays (cholesterol CHOD-PAP 11491458 and triglycerides GPO-PAP 11488872, Roche, Woerden, The Netherlands). For lipoprotein profile analysis, pooled plasma samples were fractionated using an ÅKTA fast protein liquid chromatography system (Pharmacia, Roosendaal, the Netherlands) and analyzed as reported [23]. Plasma levels of soluble vascular adhesion molecule 1 (sVCAM-1; R&D Systems, Abingdon, UK) and serum amyloid A (SAA; Life Technologies, Bleiswijk, the Netherlands) were determined by ELISA. ALAT and ASAT levels were measured in serum (unfasted sample from terminal blood, specified below) using a spectrophotometric activity assay (Reflotron Plus system, Roche). After 20 weeks of dietary treatment, mice were sacrificed by CO_2

asphyxiation and blood was collected via cardiac puncture for serum collection (unfasted). Hearts and livers were collected, and fixed in formalin and embedded in paraffin for atherosclerosis analysis (heart) and NAFLD analysis (liver).

Histological analysis of NAFLD and atherosclerosis development

For NAFLD analysis, 3 µm liver sections (medial lobe) were stained with hematoxylin and eosin and analyzed blindly using an adapted scoring method for human NAFLD [20,24]. Briefly, steatosis was expressed as the percentage of the total liver cross section affected by microvesicular steatosis or macrovesicular steatosis. Hepatic inflammation was analyzed by counting the number of inflammatory foci per section at a 100× magnification.

Atherosclerosis was analyzed blindly in 4 serial cross sections (5 µm, at 50 µm intervals) of the valve area of the aortic root. Cross sections were stained with hematoxylin-phloxine-saffron (HPS) for morphometric analysis of lesion number and area (using cell^D software, version 2.7; Olympus Soft Imaging Solutions, Hamburg, Germany) and analysis of lesion severity. Lesion severity was scored according to the classification of the American Heart Association (AHA) [21,22]. This scoring system was used to distinguish five lesion types: Type I (early fatty streak): up to ten foam cells in the intima, no other changes; Type II (regular fatty streak): ten or more foam cells in the intima, no other changes; Type III (mild plaque): foam cells in the intima with presence of a fibrotic cap; Type IV (moderate plaque): progressive lesion, infiltration into media, elastic fibers intact; Type V (severe plaque): structure of media severely disrupted with fragmented elastic fibers, cholesterol crystals, calcium deposits and necrosis may be present. The lesional macrophage content was assessed by immunohistochemical staining of MAC-3 (CD107b) positive cells (purified rat anti-mouse CD107b antibody, BD Biosciences, Breda, the Netherlands) in cross-sections adjacent to those used for the atherosclerosis analysis. The MAC-3 positive area for each individual plaque was measured using an automated macro in the image processing software ImageJ (version 1.48, NIH, Bethesda, MD, USA; [25]) and expressed as the percentage of total plaque area that was positively stained for MAC-3. The number of lesions

was counted in 4 cross sections and expressed as the average per cross-section. Furthermore, the number of lesion-free (undiseased) segments was counted and expressed as a percentage of the total number of segments (N.B. each aortic cross-section is divided into 3 segments that are demarcated by the aortic valves, making a total of 12 segments analyzed per mouse).

Hepatic gene expression analyses

Total RNA was extracted from liver tissue using RNA Bee Total RNA Isolation Kit (Bio-Connect, Huissen, the Netherlands). Spectrophotometric analysis of RNA concentration was performed using Nanodrop 1000 (Isogen Life Science, De Meern, the Netherlands) and quality of RNA was assessed using a 2100 Bioanalyzer (Agilent Technologies, Amstelveen, the Netherlands). cDNA was synthesized using a High Capacity RNA-to-cDNA™ Kit (Life Technologies, Bleiswijk, The Netherlands). Hepatic gene expression analyses were performed by RT-PCR on a 7500 Fast Real-Time PCR System (Applied Biosystems by Life Technologies) using TaqMan® Gene Expression Assays (Life Technologies). Transcripts were quantified using TaqMan® Gene Expression Assays (Life Technologies) and the following primer/probe-sets for *Srebf1* (Mm00550338_m1), *Fasn* (Mm00662319_m1), *Dgat1* (Mm00515643_m1), *Ppara* (Mm00440939_m1), *Cpt1a* (Mm01231183_m1), *Acox1* (Mm00443579_m1), *Ccl2* (Mm00441242_m1), *Tnf* (Mm00443258_m1), *Il1b* (Mm00434228_m1) and the endogenous controls *Hprt* (Mm00446968_m1) and *Ppif* (Mm01273726_m1). Changes in gene expression were calculated using the comparative Ct (ΔΔCt) method and expressed as fold-change relative to CON.

Hepatic lipid analysis

Lipids were extracted from liver homogenates using the Bligh and Dyer method [26] and separated by high performance thin layer chromatography (HPTLC) on silica gel plates as described previously [27]. Lipid spots were stained with color reagent (5g $MnCl_2 \cdot 4H_2O$, 32ml 95–97% H_2SO_4 added to 960ml CH_3OH:H_2O 1:1 v/v) and triglycerides, cholesteryl esters and free cholesterol were quantified using TINA version 2.09 software (Raytest, Straubenhardt, Germany).

Statistical analyses

All data are presented as mean±SEM. Statistical analyses were performed using SPSS software (version 22, IBM, Armonk, USA). For normally distributed variables, significance of differences between groups was tested by one-way ANOVA, followed by Fisher's Least Significant Difference (LSD) Post-Hoc Test. In case of heterogeneity between groups, variables were analyzed by ANOVA using Brown-Forsythe for differences between groups followed by Dunnett's T3 Post-Hoc Test. Non-normally distributed variables were tested by non-parametric Kruskal-Wallis test followed by Mann-Whitney U tests. To test the hypothesis that both pumpkin seed oils may have beneficial effects relative to control and that the virgin oil may have additional beneficial effects over its refined counterpart, a one-sided p-value≤0.05 was considered statistically significant.

RESULTS

The refined and virgin pumpkin seed oils used in this study were comparable in fatty acid composition (Table 1). Both oils contained 81% unsaturated fatty acids, most of which consisted of linoleic acid (C18:2n-6, 64%) and oleic acid (C18:1n-9, 17%). The virgin oil contained more phytochemicals than its refined counterpart (Table 2). Virgin pumpkin seed oil was rich in benzoic acid, vanillic acid, ferulic acid, rutin and *p*-coumaric acid, many of which were below the detection limit in the refined oil. Overall, the total phenolic content was 7.7-fold higher in the virgin oil than in the refined oil.

To investigate potential health effects of these oils on NAFLD and atherosclerosis, E3L mice were fed a standardized Western type control diet (CON) or the same diet substituted with 9% (w/w) refined pumpkin seed oil (REF) or 9% (w/w) virgin pumpkin seed oil (VIR) for 20 weeks. All diets contained 1% (w/w) cholesterol and were comparable in energy content as quantified by bomb calorimetry (CON: 20.2 kJ/g, REF: 20.0 kJ/g and VIR: 20.4 kJ/g) and food intake was comparable between groups (Supplemental Figure 1). The treatments were well tolerated and body weight increased slightly over time (percentage body weight gain relative to t=6: CON: 12.3±1.3%, REF: 8.9±1.8%, VIR: 11.1±1.6%, n.s.) in all groups (Supplemental Figure 1).

Table 1. Fatty acid composition of cocoa butter and refined and virgin pumpkin seed oil.

		Cocoa butter	Refined pumpkin seed oil	Virgin pumpkin seed oil
Poly-unsaturated fatty acids (% of total)		**2.8**	**64.4**	**64.0**
C18:2	Linoleic acid (n-6)	2.7	64.1	63.9
C18:3	alpha-Linolenic acid (n-3)	0.1	0.3	0.1
Mono-unsaturated fatty acids (% of total)		**33.0**	**17.0**	**17.8**
C18:1	Oleic acid	32.8	16.6	17.1
C16:1	Palmitoleic acid	0.2	0.3	0.2
C20:1	Eicosanoic acid	n.d.	0.1	0.4
Saturated fatty acids (% of total)		**63.7**	**18.0**	**18.1**
C16:0	Palmitic acid	26.7	12.8	12.8
C18:0	Stearic acid	35.7	4.5	4.5
C20:0	Arachidic acid (Eicosanoic acid)	1.0	0.3	0.3
C22:0	Behenic acid (Docosanoic acid)	0.2	0.2	0.2
C14:0	Myristic acid (Tetradecanoic acid)	0.1	0.1	0.1
C24:0	Lignoceric acid (Tetracosanoic acid)	n.d.	0.1	0.1
Trans fatty acids (% of total)		**n.d.**	**0.7**	**0.2**
C18:2T	Trans linoleic acid	n.d.	0.7	0.2

n.d. = not detected

Table 2. Phytochemical content of cocoa butter and refined and virgin pumpkin seed oil

	Cocoa butter	Refined pumpkin seed oil	Virgin pumpkin seed oil
Tocopherols (ppm)	246	386	577
Tocotrienols (ppm)	7	123	121
Vitamin K (µg/100g)	3.5	52.3	68.0
Total phenolic content (mg gallic acid/kg oil)	8.3	3.6	27.7
Benzoic acid (µM)	n.d.	0.1	19.3
p-coumaric acid (nM)	n.d.	n.d.	200
Vanillic acid (nM)	791	n.d.	300
Ferulic acid (nM)	n.d.	n.d.	300
Rutin (nM)	n.d.	n.d.	4
Isomer of 3-hydroxybenzoic acid (nM)	n.d.	50	8000
Isomer of protocatechuic acid (nM)	n.d.	n.d.	700
Isomer of caffeic acid (nM)	n.d.	n.d.	60
Isomer of ferulic acid (nM)	456	30	100
Isomer of naringenin (nM)	162	n.d.	2100
Isomer of 4-hydroxyphenylpropionic (nM)	522	10	700

n.d. = not detected, Tocopherols = sum of α, β, γ and δ (δ was n.d.). Tocotrienols = sum of α, γ and δ.

Both pumpkin seed oils improve dyslipidemia, with additional beneficial effects of virgin oil over refined oil

Plasma cholesterol levels rose rapidly in CON animals within the first 3 weeks and remained relatively stable until the end of the study (Figure 1A) with an average of 19.20±0.39 mM. Both REF and VIR animals had significantly lower fasting plasma cholesterol levels compared with CON at all time points (Figure 1A). Area under the curve (AUC) analysis of the plasma cholesterol levels throughout the study period showed a significantly lower AUC for cholesterol in VIR (293.6±13.6 AU), than in REF (328.8±7.0 AU, $p \leq 0.05$, Figure 1B), indicating additional cholesterol-lowering properties of VIR. These cholesterol-lowering effects were mainly confined to the VLDL-sized particles (Figure 1C). In CON animals, fasting plasma triglycerides remained at a stable and elevated level during the study (average 2.67±0.09 mM, (Figure 1D). Both pumpkin seed oils decreased fasting plasma triglyceride levels within the first 3 weeks of the study and levels remained stable at this low level thereafter (average REF 1.79±0.08 mM, average VIR 1.63±0.07 mM, Figure 1D). Overall, VIR treatment did not have additional beneficial effects on plasma triglyceride levels relative to REF as is also shown by results from the AUC analysis for plasma triglyceride levels (Figure 1E). Together, these results indicate that the observed lipid-lowering effects are predominantly attributable to the replacement of saturated by unsaturated dietary fat.

Virgin pumpkin seed oil reduces circulating markers of liver and vascular inflammation

CON diet induced plasma levels of SAA, a marker of liver inflammation, from 5.65±0.34 µg/ml at t=0 to 10.55±1.21 µg/ml at the end of the study (Figure 2A). SAA levels in REF animals were comparable to CON, while VIR attenuated SAA induction and plasma levels were significantly lower than CON at t=12 and t=20 weeks (6.77±0.44 µg/ml at t=20, -36%, $p \leq 0.01$, Figure 2A). In line with this effect on SAA, serum levels of the hepatocellular damage markers ASAT and ALAT were not affected by REF, and VIR significantly reduced both ASAT ($p \leq 0.05$) and ALAT levels ($p \leq 0.05$) (Figure 2B-C). Besides inducing liver inflammation, CON diet also gradually induced plasma levels of vascular inflammation marker sVCAM-1 from 2.45±0.09

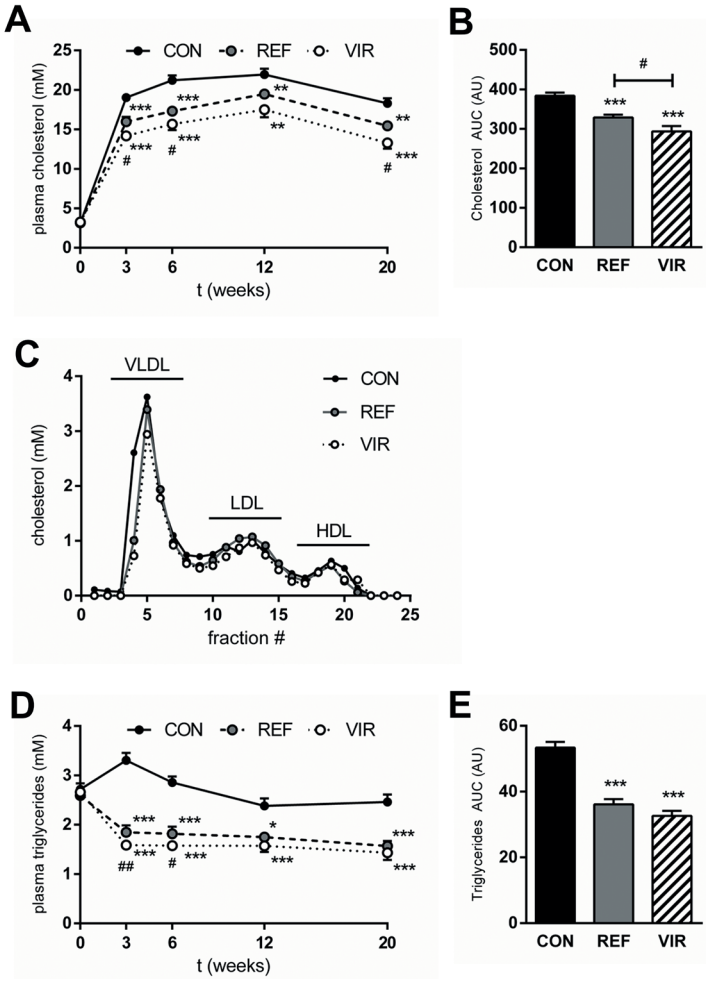


Figure 1. Refined and virgin pumpkin seed oils have beneficial effects on plasma lipids in cholesterol-fed ApoE*3Leiden mice. Mice were fed a Western type diet (CON) containing cocoa butter (15% w/w of diet) for 20 weeks. The cocoa butter was in part replaced by refined pumpkin seed oil (REF) or virgin pumpkin seed oil (VIR) (each 9% w/w of diet). (A) Plasma cholesterol levels over the course of the study, showing lower levels in REF and VIR-fed animals. (B) Area under the curve analysis (AUC, expressed in arbitrary units; AU) of plasma cholesterol levels (t=0 until t=20 weeks) shows additional cholesterol-lowering effect of VIR compared with REF. (C) Lipoprotein profile for cholesterol distribution in VLDL, LDL and HDL-sized particles shows cholesterol-lowering effect mainly confined to VLDL-sized particles. (D) Plasma triglycerides over the course of the study were lowered by both REF and VIR. (E) Area under the curve analysis of plasma triglyceride levels (t=0 until t=20 weeks) shows a reduction by VIR and REF. Data are mean±SEM. * p≤0.05, ** p≤0.01, *** p≤0.001 compared with CON. # p≤0.05, ## p≤0.01 for VIR compared with REF.

µg/ml at t=0 to 4.01±0.12 µg/ml at t=20 weeks (Figure 2D). Levels of sVCAM-1 were not affected by REF, but VIR animals showed lower sVCAM-1 throughout the study period and this effect reached significance at t=20 weeks (3.47±0.14 µg/ml, -14%, p≤0.05, Figure 2D). These data show that the phytochemicals in virgin pumpkin seed oil are responsible for the observed anti-inflammatory effects on circulating liver and vascular inflammation markers.

Virgin pumpkin seed oil attenuates development of NAFLD

Refined pumpkin seed oil reduced liver weight by 12% (CON: 5.9±0.2% of terminal body weight, REF: 5.2±0.2%, p≤0.05, Figure 3A) and this effect was even stronger in VIR (-19%), with liver weights reduced to 4.8±0.1% of terminal body weight (p≤0.01, Figure 3A). Histological examination of the livers from CON animals revealed that NAFLD developed in these mice up to the stage of non-alcoholic steatohepatitis (NASH). CON mice displayed distinctive morphological hallmarks of NASH (pronounced steatosis and lobular infiltration of inflammatory cells) and the observed pathology was less severe in REF and VIR animals (representative photomicrographs shown in Figure 3C). Quantitative scoring of NAFLD revealed that macrovesicular steatosis tended to be lower in REF (-26%, p=0.08) and was significantly reduced with VIR (-45%, p≤0.01) (Figure 3C). Microvesicular steatosis was less pronounced in both REF and VIR (-41% and -65%, respectively), but this effect did not reach statistical significance (Supplemental Figure 2). Biochemical analysis of hepatic lipid levels confirmed the histologically observed anti-steatotic effects of the pumpkin seed oils, showing reduced hepatic triglyceride content in both REF and VIR (-17%, p≤0.01 and -23%, p≤0.001 respectively, Figure 3D). Hepatic cholesterol levels, in both esterified (Figure 3E) and unesterified (Figure 3F) form, were affected only in VIR, with slightly but statistically significantly reduced levels of these lipid species in this group. Consistent with the observed effects on plasma inflammation markers, infiltration of inflammatory cells was moderately lowered by REF (-29%, n.s.), while VIR strongly and significantly reduced lobular inflammation (-73%, p≤0.001 vs CON, p≤0.001 vs REF; Figure 3G).

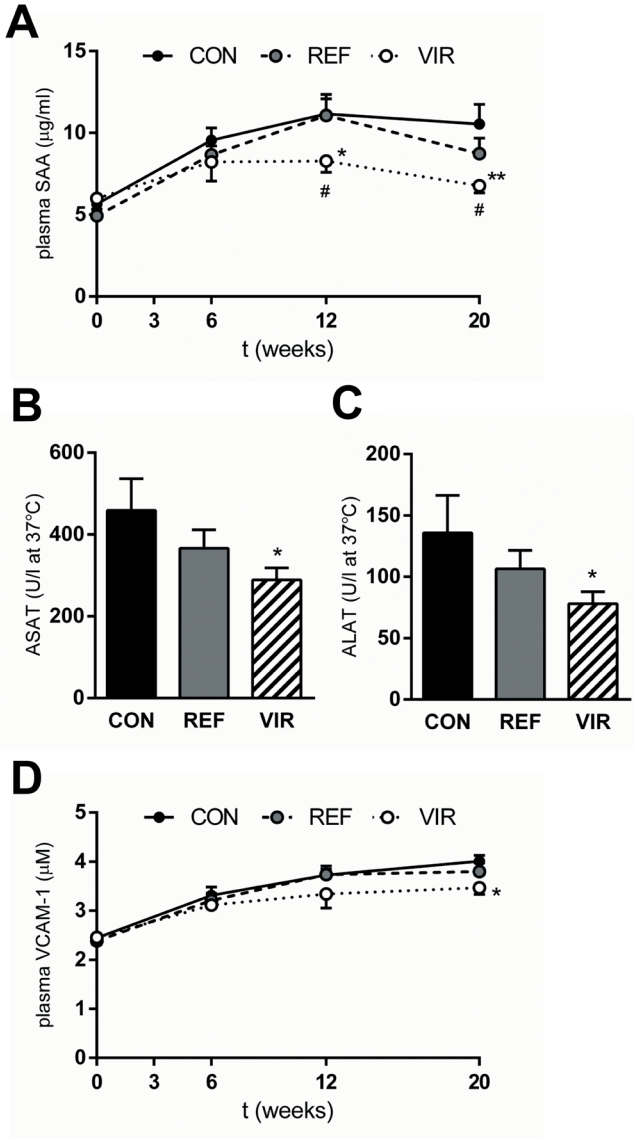


Figure 2. Virgin pumpkin seed oil reduces circulating markers of inflammation in cholesterol-fed ApoE*3Leiden mice. Mice were fed a Western type control diet (CON) or CON diet containing 9% refined pumpkin seed oil (REF) or 9% virgin pumpkin seed oil (VIR) for 20 weeks. (A) Plasma SAA levels were reduced by VIR. Liver damage marker (B) ASAT and (C) ALAT were reduced by VIR but not by REF. (D) Plasma sVCAM-1 levels in VIR animals were lower throughout the duration of the study. Data are mean±SEM. * p≤0.05, ** p≤0.01 compared with CON. # p≤0.05 for VIR compared with REF.

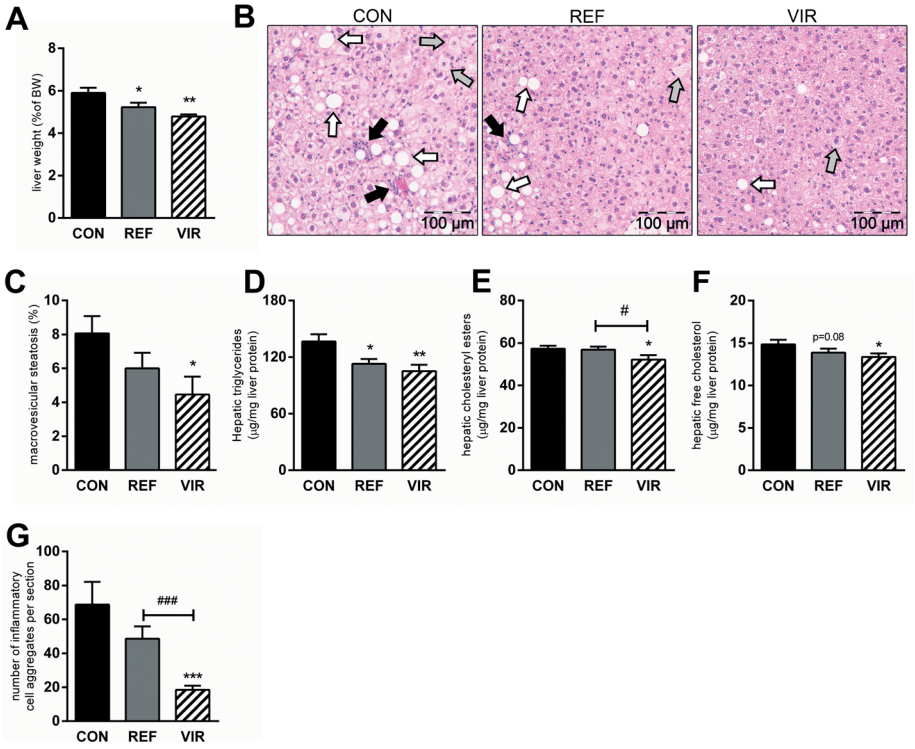


Figure 3. Virgin pumpkin seed oil attenuates development of NAFLD in cholesterol-fed ApoE*3Leiden mice. Mice were fed a Western type control diet (CON) or CON diet containing 9% refined pumpkin seed oil (REF) or 9% virgin pumpkin seed oil (VIR) for 20 weeks. (A) Liver weight (expressed as percentage of terminal body weight) was reduced by REF and VIR. (B) Representative photomicrographs of HE-stained liver sections show presence of micro- (grey arrows) and macro- (white arrows)vesicular steatosis and inflammatory cell clusters (black arrows) in CON-fed animals, which was less pronounced in REF and more strongly reduced in VIR. (C) Histological quantitative scoring of macrovesicular steatosis showed significant reduction in VIR. (D) Hepatic triglyceride levels (biochemically determined) were reduced in both REF and VIR while only VIR significantly reduced (E) hepatic cholesteryl ester content and (F) free (unesterified) cholesterol levels. (G) Histological quantification of number of inflammatory cell aggregates revealed a significant attenuation of hepatic inflammation by VIR. Data are mean±SEM. * p≤0.05, ** p≤0.01, *** p≤0.001 compared with CON. # p≤0.05, ### p≤0.001 for VIR compared with REF.

Atherosclerosis development is reduced with virgin pumpkin seed oil

Atherosclerotic lesion area and number were quantified histologically in the valve area of the aortic root. CON diet induced pronounced atherosclerosis with a total lesion area of 143765±17286 μm^2 per cross-section (Figure 4A-B). The total lesion area was reduced with REF (100594±14726 μm^2, -30%, $p \leq 0.05$, Figure 4A-B) and an even stronger effect was observed in VIR (82766±15164 μm^2, -42%, $p \leq 0.01$, Figure 4A-B). Refined morphological analysis of lesion severity revealed that the atherosclerotic lesion area in CON animals was mostly made up of large and advanced lesions (severe lesion types IV and V; Figure 4C). The observed decrease in total lesion area with REF and VIR was attributable to a significant reduction in the total area of these severe lesions specifically. Furthermore, immunohistochemical analysis of lesional macrophage content (MAC-3 positive area) showed that while there was no effect of REF or VIR on the macrophage content of mild type III lesions (not shown), the macrophage area in type V (severe) lesions was significantly reduced by both pumpkin seed oils (Figure 4D). In CON animals, 14.4±3.4% of the type 5 lesion area was MAC-3 positive and this was reduced to 6.16±1.26% in REF ($p \leq 0.05$ compared with CON) and 8.33±3.0% in VIR ($p \leq 0.05$ compared with CON). A similar, although non-significant, reduction was observed in type IV lesions (Supplemental Figure 3). The number of lesions (CON: 3.4±0.24; REF: 2.9±0.36; VIR: 2.6±0.21 lesions per cross-section; Supplemental Figure 3) and the percentage of lesion-free aortic segments (CON: 5.6±2.3; REF: 12.2±4.3; VIR: 9.5±3.3%; Supplemental Figure 3) were comparable among the groups. However the average size per lesion was significantly reduced by both oils (REF: -25%, $p \leq 0.05$; VIR: -37%, $p \leq 0.01$, Figure 4E), altogether indicating an effect on lesion growth rather than on the initiation of new lesions.

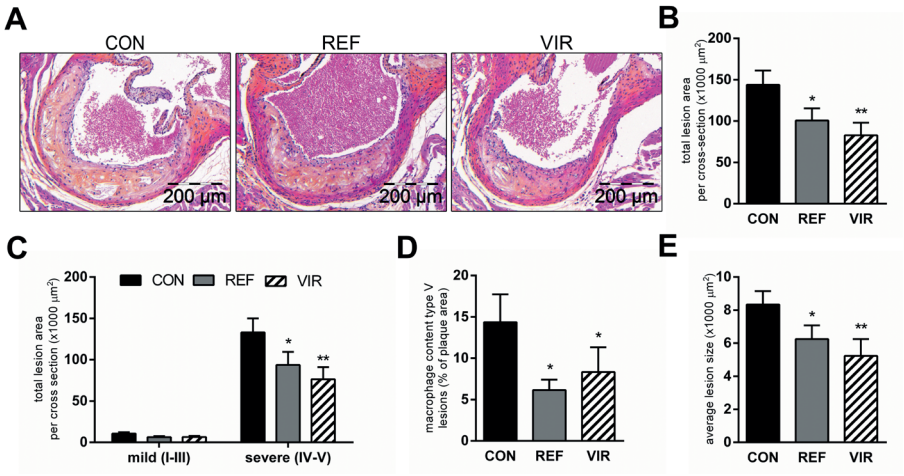


Figure 4. Atherosclerosis development is reduced with virgin pumpkin seed oil. Mice were fed a Western type control diet (CON) or CON diet containing 9% refined pumpkin seed oil (REF) or 9% virgin pumpkin seed oil (VIR) for 20 weeks. (A) Representative photomicrographs of HPS-stained cross sections of the aortic root show pronounced development of atherosclerosis in CON animals, which was less pronounced in REF and strongly reduced by VIR. (B) Morphometric analysis of lesion area revealed a significant decrease in atherosclerotic lesion area by REF and VIR. (C) Anti-atherogenic effects of pumpkin seed oils are specific on severe lesion types. (D) Average lesion size was reduced in REF and VIR. (E) Immunohistochemical staining for MAC-3 (CD107b) followed by quantification of positively stained area showed that both REF and VIR reduced the macrophage content of type V lesions. Data are mean±SEM. * p≤0.05, ** p≤0.01 compared with CON.

Both pumpkin seed oils have beneficial effects on hepatic lipid metabolism while only virgin pumpkin seed oil reduces inflammation

To provide insight into the underlying processes modulated by VIR and REF, hepatic mRNA expression of genes involved in lipid metabolism and inflammation was analyzed. In line with the observed hypolipidemic and anti-steatotic effects of REF and VIR, expression of genes involved in lipogenesis was reduced by both pumpkin seed oils (Figure 5A). Expression of SREBP-1c (*Srebf1*), a master transcriptional regulator of *de novo* fatty acid and triglyceride synthesis [28] was reduced significantly in both REF (fold-change relative to CON: 0.78±0.03, p≤0.001) and VIR (0.89±0.03, p≤0.01). In line with this, the expression of the SREBP-1c target gene Fatty acid synthase (*Fasn*), the main biosynthetic enzyme in fatty acid synthesis

[29], was also reduced in both REF (0.57±0.07, p≤0.05) and VIR (0.56±0.09, p≤0.01). Expression of Diacylglycerol acyltransferase-1 (*Dgat1*), which catalyzes the final step in triglyceride synthesis [30], was significantly reduced in REF (0.83±0.03, p≤0.001), but unaffected in VIR. Together, these results provide indication that the *de novo* synthesis of lipids is reduced in pumpkin seed oil-fed animals.

Furthermore, mRNA expression analysis of genes involved in the catabolism of fatty acids (Figure 5B) revealed that pumpkin seed oil, particularly in its virgin form, may also stimulate the breakdown of lipids. Expression of Peroxisome proliferator activated receptor α (*Ppara*), the main regulator of β-oxidation [31] was increased in both REF (1.27±0.09, p≤0.05) and VIR (1.61±0.11, p≤0.001), with additional beneficial effects of VIR over REF (p≤0.05). Carnitine palmitoyl transferase I (*Cpt1a*), which catalyzes the transport of fatty acids into the mitochondria [32] was not increased in REF (1.01±0.07) or VIR (1.16±0.06). Expression of Acyl-CoA oxidase (*Acox1)* which catalyzes the first step of β-oxidation [33], was unaffected by REF (1.06±0.05), while it was significantly increased in VIR (1.36±0.04, p≤0.001). Altogether these results indicate a stimulating effect of VIR on β-oxidation while the effects of REF on this process appear to be less pronounced.

Investigation of hepatic inflammatory gene expression (Figure 5C) revealed an anti-inflammatory effect of VIR specifically, further strengthening the notion that phytochemicals in virgin pumpkin seed oil rather than the fatty acid composition of the oil *per se* are responsible for the observed anti-inflammatory effects. Expression of Monocyte chemoattractant protein-1 (*Ccl2*), which plays an important role in the recruitment of myeloid-derived monocytes [34] was not significantly affected by REF (0.86±0.12), while it was strongly reduced in VIR (0.59±0.10, p≤0.05). Similarly, expression of the pro-inflammatory cytokines Tumor necrosis factor alpha (*Tnfa*) and Interleukin 1 beta (*Il1b*) was significantly reduced by VIR (0.59±0.08, p≤0.05 for *Tnfa*; 0.70±0.06, p≤0.05 for *Il1b*) but not by REF (0.83±0.11 for *Tnfa*; 0.96±0.10 for *Il1b*) .

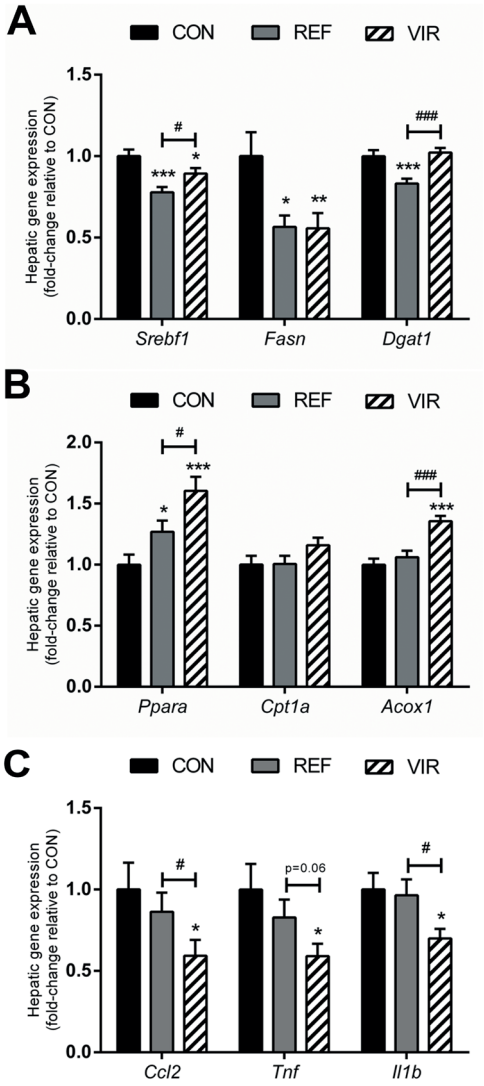


Figure 5. Refined and virgin pumpkin seed oils modulate lipid metabolism and inflammatory gene expression. Mice were fed a Western type control diet (CON) or CON diet containing 9% refined pumpkin seed oil (REF) or 9% virgin pumpkin seed oil (VIR) for 20 weeks. (A) Hepatic lipogenic gene expression (*Srebf1, Fasn, Dgat1*) was reduced in both REF and VIR. (B) Hepatic expression of genes involved in fatty acid catabolism (*Ppara, Cpt1a, Acox1*) was upregulated in VIR and to a lesser extent in REF. (C) Only VIR reduced hepatic expression of inflammatory genes (*Ccl2, Tnf, IL1b*). All gene expression data are expressed as fold-change relative to CON. Data are mean±SEM. * p≤0.05, ** p≤0.01, *** p≤0.001 compared with CON, # p≤0.05, ### p≤0.001 for VIR compared with REF.

DISCUSSION

In the study described herein, we demonstrate the potential long-term health effects of substitution of dietary fat (i.e. replacement of saturated by unsaturated fats), as well as putative additional effects of phytochemicals present in unrefined (virgin) oil. In a humanized model of disease, we show that both refined and virgin pumpkin seed oils markedly improve plasma lipids (cholesterol, triglycerides) and virgin pumpkin seed oil also reduced circulating markers of systemic and vascular inflammation. In the long run, both pumpkin seed oils attenuated the development of NAFLD and atherosclerosis, with a more pronounced effect of VIR in disease prevention.

Several epidemiological studies have shown that the development of NAFLD and CVD is associated with the type of dietary fat consumed [5-7]. To mimic diet-related long-term disease development in humans, we used the E3L model in which NAFLD and CVD are inducible by diet. These mice have a humanized lipoprotein profile, and cholesterol feeding results in a moderate elevation of plasma cholesterol (to about 18-20 mM) and combined development of NAFLD and atherosclerosis. Under the experimental conditions employed, lipid and inflammatory risk markers of future NAFLD and atherosclerosis are already induced after a few weeks, thus allowing the study of interventions on surrogate markers of disease, under conditions relevant for humans [17,19,23,35]. Replacement of a part of the cocoa butter by pumpkin seed oil markedly diminished the induction of circulating risk factors (cholesterol, triglycerides, SAA, sVCAM-1), which is in line with the short-term effects of other pumpkin seed oil preparations tested in humans and animals [12,14,15]. As these studies employed different pumpkin seed oil preparations at different doses and treatment regimens (in capsules or by oral gavage, as an addition to the regular diet), they provide evidence for a general health benefit of pumpkin seed oil, independent of how it is prepared and administered (i.e. replacement of dietary fat, or on top of regular diet).

In the present study we exchanged a part of the main fat in the CON diet, which is cocoa butter (15% w/w of the diet), with pumpkin seed oil (9% w/w of the diet) which modifies the quality of fat consumed, without affecting the caloric density of the diet. More specifically, the main fatty acids present in cocoa butter are stearic acid (C18:0, 35.7%), palmitic acid (C16:0, 26.7%) and oleic acid (C18:1n-9, 32.8%),

while linoleic acid (C18:2n-6, 2.7%) is only present in very small amounts. Replacing part of this cocoa butter with pumpkin seed oil, primarily increases the intake of linoleic acid and reduces the intake of oleic acid and the saturated fatty acids (SFA) stearic acid and palmitic acid. Linoleic acid is an essential n-6 poly-unsaturated fatty acid (PUFA) that is reported to have beneficial effects on plasma lipids (reviewed in [36]), in line with the results described herein. A possible rationale for the observed lipid-lowering effects may be found in activation of the transcription factor PPAR-α, which is known to be activated more strongly by PUFA than SFA [37]. Activation of this master regulator of lipid metabolism reportedly activates beta-oxidation in the liver and lowers plasma triglyceride levels as well as LDL cholesterol [38], consistent with observed reductions in plasma lipids in the present study. Gene expression analyses in the present study revealed an increased expression of PPAR-α in both pumpkin seed oil-fed groups, suggesting that transcriptional activity of this transcriptional regulator may be increased. Virgin pumpkin seed oil had additional effects on the expression and activation (demonstrated by increased expression of the PPAR-α target gene *Acox1*) of PPAR-α relative to the refined oil, indicating that phytochemicals present only in the virgin oil may have PPAR-α-activating properties. This is in line with findings by others, showing increased PPAR-α and PPAR-α target gene expression by tocopherols [39] and various polyphenol-rich mixtures (e.g. Apple polyphenols [40], Bilberry extract [41] and Walnut extract [42]). In contrast, there was no additional effect of the virgin oil on the reduction of lipogenic gene expression, thus indicating that these effects are attributable to the modification of the fatty acid composition of the diet, rather than effects of bioactive phytochemicals. More specifically, PUFAs are known to suppress SREBP-1c (the dominant transcriptional regulator of lipogenic genes) and rates of lipogenesis in rodents [43], in line with the effects of the PUFA-enriched pumpkin seed oil diets described herein. Remarkably, effects on lipogenic gene expression were more pronounced in the refined oil than in the virgin oil, suggesting that phytochemicals present in the virgin oil may attenuate these anti-lipogenic effects. Triglyceride and cholesterol-lowering effects comparable to those observed herein were also reported in long-term studies in E3L mice treated with long-chain PUFAs [44] or a PUFA-rich food supplement [45], as well as a pharmacological PPAR-α activator [23]. Overall, the reductions of plasma cholesterol achieved with the pumpkin seed oils are remarkably pronounced (-15%

for REF, -24% for VIR). This effect is in the range typically achieved with low-doses of hypocholesterolemic drugs such as HMG-CoA reductase inhibitors (statins) in the E3L mouse as well as in patients [46,47].

While both pumpkin seed oils had beneficial effects on dyslipidemia, only VIR reduced markers of inflammation SAA and sVCAM-1, indicating that minor components that are present in VIR but not in REF may have anti-inflammatory properties. These anti-inflammatory effects may be conferred by specific phytochemicals, including polyphenolic compounds, of which virgin pumpkin seed oil is a rich source. The total phenolic content of the VIR preparation used in the present study was 8-fold higher than in REF. Polyphenols are widely recognized for their anti-inflammatory effects [48-50], and have frequently been reported to be protective against the development of NAFLD and cardiovascular disease, both in epidemiological and experimental studies [51,52]. Under comparable experimental conditions and in the same mouse model, individual polyphenols were found to attenuate atherosclerotic lesion progression towards severe lesions [19,35], which is consistent with the observed prevention of development of severe, vulnerable atherosclerotic lesions with pumpkin seed oil. Pumpkin seed oil contains a complex mixture of polyphenols and other bioactive phytochemicals and it is unlikely that observed beneficial effects are confined to a single phytochemical or one single mechanism. It is more likely that multiple bioactives affect multiple mechanisms (alone or in combination) that culminate in the net anti-inflammatory effects observed as has been demonstrated with other complex mixtures of bioactives [13,45,53-55].

Replacement of cocoa butter with pumpkin seed oil reduces the intake of palmitic acid by 50% (from 4% of total diet to 2% of total diet). Although palmitic acid is known to have pro-inflammatory effects on liver cells, the intake of this fatty acid was comparable in REF and VIR groups and can thus not explain the marked anti-inflammatory effects of VIR. However, it is likely that the increased intake in dietary PUFAs and the reduced intake of palmitic acid, as achieved with both oils, contributed to the reduction of liver inflammation as a marked (29%) decrease in inflammatory cell content was already observed with REF.

Overall, we show that a simple lifestyle modification, i.e. a switch in the type of fat consumed without reducing total fat or calorie intake, can make a significant contribution to reducing metabolic and cardiovascular disease risk. Partial

replacement of the saturated fat-rich cocoa butter with refined pumpkin seed oil was sufficient to improve the risk factor dyslipidemia, and affect development of NAFLD and atherosclerosis. Additional anti-inflammatory effects, conferred by minor components present only in the virgin oil, lead to profound reductions in disease endpoints. Importantly, the observed effects were achieved in a translational diet-induced disease model, with moderately increased plasma lipids and low-grade metabolic inflammation as is typical for high-risk populations in humans. Under these conditions, pumpkin seed oil represents a powerful means to improve dyslipidemia, and, particularly when used in its virgin form, reduce chronic inflammation and prevent long-term disease development.

ACKNOWLEDGEMENTS

We would like to thank Aswin Menke, Erik Offerman and Karin Toet for their excellent technical assistance.

FINANCIAL SUPPORT

The study was funded partly by The Netherlands Organization for Applied Scientific Research (TNO) research program 'Healthy Nutrition' and partly by Bunge Ltd. Martine C. Morrison received funding from TNO and Top Institute Food and Nutrition (TIFN), a public-private partnership on pre-competitive research in food and nutrition. Co-author P. Mark Stavro is employed by Bunge Ltd. Bunge Ltd provided support in the form of salary for author P. Mark Stavro and had a role in data collection (analyses of fatty acid composition of the oils). Bunge Ltd had no role in the data analysis, decision to publish, or preparation of the manuscript.

DECLARATION OF INTEREST

The authors of this manuscript have the following competing interests: This study is funded in part by Bunge Ltd. P. Mark Stavro is an employee of Bunge Ltd.

REFERENCES

1. Armstrong MJ, Adams LA, Canbay A, Syn WK. Extrahepatic complications of nonalcoholic fatty liver disease. Hepatology (Baltimore, Md) 2014;59:1174-1197.
2. Farrell GC, van Rooyen D, Gan L, Chitturi S. NASH is an Inflammatory Disorder: Pathogenic, Prognostic and Therapeutic Implications. Gut and liver 2012;6:149-171.
3. Fon Tacer K, Rozman D. Nonalcoholic Fatty liver disease: focus on lipoprotein and lipid deregulation. Journal of lipids 2011;2011:783976.
4. Weber C, Noels H. Atherosclerosis: current pathogenesis and therapeutic options. Nat Med 2011;17:1410-1422.
5. Ferramosca A, Zara V. Modulation of hepatic steatosis by dietary fatty acids. World J Gastroenterol 2014;20:1746-1755.
6. Michas G, Micha R, Zampelas A. Dietary fats and cardiovascular disease: Putting together the pieces of a complicated puzzle. Atherosclerosis 2014;234:320-328.
7. Schwab U, Lauritzen L, Tholstrup T, Haldorssoni T, Riserus U, Uusitupa M, et al. Effect of the amount and type of dietary fat on cardiometabolic risk factors and risk of developing type 2 diabetes, cardiovascular diseases, and cancer: a systematic review. Food Nutr Res 2014;58:eCollection 2014.
8. Gylling H, Plat J, Turley S, Ginsberg HN, Ellegard L, Jessup W, et al. Plant sterols and plant stanols in the management of dyslipidaemia and prevention of cardiovascular disease. Atherosclerosis 2014;232:346-360.
9. Khurana S, Venkataraman K, Hollingsworth A, Piche M, Tai TC. Polyphenols: benefits to the cardiovascular system in health and in aging. Nutrients 2013;5:3779-3827.
10. Andjelkovic M, Van Camp J, Trawka A, Verhé R. Phenolic compounds and some quality parameters of pumpkin seed oil. European Journal of Lipid Science and Technology 2010;112:208-217.
11. Rezig L, Chouaibi M, Msaada K, Hamdi S. Chemical composition and profile characterisation of pumpkin (Cucurbita maxima) seed oil. Industrial Crops and Products 2012;37:82-87.
12. al-Zuhair H, Abd el-Fattah AA, Abd el Latif HA. Efficacy of simvastatin and pumpkin-seed oil in the management of dietary-induced hypercholesterolemia. Pharmacol Res 1997;35:403-408.
13. Allison GL, Lowe GM, Rahman K. Aged garlic extract and its constituents inhibit platelet aggregation through multiple mechanisms. The Journal of nutrition 2006;136:782S-788S.
14. Gossell-Williams M, Hyde C, Hunter T, Simms-Stewart D, Fletcher H, McGrowder D, et al. Improvement in HDL cholesterol in postmenopausal women supplemented with pumpkin seed oil: pilot study. Climacteric 2011;14:558-564.
15. Gossell-Williams M, Lyttle K, Clarke T, Gardner M, Simon O. Supplementation with pumpkin seed oil improves plasma lipid profile and cardiovascular outcomes of female non-ovariectomized and ovariectomized Sprague-Dawley rats. Phytother Res 2008;22:873-877.
16. Morrison MC, Liang W, Mulder P, Verschuren L, Pieterman E, Toet K, et al. Mirtoselect, an anthocyanin-rich bilberry extract, attenuates non-alcoholic steatohepatitis and associated fibrosis in ApoE *3Leiden mice. J Hepatol 2015;62:1180-1186.
17. Zadelaar S, Kleemann R, Verschuren L, de Vries-Van der Weij J, van der Hoorn J, Princen HM, et al. Mouse models for atherosclerosis and pharmaceutical modifiers. Arterioscler Thromb Vasc Biol 2007;27:1706-1721.
18. Kleemann R, Verschuren L, van Erk MJ, Nikolsky Y, Cnubben NH, Verheij ER, et al. Atherosclerosis and liver inflammation induced by increased dietary cholesterol intake: a combined transcriptomics and metabolomics analysis. Genome Biol 2007;8:R200.

19. Morrison M, van der Heijden R, Heeringa P, Kaijzel E, Verschuren L, Blomhoff R, et al. Epicatechin attenuates atherosclerosis and exerts anti-inflammatory effects on diet-induced human-CRP and NFkappaB in vivo. Atherosclerosis 2014;233:149-156.
20. Liang W, Menke AL, Driessen A, Koek GH, Lindeman JH, Stoop R, et al. Establishment of a general NAFLD scoring system for rodent models and comparison to human liver pathology. PloS one 2014;9:e115922.
21. Stary HC, Chandler AB, Dinsmore RE, Fuster V, Glagov S, Insull W, Jr., et al. A definition of advanced types of atherosclerotic lesions and a histological classification of atherosclerosis. A report from the Committee on Vascular Lesions of the Council on Arteriosclerosis, American Heart Association. Arterioscler Thromb Vasc Biol 1995;15:1512-1531.
22. Stary HC, Chandler AB, Glagov S, Guyton JR, Insull W, Jr., Rosenfeld ME, et al. A definition of initial, fatty streak, and intermediate lesions of atherosclerosis. A report from the Committee on Vascular Lesions of the Council on Arteriosclerosis, American Heart Association. Arterioscler Thromb Vasc Biol 1994;14:840-856.
23. Kooistra T, Verschuren L, de Vries-van der Weij J, Koenig W, Toet K, Princen HM, et al. Fenofibrate reduces atherogenesis in ApoE*3Leiden mice: evidence for multiple antiatherogenic effects besides lowering plasma cholesterol. Arterioscler Thromb Vasc Biol 2006;26:2322-2330.
24. Kleiner DE, Brunt EM, Van Natta M, Behling C, Contos MJ, Cummings OW, et al. Design and validation of a histological scoring system for nonalcoholic fatty liver disease. Hepatology (Baltimore, Md) 2005;41:1313-1321.
25. Schneider CA, Rasband WS, Eliceiri KW. NIH Image to ImageJ: 25 years of image analysis. Nature methods 2012;9:671-675.
26. Bligh EG, Dyer WJ. A rapid method of total lipid extraction and purification. Can J Biochem Physiol 1959;37:911-917.
27. Liang W, Lindeman JH, Menke AL, Koonen DP, Morrison M, Havekes LM, et al. Metabolically induced liver inflammation leads to NASH and differs from LPS- or IL-1beta-induced chronic inflammation. Lab Invest 2014;94:491-502.
28. Jeon TI, Osborne TF. SREBPs: metabolic integrators in physiology and metabolism. Trends Endocrinol Metab 2012;23:65-72.
29. Chirala SS, Wakil SJ. Structure and function of animal fatty acid synthase. Lipids 2004;39:1045-1053.
30. Cases S, Smith SJ, Zheng YW, Myers HM, Lear SR, Sande E, et al. Identification of a gene encoding an acyl CoA:diacylglycerol acyltransferase, a key enzyme in triacylglycerol synthesis. Proc Natl Acad Sci U S A 1998;95:13018-13023.
31. Mandard S, Muller M, Kersten S. Peroxisome proliferator-activated receptor alpha target genes. Cell Mol Life Sci 2004;61:393-416.
32. Bonnefont JP, Djouadi F, Prip-Buus C, Gobin S, Munnich A, Bastin J. Carnitine palmitoyltransferases 1 and 2: biochemical, molecular and medical aspects. Mol Aspects Med 2004;25:495-520.
33. Reddy JK, Hashimoto T. Peroxisomal beta-oxidation and peroxisome proliferator-activated receptor alpha: an adaptive metabolic system. Annu Rev Nutr 2001;21:193-230.
34. Xu L, Kitade H, Ni Y, Ota T. Roles of Chemokines and Chemokine Receptors in Obesity-Associated Insulin Resistance and Nonalcoholic Fatty Liver Disease. Biomolecules 2015;5:1563-1579.
35. Kleemann R, Verschuren L, Morrison M, Zadelaar S, van Erk MJ, Wielinga PY, et al. Anti-inflammatory, anti-proliferative and anti-atherosclerotic effects of quercetin in human in vitro and in vivo models. Atherosclerosis 2011;218:44-52.

36. Monteiro J, Leslie M, Moghadasian MH, Arendt BM, Allard JP, Ma DW. The role of n - 6 and n - 3 polyunsaturated fatty acids in the manifestation of the metabolic syndrome in cardiovascular disease and non-alcoholic fatty liver disease. Food Funct 2014;5:426-435.
37. Wahli W, Michalik L. PPARs at the crossroads of lipid signaling and inflammation. Trends Endocrinol Metab 2012;23:351-363.
38. Staels B, Dallongeville J, Auwerx J, Schoonjans K, Leitersdorf E, Fruchart JC. Mechanism of action of fibrates on lipid and lipoprotein metabolism. Circulation 1998;98:2088-2093.
39. Kim DY, Kim J, Ham HJ, Choue R. Effects of d-α-tocopherol supplements on lipid metabolism in a high-fat diet-fed animal model. Nutr Res Pract 2013;7:481-487.
40. Xu Z-R, Li J-Y, Dong X-W, Tan Z-J, Wu W-Z, Xie Q-M, et al. Apple Polyphenols Decrease Atherosclerosis and Hepatic Steatosis in ApoE−/− Mice through the ROS/MAPK/NF-κB Pathway. Nutrients 2015;7:5324.
41. Takikawa M, Inoue S, Horio F, Tsuda T. Dietary Anthocyanin-Rich Bilberry Extract Ameliorates Hyperglycemia and Insulin Sensitivity via Activation of AMP-Activated Protein Kinase in Diabetic Mice. The Journal of Nutrition 2010;140:527-533.
42. Shimoda H, Tanaka J, Kikuchi M, Fukuda T, Ito H, Hatano T, et al. Effect of Polyphenol-Rich Extract from Walnut on Diet-Induced Hypertriglyceridemia in Mice via Enhancement of Fatty Acid Oxidation in the Liver. J Agric Food Chem 2009;57:1786-1792.
43. Xu J, Nakamura MT, Cho HP, Clarke SD. Sterol regulatory element binding protein-1 expression is suppressed by dietary polyunsaturated fatty acids. A mechanism for the coordinate suppression of lipogenic genes by polyunsaturated fats. J Biol Chem 1999;274:23577-23583.
44. Wielinga PY, Harthoorn LF, Verschuren L, Schoemaker MH, Jouni ZE, van Tol EA, et al. Arachidonic acid/docosahexaenoic acid-supplemented diet in early life reduces body weight gain, plasma lipids, and adiposity in later life in ApoE*3Leiden mice. Mol Nutr Food Res 2012;56:1081-1089.
45. Verschuren L, Wielinga PY, van Duyvenvoorde W, Tijani S, Toet K, van Ommen B, et al. A dietary mixture containing fish oil, resveratrol, lycopene, catechins, and vitamins E and C reduces atherosclerosis in transgenic mice. The Journal of nutrition 2011;141:863-869.
46. van de Steeg E, Kleemann R, Jansen HT, van Duyvenvoorde W, Offerman EH, Wortelboer HM, et al. Combined analysis of pharmacokinetic and efficacy data of preclinical studies with statins markedly improves translation of drug efficacy to human trials. The Journal of pharmacology and experimental therapeutics 2013;347:635-644.
47. Verschuren L, Kleemann R, Offerman EH, Szalai AJ, Emeis SJ, Princen HM, et al. Effect of low dose atorvastatin versus diet-induced cholesterol lowering on atherosclerotic lesion progression and inflammation in apolipoprotein E*3-Leiden transgenic mice. Arterioscler Thromb Vasc Biol 2005;25:161-167.
48. Biesalski HK. Polyphenols and inflammation: basic interactions. Curr Opin Clin Nutr Metab Care 2007;10:724-728.
49. Gonzalez R, Ballester I, Lopez-Posadas R, Suarez MD, Zarzuelo A, Martinez-Augustin O, et al. Effects of flavonoids and other polyphenols on inflammation. Crit Rev Food Sci Nutr 2011;51:331-362.
50. Rahman I, Biswas SK, Kirkham PA. Regulation of inflammation and redox signaling by dietary polyphenols. Biochem Pharmacol 2006;72:1439-1452.
51. Aguirre L, Portillo MP, Hijona E, Bujanda L. Effects of resveratrol and other polyphenols in hepatic steatosis. World J Gastroenterol 2014;20:7366-7380.

52. Arts IC, Hollman PC. Polyphenols and disease risk in epidemiologic studies. Am J Clin Nutr 2005;81:317S-325S.
53. Farrell N, Norris G, Lee SG, Chun OK, Blesso CN. Anthocyanin-rich black elderberry extract improves markers of HDL function and reduces aortic cholesterol in hyperlipidemic mice. Food Funct 2015;6:1278-1287.
54. Janega P, Klimentova J, Barta A, Kovacsova M, Vrankova S, Cebova M, et al. Red wine extract decreases pro-inflammatory markers, nuclear factor-kappaB and inducible NOS, in experimental metabolic syndrome. Food Funct 2014;5:2202-2207.
55. Tang CC, Lin WL, Lee YJ, Tang YC, Wang CJ. Polyphenol-rich extract of Nelumbo nucifera leaves inhibits alcohol-induced steatohepatitis via reducing hepatic lipid accumulation and anti-inflammation in C57BL/6J mice. Food Funct 2014;5:678-687.

SUPPLEMENTAL DATA

Supplement 1. Detailed material and methods

Extraction of phenolic compounds from pumpkin seed oils

A liquid-liquid extraction (LLE) was used to isolate the phenolic fraction of the cocoa butter and pumpkin seed oil samples, both refined and virgin. The extraction was carried out following the method described by Suarez et al. [1] with some modifications. Briefly, 20 mL of methanol:water (80:20, v/v) was added to 5 g of oil and homogenized for 2 min with a Ultraturrax (IKA Labortechnik). After that, two phases were separated by centrifugation at 637×g for 10min and the hydroalcoholic phase was transferred to a balloon. This step was repeated twice and the extracts were combined in the balloon. Then, the hydroalcoholic extracts were rotatory evaporated up to a syrupy consistency at 31 °C and were dissolved in 5 mL of acetonitrile. Afterwards, the extract was washed three times with 10 mL of n-hexane and the rejected n-hexane was treated with 5 mL of acetonitrile. The acetonitrile solution was finally rotatory evaporated to dryness and then re-dissolved in 1 mL of acetonitrile and maintained at −18 °C before the chromatographic analysis. 5 µL of the eluate was directly injected into the LC-QTOF-MS. Extractions were carried out in triplicate.

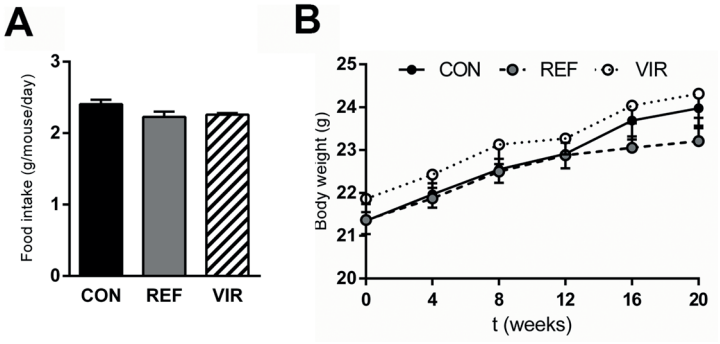
LC-QTOF-MS analysis of phenolic extracts from pumpkin seed oils

The analysis of the phenolic compounds and their metabolites in the oil samples was carried out by means of a LC-QTOF-MS system consisted of a LC-Agilent 1290Series (Agilent Technologies, Palo Alto, U.S.A.) coupled to a 6540 ESI-QTOF (Agilent Technologies) operated in negative electrospray ionization mode (ESI-). Separation was carried out using a Zorbax SB-Aq column (3.5µm, 150mm x 2.1mm i.d.) equipped with a Pre-Column Zorbax SB-C18 (3.5µm, 15mm x 2.1mm i.d.) also from Agilent. Drying gas temperature was 350°C and the flow rate was held at 12 l/min. On the other hand pressure of the gas nebulizer was 45 psi and the capillary voltage was set at 4000 V. The fragmentor was set at 120V, the skimmer at 65V and the OCT 1RF Vpp was set at 750V.

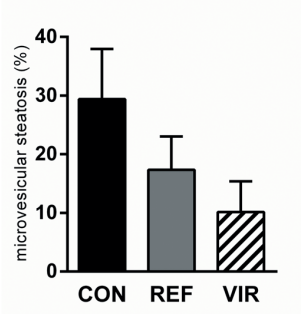
During the analysis, the column was kept at 25°C and the flow rate was 0.4 mL/min. The solvent composition was solvent A: milliQ water/acetic acid (99.8:0.2 v/v) and solvent B: acetonitrile. Solvent B was initially 5% and was gradually increased reaching 55% at 10 minutes and 95% at 12 min. Then it was maintained isocratically up to 15 min and after that it was reduced to 5% in 1 minute and was held at initial conditions during 8 minutes to re-equilibrate the column. The injection volume was set at 5 µL.

References Supplement 1

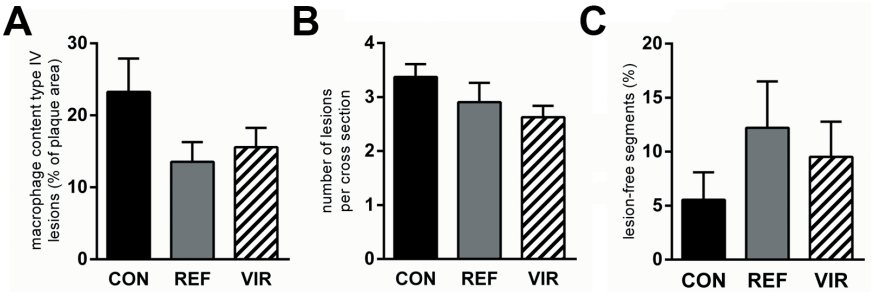
1. Suarez M, Macia A, Romero MP, Motilva MJ. Improved liquid chromatography tandem mass spectrometry method for the determination of phenolic compounds in virgin olive oil. Journal of chromatography A 2008;1214:90-99.



Supplemental Figure 1. Refined and virgin pumpkin seed oils do not affect food intake or body weight in ApoE*3Leiden mice. Mice were fed a Western type diet (CON) containing 9% refined pumpkin seed oil (REF) or 9% virgin pumpkin seed oil (VIR) for 20 weeks. (A) Average food intake was measured per cage in group-housed mice (3-4 mice per cage) and did not differ between groups. (B) Body weight was not affected by either VIR or REF and increased gradually over time. Data are mean±SEM.



Supplemental Figure 2. Refined and virgin pumpkin seed oils do not affect microvesicular steatosis in ApoE*3Leiden mice. Mice were fed a Western type diet (CON) containing 9% refined pumpkin seed oil (REF) or 9% virgin pumpkin seed oil (VIR) for 20 weeks. Microvesicular hepatosteatosis (% of total liver cross section affected) was not reduced by REF or VIR. Data are mean±SEM.



Supplemental Figure 3. Refined and virgin pumpkin seed oils do not affect number of lesions or lesion-free segments ApoE*3Leiden mice. Mice were fed a Western type diet (CON) containing 9% refined pumpkin seed oil (REF) or 9% virgin pumpkin seed oil (VIR) for 20 weeks. (A) Immunohistochemical staining for MAC-3 (CD107b) followed by quantification of positively stained area showed that the macrophage content of type IV lesions was not significantly reduced by REF or VIR. (B) number of lesions per cross section were not reduced by REF or VIR. (C) REF and VIR did not increase the percentage of lesion-free segments. Data are mean±SEM

Chapter 7

Macrovesicular steatosis is associated with development of lobular inflammation and fibrosis in diet-induced non-alcoholic steatohepatitis (NASH)

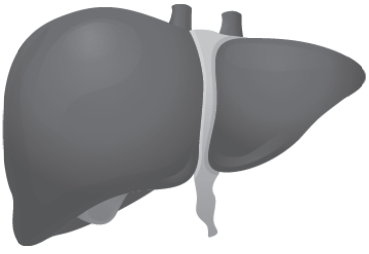
Petra Mulder[1,2], Wen Liang[1,3], P.Y. Wielinga[1], Lars Verschuren[4], Karin Toet[1], Louis M. Havekes[1,3], Anita M. van den Hoek[1]*, Robert Kleemann[1, 2, 5]*

[1] The Dutch Organization for Applied Scientific Research (TNO), Department of Metabolic Health Research, Leiden, 2333 CK, The Netherlands
[2] Leiden University Medical Center, Department of Cardiovascular Surgery, Leiden, 2333 ZA, The Netherlands
[3] Leiden University Medical Center, Department of Endocrinology and Cardiology, Leiden, 2333 ZA, The Netherlands
[4] The Dutch Organization for Applied Scientific Research (TNO), Department of Microbiology and Systems Biology, Zeist, 3704 HE, The Netherlands
[5] Wageningen University, Department of Human and Animal Physiology, Wageningen, 6709 PJ, The Netherlands

*These authors contributed equally to the manuscript

Inflammation and Cell Signaling. 2015 Jun 8;2(3).







ABSTRACT

Non-alcoholic steatohepatitis (NASH) is characterized by liver steatosis and lobular inflammation. It is unclear how the development of liver steatosis and the formation of inflammatory cell aggregates are related to each other. The present study investigated the longitudinal development of two forms of steatosis, micro- and macrovesicular steatosis, as well as lobular inflammation. ApoE*3Leiden. CETP (E3L.CETP) transgenic mice were fed a high-fat diet containing 1% w/w cholesterol (HFC) for 12 weeks to induce NASH. Livers were harvested in intervals of 4 weeks and analyzed by histological and biochemical techniques, as well as transcriptome and subsequent pathway analysis. Major findings were validated in independent NASH studies using other rodent models, i.e. HFD-treated C57BL/6J and LDLr-/-.Leiden mice. In E3L.CETP mice, microvesicular steatosis was rapidly induced and reached plateau levels after already 4 weeks of HFC treatment, while macrovesicular steatosis developed more gradually and progressed over time. Lobular inflammation increased after 4 weeks with a significant further progression towards the end of the study (12 weeks). Macrovesicular, but not microvesicular, steatosis was positively correlated with the number of inflammatory aggregates. This correlation was confirmed in a milder (C57BL/6J) and a more severe (LDLr-/-.Leiden) NASH model. Furthermore, collagen staining showed onset of perihepatocellular fibrosis in E3L.CETP mice after 12 weeks of HFC treatment and transcriptome analysis substantiated the activation of pro-fibrotic pathways and genes. Notably, macrovesicular steatosis correlated positively with liver fibrosis in LDLr-/-.Leiden mice with pronounced fibrosis. In conclusion, this study shows that macrovesicular steatosis is associated with lobular inflammation and liver fibrosis in rodent models and highlights the importance of this form of steatosis in the pathogenesis of NASH.

INTRODUCTION

Non-alcoholic fatty liver disease (NAFLD) is associated with visceral obesity, dyslipidemia and insulin resistance and has become a global threat with an estimated prevalence of 15% to 30% of the general population [1,2]. NAFLD covers a spectrum of liver disease ranging from lipid accumulation (simple steatosis) to non-alcoholic steatohepatitis (NASH). NASH is characterized by steatosis with lobular inflammation which can further progress to liver fibrosis and cirrhosis [3]. The pathophysiology that leads to NASH is not well understood, in particular the relationship between the development of steatosis and lobular inflammation is unclear.

Morphologically, hepatic steatosis can manifest in two forms of lipid accumulation, i.e. macrovesicular or microvesicular steatosis. In macrovesicular steatosis, hepatocytes contain a large, single vacuole of fat which fills the cytoplasm and displaces the nucleus to the periphery (see [4] and references therein). By contrast, hepatocytes with microvesicular steatosis contain many small lipid droplets in the cytoplasm [4]. Emerging data indicate that excessive lipid accumulation in liver cells causes lipotoxic hepatocellular injury and inflammation [5]. Lobular inflammation in NASH is characterized by the presence of inflammatory aggregates, i.e. cell clusters containing different types of immune cells such as neutrophils, lymphocytes and macrophages [6,7]. This inflammation is associated with activation of pro-fibrotic signaling cascades involving stellate cells and the production of collagen [6,8]. To date, it is unclear whether the development of inflammation is linked to a specific form of steatosis, i.e. macro- or microvesicular steatosis.

To identify a potential relationship between the two forms of steatosis and development of lobular inflammation (and the progression to fibrosis), we investigated in a longitudinal study the development of macro- and microvesicular steatosis and lobular inflammation up to the stage of early fibrosis. For this we used ApoE*3Leiden.CETP (E3L.CETP) transgenic mice which have a humanized lipoprotein metabolism and develop NASH in the context of obesity and dyslipidemia [7,9]. These mice were treated with a NASH-inducing high-fat diet

containing 24% lard fat and 1% cholesterol (HFC) for 12 weeks and compared to low-fat diet controls. Groups of mice were sacrificed in monthly intervals until NASH with early fibrosis had developed. NAFLD pathology was scored blindly using a recently established grading system for rodents which is based on the human NAS system [10]. Histological analyses and biochemical measurements in conjunction with transcriptome analysis revealed a positive association between macrovesicular steatosis and lobular inflammation as well as early fibrosis. These findings were confirmed in independent studies using diet-inducible models of NASH (i.e. C57BL/6J and LDLr-/-.Leiden mice) and the results show that macrovesicular steatosis has a critical role in the pathogenesis of NASH.

MATERIAL AND METHODS

Animal time-course experiment

Experiments were approved by an independent Animal Care and Use Committee and were in compliance with European Community specifications regarding the use of laboratory animals. APOE*3Leiden (E3L) mice were cross-bred with transgenic mice that express human- cholesteryl ester transfer protein (CETP) to obtain heterozygous E3L.CETP mice [9]. Male E3L.CETP mice (n=70, 16-19 weeks of age) were used in the present study. All animals were housed in a temperature-controlled room with 12-hour light-dark cycling and had ad libitum access to food and water. Mice received a low fat diet (LFD; 10 kcal% lard, Research Diets, New Brunswick, NJ, USA) during a 4-week run-in period. Mice were matched for body weight, plasma cholesterol and triglycerides and one group (n=10) was sacrificed to define the condition at the start of the experiment (t=0). Remaining mice were matched into 6 groups. Three groups (n=10/group) were treated with a NASH-inducing high-fat diet (HFD; D12451; 45 kcal% lard, Research Diets, New Brunswick NJ, USA) supplemented with 1% (w/w) cholesterol (HFC) [7]. As reference for transcriptome analysis, three groups (n=10/group) received a HFD control diet. At 4-week intervals, food intake and body weight were determined and EDTA plasma was collected from the tail vein after 5h of fasting. Mice were sacrificed after 4, 8 or 12 weeks of diet feeding by CO_2 asphyxiation. The

medial liver lobe was fixed in formalin and embedded in paraffin for histological analysis of NAFLD and the left lateral liver lobe (lobus sinister hepatis) was snap frozen in liquid nitrogen and stored at -80°C for liver lipids, biochemical and gene expression analyses. White adipose tissue was collected, weighed and stored at -80°C.

Histological evaluation of NAFLD

NASH development was assessed histologically in hematoxylin and eosin (HE)-stained liver sections (3 μM) using an adapted scoring method for human NASH [10]. Briefly, steatosis was determined at a 40-100x magnification and quantified as macrovesicular and microvesicular steatosis, expressed as the percentage of the total surface area. Hepatic inflammation was analyzed by counting the number of inflammatory aggregates in five fields per specimen at a 100x magnification (view size 3.1 mm^2). Inflammatory cell aggregate counts were expressed as the average number of aggregates per field. Early liver fibrosis was evaluated by collagen staining using Picro-Sirius Red (Chroma, WALDECK-Gmbh, Münster, Germany). The level of collagen deposition in the perisinusoidal area was determined relative to the total perisinusoidal area and expressed as a percentage. Correlation between the two forms of steatosis and lobular inflammation were made and validated in independent NASH studies with C57BL/6J mice and LDLr-/-.Leiden mice. More specifically, male C57BL/6J mice (n=12, 12 weeks of age) were treated with the above specified HFD (D12451) for 24 weeks to induce NASH. NAFLD was histologically scored to investigate the potential relationship between micro-/macrovesicular steatosis and lobular inflammation. Male LDLr-/-.Leiden mice (n=12, 12-16 weeks of age) were treated with HFD for 34 weeks to induce a NASH phenotype with liver fibrosis to investigate the association between steatosis and fibrosis. These models can develop NASH after long-term HFD feeding (>20 weeks) with marked lobular inflammation [10,11].

Liver lipid analysis

The intrahepatic concentration of free cholesterol triglycerides, and cholesteryl esters was analyzed as described [7]. Briefly, lipids were extracted from liver homogenates using the Bligh and Dyer method and separated by high performance thin layer chromatography (HPTLC) on silica gel plates. Lipid spots were stained

with color reagent (5g of $MnCl_{24}H_2O$, 32 ml of 95–97% H_2SO_4 added to 960 ml of CH_3OH:H2O 1:1 v/v) and triglycerides, cholesteryl esters and free cholesterol were quantified using TINA version 2.09 software (Raytest, Straubenhardt, Germany).

Biochemical analysis of metabolic parameters

Plasma levels of total cholesterol and triglycerides were measured with commercially available kits (Roche Diagnostics, Almere, The Netherlands). Plasma glucose was determined using the "Freestyle glucose measurement system" (Abbott, Heerlen, The Netherlands). Plasma insulin was quantified by ELISA (Mercodia, Uppsala, Sweden). Serum alanine transaminase (ALT) (GPT, cat. no. 10745138) and aspartate aminotransferase (AST) (GOT, cat. no. 10745120) activities were measured using Reflotron® kits (Roche Diagnostics).

RNA isolation and gene expression analysis

Transcriptome analysis was performed essentially as reported in [12] and references therein. Briefly, total RNA was extracted from individual livers using glass beads and RNAzol (Campro Scientific, Veenendaal, The Netherlands). After quality control of RNA integrity using RNA 6000 Nano Lab-on-a-Chip kit and a bioanalyzer 2100 (Agilent Technologies), biotinylated cRNA was prepared with an Illumina® TotalPrep™ RNA Amplification Kit (Ambion, art.No.AM-IL1791. Biotinylated cRNA was hybridized onto the MouseRef-8 Expression BeadChip (Illumina) by a service provider (Service XS, Leiden, the Netherlands). Genomestudio v1.1.1 software (Illumina) was used for subsequent gene expression analysis. Differentially expressed probes were identified using the limma package of R/Bioconductor. Differentially expressed probes were selected based on the cut-off value False discovery rate (FDR)<0.05. Selected differentially expressed probes were used as an input for pathway analysis using Ingenuity Pathway Analysis suite (http://www.ingenuity.com).

Statistical analysis

Data are presented as mean ± SEM. Significant differences between more than two groups were estimated by one-way ANOVA and Tukey post-hoc analysis

(parametric samples) or Kruskal–Wallis followed by Mann-Whitney U tests (non-parametric samples). Significant differences between two groups were determined by two-sided Student's t-test. Correlations between two variables were calculated by Spearman's rank (non-normally distributed variables) or Pearson's rank (normally distributed variables) correlation coefficient. A p-value<0.05 was considered statistically significant. GraphPad Prism software 6.0 was used for calculations (GraphPad Software, La Jolla, CA).

RESULTS

HFC feeding leads to liver steatosis and lobular inflammation in context of obesity, dyslipidemia and insulin resistance

E3L.CETP mice were treated with HFC up to 12 weeks. Histological analysis of livers showed that HFC-treated mice developed moderate pericentral steatosis after 4 weeks (Figure 1). This early steatosis consisted mainly of microvesicular steatosis. Steatosis intensified until the end of the study (at 12 weeks) and macrovesicular steatosis became more abundant. The development of steatosis can be attributed to a significant increase in liver lipids such as triglycerides (Table 1). With regards to lobular inflammation, first inflammatory cell aggregates were observed after 4 weeks of HFC feeding and more inflammatory aggregates were present at the end of the study (Figure 1).

During the experiment, mice developed an obese phenotype with a significant increase in body weight and visceral (epididymal and mesenteric) white adipose tissue (Table 1). Furthermore, HFC treatment induced dyslipidemia as demonstrated by significant elevations in plasma cholesterol and triglycerides. Mice developed insulin resistance as reflected by increased fasting insulin and glucose concentrations in plasma. Liver enzymes AST and ALT were significantly elevated at the end of the study demonstrating that HFC feeding resulted in hepatocellular damage. In all, HFC feeding resulted in development of NASH in context of diet-induced obesity, dyslipidemia and insulin resistance.

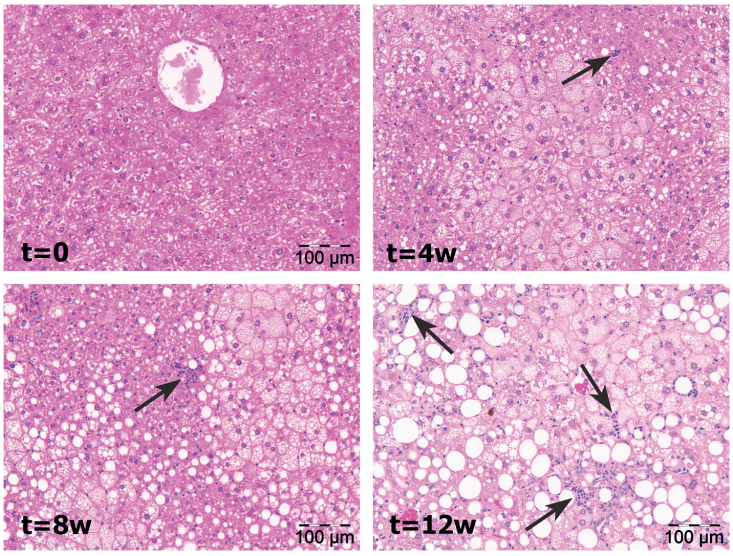


Figure 1. Histological presentation of NASH in E3L.CETP mice. Representative photomicrographs of HE-stained liver cross-sections of E3L.CETP mice fed a high-fat diet supplemented with 1% cholesterol (HFC) for 0, 4, 8 and 12 weeks showing development steatosis and increased lobular inflammation (arrows) over time. (Magnification:x200).

Table 1. Effect of HFC feeding on metabolic parameters over time.

Parameter	t=0	t=4 w	t=8 w	t=12 w
Body weight (g)	29.4 ± 0.6^{a}	36.0 ± 1.0^{b}	42.2 ± 1.6^{c}	47.6 ± 2.0^{d}
Epididymal fat (g)	0.4 ± 0.1^{a}	1.8 ± 0.3^{b}	2.3 ± 0.2^{bc}	2.5 ± 0.2^{c}
Mesenteric fat (g)	0.3 ± 0.0^{a}	0.5 ± 0.1^{a}	0.8 ± 0.1^{b}	0.8 ± 0.1^{b}
Liver (g)	1.8 ± 0.1^{a}	1.8 ± 0.1^{a}	2.4 ± 0.2^{b}	3.1 ± 0.2^{c}
Hepatic lipids (µg/mg protein):				
Triglycerides	83.5 ± 11.9^{a}	171.9 ± 86.6^{b}	321.5 ± 41.8^{c}	304.6 ± 35.8^{c}
Cholesteryl esters	17.9 ± 2.7^{a}	51.3 ± 4.8^{b}	65.8 ± 5.0^{bc}	82.8 ± 6.7^{c}
Free cholesterol	16.9 ± 1.3^{a}	19.2 ± 1.5^{a}	27.6 ± 1.6^{b}	30.5 ± 2.3^{c}
Serum levels, fasting:				
ALT (U/L)	121.7 ± 10.0^{a}	151.2 ± 39.7^{a}	100.8 ± 21.7^{a}	304.8 ± 53.6^{b}
AST (U/L)	270.0 ± 21.3^{a}	341.2 ± 111.6^{ab}	171.9 ± 20.9^{b}	519.6 ± 80.8^{c}
Plasma levels, fasting:				
Glucose (mM)	9.5 ± 0.8^{a}	12.3 ± 0.9^{b}	15.7 ± 0.7^{c}	16.0 ± 0.7^{c}
Insulin (ng/mL)	0.4 ± 0.1^{a}	2.4 ± 0.6^{b}	2.2 ± 0.4^{b}	4.4 ± 0.8^{c}
Cholesterol (mM)	6.7 ± 0.7^{a}	13.3 ± 1.1^{b}	13.7 ± 2.7^{b}	25.9 ± 2.0^{c}
Triglycerides (mM)	3.3 ± 0.5^{a}	2.9 ± 0.3^{a}	2.2 ± 0.6^{a}	6.7 ± 1.1^{b}

Mice were fed a high-fat diet supplemented with 1% (w/w) cholesterol (HFC) diet and groups (n=10) were sacrificed at regular intervals (t=0, t=4, t=8 or t=12 weeks). Values are mean±SEM. ^{a,b,c,d} Mean values within a row with unlike superscript letters are significantly different (p<0.05).

Macrovesicular steatosis is positively associated with development of lobular inflammation

In a more refined histopathological analysis, we quantified the two forms of steatosis as well as the number inflammatory aggregates during HFC feeding. At already 4 weeks of HFC treatment, a pronounced and significant increase in microvesicular steatosis was observed (38%, $p<0.05$; Figure 2A). After this rapid induction, microvesicular steatosis remained at a constant elevated level until the end of the study. By contrast, macrovesicular steatosis showed a gradual and continuous development over time (24% at week 12, $p<0.05$; Figure 2B). The number of inflammatory cell aggregates increased significantly after 4 weeks and showed a further increase at 12 weeks of HFC treatment (Figure 2C). Next, we examined whether a potential relationship exists between micro-/macrovesicular steatosis and lobular inflammation. Correlation analysis revealed a positive association between macrovesicular steatosis and inflammatory cell aggregates ($r=0.45$; $p=0.01$; Figure 2D). By contrast, microvesicular steatosis and total hepatic triglyceride content were not correlated with inflammatory cell aggregates ($r=0.05$; $p=0.8$ and $r=-0.05$; $p=0.8$, respectively). Together, these results indicate that a specific type of steatosis, macrovesicular steatosis, is critical for the development of lobular inflammation in NASH.

Macrovesicular steatosis and inflammatory cell aggregates are associated independent of the disease model

The positive association between macrovesicular steatosis and lobular inflammation observed in E3L.CETP mice was examined in other models of obesity-induced NASH. More specifically, we examined livers of a mild experimental model (HFD-treated C57BL/6J mice) and a more severe model (HFD-treated LDLr-/-.Leiden mice). C57BL/6J mice developed steatosis (macrovesicular: 23.3±2.2%; microvesicular: 59.5±2.0% of total surface area) with modest inflammation (inflammatory aggregates: 2.0±0.5 per microscopic field) (Figure 3A). LDLr-/-.Leiden mice also developed steatosis (macrovesicular: 26.5±2.3%; and microvesicular: 30.5±2.5% of total surface area), but more inflammatory aggregates (45.9±12.6 per microscopic field) and marked fibrosis (23.4±5.1%) (Figure 3A). To examine the relationship between macrovesicular steatosis and inflammation, we compared mice with a high

and low level of macrovesicular steatosis, and comparable microvesicular steatosis. In both NASH models, macrovesicular steatosis above 20% was associated with significant increases in inflammatory aggregates (Figure 3B-C). Again, macrovesicular steatosis was positively correlated with inflammatory aggregates (C57BL/6J: r=0.66, and LDLr-/-.Leiden: r=0.77; both p<0.05), while no correlation was observed for microvesicular steatosis (not shown).

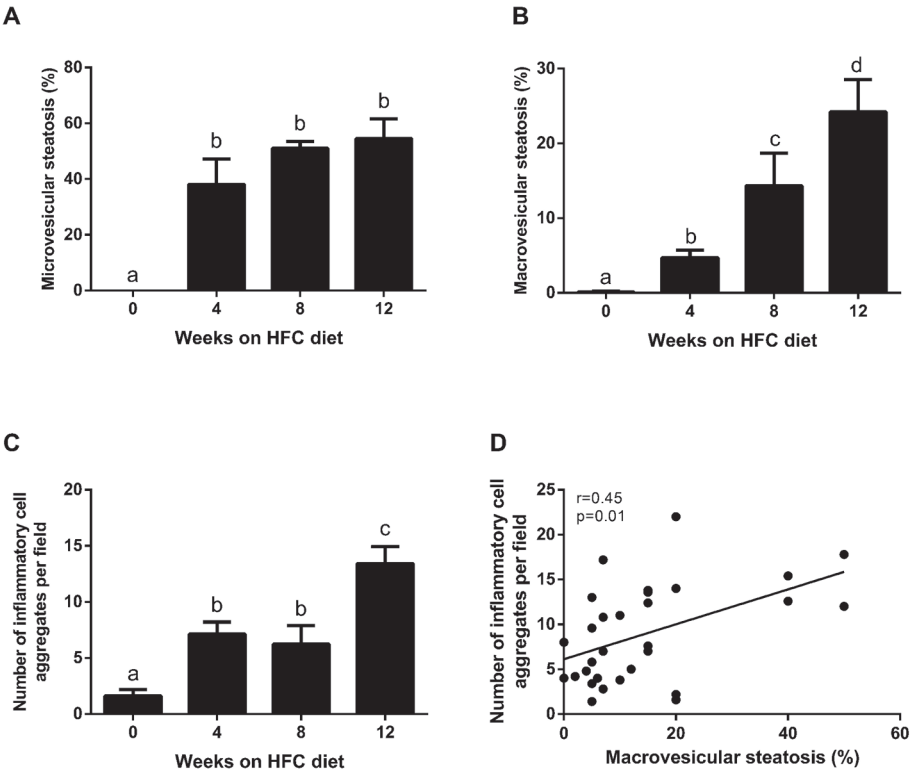


Figure 2. Quantitative histological analysis of the development of liver steatosis and inflammation in E3L.CETP mice. Quantification of the two steatosis forms (A) microvesicular steatosis and (B) macrovesicular steatosis expressed as percentage (%) of the total surface area. Microvesicular steatosis developed rapidly after 4 weeks of HFC and levels remained constant over time, whereas macrovesicular steatosis developed continuously. (C) Lobular inflammation (expressed as the number of inflammatory cell aggregates per field) was induced already after 4 weeks of HFC but increased strongly after 12 weeks of HFC feeding. (D) Macrovesicular steatosis is positively correlated with inflammatory cell aggregates as determined by Spearman's rank correlation analysis. [a,b,c,d] Mean values with unlike letters differ significantly from each other ($p \leq 0.05$).

Macrovesicular steatosis is associated with the development of fibrosis

Next, we investigated whether there is a link between the development of macrovesicular steatosis and liver fibrosis. Sirius red staining of livers from the time course experiment in E3L.CETP mice showed mild perihepatocellular fibrosis at end point (12 weeks of HFC treatment) (Figure 4A). Specifically for the 12-week time point, we observed a significant upregulation of genes involved in pro-fibrotic pathways including TGFβ, TIMP-1, Col1α1, Col1α2 and MMP13 (Figure 4B) as demonstrated by microarray pathway analysis. Of note, this onset of fibrosis was observed when macrovesicular steatosis reached levels above 20%.

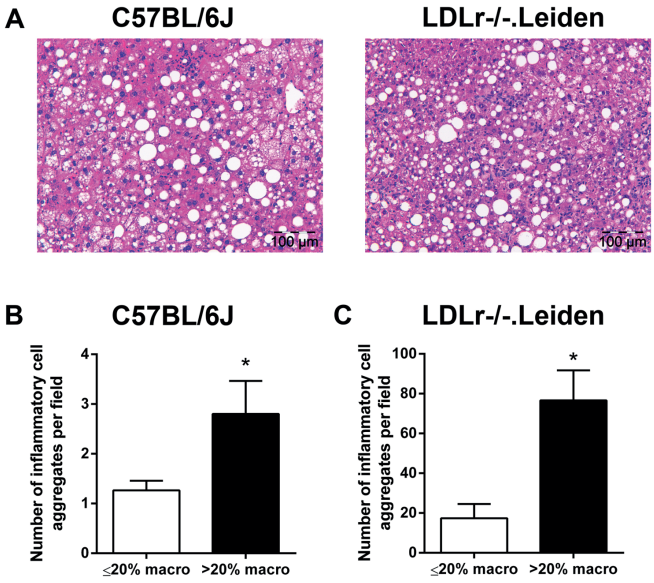


Figure 3. Histological representation and the role of macrovesicular steatosis in other diet-induced NASH mouse models. Representative photographs of HE-stained liver cross-sections from (A) male C57BL/6J mice fed a high-fat diet (HFD) for 24 weeks and male LDLr-/-.Leiden mice treated with HFD for 34 weeks. Photomicrographs on the left show C57BL/6J and on the right LDLr-/-.Leiden mice (Magnification: x200). (B) C57BL/6J mice with high levels of macrovesicular steatosis (>20%) showed more inflammatory cell aggregates then mice with low levels of macrovesicular steatosis (≤ 20%), while microvesicular steatosis was comparable (high vs. low macrovesicular steatosis: ±53% vs. ±60%, respectively). (C) LDLr-/- mice with high levels of macrovesicular (>20%) have increased lobular inflammation compared to mice with low macrovesicular steatosis (≤20%), while microvesicular steatosis was comparable between the groups (both, ±30%).

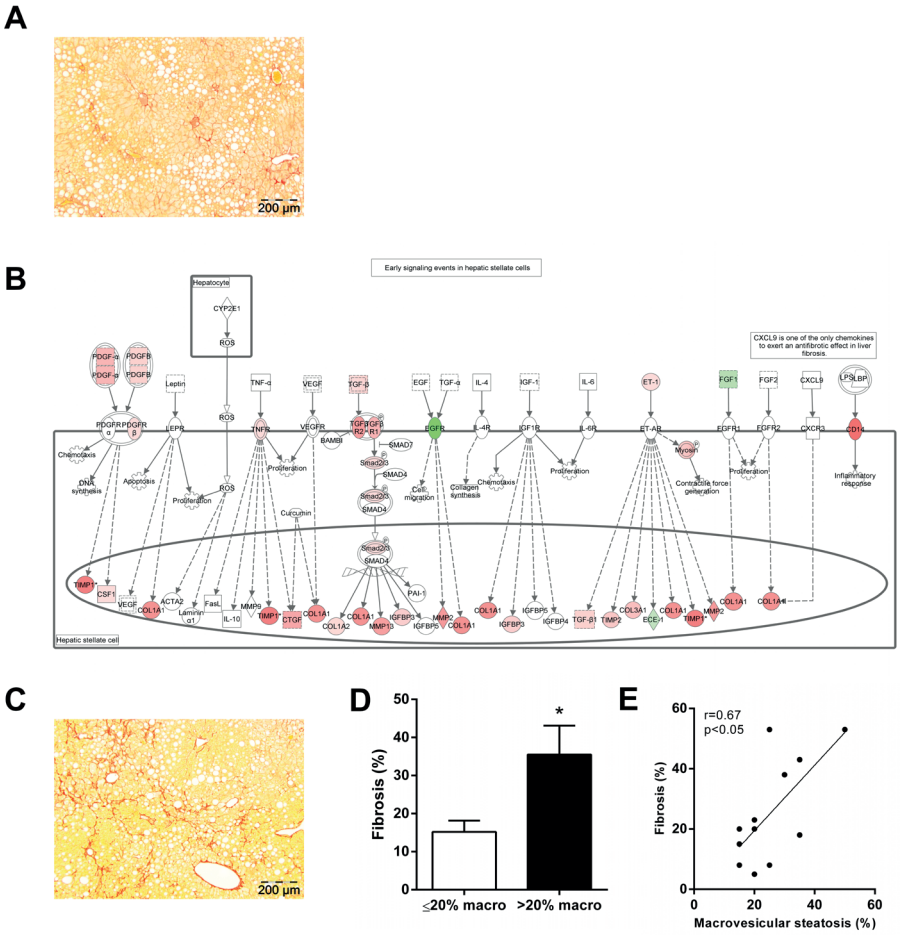


Figure 4. Onset of liver fibrosis in E3L.CETP mice and established fibrosis in LDLr-/-.Leiden mice. (A) Representative photomicrograph of pico-sirius red-stained livers from E3L.CETP mice showing mild fibrosis (Magnification x100). Arrows show perihepatocellular fibrosis. (B) Transcriptome analysis confirmed the onset of liver fibrosis as demonstrated by upregulation of pro-fibrotic signaling pathways in hepatic stellate cells and showed increased expression of pro-fibrotic genes including *Col-1α, Timp1, Smad3*. Nodes that are colored red (upregulated) or green (downregulated) indicate significant differences in fold-change in HFC-fed mice compared to HFD-fed control mice. (C) Representative photomicrograph of pico-sirius red-stained liver section showing pronounced fibrosis in LDLr-/-.Leiden mice treated with HFD feeding for 34 weeks (Magnification x100). (D) LDLr-/-.Leiden mice with high levels of macrovesicular (>20%) have more fibrosis compared to mice with low macrovesicular steatosis (≤20%). (E) Macrovesicular steatosis is positively correlated with fibrosis in HFD-fed LDLr-/-.Leiden mice.

The relationship between macrovesicular steatosis and liver fibrosis was further examined in a NASH model with pronounced fibrosis, namely LDLr-/-.Leiden mice (Figure 4C). LDLr-/-.Leiden mice with a high percentage of macrovesicular steatosis (>20%) exhibited more fibrosis than mice with a low level of macrovesicular steatosis (≤20%) (Figure 4D). Furthermore, the level of macrovesicular steatosis correlated positively with the amount of liver fibrosis ($r=0.67$, $p<0.05$, Figure 4E) while there was no correlation between microvesicular steatosis and fibrosis. Of note, the number of inflammatory cell aggregates is strongly correlated with fibrosis ($r=0.93$, $p<0.001$). Thus, the association between macrovesicular steatosis and fibrosis is likely to be a consequence of the development of macrovesicular steatosis-associated lobular inflammation. Altogether, these results support the importance of macrovesicular steatosis in the etiology of liver inflammation and, as a consequence thereof, liver fibrosis.

DISCUSSION

This study analyzed the progression of steatosis and inflammation during the pathogenesis of NASH in obesity. Specifically, we examined the relationship between the development of specific forms of steatosis and inflammatory cell aggregates in different diet-induced NASH models. In E3L.CETP mice treated with a high-fat diet containing 1% w/w cholesterol (HFC), a rapid induction of microvesicular steatosis was observed (at week 4). This form of steatosis remained at an elevated level and did not further progress. By contrast, macrovesicular steatosis showed a progressive development until the end of the study (week 12). Development of macrovesicular steatosis correlated positively with the number of inflammatory cell aggregates, whereas microvesicular steatosis did not correlate with inflammation. Further support for a positive association between macrovesicular steatosis and lobular inflammation was obtained from independent NASH studies in HFD-treated C57BL/6J and LDLr-/-.Leiden. Furthermore, macrovesicular steatosis was positively associated with perihepatocellular fibrosis in LDLr-/-.Leiden mice, a mouse model that develops

pronounced liver fibrosis on a HFD. Collectively, these results highlight the importance of macrovesicular steatosis in the pathogenesis of NASH.

In the present study, the diet-induced NASH models showed pronounced development of microvesicular and macrovesicular steatosis. Our time course analysis in E3L.CETP mice revealed that the development of microvesicular steatosis is rapid process and plateau levels were reached after 4 weeks of HFC feeding. By contrast, macrovesicular steatosis developed continuously and progressively over time. The development of these two forms of steatosis is only poorly understood. It is not clear whether the small lipid vacuoles (microvesicular steatosis) fuse to form one large vacuole (macrovesicular steatosis), or whether macrovesicular and microvesicular steatosis develop independently from each other ([13] and references therein). The most widely accepted theory of lipid droplet biogenesis implies that neutral glycerol and esters accumulate within the phospholipid bilayer of the endoplasmatic reticulum (ER) and the bilayer gradually separates from the ER to form nascent phospholipid-coated lipid droplets which bud off into the cytosol [13-15]. The most common form of further growth of these droplets is expansion by diffusion of lipids (from the ER or cytosol), i.e. triglycerides are added to the cores and phospholipids as surfactants to the surfaces of a growing lipid droplet. Notably, the fusion of small lipid vacuoles to a large vacuole is considered to be a relatively rare event [13,14]. Thus, it is possible that the observed gradual development of macrovesicular steatosis may be determined by the amount of phospholipids that are available in a hepatocyte to enlarge the microvesicular structures.

The large lipid droplets that are characteristic for macrovesicular steatosis can cause cellular stress and architectural changes to hepatocytes [13]. The injured liver cells then release immune reactive substances and hepatocellular damage will ultimately lead to ballooning, apoptosis and infiltration of immune cells [16]. Consistent with these processes, we observed a significant correlation between macrovesicular steatosis and immune cell aggregates in all models. Absence of a correlation between inflammatory cell aggregates and microvesicular steatosis suggests that the microvesicular lipid droplets are less harmful. The importance of macrovesicular steatosis as inducer of liver injury and subsequent liver fibrosis is supported by a recent study in rats [17]. A comparison of different rat strains

with either 1) solely microvesicular steatosis (Lewis rats), 2) pure macrovesicular steatosis (Sprague Dawley) and 3) mixed-type steatosis (Wistar) showed that Sprague Dawley rats with macrovesicular steatosis had the highest degree of lobular inflammation and fibrosis [17]. In line with this, we observed that the marked increase in macrovesicular steatosis between 8 and 12 weeks of HFC feeding in E3L.CETP mice is accompanied by increased number of inflammatory cell aggregates, and onset of pathways leading to liver fibrosis. Furthermore, macrovesicular steatosis and inflammatory cell aggregates correlated significantly with the level of hepatocellular fibrosis in the LDLr-/-.Leiden mice.

This study used different mouse strains and diets to investigate the development of NASH in the context of visceral obesity, insulin resistance and dyslipidemia, all of which constitute important risk factors of NAFLD in humans [1-3]. These risk factors are not or only inadequately mimicked in methionine choline deficient (MCD) diet-induced NAFLD or CCl4-induced liver fibrosis [18,19]. It is generally assumed that diets low in methionine and choline are required to induce liver fibrosis [18]. However, the present study shows that liver fibrosis can also be induced with high-fat diets (HFD) containing 45 energy percent from fat, which is translational to human diets [20]. We have previously reported that LDLr-/-.Leiden mice develop a NASH phenotype on HFD which reflects human steatohepatitis [10]. We herein show that these animals develop pronounced liver fibrosis (>20% perihepatocellular fibrosis) when the HFD treatment is prolonged (34 weeks). Consistent with this observation, others reported that mice on a LDLr-/- background constitute a physiological model particularly vulnerable to study the inflammation in NAFLD [21].

High-fat diets are often supplemented with cholesterol to induce chronic liver inflammation. In LDLr-/- mice, Bieghs and coworkers demonstrated that cholesterol feeding can cause lysosomal cholesterol accumulation in Kupffer cells which correlates with hepatic inflammation and cholesterol crystallization [22]. Similarly, E3L mice treated with a Western-type diet containing 1% (w/w) cholesterol for 20 weeks show formation of cholesterol crystals and collagen deposition in liver [23] as they have been described in humans with NASH [24]. Consistent with this pro-fibrotic effect of dietary cholesterol, HFC-fed E3L.CETP mice developed early fibrosis after already 12 weeks, and transcriptome analysis substantiated the

activation of pro-fibrotic signaling pathways in liver controlled by TNF, PDGF and TGFβ. The same pathways were activated in mouse liver with high (1% w/w) but not low (0.25% w/w) dietary cholesterol [25]. This effect was attributable to dietary cholesterol itself and not to the fat content of the diet. Therefore, it is likely that NASH-inducing diets containing high concentrations of cholesterol accentuate the above mentioned inflammatory pathways, and that other inflammatory pathways which also may contribute to NASH development (e.g. IL-6 and leptin signaling) have a relative lower contribution.

In all, our data highlight the importance of macrovesicular steatosis in the pathogenesis of experimental diet-induced NASH, because this form steatosis is tightly associated with cellular lobular inflammation and perihepatocellular fibrosis. Our study advocates a more refined morphological analysis of steatosis subtypes in addition to biochemical liver lipid analysis. Such an analysis may be of particular relevance for efficacy studies with nutritional or pharmaceutical interventions.

ACKNOWLEDGEMENTS

The authors gratefully acknowledge Erik Offerman and Wim van Duyvenvoorde for technical assistance. This study was supported by the TNO research programs ‘Personalized Prevention and Therapy/Predictive Health Technologies PHT’ (to Petra Mulder). The research was performed within the framework of CTMM, the Center for Translational Molecular Medicine (www.ctmm.nl), project PREDICCT (to Wen Liang).

REFERENCES

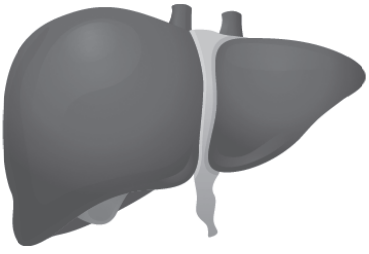
1. Vernon G, Baranova A, Younossi ZM. Systematic review: the epidemiology and natural history of non-alcoholic fatty liver disease and non-alcoholic steatohepatitis in adults. Alimentary pharmacology & therapeutics 2011;34:274-285.
2. Loomba R, Sanyal AJ. The global NAFLD epidemic. Nature reviews Gastroenterology & hepatology 2013;10:686-690.
3. Bellentani S, Marino M. Epidemiology and natural history of non-alcoholic fatty liver disease (NAFLD). Annals of hepatology 2009;8 Suppl 1:S4-8.
4. Green CJ, Hodson L. The influence of dietary fat on liver fat accumulation. Nutrients 2014;6:5018-5033.
5. Neuschwander-Tetri BA. Hepatic lipotoxicity and the pathogenesis of nonalcoholic steatohepatitis: the central role of nontriglyceride fatty acid metabolites. Hepatology 2010;52:774-788.
6. Farrell GC, van Rooyen D, Gan L, Chitturi S. NASH is an Inflammatory Disorder: Pathogenic, Prognostic and Therapeutic Implications. Gut and liver 2012;6:149-171.
7. Liang W, Lindeman JH, Menke AL, Koonen DP, Morrison M, Havekes LM, et al. Metabolically induced liver inflammation leads to NASH and differs from LPS- or IL-1beta-induced chronic inflammation. Laboratory investigation; a journal of technical methods and pathology 2014;94:491-502.
8. Ueha S, Shand FH, Matsushima K. Cellular and molecular mechanisms of chronic inflammation-associated organ fibrosis. Frontiers in immunology 2012;3:71.
9. Liang W, Tonini G, Mulder P, Kelder T, van Erk M, van den Hoek AM, et al. Coordinated and interactive expression of genes of lipid metabolism and inflammation in adipose tissue and liver during metabolic overload. PloS one 2013;8:e75290.
10. Liang W, Menke AL, Driessen A, Koek GH, Lindeman JH, Stoop R, et al. Establishment of a general NAFLD scoring system for rodent models and comparison to human liver pathology. PloS one 2014;9:e115922.
11. Ito M, Suzuki J, Tsujioka S, Sasaki M, Gomori A, Shirakura T, et al. Longitudinal analysis of murine steatohepatitis model induced by chronic exposure to high-fat diet. Hepatology research : the official journal of the Japan Society of Hepatology 2007;37:50-57.
12. Verschuren L, Wielinga PY, Kelder T, Radonjic M, Salic K, Kleemann R, et al. A systems biology approach to understand the pathophysiological mechanisms of cardiac pathological hypertrophy associated with rosiglitazone. BMC medical genomics 2014;7:35-8794-8797-8735.
13. Sahini N, Borlak J. Recent insights into the molecular pathophysiology of lipid droplet formation in hepatocytes. Progress in lipid research 2014;54:86-112.
14. Wilfling F, Wang H, Haas JT, Krahmer N, Gould TJ, Uchida A, et al. Triacylglycerol synthesis enzymes mediate lipid droplet growth by relocalizing from the ER to lipid droplets. Dev Cell 2013;24:384-399.
15. Guo Y, Cordes KR, Farese RV, Jr., Walther TC. Lipid droplets at a glance. J Cell Sci 2009;122:749-752.
16. Baffy G. Kupffer cells in non-alcoholic fatty liver disease: the emerging view. Journal of hepatology 2009;51:212-223.
17. Rosenstengel S, Stoeppeler S, Bahde R, Spiegel HU, Palmes D. Type of steatosis influences microcirculation and fibrogenesis in different rat strains. Journal of investigative surgery : the official journal of the Academy of Surgical Research 2011;24:273-282.

18. Rosso N, Chavez-Tapia NC, Tiribelli C, Bellentani S. Translational approaches: from fatty liver to non-alcoholic steatohepatitis. World journal of gastroenterology : WJG 2014;20:9038-9049.
19. Rinella ME, Green RM. The methionine-choline deficient dietary model of steatohepatitis does not exhibit insulin resistance. Journal of hepatology 2004;40:47-51.
20. Hu FB, Manson JE, Willett WC. Types of dietary fat and risk of coronary heart disease: a critical review. Journal of the American College of Nutrition 2001;20:5-19.
21. Bieghs V, Van Gorp PJ, Wouters K, Hendrikx T, Gijbels MJ, van Bilsen M, et al. LDL receptor knock-out mice are a physiological model particularly vulnerable to study the onset of inflammation in non-alcoholic fatty liver disease. PloS one 2012;7:e30668.
22. Bieghs V, Walenbergh SM, Hendrikx T, van Gorp PJ, Verheyen F, Olde Damink SW, et al. Trapping of oxidized LDL in lysosomes of Kupffer cells is a trigger for hepatic inflammation. Liver international : official journal of the International Association for the Study of the Liver 2013;33:1056-1061.
23. Morrison MC, Liang W, Mulder P, Verschuren L, Pieterman E, Toet K, et al. Mirtoselect, an anthocyanin-rich bilberry extract, attenuates non-alcoholic steatohepatitis and associated fibrosis in ApoE(*)3Leiden mice. Journal of hepatology 2015;62:1180-1186.
24. Ioannou GN, Haigh WG, Thorning D, Savard C. Hepatic cholesterol crystals and crown-like structures distinguish NASH from simple steatosis. Journal of lipid research 2013;54:1326-1334.
25. Kleemann R, Verschuren L, van Erk MJ, Nikolsky Y, Cnubben NH, Verheij ER, et al. Atherosclerosis and liver inflammation induced by increased dietary cholesterol intake: a combined transcriptomics and metabolomics analysis. Genome biology 2007;8:R200.

Chapter 8

Summary and general discussion







NAFLD is the most common cause of chronic liver disease worldwide. Prevalence estimates for NAFLD in general adult population are between 25% and 45%, and the disease incidence increases in parallel of obesity and diabetes [1]. Histologically, NAFLD comprises a wide spectrum of liver damage ranging from liver steatosis to non-alcoholic steatohepatitis (NASH) and fibrosis. Liver steatosis is considered benign in many cases [2], while NASH is a more severe condition that is characterized by steatosis and lobular inflammation with or without fibrosis. The progression from steatosis to NASH is associated with the presence of the metabolic syndrome (defined as central obesity accompanied by two or more of the following conditions: elevated fasting glucose concentration (reflecting insulin resistance), hypertension, raised triglyceride (TG) levels and lowered high-density lipoprotein cholesterol (HDL) levels) [1]. In particular patients with NASH have increased risk to develop other metabolic complications, such as cardiovascular disease, and have overall higher mortality [3-5]. Although the etiology of NASH remains largely enigmatic, it is generally accepted that inflammation is a central component of NASH pathogenesis. This inflammation may be triggered by metabolic surplus (excess energy or nutrients) and is also referred to as “metabolic inflammation”. White adipose tissue (WAT) is assumed to be largely involved in the development of metabolic inflammation. However, much remains unknown about the origin and underlying mechanisms controlling inflammation in NAFLD progression. The studies described in this thesis contributed to the understanding of the role of WAT in the development of NAFLD and provide insight into the molecular processes that cause metabolic inflammation.

THE ROLE OF WHITE ADIPOSE TISSUE IN NASH DEVELOPMENT

Adipose tissue has multiple roles in orchestrating adaptation to changes in nutrient availability [6]. It is not solely a reservoir for energy excess, but can act as an endocrine organ by transmitting soluble signals in the form of “adipokines” which can act locally and systemically. Moreover, the adipose tissue can interact extensively with immune cells which, under specific conditions, infiltrate in the

adipose tissue. Activation of the immune system in obese individuals in a so-called "chronic low-grade inflammatory state" is considered to be a crucial factor in the pathogenesis of metabolic diseases, such as NAFLD [7]. The basis of this view is that obese individuals have elevated plasma levels of inflammatory cytokines (e.g. TNFα, IL-6), increased chemokine levels that induce infiltration of immune cells, as well as elevated levels of general markers of inflammation (e.g. haptoglobin, SAA) [8].

Heterogeneity in the obese population

Although obesity is one of the major risk factors for NAFLD, some obese individuals appear 'metabolically healthy' despite having excessive body fat. These 'metabolically healthy' obese individuals have normal to high levels of insulin sensitivity, lower hepatic fat content, and a generally favorable cardiovascular profile [9]. This subgroup of obese individuals may maintain metabolic health as a result of their genetic profile or unclarified lifestyle features [10]. The factors that distinguish the "metabolically healthy" from the "metabolically unhealthy" obese are still poorly understood. A better understanding of the factors contributing to the metabolically healthy phenotype and the stratification of obesity phenotypes could lead to new prevention and therapeutic intervention strategies and thereby improve public health.

It has been postulated that some obese individuals are protected against metabolic complications because of a more favorable body fat distribution. In general, it is thought that increased visceral fat mass is linked to detrimental health effects. Studies have shown that increased visceral (intra-abdominal) fat is positively associated with metabolic disease [11,12], independent of overall adiposity [13]. On the contrary, subcutaneous adipose tissue is associated with more favorable levels of glucose and lipids [14].

As mentioned before, white adipose tissue (WAT) is not merely a storage site for excess energy, but can also act as a endocrine organ capable of secreting a variety of inflammatory mediators [15]. Hence, in the development of metabolic diseases such as NASH, the 'inflammatory status' of WAT may be even more important than the distribution of fat mass. In support of this, liver of obese subjects with

inflamed intra-abdominal (omental) WAT contain more fibro-inflammatory lesions than livers of equally obese subjects without WAT inflammation [16,17]. This observation suggests that inflammation in a specific WAT depot contributes to the inflammatory component in human NASH. The time-course experiment in an animal model for NASH, as described in **chapter 2**, supports this hypothesis. Herein, we explored the sequence of inflammatory events in different WAT depots and the liver in high-fat diet (HFD)-fed C57BL/6J mice that developed obesity. More specifically, we have investigated whether different intra-abdominal (i.e. epididymal and mesenteric) and subcutaneous (inguinal) WAT depots differ in their susceptibility to develop chronic inflammation. We found that the first depot that became inflamed was the intra-abdominal epididymal adipose tissue (eWAT) and this inflammation preceded NASH development. Moreover, we found that surgical excision of inflamed eWAT reduced liver inflammation, demonstrating that this WAT depot causally contributes to NASH development.

Adipose tissue expansion and inflammation

The susceptibility of eWAT to become inflamed, as shown herein, may be related to the fact that adipocytes in eWAT are more prone to hypertrophy than those in other WAT depots [18]. The deleterious effect of adipocyte hypertrophy was demonstrated in an *in vitro* experiment with isolated primary human adipocytes, [19] where only very hypertrophic cells were found to secrete MCP-1, a key mediator of immune cell recruitment into WAT. Consistent with this observation, adipocyte hypertrophy is associated with infiltration of macrophages and formation of crown-like structures (CLS), [20] a histological hallmark of inflamed WAT. Macrophage infiltration is positively correlated with the size of adipocytes both in visceral and subcutaneous fat [20,21]. However, visceral fat is more prone to macrophage infiltration compared to subcutaneous fat [22]. Moreover, it has been shown in obese individuals that visceral fat exhibit higher expression of inflammatory cytokines than subcutaneous fat [23]. These differences might explain the strong association between visceral obesity and NASH development.

Importantly, obese mice and humans with hyperplastic obesity (i.e. obesity without adipocyte hypertrophy) do not show CLS in WAT and remain insulin

sensitive [21,24]. The activation of peroxisome proliferator-activated receptor-γ (PPARγ) has an important role in adipocyte differentiation to stimulate fat storage via hyperplasia [25]. It has been shown that metabolic unhealthy obese (insulin resistant) patients have lower expression of PPARγ in visceral fat than (insulin sensitive) metabolically healthy obese individuals [26]. Subcutaneous WAT shows higher expression of PPARγ compared to visceral WAT [27], suggesting that this depot may be less susceptible to develop inflammation. Thus, pharmacological activation of PPARγ may be a suitable intervention strategy to stimulate fat storage via hyperplasia and thereby preventing adipocyte hypertrophy. Indeed, in **chapter 3** it was shown that intervention with a PPARγ-activator, rosiglitazone, stimulated hyperplasia specifically in the subcutaneous WAT and prevented adipocyte hypertrophy. Consequently, this depot did not become inflamed even though its mass was much greater than in control animals, an effect that was also observed in humans treated with rosiglitazone [28]. Thus, limited capacity for adipose tissue expansion, rather than obesity *per se* may underlie the development of inflammation [29,30] and leads to ectopic fat deposition in other organs such as liver [30].

Proposed mechanisms for inflamed white adipose tissue in NASH development

The removal of inflamed WAT as demonstrated in **chapter 2**, resulted in reduced NASH development. Moreover, intervention by rosiglitazone reduced WAT inflammation and subsequent NAFLD progression as shown in **chapter 3**. Both studies, showed that histological improvement of the liver was paralleled by the reduction of circulating pro-inflammatory adipokines, including leptin and saturated fatty acids. These data support a model in which secretion of inflammatory mediators (e.g. lipids, adipokines) by inflamed WAT drive NASH development as depicted in Figure 1. Excess of nutrients leads to expansion of WAT involving adipocyte hypertrophy [29]. Once adipocytes do not further increase in size and a WAT depot has reached a maximal mass, infiltration of immune cells and CLS formation are observed. Next, the inflamed WAT produces soluble inflammatory mediators that are released into the circulation driving the development of inflammatory pathologies in other organs, including the liver. The model in Figure 1 implies that intervention

strategies that can attenuate WAT inflammation may reduce NAFLD development. Strategies aiming at reducing WAT inflammation should focus on mechanisms that allow optimal WAT expansion and prevent immune cell infiltration.

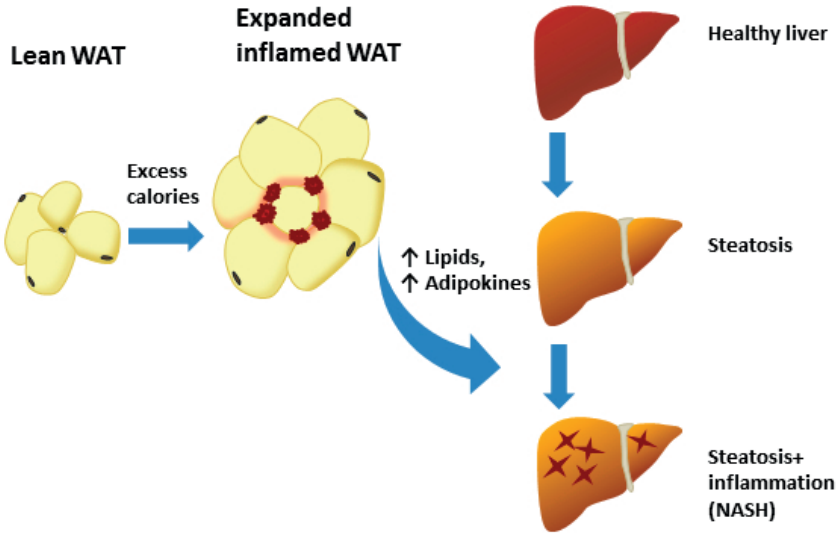


Figure 1: Limitation in expansion is critical for the development of obesity-associated inflammation and NASH. Caloric excess leads to expansion of WAT involving adipocyte hypertrophy. Infiltration of immune cells and formation of crown-like structures are observed once the adipocytes of a depot do not further increase in size and a WAT depot has reached a maximal mass. Inflamed WAT produces inflammatory mediators that can be released into the circulation driving the development of inflammatory pathologies, such as NASH. Among the inflammatory mediators are adipokines, such as TNFα, IL-6, leptin (increased) and adiponectin (decreased) as well as specific pro-inflammatory lipids like palmitic acid and stearic acid.

THE LINK BETWEEN INFLAMMATION, INSULIN RESISTANCE AND NAFLD

In 1993, Hotamisligil and colleagues were the first that described a molecular link between inflammation and obesity-associated insulin resistance [31]. They showed in rodent models of obesity and diabetes that increased expression of the pro-

inflammatory cytokine TNFα in adipose tissue correlated with insulin resistance. This study was supported by similar findings in humans, showing that elevated TNFα concentrations in both WAT and plasma were associated with decreased insulin sensitivity [32,33].

Origin of insulin resistance

Given the obvious connection between obesity and adiposity, studies have mainly focused on obesity-driven inflammation in WAT during the development of insulin resistance. However, obesity is also associated with the development of inflammation in other metabolic tissues, such as the liver. While inflammatory processes in both the WAT and liver are associated with the development of insulin resistance [34], it remains unclear to what extent both organs contribute to obesity-induced (systemic) insulin resistance. Since it is difficult to untangle this question in human subjects, we studied the inflammatory processes in both WAT and liver in a HFD-induced animal model for NAFLD (**Chapter 4**). In this time-course study, we observed that the development of tissue-specific insulin resistance was paralleled by increased infiltration of inflammatory cells in both, WAT and liver. However, adipose-specific insulin resistance was already observed after 6 weeks of HFD feeding, while hepatic insulin resistance occurred much later in time (after 24 weeks of HFD feeding). These findings support the view that hepatic inflammation contributes less to whole body insulin resistance compared to WAT inflammation, at least in early stages of diet-induced obesity, as previously hypothesized by others [15,35]. Moreover, it has been shown the degree of adipose tissue insulin resistance is associated with progressive NASH in patients [36], supporting the view that insulin resistance in WAT is an early disease symptom that may contribute to NASH development [37].

Inflammatory mechanisms underlying insulin resistance

As mentioned earlier, insulin resistance is associated with inflammation in WAT. More specifically, WAT inflammation is characterized by infiltration of macrophages that form CLS. The number of adipose tissue macrophages (ATM) is positively associated with the progression of insulin resistance [38].

The chemokine monocyte chemoattractant protein (MCP)-1 and its receptor C-C chemokine receptor-2 (CCR2) play a pivotal role in the recruitment of macrophages. In support of this, MCP-1 and CCR2 knockout mice exhibit reduced ATM content and insulin resistance [39-42]. Furthermore, prophylactic treatment with a CCR2 antagonist reduced macrophage content in WAT and hyperinsulinemia [43]. Other studies have demonstrated that CCR2 antagonists can also improve NASH [44], however, this has not been tested in a therapeutical setting so far. Therefore, we have examined in **chapter 4** whether CCR2 inhibitor, propagermanium, would attenuate NASH development in mice with manifest disease symptoms (i.e. WAT inflammation and insulin resistance). We observed that propagermanium intervention reduced insulin resistance and WAT inflammation. Moreover, propagermanium reduced macrovesicular steatosis and lobular inflammation, indicating an attenuation of NASH development. However, the beneficial effects were much more pronounced in the early intervention group compared to the late intervention group (started after 6 weeks vs. 12 weeks of HFD feeding). Hence, CCR2 inhibitors may be beneficial to treat insulin resistance and NASH, but only when administered early in the disease development. Based on existing literature [45-47], it is likely that disease pathways other than MCP1/CCR2 become upregulated at later stages of disease process (e.g. RANTES/CCR5) and that interventions merely targeting MCP1/CCR2 become less efficient. Therefore, NASH patients may benefit more from a treatment that is directed at both, the CCR2 and CCR5 pathways. The use of such a dual-CCR2/CCR5 antagonist is currently being examined in a large randomized phase 2b trial in NASH [47].

It should be noted that not only the number of ATM, but also the inflammatory phenotype of this immune cell population differs during obesity, which are typically referred to as M1 and M2 macrophages. M1 macrophages are considered pro-inflammatory as they secrete pro-inflammatory cytokines (e.g. TNFα, IL-1β), whereas M2 macrophages secrete anti-inflammatory cytokines (e.g. IL-10) [48]. In particular the accumulation of M1 macrophages, which express the CD11c surface marker, have been implicated in the development of insulin resistance [34,38]. In support of this notion, CD11c depletion in obese mice results in a rapid normalization of glucose and insulin tolerance and decreased inflammatory markers in WAT [49].

Various studies have described a shift in ATM subsets from M2 in lean mice to M1 in obese mice [48,50]. In obese humans, however, the ATM phenotype is less polarized, as both M1 and M2 markers can be detected in human ATMs [51-53]. Despite a 'mixed' ATM phenotype, these macrophages are thought to contribute to the chronic inflammatory process in obesity as they can produce extensive amounts of pro-inflammatory cytokines [53]. It has been assumed that macrophages exhibit phenotypic plasticity in response to their surrounding milieu [54]. For instance, it was shown that progressive lipid accumulation in macrophages favors M1 polarization [55]. The transcriptional factor PPARγ appears to be a key player in this macrophage polarization [56]. Indeed, we observed that administration of PPARγ activator rosiglitazone leads to decreased expression of M1 and increased expression of M2 markers in WAT as shown in **chapter 3**. This suggests that rosiglitazone partly exerts its insulin sensitizing effect by preventing M1 polarization in WAT.

Inflammation can be triggered by cytokines (e.g. TNFα) that instigate inflammatory signaling through classical activation of their cell surface receptors [34]. Alternatively, the inflammatory process can be initiated by 'danger signals', such as saturated fatty acids, that activate the NLRP3 inflammasome complex [57]. Upon inflammasome activation, caspase-1 initiates the maturation of the cytokines IL-1β and IL-18. Genetic ablation of components of the inflammasome (e.g. caspase-1) has been shown to ameliorate HFD-induced obesity and insulin resistance [58], suggesting that the inflammasome is an important mediator in the development of metabolic disease. In **chapter 5**, we examined the therapeutical value of a caspase-1 inhibitor in obesity-associated NAFLD development in LDLr-/-.Leiden mice. Treatment with this inhibitor did not affect obesity or fat mass, but did reduce inflammation in WAT, which was paralleled by improvement of whole-body insulin resistance. Moreover, intervention with caspase-1 inhibitor attenuated steatosis, inflammation and fibrosis in the liver. The inflammasome is present and of relevance in multiple tissues (e.g. WAT, liver) and cell types (e.g. hepatocytes, macrophages). Future studies should therefore address whether the observed improvement of NAFLD in LDLr-/-.Leiden mice is orchestrated by direct effects of caspase-1 inhibition on the liver or via indirect effects on WAT.

Relationship between insulin resistance and NAFLD

Obesity-associated insulin resistance is thought to play a causal role in the pathogenesis of NASH, since it is strongly associated with NAFLD severity [59,60]. However, the relationship between insulin resistance and NASH is still poorly understood. Ectopic lipid accumulation in the liver has been considered to cause insulin resistance [61]. On the other hand, insulin resistance is thought to cause NAFLD development [37]. Notably, whole body insulin resistance determined by HOMA-IR or increased plasma insulin levels may merely reflect insulin resistance in adipose tissue, rather than hepatic insulin resistance. Moreover, liver steatosis is rare in metabolic healthy obese with normal insulin-sensitive adipose tissue [36], highlighting the importance of adipose tissue in NAFLD.

Reducing inflammation in adipose tissue, via macrophage polarization or inhibiting inflammatory components (e.g. inflammasome) have been shown to improve systemic insulin resistance [62,63] and, as shown herein, is frequently accompanied by improvement in NASH. As the degree of insulin resistance in adipose tissue is associated with NASH severity [36], it is thus likely that NASH development can be attenuated by improving adipose tissue function (i.e. inflammation, insulin resistance).

PRECLINICAL NASH MODELS TO EXAMINE DIFFERENT ASPECTS OF DISEASE

NAFLD is considered a complex, multifactorial disease and its progression is difficult to study in patients. Clinical research into disease mechanisms are constrained by ethical considerations, particularly with respect to obtaining tissue biopsies (e.g. liver, WAT other than subcutaneous) and by limited ability to study interactive disease pathways over time. Although animal work contributed greatly to our understanding of the mechanisms underlying NAFLD progression, to date no optimal animal model exists that reflects all the disease aspects observed in humans. Ideally, experimental NASH models should mimic both human pathophysiology and histopathology. As multifactorial origins and processes are thought to contribute to

NASH development, animal models investigating the etiology of NAFLD have been restricted to studying specific aspects of the disease.

Histopathology of NASH

Histopathologically, fat accumulation observed in human NAFLD can manifest in two forms: macrovesicular- or microvesicular steatosis. Macrovesicular steatosis is characterized by the presence of a large lipid droplets that displaces nucleus to the periphery of liver cells, while microvesicular steatosis consists of large numbers of smaller droplets surrounding a central nucleus. In human NAFLD, the most frequent type of steatosis is macrovesicular steatosis, but a mixed pattern (macrovesicular and microvesicular) steatosis has been reported as well [64]. However, it is unclear whether a distinct type of fat storage i.e. macrovesicular or microvesicular steatosis, contributes to NAFLD progression. In **chapter 7**, we studied whether a potential relationship exists between the type of steatosis and the onset of hepatic inflammation in different experimental models of NASH. We found that macrovesicular, but not microvesicular, steatosis was positively correlated with the number of inflammatory aggregates across different disease models (i.e. ApoE3.Leiden.CETP, C57BL/6J, LDLr-/-.Leiden mice). Currently, it is unknown what factors or mechanisms that involve macrovesicular steatosis could drive disease progression. Future research should focus on how lipid droplets are formed, e.g. whether small lipid droplets characterizing microvesicular steatosis reflect newly synthesized fat droplets or if the aggregation of smaller lipid vacuoles become larger over time. Moreover, it is unknown which lipids are stored in macrovesicular steatosis and whether they differ from the lipids that accumulate in microvesicles. The latter may be of importance, because emerging data indicate that accumulation of specific types of lipids in liver cells causes lipotoxic hepatocellular injury and inflammation [65]. Therefore, it is possible that the large lipid droplets in macrovesicular steatosis contain certain toxic lipids or lipid metabolites that are absent or less abundant in liver regions with microvesicular steatosis.

Animal models of NASH

The methionine choline deficient (MCD) diet-induced NASH model is a frequently used model to study liver disease in rodents. Although this model develops pronounced (macrovesicular) steatosis, inflammation and fibrosis reflecting human histopathology, it lacks metabolic features associated with human NASH. The MCD model is associated with features that are atypical for NASH patients, i.e. weight loss, increased insulin sensitivity and low serum triglyceride (TG) levels [66]. Thus, to mimic human risk groups for NASH development, we herein used different mouse strains and diets that reflect a similar disease phenotype as observed in humans.

Inbred C57BL/6J mice fed a high-fat diet (HFD) are a frequently used model to study diet-induced obesity and associated co-morbidities, such as insulin resistance and NAFLD [67]. The development of metabolic inflammation and organ dysfunction in this model is relatively slow. Therefore, it is well-suited for longitudinal studies investigating different stages of disease development (as shown in **chapter 2, 4 and 7**). However, these mice do not develop dyslipidemia as seen in humans and they exhibit relatively low plasma TG and cholesterol levels with low levels of the atherogenic VLDL and LDL. In fact, the majority of cholesterol is confined to HDL particles. Moreover, the development of NASH is quite mild in HFD-fed C57BL/6J mice. It is likely that changes in lipid metabolism in the liver related to dyslipidemia are necessary to aggravate NASH. As dyslipidemia is considered a risk factor in NAFLD, we have used other animal models to capture this aspect of disease.

In contrast to wild-type mice, experimental models of atherosclerosis show resemblance with the human plasma lipoprotein profile. Examples are the transgenic LDL receptor deficient (LDLr-/-) mice and ApoE*Leiden (E3L) mice. LDLr-/- mice lack the LDL receptor, which is required for clearance of chylomicrons, VLDL and LDL particles. Deficiency of this receptor, results in elevated TG and cholesterol levels upon a Western-type diet. Originally, LDLr-/- mice were frequently used for atherosclerosis research. Notably, when fed a HFD, LDLr-/- mice develop obesity, hypertriglyceridemia, insulin resistance and show gradual and progressive development of NASH with fibrosis (**Chapter 5 and 7**). This makes these mice an ideal model to investigate NASH in the context of metabolic disturbances (i.e.

obesity, insulin resistance, dyslipidemia) that characterizes many NASH patients. Moreover, these mice respond to insulin sensitizing drugs, such as rosiglitazone, similarly to humans [68], as shown in **Chapter 3**.

Transgenic ApoE*Leiden (E3L) mice exhibit a humanized lipid metabolism and lipoprotein profile upon a Western-type diet that is supplemented with cholesterol. The expression of a mutated form of human ApoE results in an impaired clearance of ApoE-containing lipoprotein particles. In contrast to other experimental models for atherosclerosis (e.g. LDLr-/- and ApoE-/- mice), these mice respond to lipid-modulating drugs in a more human-like manner [69]. Moreover, prolonged treatment with a high-cholesterol diet results in the development of NASH with fibrosis in context of dyslipidemia [70]. However, metabolic disease development in E3L mice occurs in absence of obesity, WAT inflammation and insulin resistance. Even though obesity is a major risk factor in NASH development, NASH can also occur in lean individuals [71]. In these patients, the most important metabolic risk factor is considered dyslipidemia [72]. Moreover, epidemiological studies link dietary cholesterol intake to the risk and severity of NAFLD [73,74], and in particular higher cholesterol intakes are observed in lean NASH patients [73]. This potentially makes the E3L mouse model a suitable model to study cholesterol-driven NASH development independently of obesity.

The role of diet in animal models of NASH

It is generally accepted that diet has a crucial role in inflammation [75] and the development of metabolic diseases [76]. More specifically, the intake of saturated fatty acids (SFA) is associated with a greater risk of NAFLD [77], while consumption of polyunsaturated fatty acids (PUFAs) is associated with reduced disease risk [78]. As such, we investigated in **chapter 6** whether (isocaloric) replacement of dietary saturated fat with pumpkin seed oil (rich in unsaturated fat) would attenuate NAFLD and atherosclerosis development. In addition, we examined whether phytochemicals present in unrefined (virgin) pumpkin seed oil exerts additional health effects over the refined oil. We showed that pumpkin seed oil reduces dyslipidemia and attenuates NAFLD and atherosclerosis development in E3L mice. The reduced hepatic fat content by pumpkin seed oil may be the result

of increasing fatty acid β-oxidation, as well as inhibiting *de novo* hepatic fatty acid synthesis. Notably, mice receiving virgin pumpkin seed oil showed additional effects on systemic inflammation markers and hepatic inflammation. This suggests that phytochemicals present in virgin oil may have putative anti-inflammatory properties leading to more pronounced effects on disease endpoints. Numerous studies in humans have reported that various phytochemicals can indeed reduce systemic inflammatory markers (reviewed in e.g. [10,79]), but the effects of phytochemicals on disease endpoints often remain unknown. Moreover, further research is needed to determine how phytochemicals can exert beneficial effects on metabolic inflammation. An important question is whether specific phytochemicals account for the reported health effects of phytochemical-rich foods or whether the natural combination of multiple phytochemicals is important to achieve health effects.

It should be noted that the metabolically-triggered inflammatory response underlying NASH development may differ depending on the type of dietary nutrient consumed. For instance, the intake of dietary fat leads to adipocyte hypertrophy and WAT inflammation, and ultimately can lead to the development of NASH (**Chapter 2**). By contrast, increased intake of cholesterol *per se* does not necessarily lead to WAT dysfunction (unpublished results of **chapter 6**), but it can induce NASH. As demonstrated herein (**chapter 6 and 7**) and by others [35,80], dietary cholesterol is a strong inducer of inflammatory and pro-fibrotic genes in the liver. Consistent with the pro-fibrotic effect of dietary cholesterol observed in E3L mice [70], high-fat/high-cholesterol diet (HFC)-fed E3L.CETP mice show onset of fibrosis after already 12 weeks of diet feeding. More specifically, HFC feeding resulted in the activation of pro-fibrotic signaling pathways in liver controlled by TNFα, PDGF and TGFβ as shown by transcriptome analysis in **chapter 7**. The same pathways were activated in mouse liver with high (1% w/w) but not low (0.25% w/w) dietary cholesterol [81], suggesting that the pro-fibrotic effect was attributable to dietary cholesterol itself and not to the fat content of the diet. It is likely that NASH-inducing diets containing high concentrations of cholesterol accentuate specific inflammatory pathways, while other inflammatory pathways that have been associated with human NASH development (e.g. IL-6 and leptin signaling [82]) have a relative lower contribution to disease progression in this model of cholesterol-induced NASH.

Although dietary composition obviously represents one of the most important causes of NASH, the translational aspect of diets used in experimental NASH models can be debated. For example, the recommended dietary cholesterol intake for humans is no more than 300 mg/day according to the dietary guidelines for Americans [83]. At a meal size of one kilogram, this amounts to 0.03%, while diets supplemented with cholesterol ranging from 0.15% up to 2% are often used [35,84]. **Chapter 5 and 7** demonstrate that NASH and liver fibrosis can also be induced in LDLr-/- mice with a high-fat diet containing 45 energy percent from fat with only trace amounts of cholesterol (0.03%), which is translational to human diets [85]. Moreover, as shown in **chapter 7** these animals develop pronounced liver fibrosis (>20% perihepatocellular fibrosis) when the HFD treatment is prolonged (34 weeks). Importantly, **chapter 3** shows that high-fat feeding in LDLr-/- mice results in expression of several inflammatory genes that are associated with severity of human NAFLD [86]. These findings implicate that this models reflects certain processes that are also relevant in human disease development.

Taken together, many animal models have been used to study the pathogenesis of NASH and may reflect different aspects of disease, but no model completely recapitulates the characteristics of NASH in humans. Notably, the composition of the diet plays a critical role in how NASH develops, as liver inflammation may be triggered directly (e.g. via dietary cholesterol) or indirectly (e.g. via WAT). Hence, depending on the strain and diet, animal models may represent different etiologies of disease development. Although there is a clear medical need to develop novel therapies for NASH, the evaluation of therapeutic strategies is hampered by lack mechanistic insight in human disease development. Therefore, identifying causative factors in disease progression is of critical importance to further improve preclinical models of human NASH.

CONCLUDING REMARKS AND FUTURE RECOMMENDATIONS

The incidence of NAFLD is increasing dramatically along with the pandemic of obesity worldwide. Therefore, therapeutic strategies in NAFLD that target obesity can be of importance to avoid or reverse the observed deleterious health effects.

Lifestyle changes related to weight reduction are at the basis of any treatment strategy for metabolically-oriented diseases. However, many patients fail to implement lifestyle changes and pharmaceutical or nutritional interventions may be the alternative to decrease the disease burden. In this thesis, we show that a 'simple' switch in the type of fatty acid consumed can reduce metabolic overload and inflammation in the liver. Furthermore, we identified several new targets (e.g. CCR2 and caspase-1) that could be considered for pharmacological intervention.

NAFLD is a complex disease, in which mechanisms underlying disease progression are poorly understood. The complexity of this disease is highlighted by the fact that not all obese patients show disease progression, even though obesity is a major risk factor of NAFLD. The inflammatory tone of white adipose tissue, rather than its quantity, may underlie the development of obesity-associated diseases. The inflammatory state of intra-abdominal white adipose tissue shows to be a predictive marker for development of (systemic) insulin resistance and is associated with NAFLD progression. This is of great clinical significance, since it suggests that collection of intra-abdominal WAT, rather than subcutaneous fat, may have a great potential for the diagnosis of NASH. However, it should be noted that WAT inflammation in itself may not be the cause of NASH development, but rather the release of (pro-inflammatory) adipokines and fatty acids by inflamed WAT.

The lack of non-invasive biomarkers for the diagnosis of NASH is problematic in current medical practice. Liver biopsies are currently the 'golden-standard' for the diagnosis of NASH. This diagnosis is not only invasive, but also expensive and unsuitable as a tool for population screening. Hence, the most urgent need in the field of NAFLD is the discovery of biomarkers that would help a) to diagnose the stage of the disease, and b) to monitor disease progression. We potentially identified specific saturated fatty acids in the circulation associated with NASH

development that could serve as non-invasive biomarker. Future studies should validate whether these markers are suitable for the use in humans.

In conclusion, this thesis highlighted the importance of WAT in the development of NASH. Additionally, this thesis provides evidence for the contribution of specific molecular mechanisms in the development of 'metabolic inflammation' in NASH and highlights CCR2 and caspase-1 as potential targets for therapeutical intervention.

REFERENCES

1. Rinella ME. Nonalcoholic fatty liver disease: a systematic review. Jama 2015;313:2263-2273.
2. Adams LA, Ratziu V. Non-alcoholic fatty liver - perhaps not so benign. Journal of hepatology 2015;62:1002-1004.
3. Adams LA, Lymp JF, St Sauver J, Sanderson SO, Lindor KD, Feldstein A, et al. The natural history of nonalcoholic fatty liver disease: a population-based cohort study. Gastroenterology 2005;129:113-121.
4. Armstrong MJ, Adams LA, Canbay A, Syn WK. Extrahepatic complications of nonalcoholic fatty liver disease. Hepatology 2014;59:1174-1197.
5. Targher G, Marra F, Marchesini G. Increased risk of cardiovascular disease in non-alcoholic fatty liver disease: causal effect or epiphenomenon? Diabetologia 2008;51:1947-1953.
6. DiSpirito JR, Mathis D. Immunological contributions to adipose tissue homeostasis. Semin Immunol 2015;27:315-321.
7. Hotamisligil GS. Inflammation and metabolic disorders. Nature 2006;444:860-867.
8. Mirza MS. Obesity, Visceral Fat, and NAFLD: Querying the Role of Adipokines in the Progression of Nonalcoholic Fatty Liver Disease. ISRN gastroenterology 2011;2011:592404.
9. Bluher M. The distinction of metabolically 'healthy' from 'unhealthy' obese individuals. Current opinion in lipidology 2010;21:38-43.
10. Navarro E, Funtikova AN, Fito M, Schroder H. Can metabolically healthy obesity be explained by diet, genetics, and inflammation? Mol Nutr Food Res 2015;59:75-93.
11. van der Poorten D, Milner KL, Hui J, Hodge A, Trenell MI, Kench JG, et al. Visceral fat: a key mediator of steatohepatitis in metabolic liver disease. Hepatology 2008;48:449-457.
12. Wajchenberg BL, Giannella-Neto D, da Silva ME, Santos RF. Depot-specific hormonal characteristics of subcutaneous and visceral adipose tissue and their relation to the metabolic syndrome. Hormone and metabolic research = Hormon- und Stoffwechselforschung = Hormones et metabolisme 2002;34:616-621.
13. Janssen I, Katzmarzyk PT, Ross R. Waist circumference and not body mass index explains obesity-related health risk. Am J Clin Nutr 2004;79:379-384.
14. Snijder MB, Dekker JM, Visser M, Bouter LM, Stehouwer CD, Yudkin JS, et al. Trunk fat and leg fat have independent and opposite associations with fasting and postload glucose levels: the Hoorn study. Diabetes care 2004;27:372-377.
15. Item F, Konrad D. Visceral fat and metabolic inflammation: the portal theory revisited. Obesity reviews : an official journal of the International Association for the Study of Obesity 2012;13 Suppl 2:30-39.
16. Cancello R, Tordjman J, Poitou C, Guilhem G, Bouillot JL, Hugol D, et al. Increased infiltration of macrophages in omental adipose tissue is associated with marked hepatic lesions in morbid human obesity. Diabetes 2006;55:1554-1561.
17. Tordjman J, Poitou C, Hugol D, Bouillot JL, Basdevant A, Bedossa P, et al. Association between omental adipose tissue macrophages and liver histopathology in morbid obesity: influence of glycemic status. Journal of hepatology 2009;51:354-362.
18. Caesar R, Manieri M, Kelder T, Boekschoten M, Evelo C, Muller M, et al. A combined transcriptomics and lipidomics analysis of subcutaneous, epididymal and mesenteric adipose tissue reveals marked functional differences. PloS one 2010;5:e11525.

19. Skurk T, Alberti-Huber C, Herder C, Hauner H. Relationship between adipocyte size and adipokine expression and secretion. The Journal of clinical endocrinology and metabolism 2007;92:1023-1033.
20. Cinti S, Mitchell G, Barbatelli G, Murano I, Ceresi E, Faloia E, et al. Adipocyte death defines macrophage localization and function in adipose tissue of obese mice and humans. Journal of lipid research 2005;46:2347-2355.
21. Cinti S. The adipose organ. Prostaglandins, leukotrienes, and essential fatty acids 2005;73:9-15.
22. Altintas MM, Azad A, Nayer B, Contreras G, Zaias J, Faul C, et al. Mast cells, macrophages, and crown-like structures distinguish subcutaneous from visceral fat in mice. Journal of lipid research 2011;52:480-488.
23. Spoto B, Di Betta E, Mattace-Raso F, Sijbrands E, Vilardi A, Parlongo RM, et al. Pro- and anti-inflammatory cytokine gene expression in subcutaneous and visceral fat in severe obesity. Nutrition, metabolism, and cardiovascular diseases : NMCD 2014;24:1137-1143.
24. Hoffstedt J, Arner E, Wahrenberg H, Andersson DP, Qvisth V, Lofgren P, et al. Regional impact of adipose tissue morphology on the metabolic profile in morbid obesity. Diabetologia 2010;53:2496-2503.
25. Rutkowski JM, Stern JH, Scherer PE. The cell biology of fat expansion. J Cell Biol 2015;208:501-512.
26. Macias-Gonzalez M, Moreno-Santos I, Garcia-Almeida JM, Tinahones FJ, Garcia-Fuentes E. PPARgamma2 protects against obesity by means of a mechanism that mediates insulin resistance. European journal of clinical investigation 2009;39:972-979.
27. Drolet R, Richard C, Sniderman AD, Mailloux J, Fortier M, Huot C, et al. Hypertrophy and hyperplasia of abdominal adipose tissues in women. International journal of obesity 2008;32:283-291.
28. Smith U, Hammarstedt A. Antagonistic effects of thiazolidinediones and cytokines in lipotoxicity. Biochim Biophys Acta 2010;1801:377-380.
29. Lionetti L, Mollica MP, Lombardi A, Cavaliere G, Gifuni G, Barletta A. From chronic overnutrition to insulin resistance: the role of fat-storing capacity and inflammation. Nutrition, metabolism, and cardiovascular diseases : NMCD 2009;19:146-152.
30. Virtue S, Vidal-Puig A. Adipose tissue expandability, lipotoxicity and the Metabolic Syndrome--an allostatic perspective. Biochim Biophys Acta 2010;1801:338-349.
31. Hotamisligil GS, Shargill NS, Spiegelman BM. Adipose expression of tumor necrosis factor-alpha: direct role in obesity-linked insulin resistance. Science 1993;259:87-91.
32. Zinman B, Hanley AJ, Harris SB, Kwan J, Fantus IG. Circulating tumor necrosis factor-alpha concentrations in a native Canadian population with high rates of type 2 diabetes mellitus. The Journal of clinical endocrinology and metabolism 1999;84:272-278.
33. Mishima Y, Kuyama A, Tada A, Takahashi K, Ishioka T, Kibata M. Relationship between serum tumor necrosis factor-alpha and insulin resistance in obese men with Type 2 diabetes mellitus. Diabetes research and clinical practice 2001;52:119-123.
34. Olefsky JM, Glass CK. Macrophages, inflammation, and insulin resistance. Annual review of physiology 2010;72:219-246.
35. Funke A, Schreurs M, Aparicio-Vergara M, Sheedfar F, Gruben N, Kloosterhuis NJ, et al. Cholesterol-induced hepatic inflammation does not contribute to the development of insulin resistance in male LDL receptor knockout mice. Atherosclerosis 2014;232:390-396.
36. Lomonaco R, Ortiz-Lopez C, Orsak B, Webb A, Hardies J, Darland C, et al. Effect of adipose tissue insulin resistance on metabolic parameters and liver histology in obese patients with nonalcoholic fatty liver disease. Hepatology 2012;55:1389-1397.

37. Bugianesi E, McCullough AJ, Marchesini G. Insulin resistance: a metabolic pathway to chronic liver disease. Hepatology 2005;42:987-1000.
38. Osborn O, Olefsky JM. The cellular and signaling networks linking the immune system and metabolism in disease. Nat Med 2012;18:363-374.
39. Weisberg SP, Hunter D, Huber R, Lemieux J, Slaymaker S, Vaddi K, et al. CCR2 modulates inflammatory and metabolic effects of high-fat feeding. The Journal of clinical investigation 2006;116:115-124.
40. Weisberg SP, McCann D, Desai M, Rosenbaum M, Leibel RL, Ferrante AW, Jr. Obesity is associated with macrophage accumulation in adipose tissue. The Journal of clinical investigation 2003;112:1796-1808.
41. Ito A, Suganami T, Yamauchi A, Degawa-Yamauchi M, Tanaka M, Kouyama R, et al. Role of CC chemokine receptor 2 in bone marrow cells in the recruitment of macrophages into obese adipose tissue. The Journal of biological chemistry 2008;283:35715-35723.
42. Kanda H, Tateya S, Tamori Y, Kotani K, Hiasa K, Kitazawa R, et al. MCP-1 contributes to macrophage infiltration into adipose tissue, insulin resistance, and hepatic steatosis in obesity. The Journal of clinical investigation 2006;116:1494-1505.
43. Tamura Y, Sugimoto M, Murayama T, Minami M, Nishikaze Y, Ariyasu H, et al. C-C chemokine receptor 2 inhibitor improves diet-induced development of insulin resistance and hepatic steatosis in mice. Journal of atherosclerosis and thrombosis 2010;17:219-228.
44. Miura K, Yang L, van Rooijen N, Ohnishi H, Seki E. Hepatic recruitment of macrophages promotes nonalcoholic steatohepatitis through CCR2. American journal of physiology Gastrointestinal and liver physiology 2012;302:G1310-1321.
45. Seki E, De Minicis S, Gwak GY, Kluwe J, Inokuchi S, Bursill CA, et al. CCR1 and CCR5 promote hepatic fibrosis in mice. The Journal of clinical investigation 2009;119:1858-1870.
46. Kitade H, Sawamoto K, Nagashimada M, Inoue H, Yamamoto Y, Sai Y, et al. CCR5 plays a critical role in obesity-induced adipose tissue inflammation and insulin resistance by regulating both macrophage recruitment and M1/M2 status. Diabetes 2012;61:1680-1690.
47. Friedman S, Sanyal A, Goodman Z, Lefebvre E, Gottwald M, Fischer L, et al. Efficacy and safety study of cenicriviroc for the treatment of non-alcoholic steatohepatitis in adult subjects with liver fibrosis: CENTAUR Phase 2b study design. Contemporary clinical trials 2016;47:356-365.
48. Lumeng CN, Bodzin JL, Saltiel AR. Obesity induces a phenotypic switch in adipose tissue macrophage polarization. The Journal of clinical investigation 2007;117:175-184.
49. Patsouris D, Li PP, Thapar D, Chapman J, Olefsky JM, Neels JG. Ablation of CD11c-positive cells normalizes insulin sensitivity in obese insulin resistant animals. Cell metabolism 2008;8:301-309.
50. Nguyen MT, Favelyukis S, Nguyen AK, Reichart D, Scott PA, Jenn A, et al. A subpopulation of macrophages infiltrates hypertrophic adipose tissue and is activated by free fatty acids via Toll-like receptors 2 and 4 and JNK-dependent pathways. The Journal of biological chemistry 2007;282:35279-35292.
51. du Plessis J, van Pelt J, Korf H, Mathieu C, van der Schueren B, Lannoo M, et al. Association of Adipose Tissue Inflammation With Histologic Severity of Nonalcoholic Fatty Liver Disease. Gastroenterology 2015;149:635-648 e614.
52. Bourlier V, Zakaroff-Girard A, Miranville A, De Barros S, Maumus M, Sengenes C, et al. Remodeling phenotype of human subcutaneous adipose tissue macrophages. Circulation 2008;117:806-815.

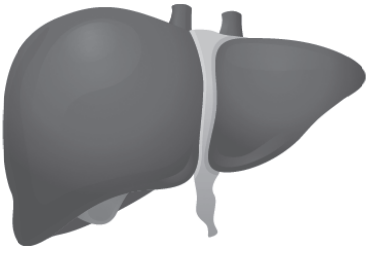
53. Zeyda M, Farmer D, Todoric J, Aszmann O, Speiser M, Gyori G, et al. Human adipose tissue macrophages are of an anti-inflammatory phenotype but capable of excessive pro-inflammatory mediator production. International journal of obesity 2007;31:1420-1428.
54. Mosser DM, Edwards JP. Exploring the full spectrum of macrophage activation. Nature reviews Immunology 2008;8:958-969.
55. Prieur X, Mok CY, Velagapudi VR, Nunez V, Fuentes L, Montaner D, et al. Differential lipid partitioning between adipocytes and tissue macrophages modulates macrophage lipotoxicity and M2/M1 polarization in obese mice. Diabetes 2011;60:797-809.
56. Odegaard JI, Ricardo-Gonzalez RR, Goforth MH, Morel CR, Subramanian V, Mukundan L, et al. Macrophage-specific PPARgamma controls alternative activation and improves insulin resistance. Nature 2007;447:1116-1120.
57. Guo H, Callaway JB, Ting JP. Inflammasomes: mechanism of action, role in disease, and therapeutics. Nat Med 2015;21:677-687.
58. Stienstra R, van Diepen JA, Tack CJ, Zaki MH, van de Veerdonk FL, Perera D, et al. Inflammasome is a central player in the induction of obesity and insulin resistance. Proceedings of the National Academy of Sciences of the United States of America 2011;108:15324-15329.
59. Bellentani S, Scaglioni F, Marino M, Bedogni G. Epidemiology of non-alcoholic fatty liver disease. Digestive diseases 2010;28:155-161.
60. Marchesini G, Bugianesi E, Forlani G, Cerrelli F, Lenzi M, Manini R, et al. Nonalcoholic fatty liver, steatohepatitis, and the metabolic syndrome. Hepatology 2003;37:917-923.
61. Boren J, Taskinen MR, Olofsson SO, Levin M. Ectopic lipid storage and insulin resistance: a harmful relationship. Journal of internal medicine 2013;274:25-40.
62. Stienstra R, Joosten LA, Koenen T, van Tits B, van Diepen JA, van den Berg SA, et al. The inflammasome-mediated caspase-1 activation controls adipocyte differentiation and insulin sensitivity. Cell metabolism 2010;12:593-605.
63. Fujisaka S, Usui I, Bukhari A, Ikutani M, Oya T, Kanatani Y, et al. Regulatory mechanisms for adipose tissue M1 and M2 macrophages in diet-induced obese mice. Diabetes 2009;58:2574-2582.
64. Brunt EM. Nonalcoholic steatohepatitis: definition and pathology. Seminars in liver disease 2001;21:3-16.
65. Neuschwander-Tetri BA. Hepatic lipotoxicity and the pathogenesis of nonalcoholic steatohepatitis: the central role of nontriglyceride fatty acid metabolites. Hepatology 2010;52:774-788.
66. Rinella ME, Green RM. The methionine-choline deficient dietary model of steatohepatitis does not exhibit insulin resistance. Journal of hepatology 2004;40:47-51.
67. Williams LM, Campbell FM, Drew JE, Koch C, Hoggard N, Rees WD, et al. The development of diet-induced obesity and glucose intolerance in C57BL/6 mice on a high-fat diet consists of distinct phases. PloS one 2014;9:e106159.
68. Neuschwander-Tetri BA, Brunt EM, Wehmeier KR, Oliver D, Bacon BR. Improved nonalcoholic steatohepatitis after 48 weeks of treatment with the PPAR-gamma ligand rosiglitazone. Hepatology 2003;38:1008-1017.
69. van de Steeg E, Kleemann R, Jansen HT, van Duyvenvoorde W, Offerman EH, Wortelboer HM, et al. Combined analysis of pharmacokinetic and efficacy data of preclinical studies with statins markedly improves translation of drug efficacy to human trials. J Pharmacol Exp Ther 2013;347:635-644.
70. Morrison MC, Liang W, Mulder P, Verschuren L, Pieterman E, Toet K, et al. Mirtoselect, an anthocyanin-rich bilberry extract, attenuates non-alcoholic steatohepatitis and

associated fibrosis in ApoE(*)3Leiden mice. Journal of hepatology 2015;62:1180-1186.
71. Das K, Das K, Mukherjee PS, Ghosh A, Ghosh S, Mridha AR, et al. Nonobese population in a developing country has a high prevalence of nonalcoholic fatty liver and significant liver disease. Hepatology 2010;51:1593-1602.
72. Kumar R, Rastogi A, Sharma MK, Bhatia V, Garg H, Bihari C, et al. Clinicopathological characteristics and metabolic profiles of non-alcoholic fatty liver disease in Indian patients with normal body mass index: Do they differ from obese or overweight non-alcoholic fatty liver disease? Indian journal of endocrinology and metabolism 2013;17:665-671.
73. Yasutake K, Nakamuta M, Shima Y, Ohyama A, Masuda K, Haruta N, et al. Nutritional investigation of non-obese patients with non-alcoholic fatty liver disease: the significance of dietary cholesterol. Scandinavian journal of gastroenterology 2009;44:471-477.
74. Musso G, Gambino R, De Michieli F, Cassader M, Rizzetto M, Durazzo M, et al. Dietary habits and their relations to insulin resistance and postprandial lipemia in nonalcoholic steatohepatitis. Hepatology 2003;37:909-916.
75. Calder PC, Albers R, Antoine JM, Blum S, Bourdet-Sicard R, Ferns GA, et al. Inflammatory disease processes and interactions with nutrition. The British journal of nutrition 2009;101 Suppl 1:S1-45.
76. Hotamisligil GS, Erbay E. Nutrient sensing and inflammation in metabolic diseases. Nature reviews Immunology 2008;8:923-934.
77. Zelber-Sagi S, Nitzan-Kaluski D, Goldsmith R, Webb M, Blendis L, Halpern Z, et al. Long term nutritional intake and the risk for non-alcoholic fatty liver disease (NAFLD): a population based study. Journal of hepatology 2007;47:711-717.
78. Oya J, Nakagami T, Sasaki S, Jimba S, Murakami K, Kasahara T, et al. Intake of n-3 polyunsaturated fatty acids and non-alcoholic fatty liver disease: a cross-sectional study in Japanese men and women. European journal of clinical nutrition 2010;64:1179-1185.
79. Gonzalez-Gallego J, Garcia-Mediavilla MV, Sanchez-Campos S, Tunon MJ. Fruit polyphenols, immunity and inflammation. The British journal of nutrition 2010;104 Suppl 3:S15-27.
80. Wouters K, van Gorp PJ, Bieghs V, Gijbels MJ, Duimel H, Lutjohann D, et al. Dietary cholesterol, rather than liver steatosis, leads to hepatic inflammation in hyperlipidemic mouse models of nonalcoholic steatohepatitis. Hepatology 2008;48:474-486.
81. Kleemann R, Verschuren L, van Erk MJ, Nikolsky Y, Cnubben NH, Verheij ER, et al. Atherosclerosis and liver inflammation induced by increased dietary cholesterol intake: a combined transcriptomics and metabolomics analysis. Genome biology 2007;8:R200.
82. Wieckowska A, Papouchado BG, Li Z, Lopez R, Zein NN, Feldstein AE. Increased hepatic and circulating interleukin-6 levels in human nonalcoholic steatohepatitis. The American journal of gastroenterology 2008;103:1372-1379.
83. Agriculture USDoHaHSaUSDo. Dietary Guidelines for Americans. 2015 – 2020 [cited 2015; 8th Edition:[Available from: http://health.gov/dietaryguidelines/2015/guidelines/
84. Charlton M, Krishnan A, Viker K, Sanderson S, Cazanave S, McConico A, et al. Fast food diet mouse: novel small animal model of NASH with ballooning, progressive fibrosis, and high physiological fidelity to the human condition. American journal of physiology Gastrointestinal and liver physiology 2011;301:G825-834.

85. Eilander A, Harika RK, Zock PL. Intake and sources of dietary fatty acids in Europe: Are current population intakes of fats aligned with dietary recommendations? European journal of lipid science and technology : EJLST 2015;117:1370-1377.
86. Moylan CA, Pang H, Dellinger A, Suzuki A, Garrett ME, Guy CD, et al. Hepatic gene expression profiles differentiate presymptomatic patients with mild versus severe nonalcoholic fatty liver disease. Hepatology 2014;59:471-482.

Chapter 9

Nederlandse samenvatting


Door de obesitas epidemie is de niet-alcoholische vetleverziekte ('non-alcoholic fatty liver disease', NAFLD) nu de meest voorkomende chronische leverziekte wereldwijd. Ongeveer 25 tot 45% van de bevolking heeft te maken met niet-alcoholische leververvetting. De prevalentiecijfers onder obese individuen lopen zelfs op tot 90%. De term 'NAFLD' omvat verschillende stadia van deze aandoening, variërend van 'simpele' vette lever gekenmerkt door ophoping van vet in de lever (steatose) en leververvetting met ontsteking (niet-alcoholische steatohepatitis, NASH), dat op den duur kan overgaan in littekenvorming (fibrose) en levercirrose. Een 'simpele' vette lever wordt vaak gezien als een relatief goedaardige aandoening, terwijl patiënten met NASH een vergroot risico hebben op het ontwikkelen van metabole ziekten, waaronder cardiovasculaire aandoeningen. Bovendien is NASH een belangrijke oorzaak van levergerelateerde morbiditeit en mortaliteit. Momenteel zijn de mogelijkheden om NASH patiënten te kunnen behandelen beperkt en daarom is het van groot belang om mechanismen te ontdekken waarop nieuwe, effectieve medicijnen kunnen aangrijpen. Hoe NAFLD ontstaat en welke onderliggende mechanismen ten grondslag liggen aan de overgang van steatose naar NASH en fibrose zijn echter onbekend. Er wordt gedacht dat ontsteking een belangrijk onderdeel vormt voor de ontwikkeling van NASH. Een hypothese stelt dat deze ontsteking veroorzaakt kan worden door metabole overbelasting van organen (door een overschot aan energie of macronutriënten) en wordt daarom ook wel 'metabole ontsteking' genoemd. Men denkt dat het vetweefsel hierin een belangrijke bron van ontsteking kan zijn. Het doel van het onderzoek beschreven in dit proefschrift was om meer inzicht te krijgen in de etiologie van NAFLD. De nadruk lag hierbij op de mogelijke rol van het vetweefsel in het ziekteproces. Daarnaast is er gekeken naar onderliggende mechanismen die ten grondslag liggen in het ontstaan van metabole ontsteking.

In **hoofdstuk 2** hebben we de opeenvolging van ontstekingsprocessen in verschillende vetweefsel depots en de lever onderzocht gedurende hoog vet dieet geïnduceerde obesitas in C57BL/6J muizen. Dit hoofdstuk laat zien dat niet alle vetweefsel depots even vatbaar zijn voor het ontwikkelen van metabole ontsteking. Het viscerale perigonadale vetweefsel (buikvet) was het eerste vetdepot waar de metabole ontsteking zich openbaarde. Deze ontsteking leek gerelateerd te zijn aan de maximale expansie van dit vetdepot en de vetcellen daarin. Het ontstaan

van ontsteking in het perigonadale vet ging vooraf aan de ontwikkeling van leverontsteking. Met andere woorden, de ontsteking in het vetweefsel ging vooraf aan de overgang van steatose naar NASH. Vervolgens hebben we onderzocht of het ontstoken vetdepot een oorzakelijke rol speelt in de progressie van NASH. We hebben hierbij laten zien dat het operatief verwijderen van het ontstoken perigonadale vetdepot, de ontwikkeling van leverontsteking verminderd en de concentratie van bepaalde circulerende ontstekingsfactoren (zoals cytokines en vetzuren) verlaagd. Deze pro-inflammatoire mediatoren, ook wel adipokines genoemd, vormen mogelijk de verbinding tussen het ontstoken vetweefsel en de ontwikkeling van NASH.

Metabole ontsteking in het vetweefsel speelt mogelijkerwijs een belangrijke rol in de ontwikkeling van metabole complicaties, zoals NAFLD en insuline resistentie (een van de voortekenen van diabetes). Daarom hebben we in **hoofdstuk 3** onderzocht of het therapeutisch behandelen met rosiglitazone, een antidiabetica met vermeende anti-inflammatoire effecten in het vetweefsel, de ontwikkeling van NAFLD kan verminderen in obese LDLr-/- muizen. De behandeling met rosiglitazone leidde tot een verbetering van diabetes symptomen (d.w.z. een verlaging van glucose en insuline concentraties in het bloed). Parallel daaraan zagen we een verminderde ontsteking in het perigonadale vetdepot en verlaagde concentraties van verschillende circulerende pro-inflammatoire adipokines. In de lever zagen we een afname van steatose, en consistent met de rol van het ontstoken vetweefsel in de ontwikkeling van leverontsteking, observeerden we een verminderde activiteit van ontstekingsgerelateerde processen in de lever. Rosiglitazone had echter geen effect op de ontwikkeling van obesitas. Mogelijk zorgde de veranderde vetopslag in het lichaam (door het stimuleren van de aanmaak van vetcellen in het ‘veilige’ onderhuidse vetdepot) voor de vermindering van de ontstekingsgraad in het perigonadale vetdepot en de daarmee geassocieerde NAFLD ontwikkeling.

Er wordt gedacht dat activatie van een bepaalde chemokine receptor (CCR2) een belangrijk onderdeel vormt in het initiëren van de ontstekingsreactie in metabole ziekten. Deze receptor is namelijk onder andere betrokken bij de infiltratie van immuuncellen (zoals macrofagen) in het vetweefsel en de lever. Daarom hebben we in **hoofdstuk 4** de effecten van een CCR2 interventie bestudeerd op de ontwikkeling van NASH in een muismodel met dieet geïnduceerde obesitas. Deze interventie

werd gestart op verschillende tijdstippen (vroeg en laat) in de ziekteontwikkeling om zo te onderzoeken of een CCR2 antagonist NASH kan verminderen. Deze studie laat zien dat de vroege ziekteverschijnselen, d.w.z. insuline resistentie en vetweefselontsteking, alleen verbeterd werden wanneer er in een vroeg stadium behandeld werd met de CCR2 antagonist. Daarnaast zagen we dat zowel de vroege als late behandeling gunstige effecten kan hebben op de mate van leverontsteking, echter leidde alleen de vroege behandeling tot uitgesproken histologische effecten in de lever. Deze resultaten suggereren dat alleen vroegtijdig behandelen met een CCR2 antagonist effectief is tegen NASH.

In **hoofdstuk 5** bestudeerden we de effecten van een interventie gericht op het NLRP3 inflammasome, één van de sensoren van metabole overbelasting, op de ontwikkeling van NAFLD. Om dit te onderzoeken zijn obese LDLr-/-.Leiden muizen behandeld met een caspase-1 remmer. Deze interventie had geen effect op de mate van obesitas of de vetweefselmassa in de muizen, maar verminderde wel de ontsteking in het perigonadale vetweefsel en parallel daaraan nam de algehele insuline resistentie af. Bovendien zorgde de behandeling voor een verminderde ontwikkeling van NAFLD wat te zien was aan de afname van steatose, ontsteking en fibrose in de lever. Dit suggereert dat beïnvloeding van het inflammasome een belangrijk aangrijpingspunt kan zijn voor het behandelen van insuline resistentie en NAFLD.

Naast de genoemde farmacologische interventies in hoofdstukken 3-5, onderzochten we in **hoofdstuk 6** de potentiële waarde van een voedingsinterventie op het verminderen van metabole ontsteking en ziekteontwikkeling. In dit hoofdstuk hebben we laten zien dat (isocalorische) vervanging van diëtair verzadigd vet met pompoenzaadolie, dat rijk is aan meervoudig onverzadigd vetzuren, de ontwikkeling van dyslipidemie verminderd in ApoE*3Leiden muizen. Daarnaast had de pompoenzaadolie gunstige effecten op NASH en de daarmee geassocieerde atherosclerose (de basis voor vele cardiovasculaire aandoeningen). Bovendien vonden we dat de ongeraffineerde variant van de pompoenzaadolie (dat fytochemische stoffen met vermeende anti-inflammatoire effecten bevat) nog bijkomende gunstige effecten hadden op het vetmetabolisme en ontsteking in de lever, wat leidde tot een uitgesproken vermindering van NAFLD en de daarmee geassocieerde atherosclerose ontwikkeling.

In **hoofdstuk 7** zijn de verschillende manieren van vetstapeling in de lever bestudeerd, om meer inzicht te krijgen hoe leververvetting kan leiden tot leverontsteking. Vetstapeling in de lever kan men op histologisch niveau onderverdelen in twee vormen van steatose, namelijk macrovesiculaire steatose en microvesiculaire steatose. Macrovesiculaire steatose wordt gekenmerkt door de aanwezigheid van één grote vetdruppel in een lever cel, terwijl microvesiculaire steatose bestaat uit grote hoeveelheden kleine vetdruppeltjes in een lever cel. Metabole overbelasting kan resulteren in zowel macrovesiculaire steatose als microvesiculaire steatose. Het is echter onbekend welke manier van leververvetting bijdraagt aan de ontwikkeling van NASH. Om dit te kunnen onderzoeken hebben we de mogelijke relatie tussen de verschillende steatose types en de ontwikkeling van leverontsteking bestudeerd in verschillende experimentele NASH modellen (in ApoE*3Leiden.CETP, C57BL/6J en LDLr-/-.Leiden muizen). Hierbij vonden we een sterke positieve correlatie tussen de mate van macrovesiculaire steatose en leverontsteking, maar niet bij microvesiculaire steatose, in de verschillende muismodellen voor NASH.

Samenvattend, dit proefschrift beschrijft dat metabole ontsteking een belangrijke rol speelt in de ontwikkeling van metabole ziekten zoals insuline resistentie, niet-alcoholische vetleverziekte (NAFLD) en atherosclerose. Bovendien is aangetoond dat het vetweefsel een oorzakelijke rol kan hebben in de progressie van obesitas geassocieerde NAFLD. Mogelijk draagt de ontstekingsgraad in het vetweefsel bij aan de uitscheiding van specifieke pro-inflammatoire factoren (zoals cytokines en vetzuren) die de lever kunnen beïnvloeden. Bij de ontwikkeling van metabole ontsteking in het vetweefsel lijkt niet de totale hoeveelheid vetmassa van belang te zijn, maar eerder de manier waarop overtollige energie wordt opgeslagen (bijvoorbeeld door het groter laten worden van bestaande vetcellen). Niet alleen de manier van vetstapeling in het vetweefsel, maar ook de wijze van vetstapeling in de lever zelf (d.w.z. meer macrovesiculaire steatose), kan betrokken zijn bij de ontwikkeling van metabole ontsteking in de lever. Tenslotte hebben we aangetoond dat interventies gericht op het onderdrukken van de metabole ontsteking waardevol kunnen zijn om de ziekteontwikkeling te voorkomen of vertragen.

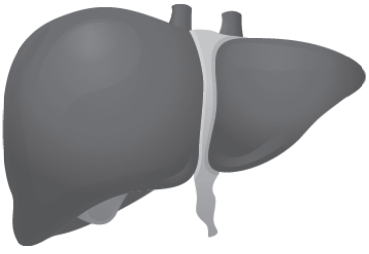
Appendices

List of publications

Curriculum Vitae

Dankwoord







LIST OF PUBLICATIONS

Reduction of obesity-associated white adipose tissue inflammation by rosiglitazone is associated with reduced non-alcoholic fatty liver disease in LDLr-deficient mice.
Mulder P, Morrison MC, Verschuren L, Liang W, van Bockel JH, Kooistra T, Wielinga PY, Kleemann R.
Scientific Reports, 2016 Aug 22; 6: 31542.

Effects of anthocyanin and flavanol compounds on lipid metabolism and adipose tissue associated systemic inflammation in diet-induced obesity.
van der Heijden RA, Morrison MC, Sheedfar F, Mulder P, Schreurs M, Hommelberg PH, Hofker MH, Schalkwjk C, Kleeman R, Tietge UJ, Koonen DP, Heeringa P.
Mediators of Inflammation. 2016 Jun 6.

Intervention with a caspase-1 inhibitor reduces obesity-associated hyperinsulinemia, non-alcoholic steatohepatitis (NASH) hepatic fibrosis in LDLr-/-.Leiden mice.
Morrison MC, Mulder P, Salic K, Verheij J, Liang W, van Duyvenvoorde W, Menke A, Kooistra T, Kleemann R, Wielinga PY.
International Journal of Obesity. 2016 Apr 28. doi: 10.1038/ijo.2016.74

Salsalate attenuates diet induced non-alcoholic steatohepatitis in mice by decreasing lipogenic and inflammatory processes.
Liang W, Verschuren L, Mulder P, van der Hoorn JW, Verheij J, van Dam AD, Boon MR, Princen HM, Havekes LM, Kleemann R, van den Hoek AM.
British journal of pharmacology. 2015 Nov 1;172(22):5293-305.

Surgical removal of inflamed epididymal white adipose tissue attenuates the development of non-alcoholic steatohepatitis in obesity.
Mulder P, Morrison MC, Wielinga PY, van Duyvenvoorde W, Kooistra T, Kleemann R.
International Journal of Obesity. 2015 Oct 26. doi:10.1038/ijo.2015.226

Replacement of dietary saturated fat by PUFA-rich pumpkin seed oil attenuates non-alcoholic fatty liver disease and atherosclerosis development, with additional health effects of virgin over refined oil.
Morrison MC, Mulder P, Stavro PM, Suárez M, Arola-Arnal A, van Duyvenvoorde W, Kooistra T, Wielinga PY, Kleemann R.
PloS one. 2015 Sep 25;10(9):e0139196.

Mirtoselect, an anthocyanin-rich bilberry extract, attenuates non-alcoholic steatohepatitis and associated fibrosis in ApoE∗ 3Leiden mice.
Morrison MC, Liang W, Mulder P, Verschuren L, Pieterman E, Toet K, Heeringa P, Wielinga PY, Kooistra T, Kleemann R.
Journal of hepatology. 2015 May 31;62(5):1180-6.

Macrovesicular steatosis is associated with development of lobular inflammation and fibrosis in diet-induced non-alcoholic steatohepatitis (NASH).
Mulder P, Liang W, Wielinga PY, Verschuren L, Toet K, Havekes LM, van den Hoek AM, Kleemann R.
Inflammation and Cell Signaling. 2015 Jun 8;2(3).

Dietary restriction reverses obesity-induced anhedonia.
Grillo CA, Mulder P, Macht VA, Kaigler KF, Wilson SP, Wilson MA, Reagan LP.
Physiology & behavior. 2014 Apr 10;128:126-32.

Coordinated and interactive expression of genes of lipid metabolism and inflammation in adipose tissue and liver during metabolic overload.
Liang W, Tonini G, Mulder P, Kelder T, van Erk M, van den Hoek AM, Mariman R, Wielinga PY, Baccini M, Kooistra T, Biggeri A, Kleemann R.
PloS one. 2013 Sep 25;8(9):e75290.

Intervention with the CCR2 inhibitor propagermanium attenuates diet-induced insulin resistance, adipose tissue inflammation and non-alcoholic steatohepatitis.
Mulder P, van den Hoek AM, Kleemann R.
Accepted - PloS one

CURRICULUM VITAE

Petra Catharina Anne Mulder werd geboren op 5 juni 1987 te Groningen. Na het behalen van haar VWO diploma (profiel Natuur en Gezondheid) aan het Dr. Aletta Jacobs college te Hoogezand in 2005, startte zij datzelfde jaar met de opleiding Life Science & Technology aan de Rijksuniversiteit Groningen. Na het behalen van haar bachelor diploma Life Science & Technology in augustus 2008, heeft zij plaatsgenomen in het bestuur van de studievereniging 'Groninger Levenswetenschappen Vereniging' Idun. In 2009, startte zij met de research master Behavioral and Cognitive Neuroscience (BCN) met als specialisatie animal and human behavior.

In het kader van haar masteropleiding heeft Petra twee onderzoeksstages afgerond. De eerste stage werd uitgevoerd bij de vakgroep neuroendocrinologie van de Rijksuniversiteit Groningen. Onder begeleiding van Prof. Dr. A.J.W. Scheurink heeft zij onderzoek gedaan naar het effect van overeten op zowel de vrijlating van het 'plezierhormoon' dopamine als de beschikbaarheid van dopamine receptoren in de hersenen. Haar tweede stage heeft zij uitgevoerd in het laboratorium van Dr. L.P. Reagan aan de University of South Carolina School of Medicine (Verenigde Staten). Hiervoor bestudeerde ze de effectiviteit van een antidepressivum om depressieve gedragingen in obese ratten te verminderen. In september 2011 behaalde zij haar master diploma cum laude.

Petra werd in maart 2012 aangesteld als promovendus bij de afdeling Heelkunde van het LUMC onder supervisie van Prof. Dr. J. Hajo van Bockel. Voor haar promotieonderzoek werd zij gedetacheerd bij de afdeling Metabolic Health Research van TNO in Leiden onder de supervisie van Dr. Robert Kleemann. Het promotieonderzoek, waarvan de resultaten zijn beschreven in dit proefschrift, is afgerond in 2016.

DANKWOORD

Het afronden van ‘mijn’ boekje was natuurlijk niet mogelijk geweest zonder de inzet en steun van een heleboel mensen. Daarom is een groot dankjewel aan iedereen die (direct of indirect) aan dit proefschrift heeft bijgedragen hier zeker op zijn plaats! Hierbij wil ik een aantal mensen in het bijzonder noemen:

Beste Robert, aan jou ben ik de meeste dank verschuldigd. Door je optimistische, enthousiaste, maar ook kritische blik leerde je me obstakels van het promoveren (die ik vooral zelf zag) te overwinnen. Bedankt voor je fijne begeleiding! Beste prof. van Bockel, Hajo, ook al zagen we elkaar niet vaak, ik heb je kritische blik en klinische inzichten ontzettend gewaardeerd. Verder gaat mijn dank uit naar de promotiecommissie: Dr. Joanne Verheij, Prof. Yvo Smulders en Prof. Louis Havekes, hartelijk dank voor het kritisch doorlezen en beoordelen van mijn proefschrift.

Anita, Hoekie, naast je wetenschappelijke bijdrage, wil ik je graag ook bedanken voor je goede adviezen, de nodige humor en ontspanning op de squashbaan. Elsbet, ik zou een heel hoofdstuk aan jou kunnen wijden om mijn dankbaarheid aan jou te tonen, maar het moet volstaan met een samenvatting: Bedankt voor je ‘commitment’ op het lab, je hulp bij ontelbare andere dingen, je smalltalk en je gezelligheid! Lars, bedankt voor je hulp bij de vele microarray analyses die een belangrijk deel van mijn proefschrift vormen. Peter, ik heb je grote interesse en betrokkenheid bij mijn onderzoek zeer gewaardeerd. Teake, bedankt voor je kritische blik en onze wetenschappelijke discussies. Karin, bedankt dat je altijd voor mij klaar stond, zowel binnen als buiten het lab. Wim en Erik, naast het vele werk in de dierstallen en op het lab, wil ik jullie ook bedanken voor de nodige gezelligheid, (ont)spanning bij het volleybal en het bijspijkeren van mijn muziekkennis.

Alle (oud)- TNO collega’s van de afdeling Metabolic Health Research: Adri, Ageeth, Angela, Anita, Anne S, Annemarie M, Anne-Marie Z, Arianne, Bea, Benno, Carla, Christa, Coen, Elly, Esther, Frans, Frits, Han, Hans, Herma, Ivana, Jan, Jessica, Joline, José, Kanita, Kirsty, Koen, Leslie, Lex, Marijke, Marjolein, Marrie, Mieke, Nanda, Natascha, Nicole, Pascalle, Reinout, Renate, Robert O, Roeland, Sabine, Sigrid, Simone, Susanna, Teun, bedankt voor jullie fijne samenwerking. Ook dank ik de collega’s van de afdeling endocrinologie van het LUMC voor hun gastvrijheid

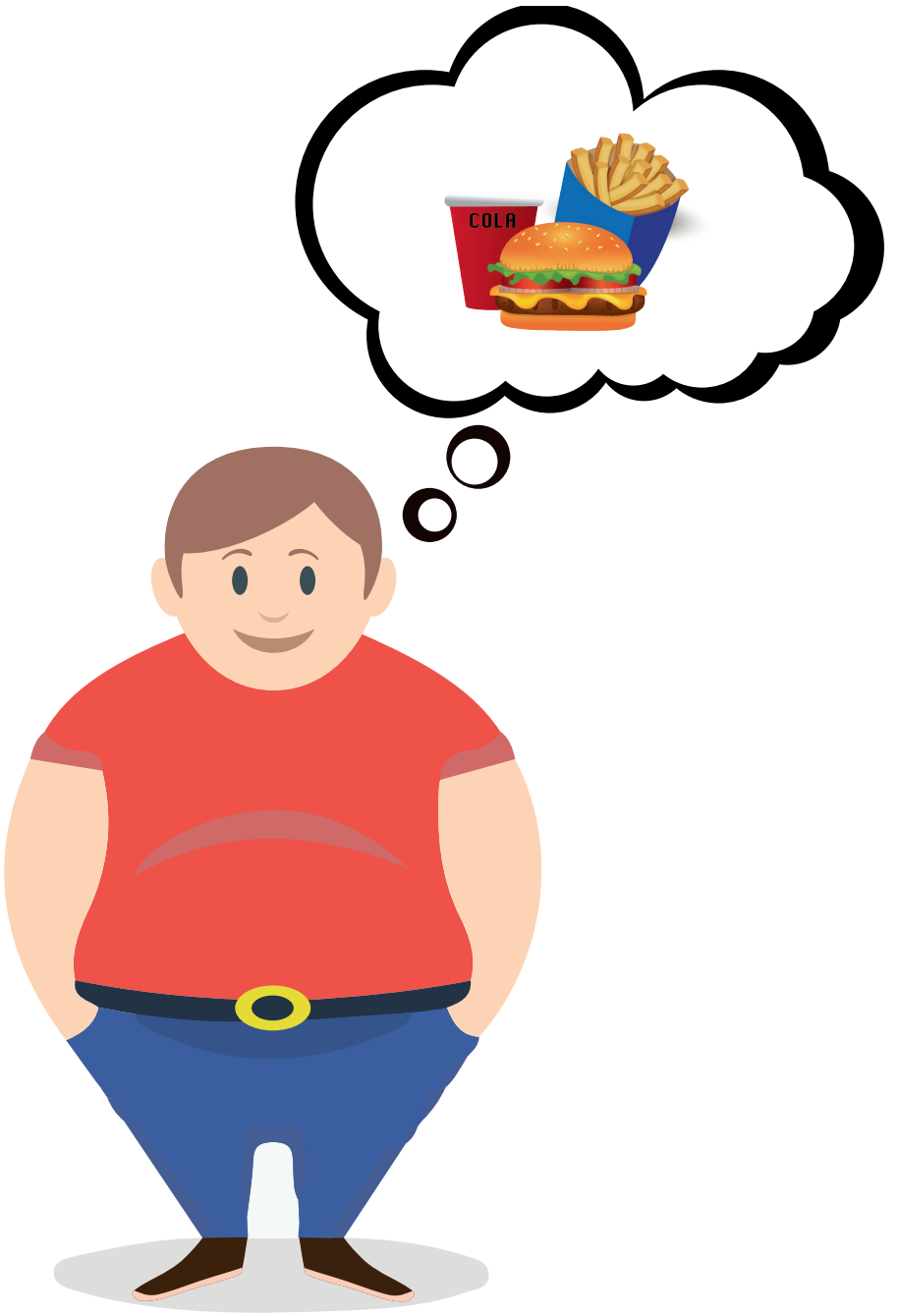
tijdens de werkbesprekingen. Speciale dank gaat uit naar Prof. Patrick Rensen en Prof. Ko Willems van Dijk voor hun kritische wetenschappelijke blik.

Het spreekwoord ‘gedeelde smart is halve smart’ gaat zeker op bij promoveren. Hierbij zijn mede-AIOs onmisbaar! Susan, Lobke, Wen, Marianne, Rob, Martine en Anne, bedankt voor al jullie hulp, enthousiasme, gezelligheid en het luisterende oor dat ik af en toe nodig had. Kamergenote Martine, bedankt voor onze leuke samenwerking, met een aantal mooie artikelen als resultaat! Anne, wat ben ik blij dat zo’n lieve meid mijn paranimf wil zijn.

Lieve Thijs en Saskia, bedankt voor onze fantastische (en hopelijk nog eeuwigdurende) vriendschap, waarbij spontaniteit en genieten (van eten) hoog in het vaandel staan! Lieve oudbestuurtjes, Adriëtte, Anne Margriet, Thijs, Bennet en Menno, ik verheug me op onze reünie bij mijn promotie. LST-vriendinnen: Marieke, Petra, Marjon, Tryanda, Aukje, Simone en Else, dank jullie wel voor de leuke en gezellige etentjes. Speciale dank aan Else, voor het altijd klaarstaan en je grote enthousiasme om samen nieuwe hobby’s te ontdekken. Ook dank voor het introduceren aan de leuke mensen van de boekenclub: Henk, Roselin en Joy. Henk, ooit zal ik je verblijden met 400 brieven van dankbaarheid. Roselin en Joy, dankjewel voor jullie blik in de wondere werelden van de geneeskunde.

Lieve pap en mam, bedankt voor alle kansen die jullie mij hebben gegeven en voor het altijd klaarstaan. Lieve Fabian, ik ben blij dat ik zo’n trotse broer naast mijn zijde heb staan tijdens mijn promotie. Bedankt dat je mijn paranimf wilt zijn en de ontelbare andere dingen die je voor me doet. Liebe Kleiners, es freut mich wahnsinnig das ihr für meine Verteidigung ‘ufe’ fahren! Mijn schoonfamilie, Piet, Diny, Annette en Michiel, bedankt voor jullie interesse. Ik voel me erg thuis bij jullie.

Lieve Adeen en Floor, jullie zijn een bron van energie voor mij, bedankt voor jullie gezelligheid. Lieve Rob, samen met jou kan ik de hele wereld aan. Bedankt voor al je liefde, steun, relativering, lieve woorden en nog zo veel meer.


COLA